The role of lipid-specific CD1a-mediated immune responses in inflammatory disease

---

A thesis submitted for the degree of Doctor of Philosophy of the University of Oxford

Lea Nußbaum

Lincoln College

Wellcome Doctoral Training Programme in Infection, Immunology and Translational Medicine

MRC Weatherall Institute of Molecular Medicine

University of Oxford

Michaelmas Term 2021

Abstract

CD1a is predominantly expressed by antigen-presenting cells in the skin, where it modulates immune responses through lipid antigen presentation to T cells. Increasing evidence supports a role of regulatory T cells (Tregs) in the control of skin immune programs. However, whether Tregs can recognise CD1a and maintain immune homeostasis remains unstudied.

The first aim of this study was to interrogate the functional interaction of Tregs with CD1a and characterise CD1a-reactive Tregs in health and psoriasis. Here, a subpopulation of polyclonal Tregs (~2%) was found to secrete the immunosuppressive cytokine IL-10, but not skin inflammation-associated cytokines, in a CD1a-dependent manner. Moreover, CD1a-reactive Tregs were demonstrated to functionally interact with CD1a presenting skin-relevant lipids. *Ex vivo* single-cell sequencing of CD1a-reactive Tregs further revealed that upon CD1a stimulation, CD1a-reactive IL-10-secreting effector/memory Tregs from healthy controls and psoriasis patients downregulate Treg lineage and phenotype markers and shift towards a central/memory phenotype. Moreover, gene expression analysis suggests that CD1a-reactive Tregs may present a subpopulation with impaired suppressive capacity.

The second aim of this study was to investigate the therapeutic potential of butyrate and related fatty acids (FAs) to modulate CD1a-reactive T cell activation *via* alteration of CD1a expression. Here, butyrate and related FAs were demonstrated to partially inhibit expression of group 1 CD1 molecules on monocyte-derived dendritic cells (moDCs) while not affecting general moDC differentiation. CD1a-mediated T cell responses by moDCs were unchanged on treatment with butyrate and related FAs, suggesting that these compounds cannot modulate CD1a expression sufficiently to influence CD1a-mediated T cell responses.

The findings presented in this study demonstrate that Tregs can functionally interact with CD1a and undergo transcriptional and phenotypic re-programming upon CD1a engagement, which in turn may influence skin immunity. While partial modulation of CD1a expression may not be sufficient to alter CD1a-mediated T cell activation, the modulation of CD1a-mediated Treg responses may present a novel therapeutic target for the treatment of skin inflammatory disease.

Acknowledgements

First, I would like to express my deepest gratitude and appreciation to my supervisors Prof Graham Ogg, Prof Tao Dong and Dr Yi-Ling Chen for their continuous support throughout my DPhil. Graham, thank you for always making time for me and for your guidance throughout. Your encouragement and enthusiasm for science was invaluable and made me feel more optimistic and motivated after every meeting. Yi-Ling, I am endlessly appreciative of your scientific and personal support, for your guidance and help with experiments no matter how busy you were, and for being a wonderful supervisor, colleague, and friend.

I would like to thank all present and past members of the lab, especially Dr Koshika Yadava, Dr Jeongmin Woo, Jessica Ng and Janina Nahler. Koshika, thank you for your supervision and guidance at the beginning of my DPhil. I would like to acknowledge Jeongmin for her immense help with the bioinformatics analysis. Thank you Jess, for your help with clinic samples and CD1a production, and for always taking a moment to have a chat. Janina, it has been an absolute pleasure to work alongside you and thank you for always lending a sympathetic ear to me and for your friendship. I would like to extend my thanks to the Churchill Hospital Dermatology Department research nurses and importantly all donors.

I would like to acknowledge Dr Joanna Hester and the TRIG, in particular Dr Amy Cross, for their invaluable advice on how to grow and work with Tregs. Thank you to Dr Mariolina Salio, Prof Sarah Rowland-Jones and Dr Joanna Hester for the scientific discussions during transfer and confirmation committees. To Prof Jim Hughes, thank you for the opportunity to first join the WIMM and for supporting my academic career. I will forever be grateful to the Wellcome Trust for funding me and to IITM and my fellow IITM students for their continuous support over the years.

Special thanks to my amazing friends around the world. To my Heidelberg friends, thank you for always being there, no matter where you currently are. Thank you to my former lab mates and now cherished friends from the Hughes lab – Matt, Caz, Rosa, Steph and Hele – for your love, support, and silliness. To my Lincoln buddy Athena and to Johannes and Jonny, thank you for many fun evenings and great friendships.

To my family, thank you for your unconditional love and support throughout my life. Thank you for believing in me and for supporting me in every way possible. Finally, and above all, I would like to thank my partner Ron. Thank you for your love, thank you for your patience and encouragement, and thank you for your silliness and optimism. I am incredibly lucky to have you in my life.

COVID-19 statement

During the Coronavirus disease 2019 (COVID-19) pandemic, my experimental work was disrupted for several months. I am listing a few of these disruptions here, since experimental work that I would have been able to perform under normal circumstances would have been part of this thesis. Before the university closed its buildings, I had to self-isolate and all running experiments had to be stopped abruptly. Due to university building closures, lab-based work was paused for three months (Mar 2020 - Jun 2020); and since July 2020 safety regulations such as limited workspaces within labs further disrupted lab access. Expanding and working with Tregs is time-consuming and the long generation process meant that only limited experiments were possible within this time. Moreover, I was unable to obtain patient blood samples for almost a year and safety regulations also restricted the access to blood samples from healthy donors. The resulting delay in progress combined with limited access to patient blood samples further meant that single-cell sequencing was performed later than initially hoped. One example of experimental work that I was not able to do due to time constrains is the transduction of identified TCRs into primary Tregs to investigate their functional and therapeutic potential.

Table of Contents

List of Figures

List of Tables

List of Abbreviations

6-PHA	6-phenylhexanoic acid
8-HOA	8-hydroxyoctanoic acid
8-POA	8-phenyloctanoic acid
9-DA	9-decenoic acid
α-GalCer	α-galactosylceramide
AD	Atopic dermatitis
AMPK	Adenosine monophosphate (AMP)-activated protein kinase
AP	Adaptor protein
APC	Antigen-presenting cell
ATP	Adenosine triphosphate
ATRA	All-*trans* retinoic acid
β_2m	β_2-microglobulin
BA	Butyric acid
BDCA	Blood dendritic cell antigen
CAR	Chimeric antigen receptor
CCL	CC-chemokine ligand
CCR	CC-chemokine receptor
CD	Cluster of differentiation
cDC	Conventional DC
cDNA	Complementary deoxyribonucleic acid
CGI	Clinical global impression
CHAPS	3-[(3-cholamidopropyl) dimethylammonio]-1-propanesulfonate hydrate
CHS	Contact hypersensitivity
CITE-seq	Cellular indexing of transcriptomes and epitopes by sequencing
CLA	Cutaneous lymphocyte antigen
CNS	Conserved noncoding sequence
C_t	Cycle threshold
CTLA-4	Cytotoxic T-lymphocyte-associated protein 4
CXCR	C-X-C motif chemokine receptor
d	Day(s)
DC	Dendritic cell
DC-SIGN	Dendritic cell-specific intracellular adhesion molecule-3 grabbing non-integrin
dDC	Dermal DC
DDM	Dideoxymycobactin
DI	Division index
dLN	Draining lymph node
DMSO	Dimethyl sulphoxide
DNA	Deoxyribonucleic acid
ECM	Extracellular matrix
EDTA	Ethylenediaminetetraacetic acid
EGFR	Epidermal growth factor receptor

ELISA	Enzyme-linked immunosorbent assay
ELISpot	Enzyme-linked immune absorbent spot
ER	Endoplasmic reticulum
FA	Fatty acid
FACS	Fluorescence activated cell sorting
FAS	Fatty acid synthase
FBS	Fetal bovine serum
FFA	Free fatty acid
Foxp3	Forkhead box P3
GARP	Glycoprotein A repetitions predominant protein
GATA	GATA binding protein
GEM	Germline-encoded mycolyl-reactive
GITR	Glucocorticoid-induced tumour necrosis factor family-related receptor
GM-CSF	Granulocyte-macrophage colony-stimulating factor
GMM	Glucose monomycolate
GPCR	G-protein-coupled receptor
GvHD	Graft-versus-host disease
h	Hour(s)
HC	Healthy control
HDAC	Histone deacetylase
HDM	House dust mite
HEPES	N-2-hydroxyethylpiperazine-N-2-ethane sulfonic acid
HIV	Human immunodeficiency virus
HLA	Human leukocyte antigen
HPGD	15-Hydroxyprostaglandin dehydrogenase
HRP	Horseradish peroxidase
HTA	Human tissue act
IC50	50% inhibitory concentration
ICOS	Inducible co-stimulatory molecule
IEF	Isoelectric focussing
IFN	Interferon
IgE	Immunoglobulin E
Ii	Invariant chain
IκBa	NFκB inhibitor alpha
IL	Interleukin
IL-10R	IL-10 receptor
IL-36R	IL-36 receptor
IL-36Ra	IL-36R antagonist
ILC	Innate lymphoid cell
iNKT cell	Invariant NKT cell
iNOS	Inducible nitric oxide synthase
IPEX	Immune dysregulation polyendocrinopathy enteropathy X-linked
iTreg	*In vitro*-induced Treg
J region	Joining region

JAK	Janus tyrosine kinase
LAMP	Lysosome-associated membrane protein
LAP	Latency-associated peptide
LAP-TGF-β	Latent TGF-β
LC	Langerhans cell
LCFA	Long-chain fatty acid
LPC	Lysophosphatidylcholine
LRRC	Leucine rich repeat containing protein
LTBP	Latent TGF-β binding protein
LTP	Lipid-transfer protein
M. tuberculosis	*Mycobacterium tuberculosis*
MACS	Magnetic-activated cell sorting
MAPK	Mitogen-activated protein kinase
MCFA	Medium-chain fatty acid
MECP	Methyl CpG binding protein
MFI	Mean fluorescent intensity
MHC	Major histocompatibility complex
min	Minute(s)
miRNA	MicroRNA
moDC	Monocyte-derived dendritic cell
MR1	MHC class I-related protein
mRNA	Messenger RNA
NEAA	Non-essential amino acids
NFκB	Nuclear factor 'kappa-light-chain-enhancer' of activated B-cells
NK cell	Natural killer cell
Nrp	Neuropilin
P. acnes	*Propionibacterium acnes*
PASI	Psoriasis area severity index
PBMC	Peripheral blood mononuclear cell
PBS	Phosphate-buffered saline
PC	Principal component
PCA	Principal component analysis
PCR	Polymerase chain reaction
PD-1	Programmed cell death protein 1
PD-L1	Programmed death-ligand 1
pDC	Plasmacytoid DC
PHA-L	Phytohemagglutinin-L
pI	Isoelectric point
PLA	Phospholipase
PPAR	Peroxisome proliferator-activated receptor
PKC	Protein kinase C
PS	Psoriasis
PSGL-1	P-selectin glycoprotein ligand 1
pTreg	Peripherally-derived Treg

PUFA	Polyunsaturated fatty acid
rh	Recombinant human
RM	Repeated measure
RNA	Ribonucleic acid
ROR	Retinoid-acid receptor-related orphan receptor
RT	Room temperature
RT-qPCR	Reverse transcription quantitative real-time PCR
S. aureus	*Staphylococcus aureus*
S. epidermidis	*Staphylococcus epidermidis*
SATB	Special AT-rich sequence binding protein
SB	Sodium butyrate
SCFA	Short-chain fatty acid
scRNA-seq	Single-cell RNA sequencing
SD	Standard deviation
sec	Second(s)
SM	Sphingomyelin
SNP	Single nucleotide polymorphism
ST	Suppression of tumorigenicity
STAT	Signal transducer and activator of transcription
TCR	T cell receptor
TGF	Transforming growth factor
TGF-βR	TGF-β receptor
Th	T helper
TIGIT	T cell immunoreceptor with Ig and ITIM domains
TIP-DC	TNF- and iNOS-producing DC
TLR	Toll-like receptor
TNF	Tumour necrosis factor
TNFR	TNF receptor
TNFRSF	TNF receptor superfamily
Treg	Regulatory T cell
Treg-DR	Treg-specific DNA hypomethylated region
T_{RM} cell	Tissue resident T cell
TSDR	Treg-specific demethylated region
TSLP	Thymic stromal lymphopoietin
TSO	Template-switch oligo
tTreg	Thymus-derived Treg
TYK2	Tyrosine kinase 2
UCP	Uncoupling protein
UMAP	Uniform manifold approximation and projection
UV	Ultraviolet
V region	Variable region
WNN	Weighted nearest neighbour

Chapter 1 Introduction

1.1 Skin

The skin is a first line of defence against physical and chemical insults, as well as continuous site of exposure to pathogens. It plays a crucial role in thermoregulation, fluid and electrolyte homeostasis, performs metabolic functions and is an important sensory organ.

1.1.1 Immune system of the skin

Many different cell types reside in or can be recruited to the skin to maintain immune homeostasis in health and upon inflammatory challenges (Fig. 1.1).

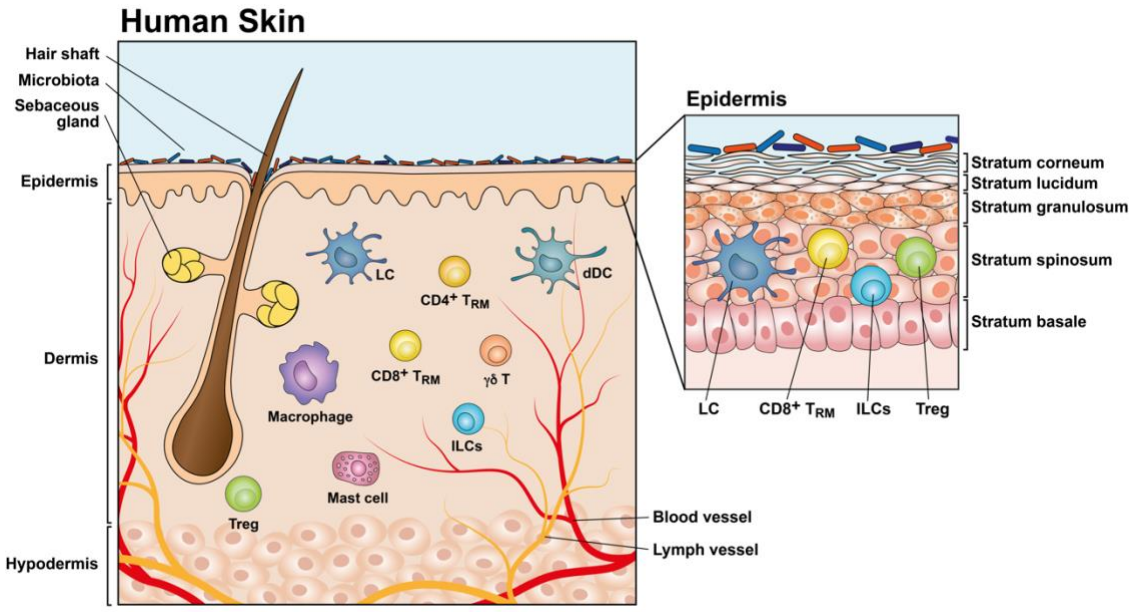

Fig. 1.1 Physical and immunological structure of the skin.
The skin forms a physical and immunological barrier that defends against physical and chemical insults, external pathogens, and allergens. During immune homeostasis, the human epidermis is populated with Langerhans cells (LCs), innate lymphoid cells (ILCs), resident memory $CD8^+$ T cells ($CD8^+$ T_{RM}) and regulatory T cells (Tregs)[1-3]. The dermis is home to a range of innate and adaptive immune cells, including LCs, dermal dendritic cells (dDCs), ILCs, macrophages, mast cells, $CD4^+$ T_{RM}, $CD8^+$ T_{RM}, γδ T cells (γδ T) and Tregs[1-3].

1.1.1.1 Epidermis

Immune cell types residing in the epidermis include Langerhans cells (LCs), innate lymphoid cells (ILCs), non-circulating resident memory $CD8^+$ T cells ($CD8^+$ T_{RM} cells) and regulatory T cells (Tregs). LCs are a subset of professional antigen-presenting cells (APCs) that next to classical major histocompatibility complex (MHC) molecules also express non-classical antigen-presenting molecules, such as CD1a, involved in lipid antigen presentation to T cells[4,5]. CD1a lipid antigen presentation by LCs has further been shown to amplify the inflammatory response in psoriasis and allergic contact dermatitis[6]. Epidermal LCs are located between keratinocytes where they prime $CD8^+$ T_{RM} cell responses and contribute to the maintenance of immune homeostasis *via* activation and induction of proliferation of Tregs[7-9]. During inflammation, activated LCs elongate their dendrites through keratinocyte tight junctions, reaching to the bottom of the stratum corneum, where they survey for external antigens[10]. ILCs are a diverse family of innate immune cells that can be divided into three groups according to cytokine expression and transcriptional profile: ILC1s (ILC1s and natural killer (NK) cells), ILC2s, and ILC3s (ILC3s and lymphoid tissue inducers). They influence adaptive immune responses through cytokine production and direct contact with other immune cells such as T cells and have been implicated in skin barrier sensing. Although cells of all three subgroups can be found in the skin, only ILC2s and ILC3s have been reported in the epidermis specifically[11-13]. Both ILC2s and ILC3s have been shown to contribute to the pathogenesis of skin inflammatory diseases such as AD and psoriasis[13-17]. Moreover, skin ILC2s have been shown to express CD1a and are capable of presenting lipid antigens to CD1a-reactive T cells[14]. At particularly high levels in mice, γδ T cells are also present in the epidermis where they provide an early immune response and have been shown to play a major role in imiquimod-induced psoriasis mouse models[16,18-21]. Although γδ T cells are rare in the human epidermis at steady state, the pro-inflammatory

Vγ9Vδ2$^+$ subset is recruited to the skin during psoriasis and the number of circulating Vγ9Vδ2$^+$ T cells is correlated to disease severity[22]. Next to lymphocytes, also keratinocytes play an important role in skin immune homeostasis. As part of the innate immune system, they produce a variety of cytokines, including interleukin-1 (IL-1) family members, IL-33, thymic stromal lymphopoietin (TSLP), and tumour necrosis factor (TNF), which are essential for immune cell recruitment and the activation of skin-resident immune cells[1,23].

1.1.1.2 Hair follicles and immune privilege

Although the stratum corneum blocks entry and exit of hydrophilic substances, this barrier is interrupted at skin appendages such as hair follicles and sweat glands. Hair follicles constitutively express chemoattractants, such as CC-chemokine receptor 2 (CCR2) and CCR6, that facilitate the recruitment of monocytes, and were suggested as point of entry for LC precursors into the epidermis[24]. In contrast, hair follicles show a paucity of effector T cells and have been classified as a site of immune privilege. The reason for this is still unknown; however, it may be beneficial for discrimination of self- and non-self-antigens in an environment of constant exposure to colonising microorganisms. The lack of effector T cells is a result of several mechanisms, including MHC class I downregulation in follicular keratinocytes, local production of immunosuppressants such as IL-10 and transforming growth factor β1 (TGF-β1), and deletion of autoreactive fatty acid synthase (FAS)-reactive T cells *via* production of FAS ligands[25]. Unlike effector T cells, skin Tregs are mostly localised to the hair follicles. These CD4$^+$ forkhead box P3 (Foxp3)$^+$ Tregs show a memory phenotype and due to lack of CCR7 expression are non-migratory[26]. They have been implicated in preservation of the immune privilege by interacting with hair follicular stem cells and thus maintaining a functional hair cycle[27,28]. Skin Tregs are further involved in wound healing and promote adaptive immune tolerance to commensals[28-30]. In addition to

Tregs, also skin-resident $CD4^+$ and $CD8^+$ T_{RM} cells reside around hair follicles, where they play an important role in long-term skin immunity[31].

1.1.1.3 Skin lipids in immunity

Skin lipids are important in skin immune homeostasis. Lipids released from lamellar granules, such as sphingomyelin, glucosylceramides, and phospholipids, are converted into sphingosine and dihydrosphingosine, which have antimicrobial properties against certain bacterial strains including *Staphylococcus aureus* (*S. aureus*) and *Propionibacterium acnes* (*P. acnes*)[32,33]. Many skin lipids further influence skin immunity through lipid antigen presentation *via* CD1a expressed on LCs and subsets of dermal dendritic cells (DCs). As described in more detail below, CD1a-reactive T cells recognise a variety of endogenous skin lipids including fatty acids (FAs), squalene, triacylglycerol, and wax ester[34]. Thus, changes in skin lipid profiles, as seen in several skin inflammatory diseases[35,36], may affect CD1a-mediated immune responses. Additionally, sebum produced by sebocytes residing in sebaceous glands is rich in relevant lipids such as wax esters, triacylglycerol and squalene[37]. It is thought to serve as lipid seal for the hair follicles to prevent entry of microbes into deeper skin layers. Moreover, skin commensal bacteria can process sebum lipids to free fatty acids (FFAs) which in turn induce defensin expression by sebocytes[38,39].

1.1.1.4 Skin microbiota

The skin is home to numerous microorganisms, termed the microbiota, that can influence cutaneous immunity[40,41]. It is unknown how the cutaneous immune system discriminates between commensal and pathogenic microorganisms, but there is emerging evidence that non-classical MHC molecules can play a role[42,43]. One major population of skin commensal bacteria is *Staphylococcus epidermidis (S. epidermidis)*. It inhibits inflammatory cytokine release by secreting lipoteichoic acid that selectively acts on keratinocytes *via* the Toll-like

receptor 3 (TLR3)[44]. *S. epidermidis* is also captured by dermal APCs and bacterial antigens are presented by non-classical MHC class I molecules in the draining lymph nodes. This leads to the recruitment of *S. epidermidis*-specific $CD8^+$ T cells, expressing IL-17A or interferon-γ (IFNγ), to the skin and in turn promotes keratinocyte proliferation and wound healing[42,45]. The colonisation of the skin is not only essential for protective immunity, for example against the parasite *Leishmania major*[46], but it is also becoming increasingly evident that alterations in the skin microbiota are associated with skin inflammatory disease. *S. aureus* is a common cause of skin infections and is frequently found on the skin of patients with atopic dermatitis (AD)[47]. *S. aureus* releases γ-toxin which activates mast cells and thereby promotes innate and adaptive T helper cell type 2 (Th2) immune responses[48].

1.1.1.5 Dermis

Recruitment of immune cells and their precursors to the dermis is facilitated by the extracellular matrix (ECM) and a network of blood vessels[49]. The dermis houses several types of innate immune cells, including dermal DCs, ILCs, macrophages, mast cells and γδ T cells[12-14,50-56]. In addition, $CD4^+$ and $CD8^+$ T cells survey the dermis for pathogens[50]. Upon antigen capture, dermal DCs migrate through the lymphatics to the draining lymph nodes[57]. During cutaneous inflammation, inducible skin-associated lymphoid tissues (iSALT) consisting of DCs, T cells, and perivascular macrophages form around postcapillary venules. These clusters are important sites of antigen presentation and essential for the induction of adaptive immune responses[58]. As effector T cells do not require co-stimulatory molecules for activation[59], also cells other than DCs and LCs can act as cutaneous APCs in pathological conditions. For example, in a model of T cell-induced skin inflammation, mast cells have been shown to acquire MHC class II molecules from DCs[60]. The neuronal network in the dermis further communicates with resident immune cells such

as dermal DCs, many of which are located close to neurons[61,62]. These neuro-immune interactions also play a role in skin inflammatory diseases. In an imiquimod-induced mouse model of psoriasis, IL-23 production by dermal DCs, which resulted in skin inflammation *via* IL-17A production by γδ T cells, was significantly suppressed upon pharmacological ablation of transient receptor potential subfamily V member 1 (TRPV1)-expressing sensory nerves[62].

1.2 Lipid antigen presentation and CD1a

Antigen presentation is crucial for the induction of an effective adaptive immune response[63]. Peptide antigens are presented by highly polymorphic 'classical' MHC molecules, which modulate immune responses by direct interaction with the T cell receptor (TCR) of 'conventional' T cells. MHC molecules are encoded in the MHC region on chromosome 6 of the human genome. While MHC class II molecules consist of two homogenous transmembrane proteins, α and β chain, MHC class I molecules are composed of a larger transmembrane α chain which is associated with β_2-microglobulin (β_2m). Due to their high polymorphism, both MHC class I and class II molecules can present a large variety of peptides. In addition to these 'classical' MHC molecules, also less polymorphic 'non-classical' MHC class Ib molecules present peptide and non-peptide antigens to T cells. While some of these non-classical antigen-presenting molecules are encoded in the MHC region, others are encoded on different chromosomal regions. Non-classical antigen-presenting molecules, such as CD1 and MHC class I-related protein (MR1), play an important role in immune responses to infection, inflammation, and other diseases[64].

1.2.1 CD1 family

CD1 proteins are a family of non-classical antigen-presenting molecules involved in lipid antigen presentation to T cells[4,5]. The human CD1 family is encoded on chromosome 1 and consists of 5 isotypes (CD1a-e). Based on sequence homology, expression pattern and function, they can be divided into three groups: group 1 is comprised of CD1a, CD1b and CD1c, group 2 of CD1d, and group 3 of CD1e. Group 1 and group 2 CD1 proteins are expressed on the cell surface and can bind and present lipid antigens to T cells[5]. Group 1 CD1 molecules are predominantly expressed by specific antigen-presenting cells, including DCs and LCs, and thymocytes[65,66]. CD1d is expressed on most cells of haematopoietic

lineage, hepatocytes, epithelial cells, keratinocytes, and activated T cells[65-67]. In contrast, CD1e is expressed in the endosomal compartment where it plays a role in lipid antigen processing and CD1 loading[68,69].

On a transcriptional level, CD1a, CD1b, CD1c and CD1d are regulated differentially. While all group 1 CD1 proteins can be induced during *in vitro* differentiation of monocytes using granulocyte-macrophage colony-stimulating factor (GM-CSF), upon maturation CD1a is down- and CD1b and CD1c are upregulated[70,71]. CD1d expression in DCs is controlled by peroxisome proliferator-activated receptor γ (PPARγ) *via* triggering the synthesis of retinoic acid[72-76]. Some evidence points towards PPARγ activation also playing a role in group 1 CD1 transcriptional regulation[72-75]. However, also mycobacterial cell wall lipids can differentially induce group 1, but not group 2, CD1 protein expression *via* TLR2[77,78]. Moreover, inhibition of histone deacetylase (HDAC) can block CD1a acquisition during *in vitro* monocyte-derived DC (moDC) differentiation and partially upregulate CD1d expression[79,80]. Therefore, the exact mechanisms of CD1 transcriptional regulation remain elusive. Interestingly, several pathogens have been shown to modulate CD1 expression, thereby potentially mediating immune evasion. One example is human immunodeficiency virus (HIV) that downregulates CD1d and CD1a, while only marginally affecting CD1c expression[81-84].

Structurally, CD1 molecules show similarities to MHC class I proteins and are non-covalently linked to β_2m. However, unlike MHC class I and class II, CD1 exhibits low levels of polymorphism. The antigen binding cleft of CD1 is structurally related to MHC class I, with two α-helices and a β-sheet floor. CD1 binding clefts are composed of two major channels, A' and F', which are deeper, narrower, and more hydrophobic compared to MHC binding grooves[4,85]. Diverse structural differences and additional features in the

antigen-binding clefts of the different CD1 molecules (see Fig. 1.2) allows the binding and presentation of a broad variety of lipid antigens despite minimal genomic polymorphism[86-89].

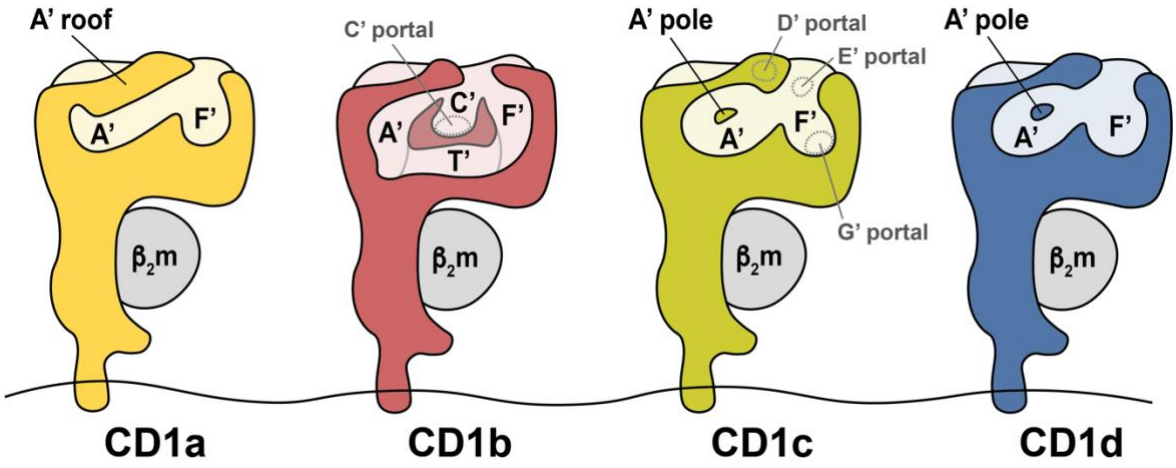

Fig. 1.2 CD1 antigen binding cleft architecture.
CD1 antigen binding clefts are composed of two major channels (A' and F'), with CD1b having two additional pockets (C' and T'). Moreover, some CD1 proteins contain accessory portals through which antigens can protrude from the binding clefts. Adapted from Current Opinion in Immunology, Vol. 46, Moody *et al.*, Four Pathways of CD1 Antigen Presentation to T cells, page no. 127-133, Copyright (2017) with permission from Elsevier[90].

1.2.1.1 CD1 lipid antigen presentation

Distinct intracellular trafficking patterns of the different CD1 isoforms defines compartments of antigen sampling and loading and thereby influence the variety of lipid species loaded. CD1 molecules are synthesised in the lumen of the endoplasmic reticulum (ER), where they capture endogenous ER-resident lipids, and traffic to the cell surface *via* the secretory pathway[4,91-93]. Before reinternalization into the endo-lysosomal compartment, CD1 molecules, particularly CD1a, can capture exogenous lipids at the cell surface[4,90,94]. The pattern of intracellular trafficking varies between the isoforms. The cytoplasmic tails of CD1b, CD1c and CD1d contain tyrosine-containing motifs that mediate binding to adaptor

protein (AP) complexes and trafficking to early and late endosomal compartments, which is essential for antigen presentation[4,90,95,96]. CD1c and CD1d are distributed throughout the early and late endosomal compartment, while CD1b is targeted to late-endosomal/lysosomal vesicles and co-localises with lysosome-associated membrane protein-1 (LAMP-1)[4,90,97]. Whereas CD1b antigen presentation is dependent on endosomal acidification, and CD1d antigen capture is less efficient when endosomal targeting is disrupted, CD1a and CD1c antigen presentation seem independent of acidification[97-100]. The low pH in the late endosome and lysosome (pH 4.5-5.5) facilitates antigen capture in multiple ways: it aids the binding of lipids with long alkyl chains, promotes lipid binding by relaxing the conformation of the CD1b-β_2m complex, and affects the stability of CD1d-lipid complexes, thus assisting lipid displacement[101-103]. In contrast to the other isoforms, CD1a associates with invariant chain (Ii) at the cell surface within lipid rafts and is internalised to the early/sorting and early/recycling endosomes[104,105]. The distribution of the different CD1 molecules within distinct intracellular sites allows the sampling of antigens in various compartments. Lipids antigens harbouring short or unsaturated alkyl chains get delivered to endocytic recycling compartments, whereas lipid antigens with long saturated alkyl chains traffic to late endocytic compartments[106]. Lipid processing and loading within the endo-lysosomal compartment is facilitated by a number of proteins, including lipid processing proteins such as glycosidases, lipid-transfer proteins (LTPs) such as saposins, and CD1e[107-109]. CD1e accumulates in the Golgi and the endosomal compartment in immature DCs and mainly in the lysosome in mature DCs[110]. It is cleaved into a soluble form that is involved in editing and processing of large complex glycolipids for loading onto CD1b and has further been proposed to extract self-lipids from the endosomal membrane, enabling their processing and presentation[109].

The variety of lipids that can be bound and presented by CD1 molecules is broadened even further by the use of short FAs or hydrophobic lipids as spacer or scaffold lipids. These lipids stabilise the CD1 protein structure and enable presentation of lipids smaller than the CD1b and CD1c binding grooves by helping in meeting the energy requirements for expelling water from the binding clefts[111].

In accordance with antigen cleft structure and size, as well as intracellular localisation, the different CD1 isoforms bind to and present a diverse range of endogenous and exogenous lipid antigens[5,64]. The main groups of self-lipid antigens are glycosphingolipids such as sulfatides[112,113] and phosphoglycerolipids including phosphatidylcholine, sphingomyelin and gangliosides[34,81,114-120]. While sulfatides and phosphatidylcholine bind to all group 1 and 2 CD1 molecules, sphingomyelin binds to CD1a, CD1c and CD1d, and gangliosides bind to CD1a, CD1b and CD1d. CD1a has further been shown to bind highly hydrophobic headless antigens such as short FAs, squalene, and wax esters[34]. In addition to self-antigens, all group 1 CD1 molecules can present mycobacterial antigens. CD1a has been shown to bind and present dideoxymycobactin (DDM) antigens from *Mycobacterium tuberculosis (M. tuberculosis)*[121,122], whereas CD1b presents mycolyl lipid antigens, such as mycolic acid, glucose- and glycerol-monomycolates from *Mycobacterium* and other bacterial species[123-125], and CD1c can bind lipids derived from the cell wall of several *Mycobacterium* species[126]. In contrast, CD1d can present glycosphingolipids, such as α-galactosylceramide (α-GalCer), produced by commensal or ubiquitous bacteria, and fungi[127-129].

1.2.1.2 Models for CD1 antigen presentation

Similar to the TCR-peptide-MHC model, the classical model of CD1-antigen recognition is based on head group discrimination. The antigen alkyl chain lies within the CD1 binding cleft, while the headgroup, such as phosphate or peptide, protrudes above the cleft surface

where it interacts with the TCR. High specificity is achieved through TCR contact with both antigen and CD1. This model has been shown to hold true for CD1b and CD1d antigen recognition[130,131].

A second model, termed CD1 remodelling model, was proposed due to structural reorganisation upon antigen binding seen in CD1c[132]. Ligand binding creates new contacts within the CD1c protein that result in the formation of a roof over the F' pocket and a new G' portal that opens to the right side of the F' pocket. Recently, also CD1a has been shown to undergo lipid-mediated molecular rearrangement that negatively impacted binding of the TCR to the A' roof[133,134]. While CD1 remodelling may serve to modify TCR binding epitopes, it does not exclude that the TCR may also directly interact with the antigen[90].

A third model termed 'absence of interference' emerged after the first CD1a-lipid-TCR structure was solved[133]. While autoreactive TCRs can bind to the CD1a A' roof without contact to the loaded lipid, lipid antigens with large headgroups block this TCR-CD1a interaction. Therefore, small lipids that lack head groups and do not protrude from the cleft do not interfere with the binding of the TCR to the CD1a A' roof and provide 'absence of interference'. This model explains the presentation of a large variety of structurally diverse CD1a-presented autoantigens that lack hydrophilic head groups, including squalene and FFAs[34]. Unlike symmetrical positioning of peptides on MHC proteins, TCRs binding to CD1a are positioned to the left side of CD1a allowing ligands to emerge from the F' portal on the right side of the roof[90]. Moreover, mutations of the outer surface of the CD1a A' roof were shown to block CD1a-mediated T cell responses, supporting TCR specificity to CD1a itself rather than carried antigens[135]. Similarly, CD1c has been shown to present a variety of permissive ligands, indicating that T cell autoreactivity may also be directed towards CD1c itself[117]. In contrast to models in which CD1 or MHC antigen binding initiates T cell

modulation, these data suggest an antigen-regulated "on until off" mode of regulation for CD1a and CD1c[136].

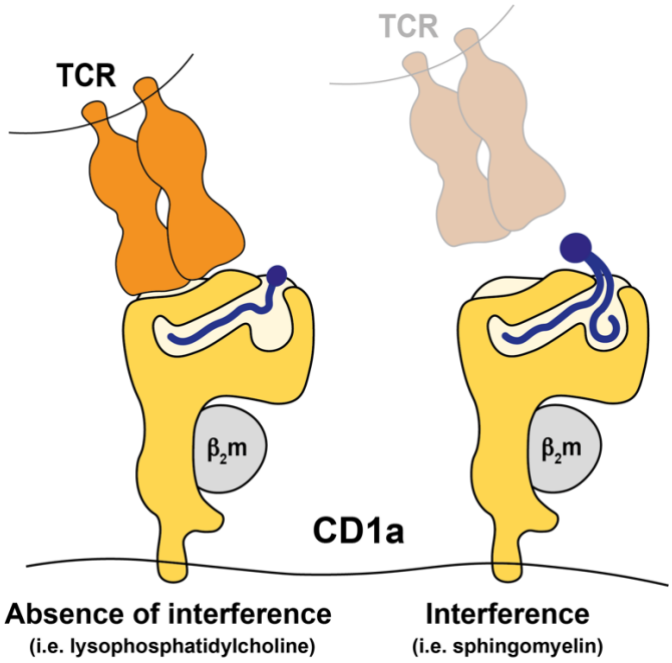

Fig. 1.3 Absence of interference model.

Autoreactive TCRs interact with the CD1a A' roof, without interacting with the ligand bound to CD1a. While some ligands (i.e. lysophosphatidylcholine) do not interfere with TCR binding to the A' roof and therefore provide 'absence of interference', other ligands (i.e. sphingomyelin 24:1) interfere with TCR binding, either by steric interference or *via* remodelling of the A' roof[133,135]. Adapted from *Current Opinion in Immunology,* Vol. 46, Moody *et al*., Four Pathways of CD1 Antigen Presentation to T cells, page no. 127-133, Copyright (2017) with permission from Elsevier[90].

1.2.1.3 CD1-reactive T cells

CD1-reactive T cells form a bridge between the innate and adaptive immune response. They are composed of a variety of αβ and γδ T cells that respond to many different self and foreign lipids presented by CD1 molecules[66,71,123,137-139]. While most group 1 CD1-reactive T cells express polyclonal TCRs, the majority of group 2 CD1-reactive T cells have a semi-invariant TCR[140].

CD1d-reactive T cells are termed natural killer T cells (NKT cells) as they express T cell and NK cell markers. They can be divided into type I cells, also called invariant NKT cells (iNKT) that express a semi-invariant TCR (Vα24-Jα18 and Vβ11), and type II NKT cells that express polyclonal TCRs[140-142]. iNKT cells are classed as innate-like cells as they can respond to innate signals without TCR engagement and release vast amounts of cytokines upon stimulation[143,144]. Activation of iNKT cells further initiates cross talk with other immune cells, including DCs, NK cells and B cells, thus promoting adaptive T cell and antibody responses, and bridging innate and adaptive immunity[145-148]. NKT cells have numerous important immune-regulatory roles in protection from infection, tumour immunosurveillance and autoimmunity[64]. However, a pathogenic role has been suggested in ulcerative colitis, where lyso-sulfatide-reactive CD1d-reactive type II NKT cells show cytotoxic activity against the intestinal epithelium, thus exacerbating disease[149].

In contrast to iNKT cells, T cells reactive to CD1a, CD1b and CD1c show adaptive-like phenotypes. Generally, these T cells express a polyclonal TCR repertoire and display Th0-, Th1-, Th2-, or Th17-like phenotypes[64,150-152]. Amongst CD1b-reactive T cells, a semi-invariant population has been identified by tetramer staining with glucose monomycolate (GMM)-loaded CD1b. These germline-encoded mycolyl-reactive (GEM) T cells are rarely detected in healthy individuals but are frequently found in genetically unrelated patients with tuberculosis[153,154]. While CD1b-autoreactive T cells are only found at low frequency in peripheral blood of healthy individuals, CD1a- and CD1c-autoreactive T cells are much more prevalent[151]. Similar to CD1b-reactive T cells, CD1c-reactive T cells expand during mycobacterial infection[155,156]. In addition, DDM-responsive CD1a-reactive T cells can be detected in blood of tuberculosis patients[157]. A protective role for CD1a-reactive T cells in tuberculosis is supported by increased susceptibility to disease in the presence of a single nucleotide polymorphism (SNP) in the CD1a gene that causes CD1a

deficiency[158,159]. In addition to mediating immune responses to infections, CD1c-reactive T cells have further been shown to respond to self-lipid antigens that accumulate in leukaemia cells and data from a mouse model suggests that these lipid-specific T cells may have a protective phenotype[152]. CD1a-autoreactive T cells have been suggested to play a crucial role in maintaining cutaneous immune homeostasis and are further involved in allergic reactions and skin inflammatory diseases (see 2.1.1 CD1a-reactive T cells).

1.2.2 CD1a structure and function

CD1a is predominantly expressed on LCs, subsets of dermal DCs and thymocytes, and is inducible on ILC2s[14,160]. Peripheral mature T cells do not express CD1a[161], however, polyclonal $CD1a^+$ T cells have been detected in Langerhans Cell Histiocytosis lesions[162]. The intensity of cellular CD1a expression, unlike CD1b and CD1c, is highly variable among healthy individuals[159]. Several SNPs in the CD1a gene have been reported, some of which influence protein expression and lead to CD1a deficiency[157,159]. Moreover, CD1a-deficient DCs are unable to present the mycobacterial lipopeptide DDM to CD1a-reactive T cells and one of the SNPs causing CD1a-deficiency (rs411089) has been associated with susceptibility to tuberculosis[158,159]. It has further been proposed that this genetically regulated mechanism for CD1a-mediated lipid antigen presentation may allow differences of CD1a expression on a population level despite limited structural variation within CD1a[159].

In contrast to other CD1 isoforms, CD1a lacks a tyrosine-based cytoplasmic motif, resulting in localisation on the cell surface and in the early endocytic recycling compartment, where it loads lipid antigens at neutral pH[97,163]. The CD1a antigen-binding cleft is the smallest of the CD1 isoforms[4,88]. The A' pocket is narrow with a fixed end and due to this constriction has been proposed to act as a 'molecular ruler'. It can only accommodate relatively short alkyl chains of 18 to 23 carbons (C_{18}-C_{23}). In contrast, the F' pocket is wider and can

accommodate alkyl chains as well as peptide fragments. In total, the CD1a binding cleft is thought to have a capacity of C_{32}-C_{42}, as longer lipid chains may not be efficiently bound and buried within the cleft[89,164]. This limited capacity paired with enhanced accessibility compared to other CD1 isoforms may allow CD1a to more readily load antigens at the cell surface and in the secretory pathway without the requirement for an acidic pH[89]. CD1a has been shown to bind and present endogneous as well as exogenous lipid antigens to CD1a-reactive T cells (see 1.2.2.1 CD1a lipid antigens), and recognition of CD1a-presented lipid antigens by TCRs occurs *via* binding of the TCR to the CD1a A' roof (see 1.2.1.2 Models for CD1 antigen presentation).

1.2.2.1 CD1a lipid antigens

Although CD1a has the smallest antigen-binding cleft of all CD1 isoforms, it can accommodate a wide range of endogenous and exogenous lipid antigens[88,165]. Most prominent among CD1a self-lipids are headless antigens which have been shown to stimulate CD1a-autoreactive T cell responses by 'absence of interference' *via* TCR binding to the CD1a A' roof. This group of permissive CD1a lipid antigens includes many natural skin oils such as FAs, triacylglyceride, wax esters and squalene[34]. In contrast to these activating self-ligands, several sphingolipids, including sulfatide and longer sphingomyelins, have been identified as non-permissive self-ligands that disrupt CD1a-TCR interaction[133]. Self-lipid antigens further play a role in allergic reactions. House dust mite (HDM)- as well as bee and wasp venom-derived phospholipase A2 (PLA_2) generates neo-lipid antigens, such as FFAs and lysophospholipids, that induce CD1a-mediated immune responses[166-168]. Only few exogenous lipid antigens binding to CD1a have been defined. The first foreign lipopeptide antigen to be identified was DDM produced by *M. tuberculosis*[121]. In addition, plant pollen-derived phosphatidylcholine and

phosphatidylethanolamine, and poison ivy-derived urushiol have been described as CD1a antigens[6,169].

1.2.2.2 CD1a presentation of skin lipid antigens

The skin surface is covered by lipids derived from sebocytes and keratinocytes, including triglycerides, wax esters, cholesterol and squalene. Triglycerides and phospholipids are further processed by endogenous enzymes, skin-resident commensal bacteria and fungi to produce FFAs. In the stratum corneum, the extracellular lipid matrix comprises phospholipids, cholesterol and its esters, glycosyl-ceramides, and sphingomyelin[37-39]. Cutaneous immune responses are largely dependent on antigen presentation by skin-resident DCs, which next to MHC also express CD1 molecules including CD1a[170,171]. CD1a has been shown to present natural skin oils, glycolipids, and phospholipids, thereby modulating CD1a-reactive T cell responses[34,134]. Although CD1 molecules can capture bacteria-derived lipid antigens and promote skin immune homeostasis, they are also implicated in skin diseases[165,172,173]. In skin inflammatory disease, changes in lipid profiles are commonly observed[35,36] and CD1a-antigen presentation has been shown to exacerbate disease[6,167,174]. These findings highlight the importance of lipid antigen presentation in the skin in health and disease and emphasize the therapeutic potential of modulating immune responses driven by CD1a lipid antigen presentation.

1.2.3 CD1a in skin inflammatory disease

The skin and mucosal barriers are the first line of defence against pathogenic microbes while at the same time harbouring commensal bacteria that contribute to immune homeostasis[175]. Bacteria are not only abundant in lipid-rich areas of the skin but also dynamically affect the local lipid profile[176]. In the skin, lipids play an important role in maintaining barrier integrity, but when barrier function is compromised, these lipids can pass into underlying layers. One

of the main immune sentinels in the skin and the mucosal epithelium are CD1a-expressing DCs and LCs, and thus CD1a-mediated immune responses play an important role in skin homeostasis and skin inflammatory diseases. In inflammatory skin diseases such as psoriasis and AD, CD1a-expressing DC subsets are increased and LC migration is reduced[177-179]. Moreover, $CD1a^+$ DCs co-expressing blood dendritic cell antigen 2 (BDCA-2) and CD123 have been shown to infiltrate the skin during acute sterile skin inflammation[180].

In the context of psoriasis, changes in skin microbiota and lipid profile contribute to inflammation[176,181-184] and CD1a increases model psoriasis-like inflammation *via* CD1a-reactive inflammatory T cells[6,174]. Aggravation of psoriasis can be mediated by self-lipids generated from mast cell-derived PLA_2. Mast cells from patients with psoriasis release high levels of PLA_2 and PLA_2-generated neolipids have been shown to activate CD1a-reactive T cells to produce IL-22 and IL-17A[174]. A study in CD1a-transgenic mice further showed strong activation of CD1a-mediated immune responses in skin inflammation triggered by poison-ivy derived urushiol[6]. Most patients with AD show elevated levels of serum immunoglobulin E (IgE), which recognises environmental allergens such as HDM allergens[185]. Similar to psoriasis, CD1a-reactive T cells responsive to neolipid antigens generated by HDM-derived PLA_2 are elevated in patients with AD[167]. Interestingly, the skin barrier protein filaggrin is deleted in a large population of AD patients[186]. Filaggrin inhibits PLA_2 activity and is thought to play a protective role against CD1a-mediated T cell activation[167]. In both diseases, CD1a-reactive T cells show an inflammatory phenotype, secreting cytokines such as IFNγ, GM-CSF, IL-13 and IL-17A, thereby contributing to disease phenotype[6,167,174]. In psoriasis, CD1a-reactive T cells can also secrete IL-22[6,174]. While IL-22 is important for wound healing and skin immune homeostasis, in the context of psoriasis it mediates inflammation and keratinocyte hyperplasia[187]. Moreover,

CD1a-reactive T cells have been shown to respond to CD1a-loaded contact dermatitis allergens, implicating CD1a-mediated immune responses in skin hypersensitivity[188].

In addition to dermal DCs and LCs, also ILC2s in the skin can express CD1a and present lipid antigens to CD1a-autoreactive T cells[14]. *In vitro* assays showed that CD1a expression in ILC2s is upregulated by TSLP at levels comparable to those observed in the skin of AD patients, and that subsequent CD1a-mediated T cell responses were dependent on PLA_2. Moreover, ILC2s can exploit this pathway to promote skin inflammation during *S. aureus* infection, which is known to exacerbate AD in a TLR-dependent manner[14,189]. This study not only gives insight into *S. aureus*-induced AD, but also defines a role for ILC2s in lipid surveillance and skin immunity.

1.2.4 CD1 therapeutics

The high genetic diversity of classical MHC-encoded antigen-presenting molecules presents a considerable obstacle for the development of MHC-peptide-based immunomodulatory therapies. In contrast, the low polymorphism of CD1 offers the possibility for the discovery and design of broadly acting immunomodulatory antigens[190]. Modulation of CD1-mediated immune responses *via* lipid antigens, many of which are bioavailable, may present a novel therapeutic approach. While showing limited therapeutic success in small-scale cancer and vaccine trials, glycolipid antigens have been shown to consistently activate NKT cell responses in patients of different genetic backgrounds[191-195]. Moreover, mycobacterial lipid antigens have been investigated for treatment of tuberculosis. In a transgenic mouse model expressing CD1 and a CD1b-reactive mycolic acid-specific TCR (DN1), *M. tuberculosis* challenge resulted in DN1 T cells localising in lung granulomas and partially protecting from infection[196]. Further, immunisation of guinea pigs (which express homologs of human CD1a, CD1b and CD1c) with lipids including mycolic acid, diacylated sulfoglycolipids and

phosphatidylinositol dimannosides reduced lung inflammation and bacterial burden upon challenge[197,198]. Lipid antigen vaccination did not protect as efficiently as the current tuberculosis vaccine, but it is not known whether the current whole cell vaccine contains antigenic lipids and thus may elicit lipid-specific CD1-mediated immune responses.

Several factors need to be taken into consideration for the design of new immunomodulatory drugs or vaccines based on antigenic lipids. Firstly, differential interaction of TCRs with different CD1 molecules may allow targeting of specific CD1 and T cell populations[190]. CD1-TCR interactions depending on 'absence of interference' could be broadly interrupted using large lipids or lipids with polar head groups, while those depending on CD1 remodelling may be modified with small lipid agonists lacking head groups that are readily loaded into the binding cleft. Further, modulation of CD1-mediated T cell responses by chemically modifying antigen head groups has been shown to alter the immunological properties of α-GalCer variants[192]. Secondly, possible modes of lipid antigen delivery differ between CD1 molecules, depending on their cellular and anatomical location. One example is the use of cell type-specific markers for targeted antigen delivery. Liposomes coated with a sialic acid analogue targeting Siglec-7 were shown to deliver the mycobacterial antigen GMM to moDCs *in vitro* and induce GMM-mediated CD1b-reactive T cell activation[199]. Another example is the formulation of lipid antigens into skin creams for the treatment of skin diseases[190]. Contact dermatitis allergens have been shown to bind to CD1a and induce CD1a-mediated T cell responses *in vitro*[200]. CD1a is highly expressed in the skin and CD1a-mediated immune responses are implicated in skin inflammatory diseases[14,167,170,171,174], highlighting the potential of topical treatments to modulate CD1a-mediated immune responses. Lastly, biochemical pathways that generate antigenic self-lipids and the regulation of CD1 expression may present additional therapeutic targets. Short-chain fatty acids (SCFAs) are produced by many commensal and pathogenic bacteria

and the SCFA butyrate has been shown to modulate CD1 expression in moDCs[201-203]. Modulation of CD1-mediated immune responses *via* regulation of CD1 expression may therefore have great therapeutic potential.

1.3 Regulatory T cells

$CD4^+$ Tregs expressing CD25 (IL2 receptor α chain) and Foxp3 are a subpopulation of T lymphocytes responsible for suppressing immune responses and preserving immune homeostasis[204]. The transcription factor Foxp3 is an essential regulator of Treg development, maintenance and function, and the absence of Foxp3-expressing Tregs results in the development of severe autoimmunity[205-207].

Based on origin, natural Foxp3-expressing Tregs can be divided into thymus-derived Tregs (tTregs), which develop from $CD4^+$ T cell precursors following intermediate TCR reactivity against self-antigens[208,209], and peripherally-derived Tregs (pTregs), which differentiate from naïve $CD4^+$ T cells following TCR recognition of antigens thought to be non-self[208-210]. Stable maintenance of Treg-specific gene expression is highly dependent on epigenetic mechanisms, especially deoxyribonucleic acid (DNA) methylation/demethylation[211-214]. Natural Tregs possess Treg-specific hypomethylated regions, one of which is the Treg-specific demethylated region (TSDR) located in the conserved noncoding sequence 2 (CNS2) within the *Foxp3* gene. Treg-specific hypomethylation is also found in several other important Treg signature genes, such as *Il2ra* (*Cd25*), *Ctla4* and *Ikzf2* (encoding *Helios)*. Collectively, these regions are termed Treg-specific DNA hypomethylated regions (Treg-DRs)[211-213]. Only a few studies have distinguished between tTregs and pTregs. While murine studies show that CNS1 in the *Foxp3* locus, containing a TGF-β/Smad response element, is crucial for pTreg, but not tTreg, development[215-217], several studies suggest that pTregs can acquire demethylation of Treg-DRs similar to tTregs[212,214,218]. tTregs can be distinguished from pTregs by expression of the transcription factor Helios[219] and the membrane protein neuropilin-1 (Nrp1)[220,221]. However, in certain circumstances, these markers can also be expressed by pTregs and thus are not perfect markers[222-225]. Foxp3 is

important for development and maintenance of Tregs, and in combination with expression of CD4 and CD25 and lack of CD127 expression, serves as a reliable Treg marker. However, it is important to note that Foxp3 is not exclusively expressed by Tregs and can be upregulated in activated effector T cells. This upregulation is usually transient and at lower levels, and expression does not seem to confer significant suppressive capacity[226]. Moreover, a number of other intracellular and surface markers are associated with Tregs, including cytotoxic T-lymphocyte-associated protein 4 (CTLA-4)[227,228] and glucocorticoid-induced tumour necrosis factor family-related receptor (GITR)[229]. In addition to natural Tregs, Tregs can be induced *in vitro* from naïve $CD4^+$ T cells using IL-2 and TGF-β[211,230]. Although these *in vitro*-induced Tregs (iTregs) show phenotypical similarities to natural Tregs, they differ in their epigenetic signature for example. iTregs do not possess stable TSDR demethylation and thus show unstable Foxp3 expression and lineage instability[212,214].

Under normal physiological conditions, $Foxp3^+$ Tregs, and in particular effector-type Tregs, are in a highly proliferative state, which is thought to result from continuous recognition of self- and commensal antigens[231,232]. Although TCR activation is required for Tregs to exert inhibitory functions, once activated they can suppress in antigen-nonspecific ways[233]. During immune homeostasis, Tregs control the activation of effector T cells and are responsible for maintenance of self-tolerance[204]. They further play an important role in the suppression of aberrant responses to microbial and environmental antigens[234,235]. Treg anomalies have been shown to cause various immunological diseases such as autoimmune disease and allergy[236,237]. Moreover, Tregs play a role in many other processes and diseases, including tissue regeneration, foetal-maternal tolerance, immunometabolic diseases, and degenerative diseases with inflammatory elements like atherosclerosis[238-241]. The role of $Foxp3^+$ Tregs is further highlighted by the severe autoimmune/inflammatory disease caused

by loss-of-function mutations in the *Foxp3* gene. Foxp3-mutant scurfy mice spontaneously develop fatal systemic autoimmune/inflammatory disease[242]. Similarly, humans with deficient or dysfunctional Tregs due to Foxp3 mutations develop immune dysregulation polyendocrinopathy enteropathy X-linked (IPEX) syndrome, which is characterised by several severe autoimmune and inflammatory diseases such as type 1 diabetes, allergy, inflammatory bowel disease and thyroiditis[243,244]. Further, deficiency of CD25, CTLA-4, or IL-2 have been shown to cause severe autoimmune/inflammatory diseases with phenotypes similar to scurfy disease, suggesting that these molecules are crucial for Treg suppressive function[245,246].

1.3.1 Mechanisms of suppression

Tregs can mediate their suppressive function though many different cell-cell contact-dependent and humoral factor-mediated mechanisms[247,248]. One mechanism of cell-cell contact-dependent suppression by Tregs is direct cytotoxic action (i.e. against NK cells and cytotoxic T lymphocytes) *via* granzyme B and perforin release[249,250]. Tregs can further exert their suppressive function by delivering negative signals to responder T cells. This includes interaction of CTLA-4 with CD80 and CD86 expressed on T cells[251] and the generation of pericellular anti-inflammatory adenosine *via* the ectonucleotidases CD39 and CD73 expressed on Tregs[252]. In addition to acting directly on effector T cells, Tregs can also modulate APC function. CTLA-4 expressed by Tregs competes with CD28 for binding to CD80/CD86 and can downregulate CD80/CD86 expression on APCs such as DCs, thereby reducing CD28-mediated co-stimulatory signals for responder T cells[253-255]. It has further been proposed that CTLA-4 expressed by Tregs can also deplete these molecules from the cell surface of APCs *via* trans-endocytosis[256].

One of the main cell-cell contact-independent mechanisms of Treg suppression is the generation and secretion of suppressive cytokines, such as IL-10, TGF-β and IL-35[248] (detailed description of the roles of IL-10 and TGF-β in sections 1.3.1.1 IL-10 and 1.3.1.2 TGF-β). Tregs have further been shown to mediate suppression *via* IL-2 deprivation. Tregs rarely produce IL-2 as the *Il2* gene is suppressed by Foxp3 and therefore Tregs are highly dependent on exogenous IL-2[257,258]. Due to constitutive expression of the high-affinity IL-2 receptor (CD25), Tregs bind high amounts of IL-2. This depletion of IL-2 from the surrounding environment contributes to suppression of differentiation and expansion of different cell types such as effector T cells and NK cells[259,260]. In addition, the production of IL-2 by activated T cells further stabilises Foxp3 expression and thus through a negative-feedback mechanism enhances Treg suppression[207].

1.3.1.1 IL-10

IL-10 is an anti-inflammatory immunosuppressive cytokine that is secreted by a variety of innate and adaptive immune cells, such as T cells (including Tregs), B cells, mast cells, macrophages and DCs[261,262]. It is secreted as a homodimer that binds to and signals through a receptor complex consisting of two IL-10 receptor 1 (IL-10R1) and two IL-10R2 chains *via* Janus tyrosine kinase (JAK)/tyrosine kinase 2 (TYK2)-signal transducer and activator of transcription (STAT) signalling[263-267]. IL-10 directly and indirectly inhibits production of pro-inflammatory cytokines, chemokines and chemokine receptors of many cell types, including T cells, B cells, NK cells, monocytes, mast cells and DCs[261,262]. In addition, IL-10 can modulate APC function, i.e. *via* downregulation of MHC class II and co-stimulatory molecules (such as CD86), thus indirectly inhibiting T cell activation[268]. IL-10 can also inhibit T cell proliferation and cytokine production *via* suppression of CD28- and inducible co-stimulatory molecule (ICOS)-mediated co-stimulation[269-271]. Moreover, Treg immunoregulatory functions are amplified by IL-10 acting in a feedback loop to maintain

Foxp3 expression and thus Treg function[272]. Treg-specific deficiency of IL-10 leads to multiorgan inflammation, particularly at environmental surfaces, but does not cause systemic autoimmunity[273]. Moreover, IL-10 is crucial for Treg-mediated inhibition of IFNγ production by T cells in inflamed skin, but not in the lymph node[274]. These studies highlight the important role of IL-10 in Treg-mediated immunity, but also suggest that Tregs use multiple suppressive mechanisms to control different aspects of inflammation.

1.3.1.2 TGF-β

The TGF-β family has three highly homologous members: TGF-β1, TGF-β2, and TGF-β3. They are synthesised as precursors consisting of a signal peptide, latency-associated peptide (LAP), and the mature TGF-β peptide. As a result of post-transcriptional modifications in the ER, the mature TGF-β peptide is cleaved from LAP. The mature TGF-β then forms a homodimer that remains non-covalently associated with a homodimer of LAP. In this small latent complex, the active TGF-β cytokine is encircled by LAP, covering all receptor contact sites[275-277]. LAP can further cross-link to latent TGF-β binding proteins (LTBPs), which interact with components of the ECM, to form the large latent complex[275,276]. Moreover, TGF-β can tether to the cell surface through association with transmembrane proteins such as glycoprotein A repetitions predominant protein (GARP; LRRC32, leucine rich repeat containing protein 32), which is expressed on Tregs[278-280]. TGF-β is always produced as an inactive complex that requires activation *via* the dissociation of TGF-β from the latent complex. This activation serves as a crucial layer of regulation to control TGF-β function[281]. Activation can be achieved through several routes. The main mechanisms include: cleavage of the LAP domain by extracellular proteases (such as plasmin and several metalloproteases); cell contraction-created integrin-transmitted tension on the large latent complex tethered to the ECM; and integrin-mediated release of active TGF-β *via* tethering

of the small latent complex to GARP on the cell surface[281]. TGF-β signals through the TGF-β receptor complex, which is composed of two type I TGF-β receptors (TGF-βRI) and two type II TGF-β receptors (TGF-βRII), thereby activating SMAD signalling pathways[282]. Moreover, TGF-β can signal through SMAD-independent pathways, such as mitogen-activated protein kinase (MAPK)[282]. Several of the downstream pathways also act as feedback loops to prevent exuberant responses[283-285].

The functional roles of TGF-β are diverse and highly context-specific[281]. TGF-β is important for the differentiation of many cell types, including Th17 cells and iTregs. It further modulates adaptive immune responses, either by suppressing or promoting them, and can indirectly affect Treg function, i.e. *via* enhancing Foxp3 expression[281,282]. Tregs can produce large amounts of soluble and membrane-bound TGF-β; and TGF-β presents one of the mechanisms that Tregs employ for immunosuppression. Examples include TGF-β-dependent suppression of NK cell function and $CD8^+$ cytotoxic T lymphocytes[286-290]. Next to directly or indirectly modulating T cell function, TGF-β secretion by Tregs further facilitates the conversion of naïve T cells into cells with suppressive capacities, termed 'infectious tolerance'[291,292]. Although mice deficient for TGF-β signalling in T cells or all cells develop T cell-mediated autoimmunity early in life, mice lacking TGF-β1 specifically in $Foxp3^+$ Tregs do not develop inflammation[282,293-298]. However, TGF-β1-deficient mice show reduced peripheral Treg numbers and in a murine colitis model DC-derived TGF-β was critical for the prevention of disease *via* the induction of Tregs[294,299,300].

1.3.2 Tregs in the skin

Tissue-resident Tregs have tissue-specific functions and are highly heterogeneous. Increasing evidence supports that not only their phenotype, but also metabolism and

transcriptome differ from their counterparts in circulation and secondary lymphoid organs[301-305]. Tissue-specific adaptation seems closely linked to environmental and physiological signals and the activated effector phenotype of tissue-resident Tregs emphasizes their continuous exposure to antigenic challenges[303,305,306]. Single-cell transcriptomics by Miragaia and colleagues further suggests that Tregs at barrier sites, in skin and colon, share core transcriptomic signatures and that transcriptomic adaptation starts as early as during the transition from lymph node to tissue[302]. They further revealed metabolic differences between draining lymph node (dLN) Tregs and tissue-resident Tregs. While dLN Tregs were associated with the expression of genes involved in glycolysis, colonic and skin Tregs preferentially expressed genes associated with fatty-acid metabolism[302]. This suggests that fatty-acid metabolism may play a central role in Treg adaptation to lipid-rich barrier sites[305].

Tregs in the skin play an important role in maintaining cutaneous immune homeostasis[28,307], but also modulate many other important skin processes such as hair-follicle regeneration, wound healing, and adaptive immune tolerance to skin commensals[28]. The importance of Tregs in maintaining skin immune homeostasis is particularly evident in patients suffering from IPEX syndrome, in whom mutations in Foxp3 result in absent or dysfunctional Tregs. These patients commonly present with cutaneous manifestations such as atopic dermatitis or psoriasis[308]. Genetic impairment of several skin-homing receptors, including CCR4 and CD103, has further been shown to impair Treg-mediated suppression of skin inflammation[307,309,310].

$CD4^+CD25^+$ Tregs constitute about 3% of peripheral blood mononuclear cells (PBMCs) and about 5-15% of $CD4^+$ T cells in peripheral blood[26,311-315], with 68-90% and 62-84% of circulating $CD4^+CD25^+Foxp3^+$ Tregs expressing the skin-homing receptors cutaneous lymphocyte antigen (CLA) and CCR6, respectively[316-318]. In contrast, $Foxp3^+$ Tregs

represent approximately 20% of $CD4^+$ T cells in the skin. More than 95% of these express the memory T cell marker CD45RO[26]. Recent mouse studies suggest that most skin Tregs express GATA binding protein 3 (GATA3) and Nrp1-Helios, indicating that the skin Treg pool may be dominated by tTregs[319-322]. Mice with deletions in GATA3 or the retinoid-acid receptor-related orphan receptor RORα in Foxp3-expressing cells further showed increased type 2 skin inflammation, suggesting that these skin tTregs may be important in preventing aberrant cutaneous inflammatory responses[319,323].

From mouse studies it is known that the first colonisation of the skin with Tregs occurs in a wave of highly activated Tregs during the first weeks of life[324]. In mouse and human skin, Tregs localise early to hair follicles[26,325] and the development of hair follicles facilitates the accumulation of Tregs[326]. Moreover, Tregs have been shown to promote proliferation and differentiation of stem cells to stimulate the regeneration of hair follicles[27]. Further accumulation of highly activated Tregs in the skin occurs early after wounding. These Tregs attenuate IFNγ production and the accumulation of pro-inflammatory macrophages and can produce epidermal growth factor receptor (EGFR) thus facilitating wound healing[29].

While it is well established that intestinal Tregs are heavily influenced by the gut microbiota[305], data on skin Treg-microbiome interactions are limited. Several murine studies indicate that the skin microbiota may dynamically regulate skin-resident Treg numbers during ontogeny and depending on skin site[46,326]. Moreover, neonatal cutaneous microbiome colonisation seems to facilitate immune tolerance by inducing antigen-specific Tregs in skin and lymph nodes[324,327]. There are limited data on the recognition of non-peptide antigens by human Tregs.

1.3.3 Therapeutics

Increasing evidence supports a significant role of Tregs in various immunological and inflammatory diseases and the modulation of these Tregs may prove beneficial for treatment[328].

For diseases in which immunological tolerance needs to be re-established, such as autoimmune diseases and allergy, expansion of Tregs and/or enhancement of suppressive functions may present a viable treatment. Such 'Treg-up' strategies could also suppress undesirable immune responses like the rejection of transplanted organs[328]. Possible methods for expansion and increased functional activity of Tregs include Treg adoptive cell therapy, *in vivo* expansion of natural Tregs and conversion of conventional T cells to Tregs.

Treg adoptive cell therapy is based on *in vitro* expansion of patient Tregs that are subsequently transferred back to the patient[329-331]. Treg transfer has proven safe in patients with graft-versus-host disease (GvHD) or type 1 diabetes, where transferred Tregs persisted for over a year[329,330]. Moreover, pre-clinical data indicate effectiveness in some settings such as GvHD[330,332]. In kidney transplant recipients, immune modulation with autologous polyclonal Treg therapy has been shown to induce a long-lasting increase in peripheral Tregs and restoration of immune cell composition[333,334]. Further, Treg cell therapy resulted in fewer episodes of common viral infection, allowed for reduction of immunosuppression, and reduced transplant rejection. Limiting factors for Treg adoptive cell therapy are low Treg numbers in peripheral blood and limited *in vitro* expansion potential of Tregs. Advancements in *in vitro* Treg expansion protocols for clinical trials[335,336] and the identification of makers determining therapeutic efficacy of expanded Tregs such as CD27 and CD70 may help overcome these limitations[337-341]. Moreover, designing chimeric antigen

receptor (CAR)-Tregs, which have shown promising results in pre-clinical models of transplantation and autoimmune diseases, may help resolve these issues[342-345].

In vivo expansion of natural Tregs can be achieved *via* administration of low-dose IL-2. Tregs constitutively express the high-affinity IL-2 receptor (CD25) and require IL-2 for differentiation and suppressive function. Treatment with low-dose IL-2 has been shown to increase Treg frequency in several disease settings, including GvHD, type 1 diabetes, alopecia areata and systemic lupus erythematosus[346-351]. While Tregs are sensitive to IL-2 due to the expression of CD25, IL-2 acts on a broad range of cells and thus potential side effects of IL-2 treatment include increased NK cell frequency and eosinophilia[352-354]. Generation of mutated IL-2 molecules that allow activation in a CD25-dependent manner could potentially minimise unspecific reactivity[355]. In a recent phase I-IIa study, patients suffering from a variety of autoimmune diseases were treated with low-dose IL-2. Patients across all diseases showed expansion of Tregs and improved CGI (clinical global impression) scores suggesting clinical effectiveness[356].

Another approach to increase Treg frequencies is the *in vivo* conversion of conventional T cells into iTregs. *In vitro*, iTregs can be induced from naïve T cells by antigen stimulation in the presence of TGF-β and IL-2[211,230]. The induction of iTregs using SCFAs or retinoic acid is similarly dependent on TGF-β[211]. Moreover, inhibition of the AKT signalling pathway (i.e. by rapamycin) can induce Foxp3 expression when combined with premature termination of TCR signalling[357,358]. However, iTregs lack Treg-specific epigenetic changes such as TSDR demethylation making them functionally unstable[212,214], thus further studies are necessary to achieve the induction of stable iTregs.

While Treg-up strategies can be beneficial for treatment of diseases in which immunological tolerance needs to be re-established, the reduction of Treg numbers or suppressive capacity

by 'Treg-down' strategies can enhance antimicrobial immunity in chronic infections or evoke antitumor responses[328]. One example of a Treg-down approach is the depletion of Tregs by small molecules or monoclonal antibodies. Although the depletion of Tregs has been shown to efficiently evoke an antitumor response in experimental models[359], due to the key role of Tregs in immunological self-tolerance such a depletion has the potential to elicit autoimmunity. It is therefore crucial to target i.e. tumour-infiltrating Tregs without affecting Tregs in other tissues or conventional T cells[328]. To target tumour-infiltrating Tregs, cell surface molecules that are selectively upregulated on these cells, such as CD25 and CTLA-4, present viable targets for antibody-mediated Treg depletion[360,361]. While CTLA-4 is constitutively expressed by Tregs, conventional T cells express CTLA-4 only upon activation; thus, targeting CTLA-4 may reduce potential side effects[328]. Moreover, CTLA-4 is often highly upregulated in tumour-infiltrating lymphocytes[361]. Anti-CTLA-4 monoclonal antibodies have shown promising results in pre-clinical models, reducing tumour Tregs while increasing $CD8^+$ T cell numbers and thus enhancing antitumor immunity[361-363].

1.4 Overall aims

The overall aim of this thesis was to expand our understanding of CD1a-mediated immune responses in skin immune homeostasis and skin inflammatory disease. CD1a-mediated T cell responses play an important role in skin inflammatory diseases (see 1.2.3 CD1a in skin inflammatory disease) and while increasing evidence supports a role for Tregs in the control of skin inflammation and skin immunity (see 1.3.2 Tregs in the skin), it remains unknown whether Tregs can respond to CD1a. I hypothesised that Tregs may functionally interact with CD1a and thereby modulate skin immunity. Therefore, I aimed to determine whether Tregs can respond to CD1a stimulation, characterise CD1a-reactive Treg responses, define CD1a-specific Treg-TCR sequences, and investigate CD1a-mediated modulation of Treg suppressive functionality (Chapter 2). To gain insights into the role of CD1a-reactive Tregs in skin inflammatory disease, single-cell sequencing of CD1a-reactive Tregs form healthy individuals and psoriasis patients was performed and analysed (Chapter 3). Additionally, I hypothesised that modulation of CD1a expression *via* fatty acids may impact CD1a-mediated T cell responses. I therefore aimed to investigate CD1 modulation by different short- and medium-chain fatty acids and the impact of CD1a modulation on CD1a-reactive T cell responses (Chapter 4). Detailed hypotheses and aims are outlined in the respective chapters.

Chapter 2 Regulatory T cells recognise and functionally interact with CD1a

2.1 Introduction and Aims

2.1.1 CD1a-reactive T cells

CD1a-autoreactive T cells can be found circulating in peripheral blood and residing in the skin. Of peripheral blood memory T cells, 0.02-0.4% produce IFNγ in response to CD1a stimulation. These cells express skin-homing markers such as CLA, CCR4, CCR6, and CCR10 and many home to the skin[150]. Further, skin-resident T cells can be stained with "unloaded" CD1a-Tetramer and can secrete IL-22 in response to CD1a stimulation[135]. CD1a-autoreactive T cells have been described as part of the αβ T cell repertoire[150], but also γδ T cells have been shown to respond to CD1a-presented lipid antigens (unpublished data, Dr Yi-Ling Chen). Unlike CD1d-reactive iNKT cells and CD1b-reactive GEM T cells, CD1a-reactive T cells express diverse TCRs[141,142,150,151,153,154]. Most CD1a-reactive T cells express CD4, but also $CD8^+$ and double-negative T cells have been described[6,121,138,150,151,364-366]. Therefore, co-receptor expression may not be required for CD1a-mediated immune responses. In response to CD1a stimulation, CD1a-reactive T cells can secrete a range of different cytokines including IFNγ, TNFα, IL-2, IL-13, IL-17A, IL-22 and GM-CSF[150,151,167,168,174]. CD1a-autoreactive T cells have been suggested to play a crucial role in maintaining cutaneous immune homeostasis[150,367], as IL-22 is not only involved in skin inflammation, but also keratinocyte proliferation, wound healing, and skin immunity[368]. CD1a-autoreactive T cells further respond to a large variety of natural skin oils[34] and CD1a-mediated T cell responses play an important role in skin inflammatory diseases, which is reviewed in section '1.2.3 CD1a in skin inflammatory disease'. Moreover,

during allergic reactions to bee and wasp venom as well as HDM, PLA_2-generated neolipid antigens stimulate CD1a-reactive T cells to infiltrate the skin and produce inflammatory cytokines such as IFNγ, GM-CSF, and IL-13[166,167]. This process is not only dependent on CD1a but also the availability of cellular membrane for processing and release of self-lipids[166]. Further, bee and wasp venom allergic individuals show a higher frequency of CD1a-reactive T cells[166]. CD1a-reactive T cells have also been implicated in autoimmune diseases such as Graves' disease and Hashimoto's thyroiditis and may play a protective role in mycobacterial infections[121,158,369].

2.1.2 Treg TCR repertoire

Tregs display a high level of TCR diversity and the TCR repertoire of Tregs is mostly, but not entirely, distinct from non-Treg cells[370-374]. TCR diversity plays a crucial role in thymic selection and differentiation of Tregs and may be important for suppressive function and prevention of autoimmune disease[375-378]. While the TCR repertoire of pTregs and tTregs are similar, they are not identical[370,379]. Moreover, TCR signalling and signal strength influence Treg transcriptional identity resulting in phenotypic distinct Treg subsets with specific regulatory activities[380-383]. Overall, there are limited data on specific human Treg peptide antigens. Examples of identified peptide antigens include peptides derived from a prostate-specific protein (Tcaf3), an apolipoprotein B peptide that is associated with atherosclerosis, and tumour peptide antigens[384-386]. The highly proliferative state of Tregs, especially effector-type Tregs, under normal physiological conditions is thought to result from continuous recognition of self- and commensal antigens[231,232]. While TCR activation is required for Treg suppressive function, once activated they can also suppress in antigen-nonspecific ways[233,387,388].

Tregs in the skin play an important role in maintaining skin immunity (see 1.3.2 Tregs in the skin). Skin Tregs respond to self as well as non-self antigens, but knowledge on specific antigens is lacking. Using sequencing of the TCR β-chain, Sanchez Rodriguez *et al.* showed that skin memory $CD4^+$ conventional T cells and skin memory Tregs may recognise predominantly different antigens[26]. The potential targeting of non-peptide antigens by human Tregs has not been extensively investigated.

2.1.3 Hypothesis and aims

Through the non-classical antigen-presenting molecule CD1a, which is predominantly expressed on LCs and dermal DCs in the skin[160], skin APCs can present lipid antigens to T cells and modulate the skin immune response (see 2.1.1 CD1a-reactive T cells). Tregs are crucial for preservation of immune homeostasis (see 1.3 Regulatory T cells) and increasing evidence supports an important role for Tregs in the control of skin inflammation and skin immunity (see 1.3.2 Tregs in the skin). It has been recently appreciated that effector T cells can respond to CD1a, *via* CD1a-TCR interaction, and contribute to the exacerbation of skin inflammation and skin diseases such as psoriasis (see 1.2.3 CD1a in skin inflammatory disease). However, whether Tregs can recognise CD1a and maintain immune homeostasis remains elusive. For these reasons, I hypothesised that Tregs can bind to and functionally interact with CD1a, and that CD1a-reactive Tregs contribute to immune regulation.

The aims of this project included:

- Determine whether Tregs can bind to and functionally interact with CD1a
- Study the interaction of CD1a-reactive Tregs with CD1a presenting skin-relevant lipids
- Assess the potential of CD1a-reactive Tregs to secrete skin inflammation-associated cytokines
- Investigate TCR expression and usage of CD1a-reactive Tregs
- Investigate the effect of CD1a stimulation on CD1a-reactive Treg functionality
- Generate and phenotype CD1a-reactive Treg clones

2.2 Results

2.2.1 Polyclonal Treg expansion and suppressive functionality

The use of primary $CD4^+CD25^+CD127^{low}Foxp3^+$ Tregs as an experimental model is limited by low numbers present in peripheral blood[26,311-315]. To study Tregs *in vitro*, polyclonal Tregs were isolated from circulating PBMCs and expanded *in vitro* using high levels of IL-2 and stimulation with anti-CD3 and anti-CD28 (see 6.4.5 Treg isolation and expansion). To confirm the Treg phenotype post expansion, Treg lineage marker expression was analysed by flow cytometry. Expanded polyclonal Tregs expressed CD3, CD4 and CD25, while CD127 expression was non-detectable or very low (Fig. 2.1, A). Moreover, the majority of Tregs stained positive for GITR and intracellular CTLA-4 (Fig. 2.1, B). Foxp3 expression was consistently high in expanded Tregs with 86.46% ± 13.03 Tregs expressing Foxp3 (gated on live single cells; n=23). Suppressive functionality of expanded Tregs was confirmed by proliferation suppression assays. For this, Tregs were co-cultured at varying ratios with autologous PBMCs in the presence of anti-CD3/anti-CD28 microbeads for T cell expansion. Suppression of $CD4^+$ and $CD8^+$ T cell proliferation was determined by calculating the division index using $CD4^+$ and $CD8^+$ T cell proliferation in the absence of Tregs as baseline. Expanded Tregs inhibited $CD4^+$ and $CD8^+$ T cell proliferation by 93.52% ± 5.76 and 90.22% ± 7.79 at a ratio of 1:1 PBMC:Treg, respectively (Fig. 2.1, C). At a ratio of 8:1 PBMC:Treg, $CD4^+$ and $CD8^+$ T cell proliferation were still inhibited by 61.57% ± 15.21 and 53.14% ± 16.09, respectively. Overall, Tregs retained the expression of phenotypic Treg markers and suppressive functionality throughout the expansion process.

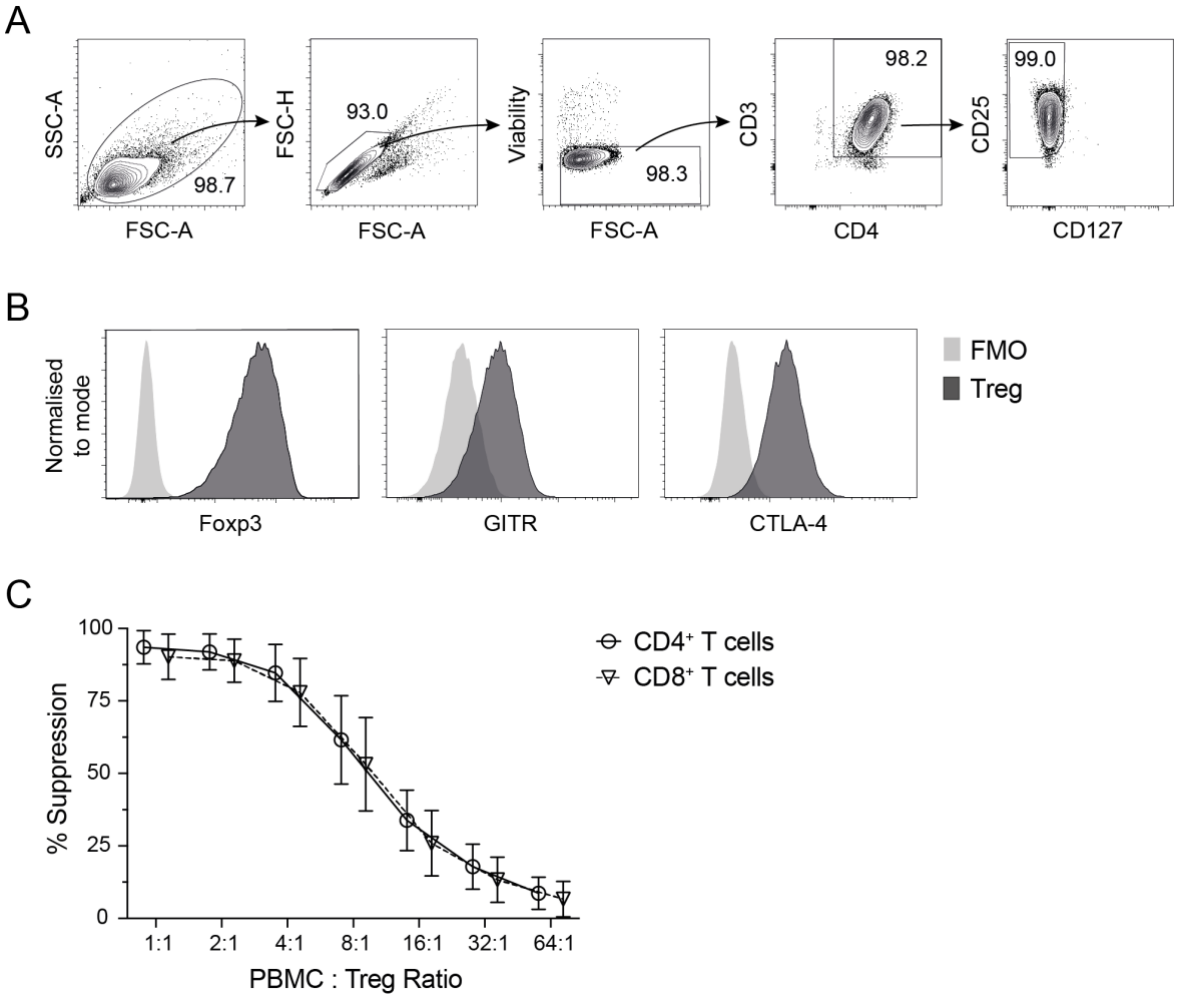

Fig. 2.1 Lineage staining and suppressive functionality of expanded polyclonal Tregs.

Circulating Tregs were expanded for 12-14 days and rested for 1-2 days before phenotyping. **(A)** Flow cytometry gating strategy for Tregs using the surface markers CD3, CD4, CD25 and CD127. Arrows indicate gating on the parent population. Numbers indicate the percentage of cells in or next to the respective gate. **(B)** Foxp3, GITR and intracellular CLTA-4 staining of $CD3^+CD4^+CD25^+CD127^{low}$ expanded Tregs. **(C)** Suppression of autologous $CD4^+$ and $CD8^+$ T cell proliferation by expanded Tregs as determined by division index. Tregs were co-cultured with autologous PBMCs in the presence of anti-CD3/anti-CD28 microbeads (5:1 PBMC:bead ratio) for 3 days. Suppression was calculated relative to $CD4^+$ and $CD8^+$ T cell proliferation in the absence of Tregs, respectively. (n=16 donors; 6 independent experiments) (mean ± SD).

2.2.2 Polyclonal Tregs secrete IL-10 in a CD1a-dependent manner

Tregs exert their suppressive function through a variety of different cell-cell contact-dependent and -independent mechanisms[247,248]. One important suppressive mechanism is the generation and secretion of the immunomodulatory cytokine IL-10. To study the functional engagement of Tregs with CD1a, two different CD1a stimulation systems were used. Firstly, an artificial antigen-presenting cell system mimicking CD1a antigen presentation by APCs in the skin. For this, Tregs were co-cultured with K562 cells stably expressing CD1a (K562-CD1a) or an empty vector control (K562-EV) (gift from Prof Branch Moody, Harvard). Secondly, an artificial cell-free CD1a stimulation system eliminating all other stimulatory factors present on APCs. In this system, Tregs were stimulated with CD1a-coated beads, using empty beads as a control. In both systems, IL-2 was present throughout stimulation and Tregs were co-stimulated with anti-CD11a (unless otherwise indicated). IL-2 is essential for Treg function[209], while stimulation *via* CD11a is involved in T cell activation and has previously been published to aid CD1a-mediated T cell responses in cell-free plate-binding assays[6,34,166,200,389]. As production of IL-10 is an important mechanism through which Tregs exert their suppressive function[247,248], the effect of CD1a stimulation on Tregs was quantified by measuring IL-10 secretion.

2.2.2.1 CD1a stimulation of polyclonal Tregs using an artificial antigen-presenting cell system

Tregs co-cultured with K562-EV cells showed a background IL-10 secretion of 0.43% ± 0.15, which was significantly increased to 2.14% ± 0.15 in the presence of K562-CD1a cells (Fig. 2.2, A, B). CD1a stimulation increased IL-10 secretion by polyclonal Tregs 5.37-fold (± 2.65) compared to the control (Fig. 2.2, C). Blocking of CD1a with anti-CD1a antibody reduced IL-10 secretion significantly, although not completely, to 0.71% ± 0.33,

which was not observed when adding the respective isotype control (2.14% ± 1.11) (Fig. 2.2, A, B). These results indicate that CD1a stimulation induces CD1a-dependent IL-10 secretion in a subpopulation of polyclonal Tregs.

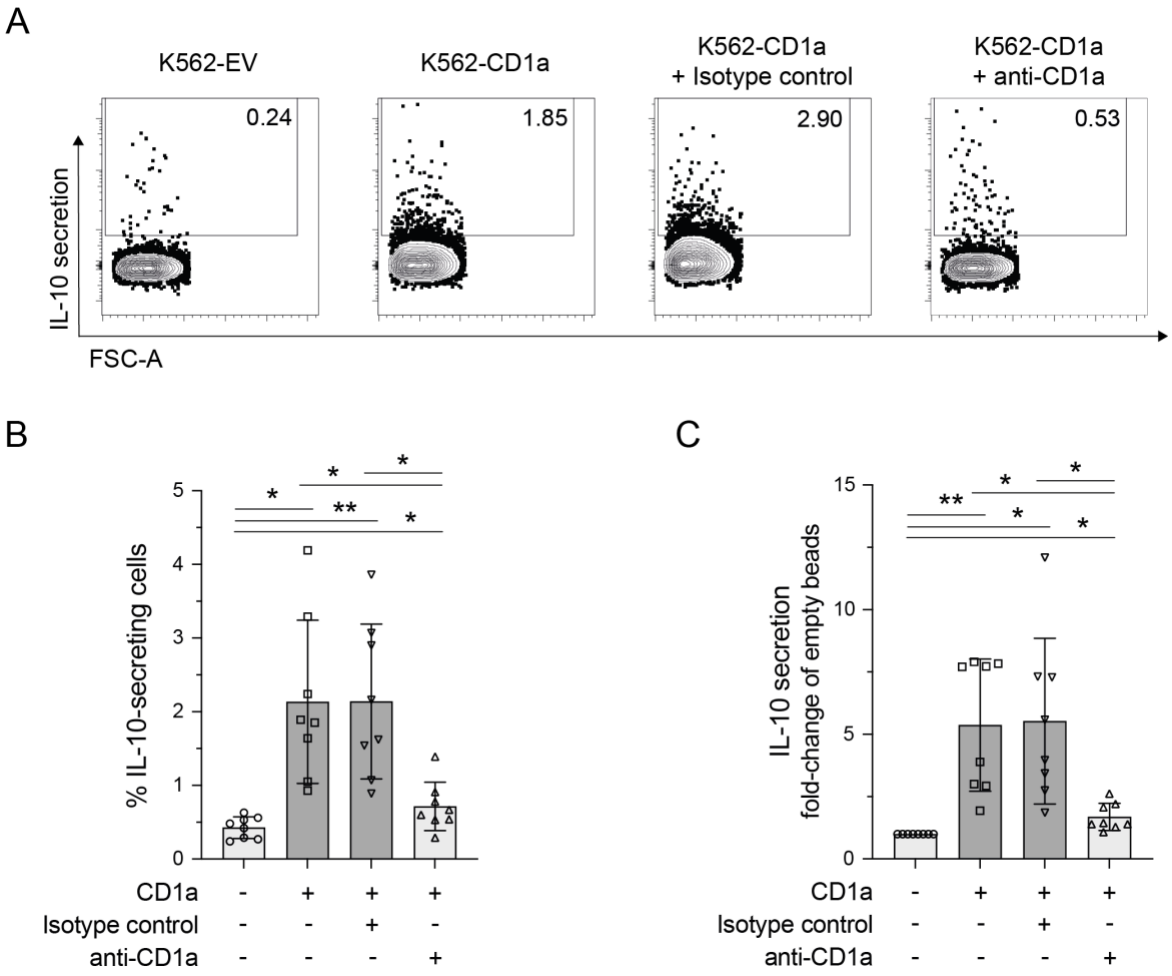

Fig. 2.2 A subpopulation of polyclonal Tregs secretes IL-10 in a CD1a-dependent manner. **(A)** Expanded Tregs were co-cultured with K562-CD1a cells or K562-EV cells as a control in the absence or presence of anti-CD1a antibody (clone HI149) or an isotype control. Cells were co-stimulated with IL-2 only or IL-2 and anti-CD11a. Secretion of IL-10 by Tregs was determined by IL-10 secretion assay. Numbers indicate percentages of cells within the indicated gates; gated on live $CD3^+CD4^+CD25^+CD127^{low}$ cells. Plots representative of n=8. **(B, C)** Summary of IL-10 secretion by Tregs upon CD1a stimulation as **(B)** percentage of IL-10-secreting Tregs gated on live $CD3^+CD4^+CD25^+CD127^{low}$ cells, and **(C)** fold-change of IL-10 secretion of Tregs compared to the K562-EV control. (n=8 donors; 4 independent experiments). *P < 0.05; **P < 0.01; ***P < 0.001; RM One-way ANOVA with Tukey's correction for multiple comparison (mean ± SD).

2.2.2.2 Optimisation of CD1a stimulation by CD1a-coated beads

To optimise the CD1a-coated bead stimulation assay, polyclonal Tregs were stimulated with CD1a-coated beads at different bead:Treg ratios, measuring IL-10 secretion in the presence of different co-stimulatory antibodies and cytokines. Anti-CD11a can activate T cells and has been shown to aid CD1a-mediated T cell responses in cell-free plate-binding assays[6,34,166,200,389]. Anti-CD3 and anti-CD28 are well characterised T cell stimulators and commonly used to stimulate Tregs during *in vitro* expansion. While anti-CD137 (anti-4-1BB) can negatively regulate Treg function, it has also been proposed to aid expansion and function of Tregs, depending on experimental system and environment[390,391]. In an initial test with a single Treg donor, co-stimulation with anti-CD11a, anti-CD3 and anti-CD28, or anti-CD137 showed increased IL-10 secretion upon CD1a stimulation (1.49%, 2.02% and 0.78%, respectively) in comparison to co-stimulation with IL-2 only (0.39%) (Fig. 2.3, A). Comparing IL-10 secretion to the empty bead control revealed that co-stimulation with anti-CD11a showed the highest CD1a-specific increase in IL-10 secretion (45.2-fold). While addition of anti-CD3/anti-CD28 increased IL-10 secretion upon CD1a stimulation to a higher percentage compared to the other co-stimulations, also background IL-10 secretion was increased thus reducing the fold-change increase (5.6-fold). Increasing the bead:Treg ratio during stimulation from 1:1 to 3:1 reduced IL-10 secretion for all conditions (Fig. 2.3, A). Therefore, a bead:Treg ratio of 1:1 was chosen for subsequent experiments.

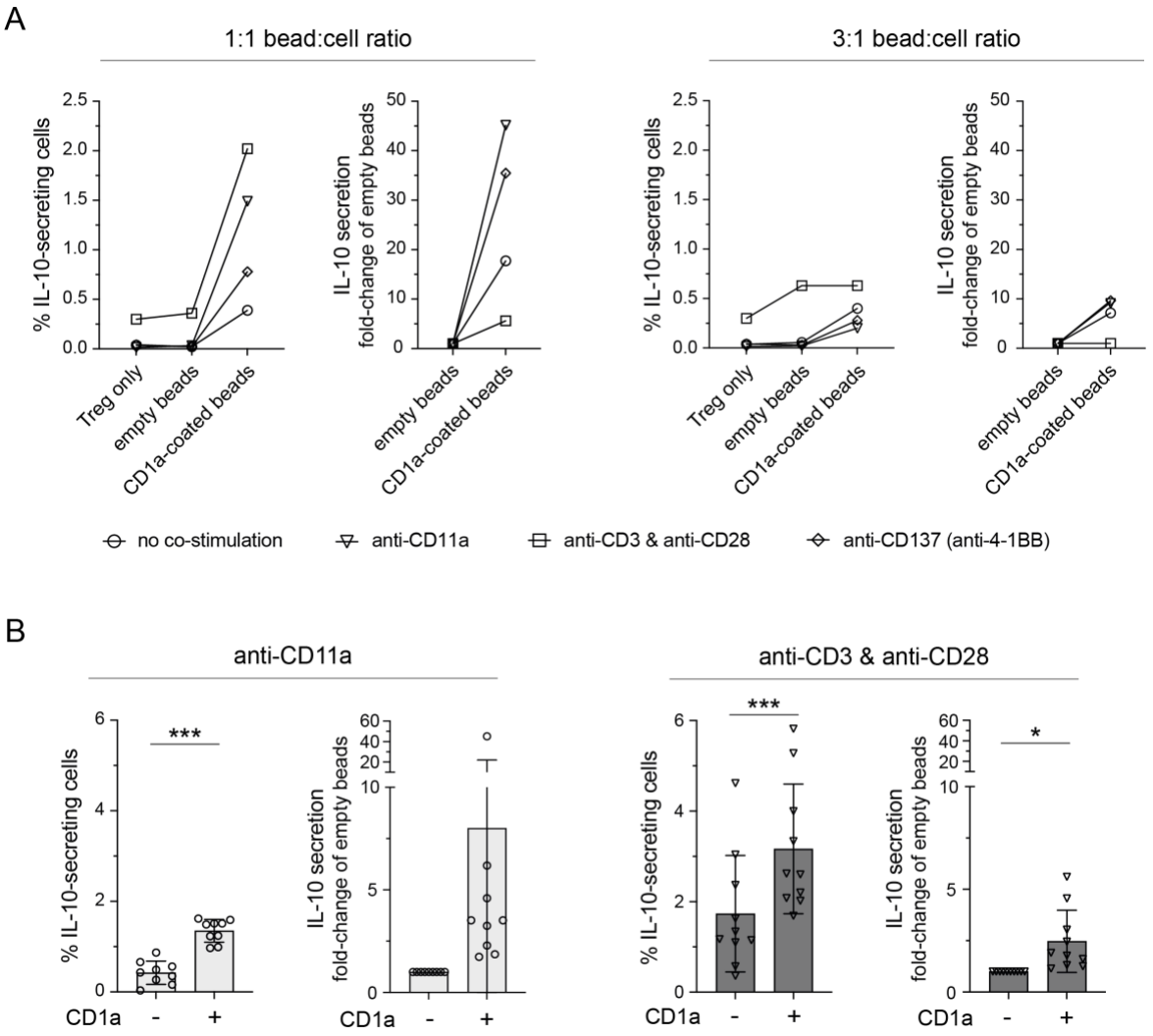

Fig. 2.3 Effect of different co-stimulations on CD1a-dependent IL-10 secretion by Tregs.
Expanded Tregs were co-cultured with CD1a-coated beads or empty beads as control. Secretion of IL-10 by Tregs (gated on live $CD3^+CD4^+CD25^+CD127^{low}$ cells) was determined by IL-10 secretion assay. IL-2 was present in all conditions. **(A)** IL-10 secretion as percentage and fold-change of the empty bead control for Tregs co-cultured with CD1a-coated (coated with 0.32mg/ml CD1a) or empty beads at bead:Treg ratios of 1:1 and 3:1. Tregs were co-stimulated with 2500ng/ml anti-CD11a, anti-CD3 and anti-CD28, or anti-CD137 (n=1 donor). **(B)** IL-10 secretion as percentage and fold-change of the empty bead control by Tregs co-cultured with CD1a-coated (coated with 0.10-0.32mg/ml CD1a) or empty beads at a ratio of 1:1, co-stimulated with 2500ng/ml anti-CD11a or anti-CD3 and anti-CD28. (n=9-10 donors; 3 independent experiments). *P < 0.05; **P < 0.01; ***P < 0.001; Two-tailed paired t-test (mean ± SD).

As co-stimulation with anti-CD11a and with a combination of anti-CD3 and anti-CD28 showed high IL-10 secretion of polyclonal Tregs upon CD1a stimulation, these conditions were repeated for additional donors (Fig. 2.3, B). In line with previous results, CD1a-stimulated Tregs co-stimulated with anti-CD3/anti-CD28 showed higher IL-10 secretion (3.17% ± 1.43) compared to co-stimulation with anti-CD11a (1.35% ± 0.25). However, as expected, IL-10 secretion in response to the empty bead control was also increased in the presence of anti-CD3/anti-CD28 (1.74% ± 1.29 compared to 0.43% ± 0.26 for anti-CD11a), thus showing a lower fold-change increase of CD1a-specific IL-10 secretion in comparison to anti-CD11a (2.5- and 8-fold, respectively). Therefore, anti-CD11a co-stimulation was chosen for subsequent experiments.

Several cytokines have been shown to modulate IL-10 production and/or Treg function. Tregs use TGF-β to exert their suppressive functions, but TGF-β also plays an important role in Treg induction and affects Treg function (see 1.3.1.2 TGF-β). IL-4 has been proposed to enhance IL-10 production in Th1 cells and support Treg suppressive immune responses[392-394]. TCR priming in the presence of IL-21 has been proposed to result in the accumulation of T cells with an IL-10-dependent immunosuppressive phenotype, and IL-21 induction *via* IL-27 has been shown to induce IL-10 production by Tr1 cells[395,396]. To test whether the addition of these cytokines may increase CD1a-specific IL-10 secretion by Tregs, polyclonal Tregs were stimulated with empty or CD1a-coated beads in the presence of anti-CD11a and TGF-β1, IL-4 or IL-21 (Fig. 2.4). While the addition of IL-4 showed no effect on CD1a-mediated IL-10 secretion, the addition of TGF-β1 decreased CD1a-mediated IL-10 secretion by Tregs (Fig. 2.4). The addition of IL-21 increased IL-10 secretion upon CD1a stimulation slightly (1.48% ± 0.13) compared to anti-CD11a only (1.24% ± 0.01). However, IL-10 secretion was also increased for stimulation with empty beads in the presence of IL-21 thus reducing the fold-change increase of IL-10 secretion to 3.3-fold

compared to 4.1-fold for anti-CD11a only (Fig. 2.4). Therefore, co-stimulation with anti-CD11a only was chosen for subsequent bead stimulation assays.

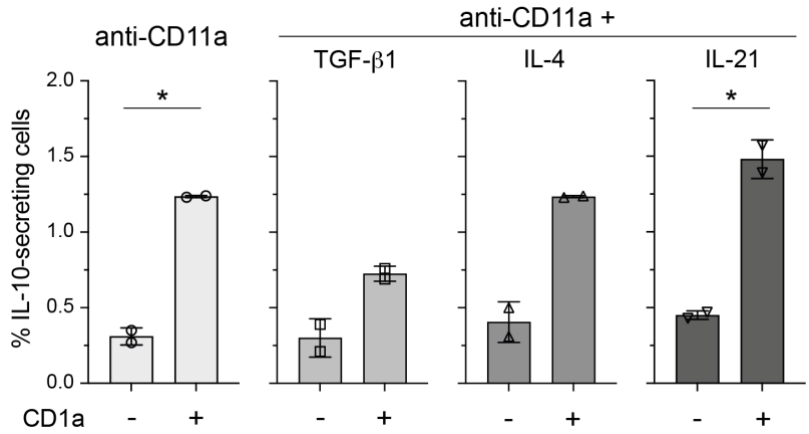

Fig. 2.4 Effect of cytokine co-stimulation on CD1a-dependent IL-10 secretion by Tregs.
Expanded Tregs were co-cultured with CD1a-coated beads (coated with 0.15mg/ml) or empty beads as control, at ratio of 1:1 bead:Treg. Secretion of IL-10 by Tregs (gated on live $CD3^+CD4^+CD25^+CD127^{low}$ cells) was determined by IL-10 secretion assay. Tregs were co-stimulated with 2500ng/ml anti-CD11a in the presence or absence of 10ng/ml TGF-β1, 20ng/ml IL-4, or 20ng/ml IL-21. (n=2 donors; 1 experiment). *P < 0.05; **P < 0.01; ***P < 0.001; Two-tailed paired t-test (mean ± SD).

The amount of CD1a coated onto beads used for cell-free CD1a stimulation may impact the ability of CD1a-coated beads to stimulate Treg responses. To assess this, beads were incubated with different concentrations of CD1a and subsequently used for Treg stimulation, measuring IL-10 secretion as read-out. Although the coating of beads with 0.32mg/ml CD1a resulted in consistent induction of IL-10 secretion by Tregs initially (Fig. 2.3, A, B), subsequent experiments showed varying IL-10 secretion, with some donors showing no increase upon CD1a stimulation by CD1a-coated beads (Fig. 2.5, A). Coating beads with 0.15mg/ml CD1a led to an equally strong but potentially more consistent CD1a stimulation of Tregs (Fig. 2.5, A). To further optimise the coating of beads for most efficient CD1a stimulation, beads were coated with 0.15, 0.10 and 0.05mg/ml CD1a and IL-10 secretion of

Tregs upon stimulation with these CD1a-coated beads was compared (Fig. 2.5, B). CD1a-coated beads from all three conditions were able to induce IL-10 secretion of Tregs (0.66% ± 0.06, 1.04% ± 0.21 and 0.52% ±0.07, respectively). However, coating beads with 0.10mg/ml CD1a showed the highest percentage and fold-change of IL-10 secretion (3.3-fold; compared to 2.2-fold for 0.15mg/ml and 1.7-fold for 0.05mg/ml) and was therefore used for all subsequent experiments. On the cell surface, CD1a accumulates in lipid rafts[104] and therefore low density of CD1a on beads may result in weak TCR stimulation due to limited TCR-CD1a interactions, while high density may result in steric interference of TCR engagement with CD1a.

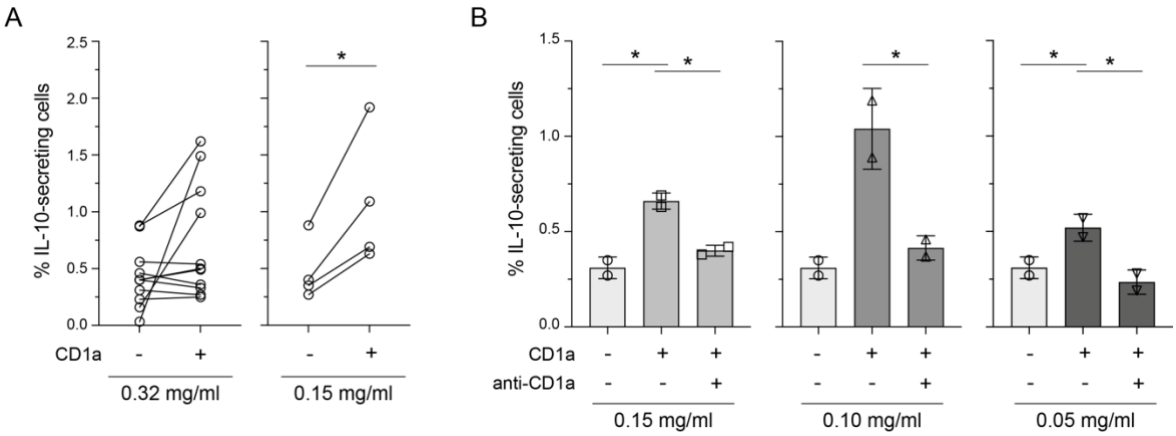

Fig. 2.5 CD1a-dependent IL-10 secretion of Tregs varies with CD1a density on CD1a-coated beads used for stimulation.

Expanded Tregs were co-cultured with CD1a-coated beads or empty beads as control in the absence or presence of anti-CD1a antibody (clone HI149). Tregs were co-stimulated with IL-2 and anti-CD11a. Beads were coated with CD1a at concentrations of **(A)** 0.32mg/ml and 0.15mg/ml, or **(B)** 0.15mg/ml, 0.10mg/ml and 0.05mg/ml. Secretion of IL-10 by Tregs (gated on live $CD3^+CD4^+CD25^+CD127^{low}$ cells) was determined by IL-10 secretion assay. ((A) left: n=11 donors, 5 independent experiments; right: n=4 donors, 2 independent experiments. (B) n=2 donors, 1 experiment). *P < 0.05; **P < 0.01; ***P < 0.001; (A) Two-tailed paired t-test. (B) RM One-way ANOVA with Tukey's correction for multiple comparison (mean ± SD).

2.2.2.3 CD1a stimulation of polyclonal Tregs using a cell-free stimulation system

The previously optimised cell-free CD1a stimulation system (see 2.2.2.2 Optimisation of CD1a stimulation by CD1a-coated beads) was used to study CD1a-mediated IL-10 secretion of polyclonal Tregs independent of other stimulatory factors present on antigen-presenting cells. Tregs stimulated with empty beads showed 0.49% ± 0.36 IL-10 secretion which was significantly increased to 1.83% ± 0.92 when stimulated with CD1a-coated beads (Fig. 2.6, A, B). IL-10 secretion of Tregs upon CD1a stimulation was increased by 4.8-fold compared to the empty bead control (Fig. 2.6, C). Blocking of CD1a with an anti-CD1a antibody reduced IL-10 secretion significantly to background level (0.56% ± 0.31), while adding the respective isotype control did not change IL-10 secretion (2.08% ± 1.09) (Fig. 2.6, A, B). These results confirm and strengthen previous results (Fig. 2.2) that a subset of polyclonal Tregs can secrete IL-10 in a CD1a-dependent manner. They further indicate that additional APC-mediated stimulation may not be required for the functional interaction of Tregs with CD1a.

To assess whether CD1a stimulation induces IL-10 transcription, polyclonal Tregs were co-cultured for 2h or 4h with CD1a-coated beads or empty beads as control in the absence and presence of anti-CD1a antibody or an isotype control. *IL10* messenger RNA (mRNA) levels relative to *CD2* were measured by RT-qPCR. No CD1a-dependent change in *IL10* transcription could be observed upon CD1a stimulation (Fig. 2.7). As only a subpopulation of polyclonal Tregs shows CD1a-mediated secretion of IL-10 (Fig. 2.2, Fig. 2.6), transcriptional changes in a subpopulation may be masked by non-reactive Tregs. Further, C_t values for *IL10* ranged from 30-35, depending on donor (C_t values > 34 were excluded from analysis). Due to lack of RT-qPCR sensitivity, following experiments focussed on cytokine secretion.

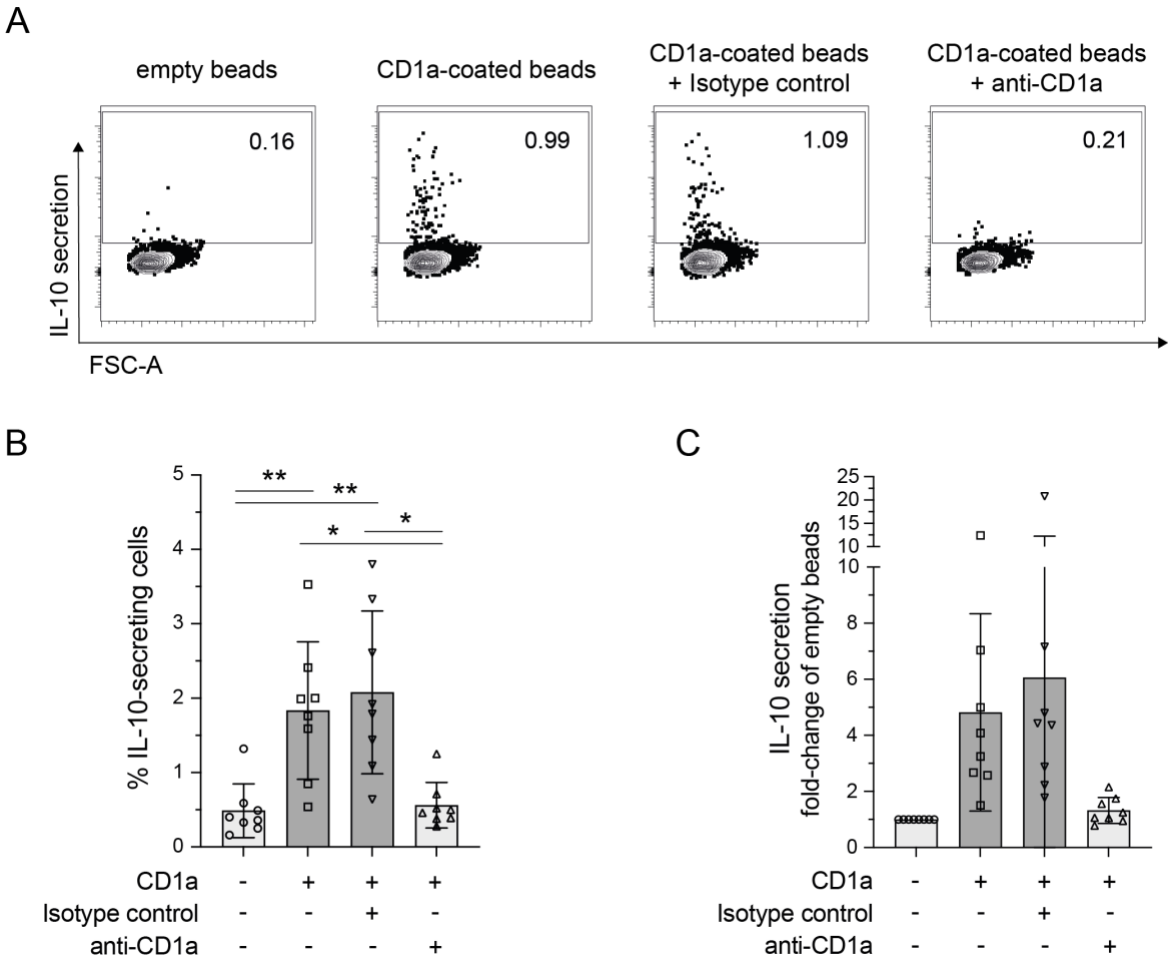

Fig. 2.6 Polyclonal Tregs secrete IL-10 in a CD1a-dependent manner in a cell-free system.

(A) Expanded Tregs were co-cultured with CD1a-coated beads or empty beads as control in the absence or presence of anti-CD1a antibody (clone HI149) or an isotype control. Cells were co-stimulated with IL-2 and anti-CD11a. Secretion of IL-10 by Tregs was determined by IL-10 secretion assay. Numbers indicate percentages of cells within the indicated gates; gated on live $CD3^+CD4^+CD25^+CD127^{low}$ cells. Plots representative of n=8. **(B, C)** Summary of IL-10 secretion by Tregs upon CD1a stimulation as **(B)** percentage of IL-10-secreting Tregs gated on live $CD3^+CD4^+CD25^+CD127^{low}$ cells, and **(C)** fold-change of IL-10 secretion compared to the empty bead control. (n=8 donors; 4 independent experiments). *P < 0.05; **P < 0.01; ***P < 0.001; RM One-way ANOVA with Tukey's correction for multiple comparison (mean ± SD).

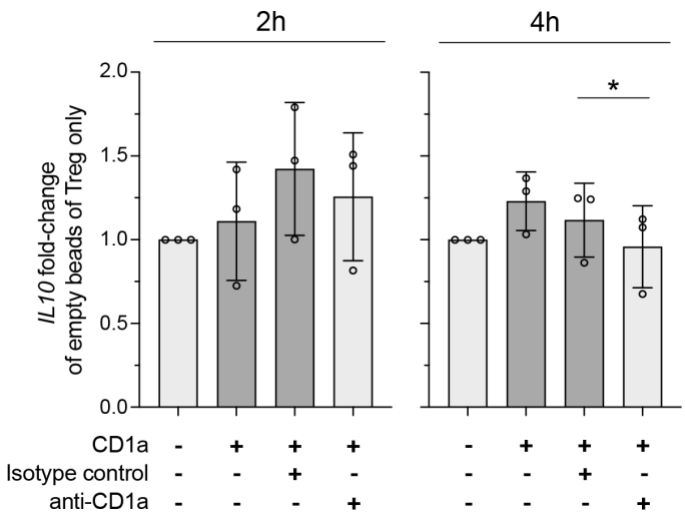

Fig. 2.7 *IL10* mRNA expression in polyclonal Tregs stimulated with CD1a-coated beads.
Expanded Tregs were co-cultured for 2h or 4h with CD1a-coated beads or empty beads as control in the absence or presence of anti-CD1a antibody (clone HI149) or an isotype control. Tregs were co-stimulated with IL-2 and anti-CD11a. *IL10* mRNA expression relative to *CD2* was measured by RT-qPCR and is shown as fold-change of the empty bead control. (n=3 donors; 1 experiment). ns > 0.05; *P < 0.05; RM One-way ANOVA with Tukey's correction for multiple comparison (mean ± SD).

Different anti-CD1a antibody clones bind to different targets on CD1a and therefore may differentially affect CD1a-mediated T cell responses. To investigate differential blocking of CD1a-mediated IL-10 secretion of polyclonal Tregs by different anti-CD1a antibodies, CD1a-coated beads were incubated with anti-CD1a clones HI149, OKT6 or SK9 before Treg stimulation. CD1a-mediated secretion of IL-10 by Tregs was abrogated when CD1a-coated beads were blocked with anti-CD1a clone HI149 (Fig. 2.8, A, B). In contrast, blocking of CD1a-coated beads with anti-CD1a clone OKT6 reduced IL-10 secretion only marginally and not significantly, and blocking with anti-CD1a clone SK9 had no effect on IL-10 secretion by Tregs. These results may indicate that either the binding sites of Treg-TCRs to CD1a may overlap with the binding site of clone HI149 and partially with the binding site clone OKT6, or that binding of these antibody clones may induce conformational changes in CD1a thereby disrupting Treg-TCRs binding to CD1a.

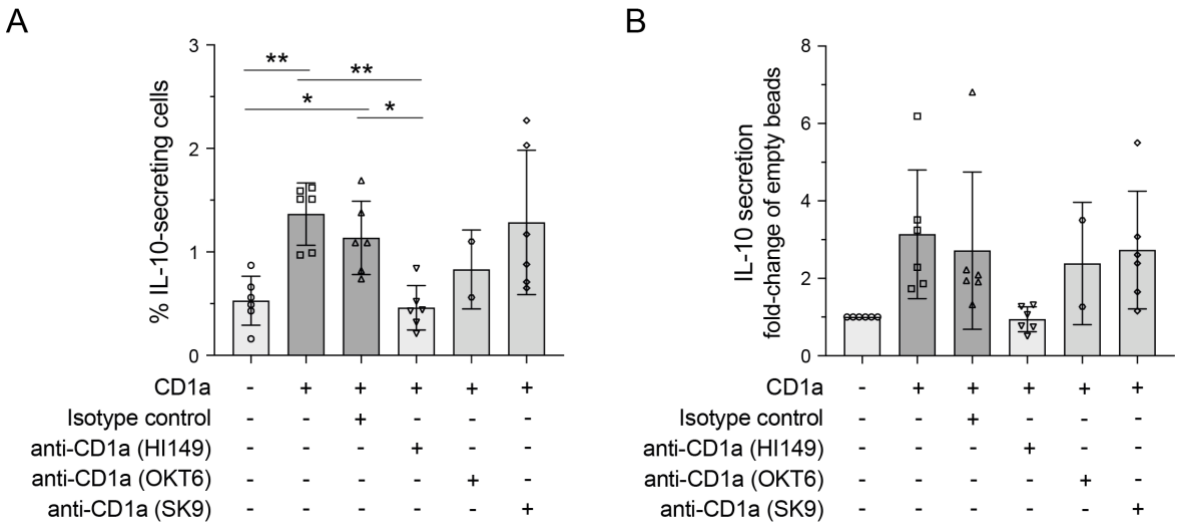

Fig. 2.8 Differential blocking of CD1a-mediated IL-10 secretion of polyclonal Tregs by different CD1a blocking antibodies.

Expanded Tregs were co-cultured with CD1a-coated beads (coated with 0.10 or 0.32mg/ml CD1a) or empty beads as control in the absence or presence anti-CD1a antibody clone HI149, clone OKT6 or clone SK9, or an isotype control (mouse IgG1). Cells were co-stimulated with IL-2 and anti-CD11a. Secretion of IL-10 by Tregs (gated on live $CD3^{+}CD4^{+}CD25^{+}CD127^{low}$ cells) was measured by secretion assay and is shown as **(A)** percentage and **(B)** fold-change compared to the empty bead control. (n=2-6 donors; 1-2 independent experiments). *P < 0.05; **P < 0.01; ***P < 0.001; RM One-way ANOVA with Tukey's correction for multiple comparison (mean ± SD).

2.2.2.4 CD1a-reactive IL-10-secreting polyclonal Tregs express α/β T cell receptors

CD1a-reactive effector T cells are part of the α/β T cell receptor repertoire[150]. To determine whether CD1a-reactive Tregs express α/β TCRs, expanded polyclonal Tregs were stimulated with CD1a and analysed for TCRαβ and TCRγδ surface expression by flow cytometry. The majority of expanded polyclonal Tregs stained positive for TCRαβ (96.45% ± 0.29) (Fig. 2.9, A), while only few Tregs stained positive for TCRγδ (0.59% ± 0.40). Tregs co-cultured with K562 cells in the absence or presence of anti-CD1a antibody or an isotype control showed comparable TCRαβ expression (Fig. 2.9, B). 91.22% ± 3.95 of Tregs that secreted IL-10 in response to CD1a stimulation stained positive for TCRαβ, while only 3.78% ± 2.96 stained positive for TCRγδ (Fig. 2.9, C, D). This did not change significantly between stimulation with K562-EV or K562-CD1a cells or in the presence of anti-CD1a antibody or an isotype control (Fig. 2.9, D). These data suggest that like CD1a-reactive effector T cells, CD1a-reactive IL-10-secreting Tregs express α/β TCRs.

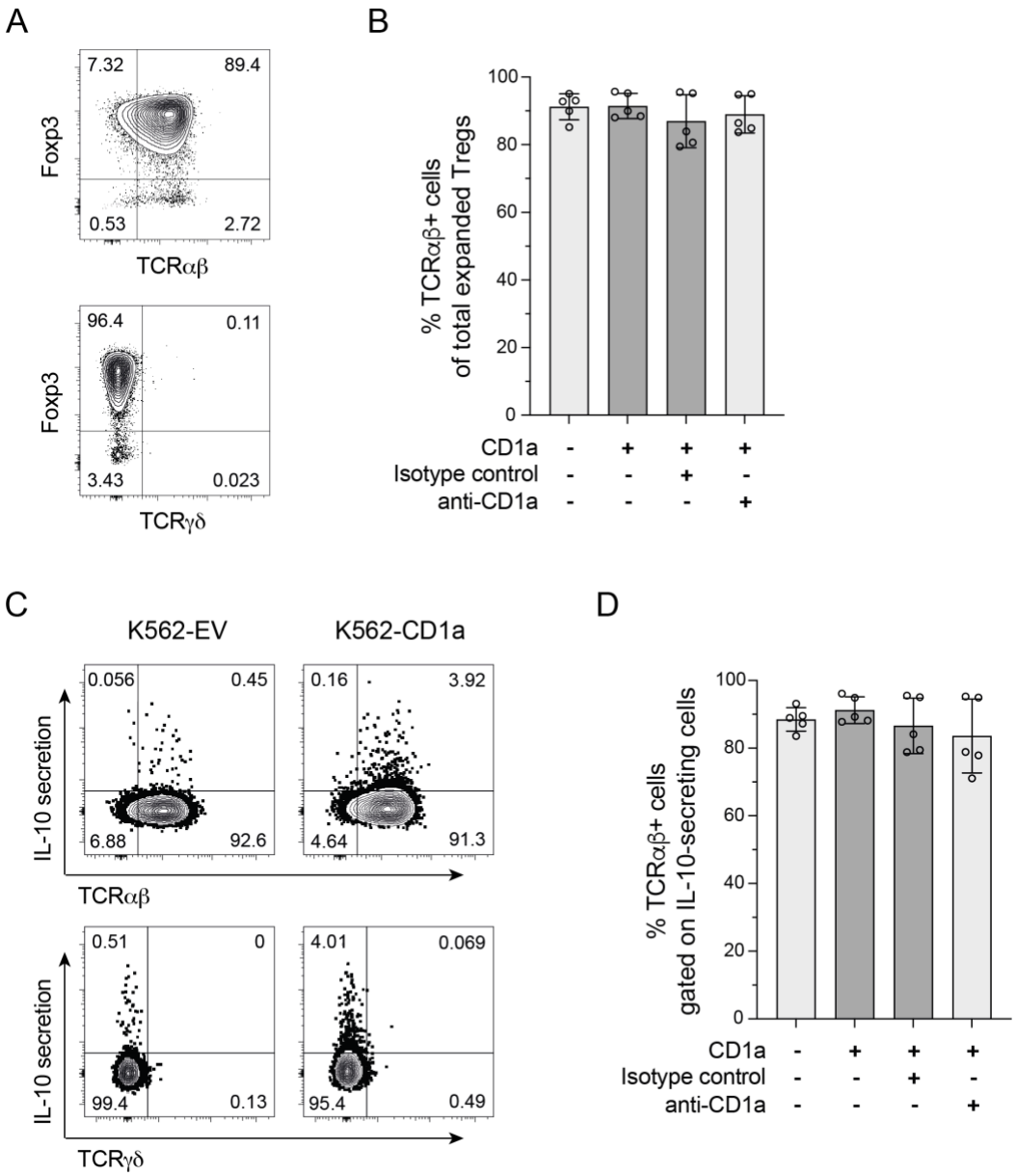

Fig. 2.9 CD1a-reactive IL-10-secreting Tregs express α/β T cell receptors.

(A) Flow cytometry analysis of TCRαβ and TCRγδ surface expression on expanded polyclonal Tregs, gated on live $CD3^+CD4^+CD25^+CD127^{low}$ cells. Plots representative of n=5. **(B)** Summary of surface expression of TCRαβ on polyclonal Tregs. (n=5 donors; 2 independent experiments). **(C-D)** Expanded polyclonal Tregs were co-cultured with K562-CD1a cells or K562-EV cells as control in the absence or presence of anti-CD1a antibody (clone HI149) or an isotype control. Cells were co-stimulated with IL-2 and anti-CD11a. Tregs were gated on live $CD3^+CD4^+CD25^+CD127^{low}$ cells and secretion of IL-10 by Tregs was determined by IL-10 secretion assay. **(C)** Flow cytometry analysis of TCRαβ and TCRγδ expression on CD1a-reactive IL-10-secreting Tregs. Plots representative of n=5. **(D)** Summary of surface expression of TCRαβ on CD1a-reactive IL-10-secreting Tregs. (n=5 donors; 2 independent experiments). ns > 0.05; *P < 0.05; RM One-way ANOVA with Tukey's correction for multiple comparison (mean ± SD).

2.2.3 LAP-TGF-β secretion of polyclonal Tregs in response to CD1a stimulation

In addition to secretion of IL-10, Tregs can also exert their suppressive function *via* the immunomodulatory cytokine TGF-β[248]. For this reason, TGF-β expression of CD1a-reactive Tregs was investigated. However, TGF-β is produced by many cell types, including K562 cells. To determine TGF-β expression in the K562 cell lines used herein, secretion of latent TGF-β (LAP-TGF-β) was quantified by ELISA and *TGFB1* mRNA levels were measured by RT-qPCR. K562-CD1a cells secreted significantly higher levels of LAP-TGF-β (12.20ng/ml ± 3.80) compared to K562-EV cells (3.60ng/ml ± 1.54) (Fig. 2.10, A) and expressed 1.45-fold higher levels of *TGFB1* mRNA (Fig. 2.10, B). As TGF-β does not only act as an immunomodulatory cytokine but also modulates Treg function (see 1.3.1.2 TGF-β), the antigen-presenting cell system that uses K562 cells for CD1a stimulation of Tregs could not be used to investigate CD1a-mediated expression of TGF-β by Tregs.

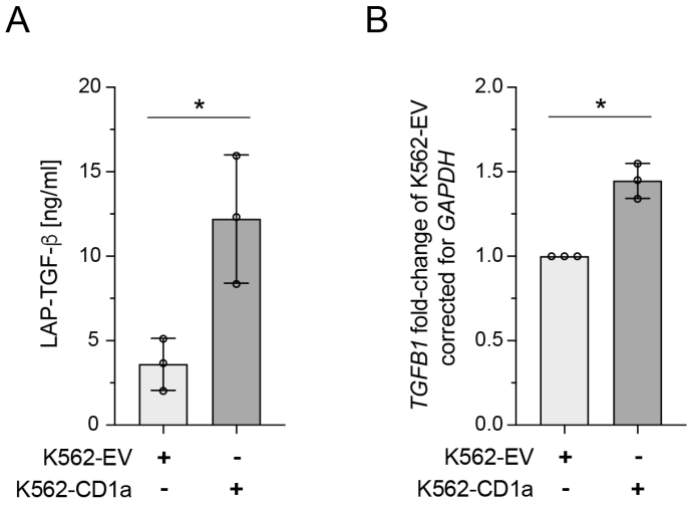

Fig. 2.10 K562-CD1a cells express higher levels of TGF-β compared to K562-EV cells.
(A) LAP-TGF-β secretion of K562-EV and K562-CD1a cells, as measured by ELISA. **(B)** *TGFB1* mRNA expression relative to *GAPDH* measured by RT-qPCR and shown as fold-change of K562-EV. (n=3 donors; (A) 3 and (B) 2 independent experiments). *P < 0.05; **P < 0.01; ***P < 0.001; Two-tailed paired t-test (mean ± SD).

For this reason, cell-free CD1a stimulation using CD1a-coated beads was employed to study TGF-β secretion by polyclonal Tregs. Antibodies binding the active form of TGF-β are not commercially available and, at the time of the presented experiments, no assays detecting active TGF-β secretion were available. Therefore, secretion of LAP-TGF-β was studied using a home-made LAP-TGF-β secretion assay (see 6.7.2.2 LAP-TGF-β Secretion Assay). Stimulating polyclonal Tregs with CD1a-coated beads showed a non-significant trend towards increased LAP-TGF-β secretion (2.41% ± 1.58) compared to the empty bead control (1.73% ± 0.95) (Fig. 2.11, A, B). This increase in LAP-TGF-β secretion was CD1a-dependent, as blocking of CD1a using anti-CD1a antibody reduced LAP-TGF-β secretion (1.81% ± 1.06) to a similar level as the empty bead control. CD1a stimulation-induced secretion of LAP-TGF-β by Tregs was negatively correlated with secretion of IL-10 (Fig. 2.11, C, D). Comparing secretion of LAP-TGF-β and IL-10 upon CD1a-coated bead stimulation, the Pearson correlation coefficient was -0.6862 (95% confidence interval: -0.9375 to 0.0358; not significant) (Fig. 2.11, C). When comparing LAP-TGF-β secretion upon stimulation with CD1a-coated beads with IL-10 secretion upon stimulation with K562-CD1a cells, the negative correlation was significant with a Pearson correlation coefficient of -0.8155 (95% confidence interval: -0.9718 to -0.1619; p=0.025) (Fig. 2.11, D).

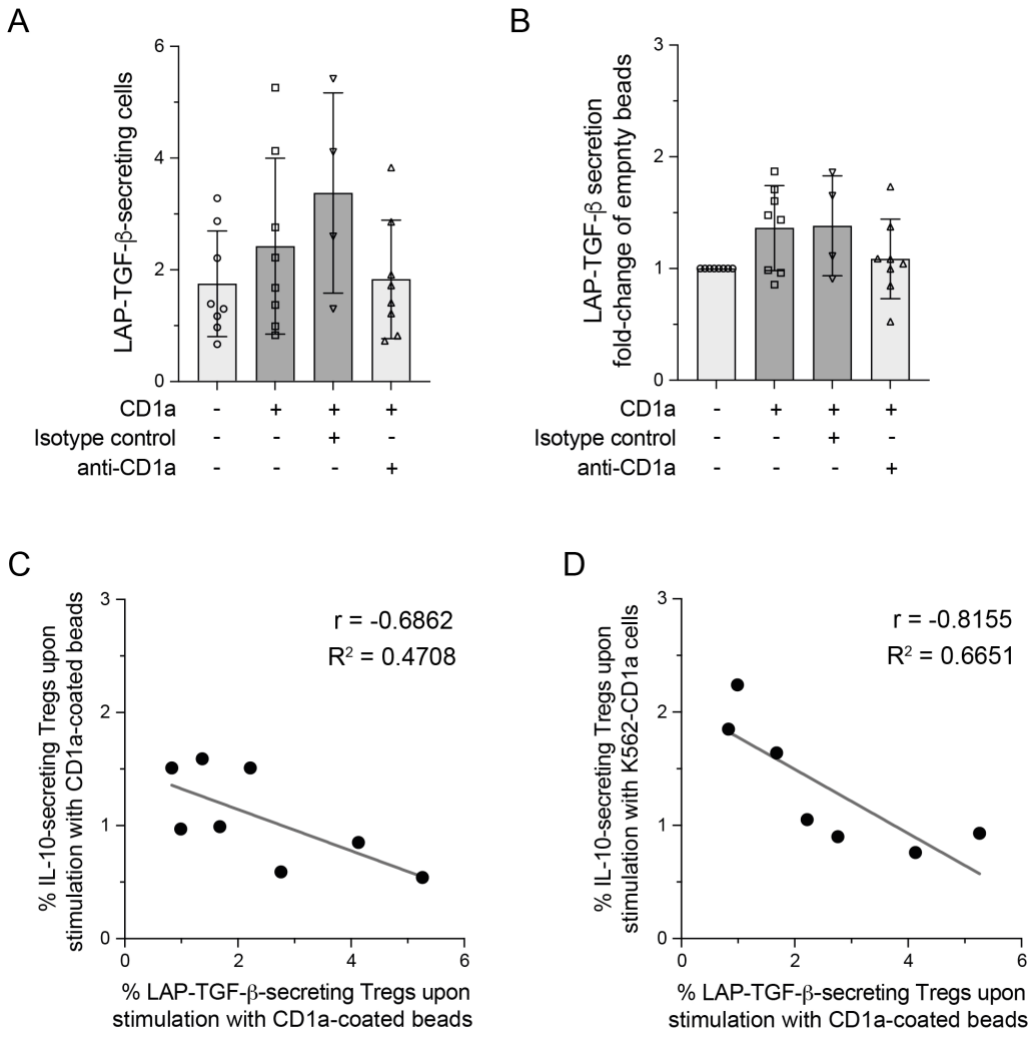

Fig. 2.11 LAP-TGF-β secretion of CD1a-stimulated polyclonal Tregs.

Expanded Tregs were co-cultured with CD1a-coated beads or empty beads as control in the absence or presence of anti-CD1a antibody (clone HI149) or an isotype control. Tregs were co-stimulated with IL-2 and anti-CD11a. **(A, B)** Secretion of LAP-TGF-β by Tregs measured by secretion assay as **(A)** percentage of Tregs, gated on live $CD3^+CD4^+CD25^+CD127^{low}$ cells, and **(B)** fold-change of the empty bead control. **(C, D)** Correlation between LAP-TGF-β secretion of Tregs upon CD1a-coated beads stimulation and IL-10 secretion upon stimulation with **(C)** CD1a-coated beads or **(D)** K562-CD1a cells. r indicates the Pearson correlation coefficient; R^2 indicates the coefficient of correlation for the linear fit. (n=4-8 donors; 2 independent experiments). ns > 0.05; *P < 0.05; RM Mixed-effects analysis with Tukey's correction for multiple comparison (mean ± SD).

To investigate whether CD1a stimulation induces *TGFB1* transcription, polyclonal Tregs were co-cultured for 2h or 4h with CD1a-coated beads or empty beads as control in the absence and presence of anti-CD1a antibody or an isotype control. *TGFB1* mRNA levels relative to *CD2* were measured by RT-qPCR. *TGFB1* transcription was slightly increased for all conditions in which CD1a-coated beads were present (Fig. 2.12). This reached significance for Tregs stimulated with CD1a-caoted beads in the presence of the isotype control at 4h, showing a 1.36-fold increase of *TGFB1* mRNA expression compared to the empty bead control. However, the observed increase did not seem to be CD1a-specific, as blocking of CD1a with anti-CD1a antibody did not reduce *TGFB1* mRNA levels back to the level observed for empty beads (1.30-fold increased compared to empty beads at 4h).

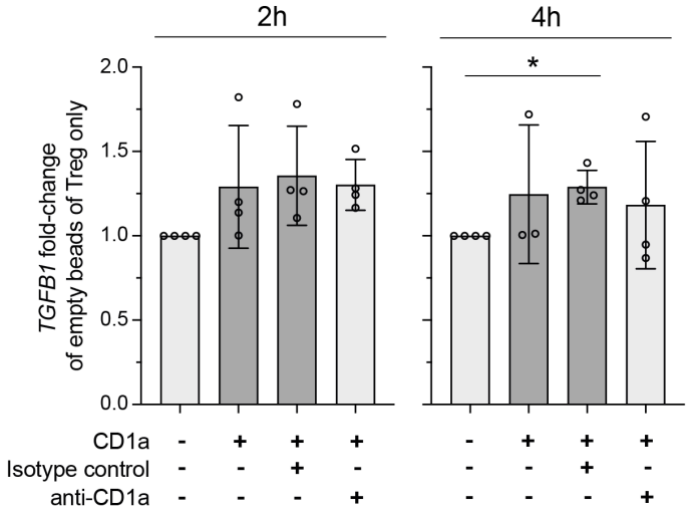

Fig. 2.12 *TGFB1* mRNA expression in polyclonal Tregs stimulated with CD1a-coated beads. Expanded Tregs were co-cultured for 2h or 4h with CD1a-coated beads or empty beads as control in the absence or presence of anti-CD1a antibody (clone HI149) or an isotype control. Tregs were co-stimulated with IL-2 and anti-CD11a. *TGFB1* mRNA expression relative to *CD2* was measured by RT-qPCR and is shown as fold-change of the empty bead control. (n=3-4 donors; 1 experiment). *P < 0.05; **P < 0.01; ***P < 0.001; RM One-way ANOVA (2h) or RM Mixed-effects analysis (4h) with Tukey's correction for multiple comparison (mean ± SD).

2.2.4 Polyclonal Tregs do not secrete skin inflammation-associated cytokines in a CD1a-dependent manner

Several cytokines, including GM-CSF, IL-13, IL-17A, IL-22 and IFNγ, contribute to the pathogenesis of skin inflammatory diseases such as psoriasis[397-399]. To investigate whether polyclonal Tregs secrete skin inflammation-associated cytokines in a CD1a-dependent manner, Tregs were stimulated with CD1a, and secretion of these cytokines was determined by secretion assays. Cytokine secretion by polyclonal Tregs was measured upon CD1a stimulation with K562-CD1a cells (Fig. 2.13, A) or CD1a-coated beads (Fig. 2.13, B). Secretion of all measured cytokines was ≤ 1% for Tregs stimulated with K562 cells. When Tregs were stimulated with beads, GM-CSF, IL-13 and IL-22 secretion was increased to approximately 5.0%, 2.2% and 4.7%, respectively. The presence of CD1a and the addition of the isotype control or anti-CD1a antibody led to a small increase in cytokines secretion for most cytokines compared to the K562-EV and empty bead control. This increase was significant for IL-13 and IL-17A secretion of Tregs stimulated with CD1a in the presence of anti-CD1a antibody compared to the K562-EV or empty bead control (Fig. 2.13, A, B). Moreover, the increase of IL-17A secretion by Tregs stimulated with CD1a-coated beads in the presence of the isotype control compared to CD1a-coated beads alone was significant. However, all increases were minimal compared to the baseline secretion for co-culture with K562-EV cells or empty beads and blocking of CD1a did not reduce cytokine secretion (Fig. 2.13, A, B). Taken together, these results suggest that Tregs do not secrete GM-CSF, IL-13, IL-17A, IL-22 or IFNγ in a CD1a-dependent manner.

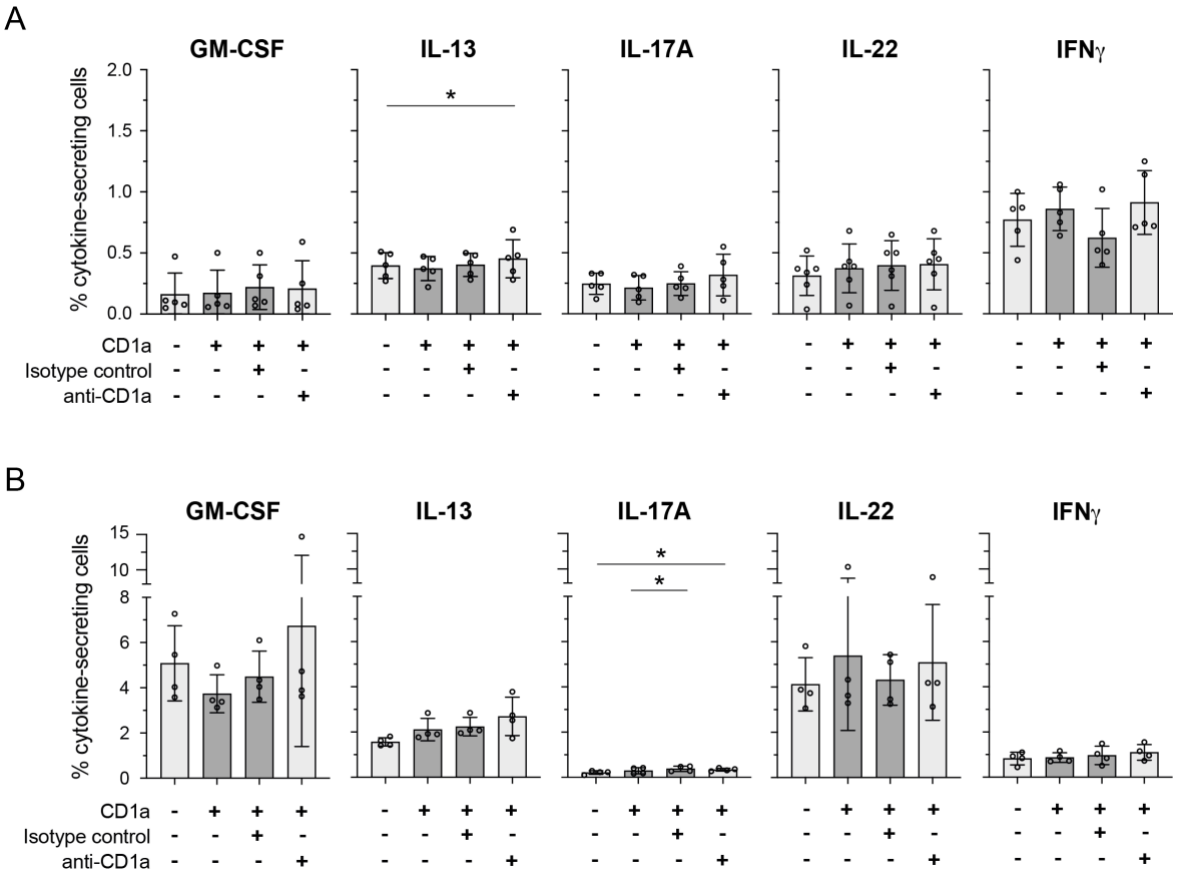

Fig. 2.13 Polyclonal Tregs do not secrete skin inflammation-associated cytokines in a CD1a-dependent manner.

Secretion of GM-CSF, IL-13, IL-17A, IL-22 and IFNγ by expanded polyclonal Tregs upon CD1a stimulation. Tregs were stimulated with **(A)** K562-CD1a cells or **(B)** CD1a-coated beads in the presence and absence of anti-CD1a (clone HI149) or an isotype control. K562-EV cells and empty beads served as control, respectively. Cells were co-stimulated with IL-2 and anti-CD11a, and secretion was determined by cytokine secretion assays, gating on live $CD3^{+}CD4^{+}CD25^{+}CD127^{low}$ cells. (n=4-6 donors; 2 (A) or 1 (B) independent experiments). *P < 0.05; **P < 0.01; ***P < 0.001; RM One-way ANOVA with Tukey's correction for multiple comparison (mean ± SD).

2.2.5 CD1a-reactive Tregs can secrete IL-10 in response to CD1a presenting skin-relevant lipids

CD1a can bind and present a variety of lipids present in the skin, including lysophosphatidylcholine (LPC) and sphingomyelin (SM)[34,134,135]. LPC is generated by PLA_2-mediated cleavage of phosphatidylcholine, which is a major component of mammalian cell membranes. PLA_2 from bee venom has further been shown to induce CD1a-mediated T cell responses[166,168]. Moreover, PLA_2 activity and LPC levels are increased in psoriatic skin[400-404]. SM is enriched in plasma membranes and SMs of differing length and saturation have been shown to differentially modulate CD1a-mediated effector T cell responses[34,134]. While CD1a-Tetramers loaded with SM 18:1 can bind to several CD1a-reactive T cell clones, the binding is partially blocked when CD1a is loaded with SM 24:0 and completely blocked when CD1a is loaded with SM 24:1[134]. In addition to self-lipids, the plant-derived lipid urushiol (C15:2) has been demonstrated to bind to CD1a, activate CD1a-mediated T cell responses and trigger CD1a-dependent skin inflammation[6].

To investigate the effect of these lipids on CD1a-mediated Treg responses, polyclonal Tregs were stimulated with lipid-pulsed K562 cells or beads coated with lipid-loaded CD1a. CD1a reactivity of Tregs was measured by IL-10 secretion assay. LPC, SM 18:1, SM 24:0 and SM 24:1 were dissolved in 0.5% CHAPS. Urushiol was dissolved in DMSO. IL-10 secretion of Tregs was unchanged in the presence of the solvent controls (0.5% CHAPS and DMSO) (Fig. 2.14, A, C). Pulsing of K562-CD1a cells with LPC and SM 18:1 showed a slight trend towards higher IL-10 secretion by Tregs compared to the unpulsed control (1.14- and 1.09-fold of the unpulsed control, respectively) (Fig. 2.14, B). In contrast, when K562-CD1a cells were pulsed with SM 24:0, secretion of IL-10 by Tregs was significantly decreased to 0.78-fold compared to the unpulsed control. Pulsing with SM 24:1 showed a non-significant

trend towards lower IL-10 secretion (0.90-fold of unpulsed control) (Fig. 2.14, B). When Tregs were stimulated with CD1a-coated beads (Fig. 2.14, D), loading of CD1a with LPC and SM 18:1 increased IL-10 secretion significantly by 1.61- and 1.34-fold compared to unloaded CD1a-coated beads, respectively. Comparing IL-10 secretion upon Treg stimulation with CD1a-coated beads loaded with different SMs, a gradual decrease of IL-10 secretion with rising chain length and unsaturation could be observed. While CD1a loaded with SM 18:1 induced an 1.34-fold increase in IL-10 secretion compared to the unloaded control, SM 24:0 slightly but not significantly increased IL-10 secretion by 1.19-fold, while IL-10 secretion was unchanged for CD1a loaded with SM 24:1. Stimulating Tregs with beads coated with urushiol-loaded CD1a, a slight but not significant 1.31-fold increase in IL-10 secretion compared to the unloaded control could be observed (Fig. 2.14, D). These results indicate that CD1a-reactive Tregs differentially recognise CD1a loaded with skin-relevant lipids, and that skin-relevant lipids may modulate TCR-CD1a interactions of Tregs similar but not identical to those of CD1a-reactive effector T cells.

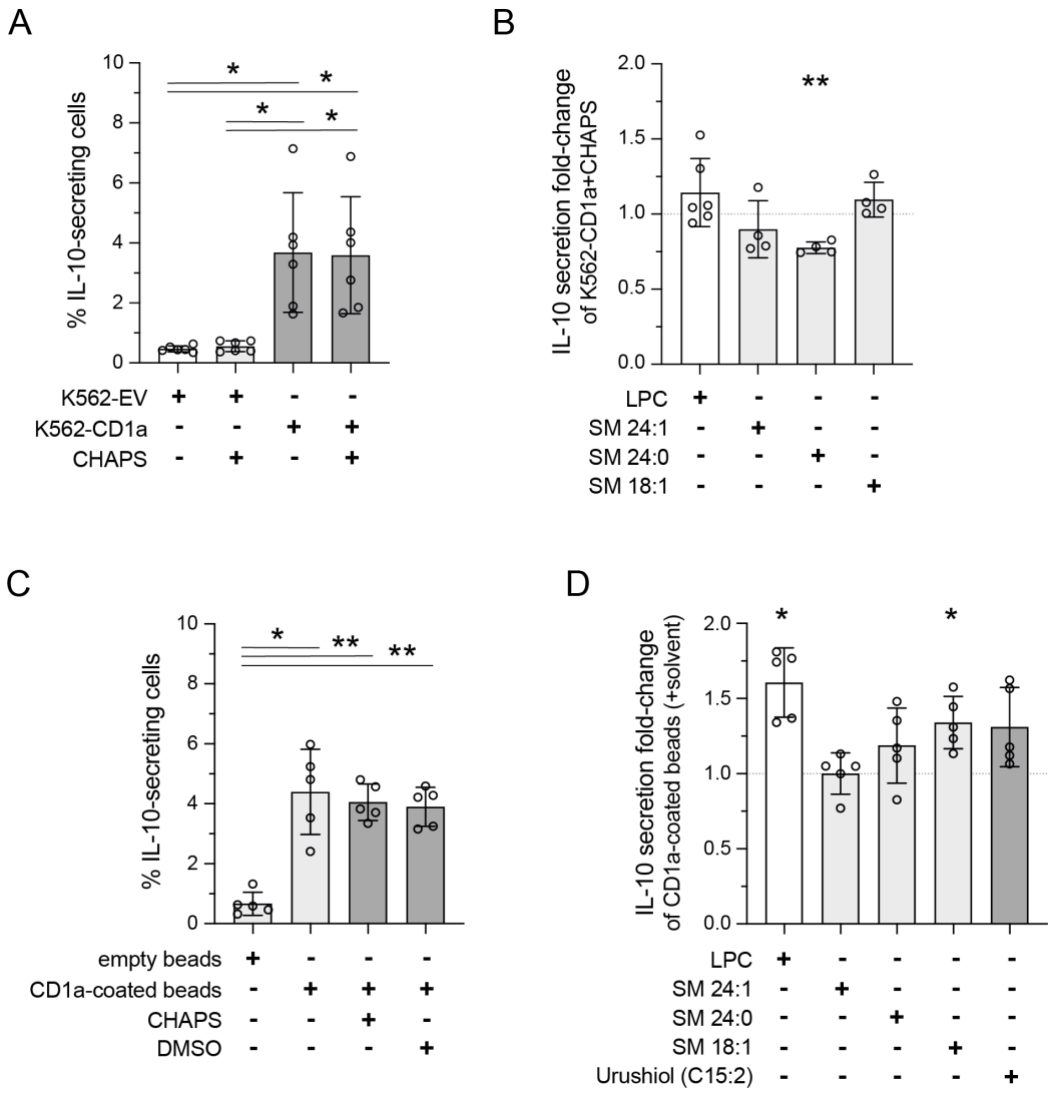

Fig. 2.14 CD1a-reactive IL-10-secreting Tregs recognise CD1a loaded with skin-relevant lipids. IL-10 secretion of expanded polyclonal Tregs upon stimulation with lipid-loaded CD1a. Tregs were either stimulated with **(A, B)** K562-CD1a cells or K562-EV cells as control, or **(C, D)** CD1a-coated beads using empty beads as control. Cells were co-stimulated with IL-2 and anti-CD11a. IL-10 secretion was determined by IL-10 secretion assay (gating on live $CD3^+CD4^+CD25^+CD127^{low}$ cells). **(A, B)** IL-10 secretion of Tregs upon co-culture with K562 cells pulsed with **(A)** the solvent control (0.5% CHAPS), or **(B)** 150-250µM of lysophosphatidylcholine (LPC), sphingomyelin (SM) 24:1, SM 24:0 or SM 18:1, as fold-change of K562-CD1a cells pulsed with 0.5% CHAPS. **(C, D)** IL-10 secretion of Tregs upon co-culture with beads coated with CD1a loaded with **(C)** the solvent controls (0.5% CHAPS or DMSO), or **(D)** LPC, SM 24:1, SM 24:0, SM 18:1, or urushiol (C15:2), as fold-change of CD1a-coated beads with the respective solvent control (DMSO for urushiol, CHAPS for the remainder). (n=4-6 donors; 2-3 independent experiments). *P < 0.05; **P < 0.01; ***P < 0.001; RM One-way ANOVA with (A, C) Tukey's or (B, D) Dunnett's correction for multiple comparison (mean ± SD).

2.2.6 CD1a-reactive IL-10-secreting Treg clones

Only a small subpopulation of circulating polyclonal Tregs (~2%) secretes IL-10 in a CD1a-dependent manner (Fig. 2.2, Fig. 2.6). To study suppressive functionality and identify CD1a-reactive TCRs, single-cell clones of CD1a-reactive IL-10-secreting Tregs were generated and expanded to sufficient numbers for functional assays (Fig. 2.15, A).

2.2.6.1 Generation of CD1a-reactive IL-10-secreting Treg clones

Polyclonal Tregs were isolated from peripheral blood of healthy donors and expanded for one week with anti-CD3/anti-CD28 microbeads, and rested overnight before stimulation with CD1a-coated beads (coated with CD1a-"endo" containing endogenous lipids from cell of origin, or LPC-loaded CD1a). IL-10-secreting Tregs were single-cell sorted, gating on live $CD3^{+}CD4^{+}CD25^{+}CD127^{low}$ cells (Fig. 2.15, B), and stimulated with feeder cells in the presence of high levels of IL-2 (see 6.4.6 Generation and culture of CD1a-reactive Treg clones). Treg clones were re-fed with fresh feeders after 3 weeks and subsequently every 2-3 weeks. In total, 30 Treg clones from 3 donors (13, 10 and 7 from one donor each) expanded enough for further analysis.

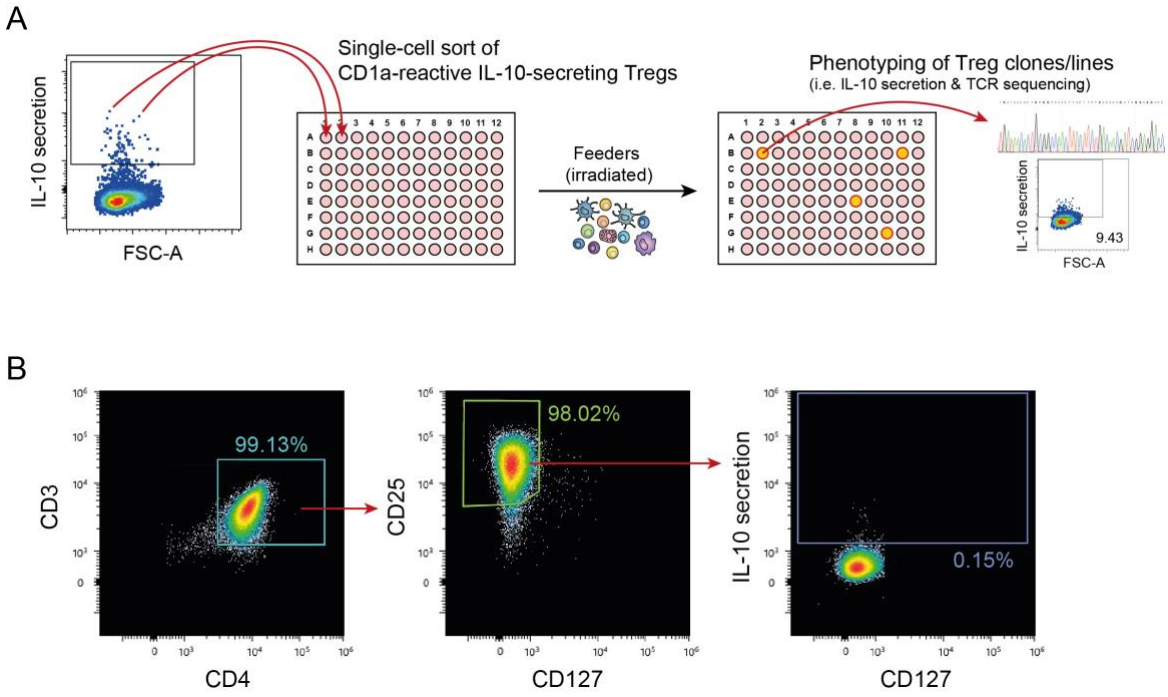

Fig. 2.15 Generation of Treg clones.

(A) Schematic of the single-cell Treg clone generation process. **(B)** Flow cytometry gating strategy for sorting of CD1a-reactive IL-10-secreting Treg clones. Arrows indicate gating on the parent population. Numbers indicate percentages of cells in the adjacent gates.

2.2.6.2 Phenotyping of IL-10-secreting CD1a-reactive Treg clones

To assess whether Treg clones maintained the expression of Treg lineage markers after the first expansion, CD127, CD25 and Foxp3 expression were determined by flow cytometry. Treg clones showed mostly low or minor expression of CD127, while expression of CD25 and Foxp3 was highly variable between Treg clones (Fig. 2.16).

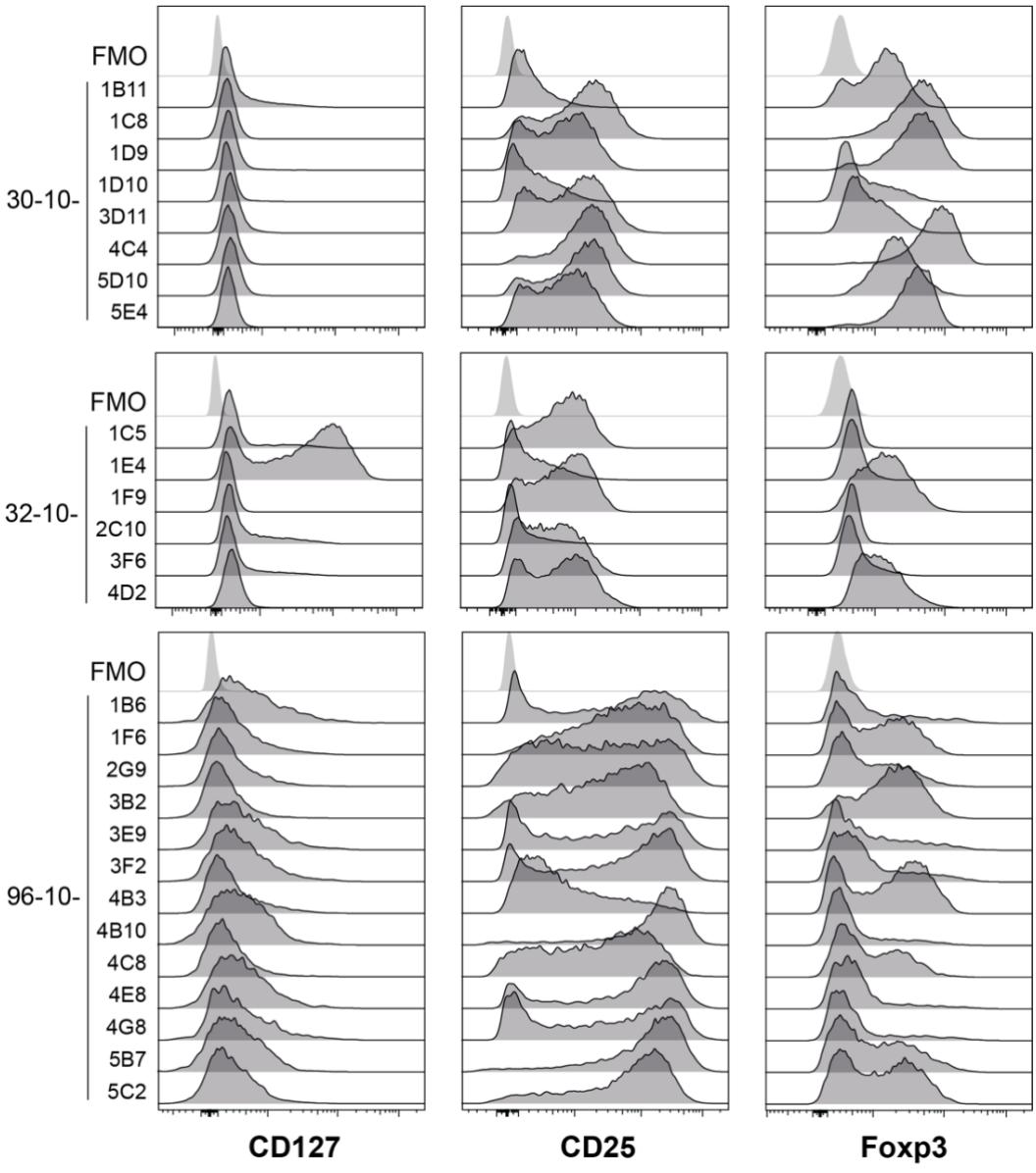

Fig. 2.16 Treg clones show varying expression of Treg lineage markers post expansion. Surface staining of CD127 and CD25 and intracellular staining for Foxp3 on individual Treg clones after the first expansion post single-cell sorting, gated on live $CD3^+CD4^+$ cells.

While some clones maintained high expression of both CD25 and Foxp3, i.e. 30-10-1C8, 32-10-1F9 and 96-10-3B2, other clones partially or completely lost CD25 and Foxp3 expression, i.e. 30-10-1D10, 32-10-1E4 and 96-10-4G8. Three Treg clones were not included in this initial analysis as re-feeding of these slower growing Treg clones was needed. CD25 expression was highly dependent on the activation status of the cells and varied depending on the time elapsed post feeding. Foxp3 expression also varied between feedings but overall declined the longer the Treg clones were kept in culture. Freshly thawed and re-fed Treg clones (frozen after 3 feedings post sorting) showed low to medium Foxp3 expression, but high CD25 expression (Fig. 2.17). Additionally, Treg clones showed varying expression of GITR and intracellular CTLA-4 with most Treg clones expressing medium to high levels (Fig. 2.17).

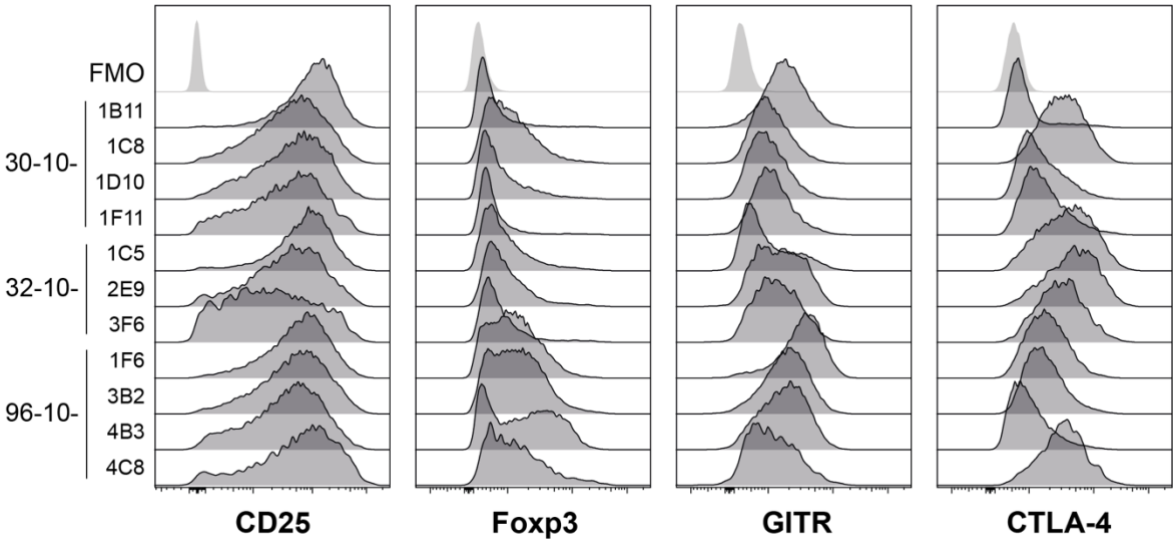

Fig. 2.17 Most Treg clones lose Foxp3 expression but retain varying expression of CD25, GITR and CTLA-4 during repeated rounds of expansion.

Surface staining of CD25 and GITR and intracellular staining for Foxp3 and CTLA-4 on individual Treg clones after freezing and expansion (feeding), gated on live $CD3^{+}CD4^{+}$ cells.

To determine whether CD1a-reactive Treg clones retained suppressive functionality, Treg clones were co-cultured at varying ratios with autologous PBMCs in the presence of anti-CD3/anti-CD28 microbeads for stimulation of T cell proliferation. Suppression of $CD4^+$ and $CD8^+$ T cell proliferation was determined by calculating the division index of each condition in comparison to $CD4^+$ and $CD8^+$ T cell proliferation in the absence of Tregs. The tested Treg clones were fed and expanded a total of 5 times at the time of the suppression assay. Several Treg clones efficiently inhibited T cell proliferation (Fig. 2.18). Treg clone 32-10-1C5 showed the highest suppressive capacity, suppressing 95% and 93% of $CD4^+$ and $CD8^+$ T cell proliferation at a 1:1 PBMC:Treg ratio, respectively, and still inhibiting proliferation by 49% and 48% at a ratio of 4:1, respectively. Overall, the inhibition of T cell proliferation by Treg clones was highly variable between different Treg clones, ranging between 32-95% (73.82% ± 23.35) and 10-93% (63.73% ± 28.01) for suppression of $CD4^+$ and $CD8^+$ T cell proliferation at a 1:1 PBMC:Treg ratio, respectively. Suppressive functionality did not generally correlate with expression of Treg markers such as Foxp3, CTLA-4 and GITR. For example, Treg clone 32-10-1C5 showed high suppressive capacity (Fig. 2.18) and expressed CTLA-4 and low levels of GITR and Foxp3 (Fig. 2.17), whereas 96-10-3B2 retained moderate levels of Foxp3 and GITR expression (Fig. 2.17) but showed low suppressive functionality (Fig. 2.18). It should be noted that the suppressive functionality of Treg clones was variable between feedings and time points and efficient suppression of T cell proliferation was not observed in every circumstance.

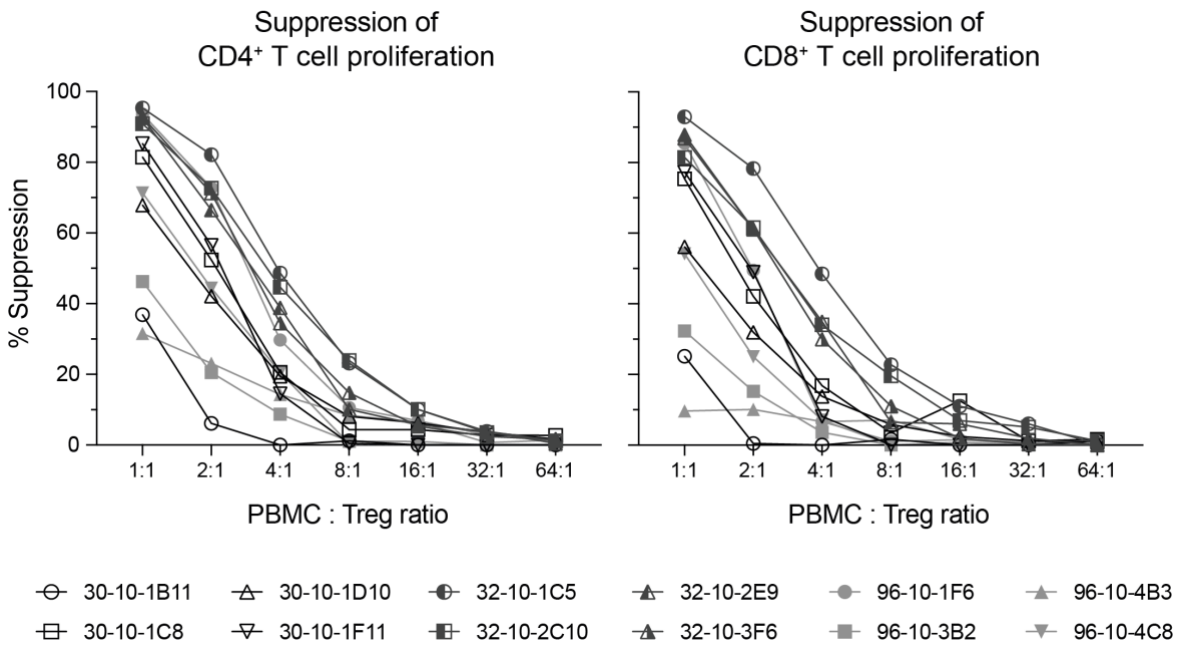

Fig. 2.18 Several Treg clones retain suppressive functionality.

Suppression of autologous $CD4^+$ and $CD8^+$ T cell proliferation by Treg clones as determined by division index. Treg clones were co-cultured with autologous PBMCs in the presence of anti-CD3/anti-CD28 microbeads (5:1 ratio PBMC:bead) for 3 days. Suppression was calculated relative to $CD4^+$ and $CD8^+$ T cell proliferation in the absence of Tregs, respectively. (n=12 Treg clones; 1 experiment).

2.2.6.3 CD1a-reactive IL-10-secreting Treg clones retain the ability to secrete IL-10 in a CD1-dependent manner

To assess whether Treg clones retained the ability to secrete IL-10 in response to CD1a stimulation, IL-10 secretion of Treg clones was measured upon stimulation with K562-CD1a cells or CD1a-coated beads. The stimulation of Treg clones with K562-CD1a cells showed a significant 6.3-fold increase in IL-10 secretion (8.26% ± 4.08) compared to the K562-EV control (1.92% ± 1.84) (Fig. 2.19, A, B). Addition of the isotype control did not change this increase significantly (7.98% ± 3.88), but IL-10 secretion was reduced to similar levels as the K562-EV control when CD1a was blocked with anti-CD1a (2.49% ± 2.75) (Fig. 2.19, A). Stimulating Treg clones in a cell-free assay using CD1a-coated beads, Treg clones showed a comparably lower but nevertheless significant increase in IL-10

secretion (5.30% ± 2.41) compared to the empty bead control (2.40% ± 1.39) (Fig. 2.19, C). This CD1a-induced IL-10 secretion was abrogated by CD1a blocking with anti-CD1a antibody (2.97% ± 2.26) but did not change in the presence of the isotype control (5.89% ± 3.03). CD1a-dependent IL-10 secretion of Treg clones could be observed, with some variation to levels of IL-10 secretion, after repeated feeding and expansion (≥ 5 times). Taken together, these data suggest that Treg clones retain the ability to secrete IL-10 in a CD1a-dependent manner. However, while IL-10 secretion was increased by 6.3-fold in the K562 cell stimulation system, this increase was much lower (2.4-fold) in the cell-free assay (Fig. 2.19, B, D). Additionally, unlike polyclonal Tregs (Fig. 2.2, Fig. 2.6), CD1a-reactive Treg clones secrete higher levels of IL-10 in the presence of antigen-presenting cells compared to cell-free CD1a stimulation (Fig. 2.19, A, C). This indicates that Treg clones may require additional co-stimulatory factors to efficiently interact with CD1a.

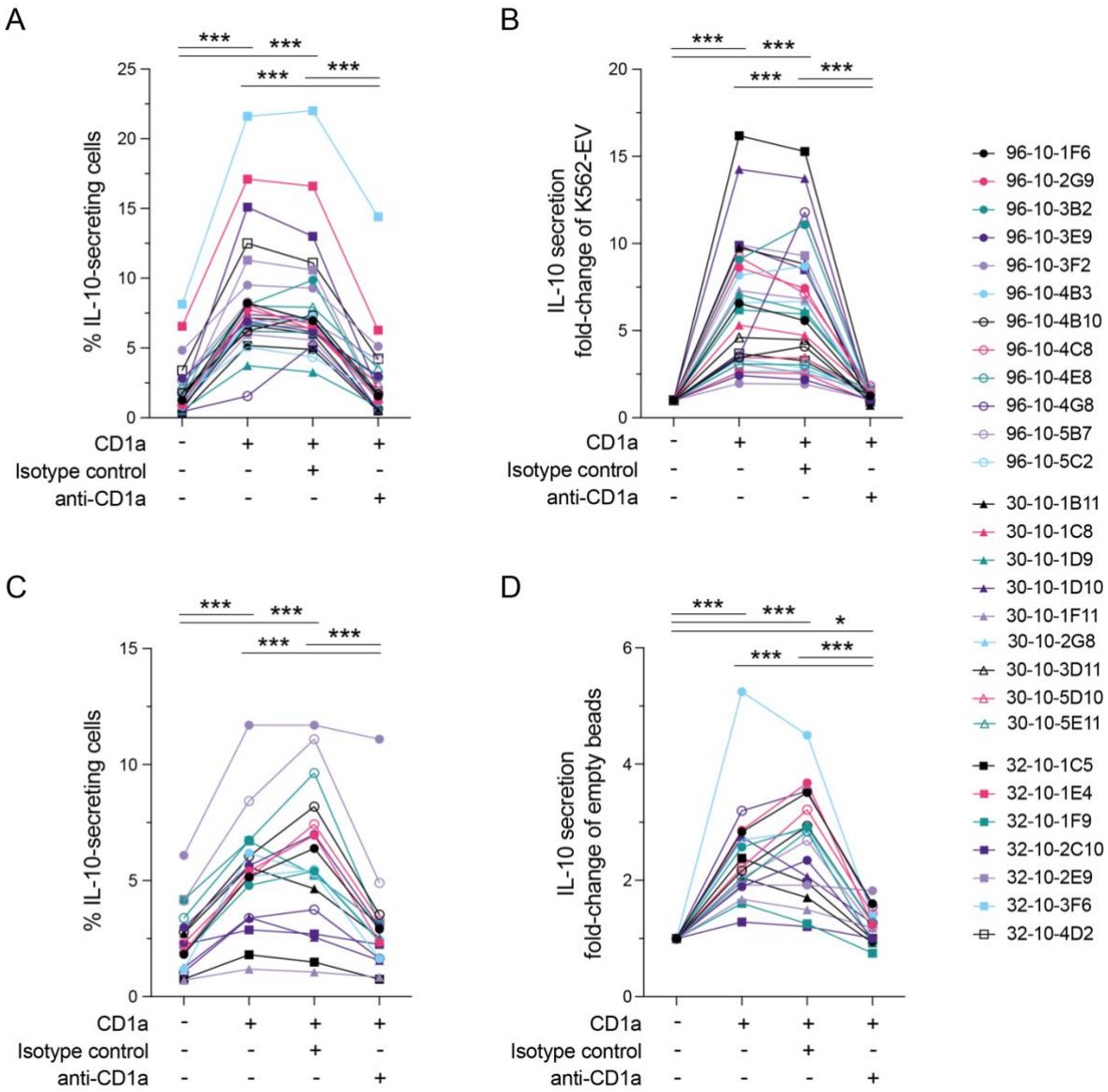

Fig. 2.19 Treg clones retain the ability to secrete IL-10 in a CD1a-dependent manner.

IL-10 secretion by Treg clones upon CD1a stimulation with **(A, B)** K562-CD1a cells or **(C, D)** CD1a-coated beads in the presence and absence of anti-CD1a (clone HI149) or an isotype control. Cells were co-stimulated with IL-2 and anti-CD11a. Secretion of IL-10 by Tregs was determined by IL-10 secretion assay, gating on live $CD3^+CD4^+$ cells. Every data point represents a different Treg clone, with lines connecting the same clone for different conditions. **(A, B)** IL-10 secretion upon co-culture with K562-CD1a cells or an K562-EV cells as control, as **(A)** percentage of live $CD3^+CD4^+$ cells and **(B)** fold-change of the K562-EV control. **(C, D)** IL-10 secretion upon stimulation with CD1a-coated beads or empty beads as control, as **(C)** percentage of live $CD3^+CD4^+$ cells and **(D)** fold-change of the empty bead control. (n=18-28 Treg clones; data shown is representative for ≥ 3 experiments). *P < 0.05; **P < 0.01; ***P < 0.001; RM One-way ANOVA with Tukey's correction for multiple comparison.

2.2.6.4 Effect of different co-stimulations on IL-10 secretion by CD1a-reactive Treg clones

Anti-CD3 and anti-CD28 are known T cell stimulators and are commonly used to stimulate Tregs during *in vitro* expansion. Previous experiments using polyclonal Tregs showed that anti-CD3/anti-CD28 co-stimulation can efficiently stimulate Tregs to secrete IL-10 in response to CD1a stimulation but also increases unspecific IL-10 secretion (Fig. 2.3, B). To investigate whether co-stimulation with anti-CD3 and anti-CD28 may increase CD1a-mediated IL-10 secretion of Treg clones, Tregs were stimulated with CD1a using CD1a-coated beads or K562-CD1a cells in the presence of different concentrations of anti-CD3 and anti-CD28. When Treg clones were stimulated with CD1a-coated beads in the presence of 2500ng/ml anti-CD3 and anti-CD28, several of the tested Treg clones showed high IL-10 secretion independent of stimulation with CD1a-coated beads (0.38-65.70%, 16.53% ± 22.23) or the empty bead control (0.17-67.90%, 15.74% ± 21.61) (Fig. 2.20, A). Reducing the concentration of anti-CD3/anti-CD28 co-stimulation to 200ng/ml reduced IL-10 secretion by Treg clones, but secretion remained comparable between stimulation with empty beads (0.05-23.90%, 6.17% ± 8.05) and CD1a-coated beads (0.36-21.90%, 7.38% ± 7.82) (Fig. 2.20, A). Using K562-CD1a cells for CD1a stimulation, Treg clones showed significantly increased IL-10 secretion when CD1a was present compared to the K562-EV control for all tested concentrations of anti-CD3/anti-CD28 co-stimulation (Fig. 2.20, B). Co-stimulating with 200ng/ml anti-CD3/anti-CD28, Treg clones showed 5.11% ± 9.66 (0.16-35.10%) IL-10 secretion when co-cultured with the K562-EV control, which was significantly increased to 34.77% ± 37.48 (0.99-98.20%) in the presence of CD1a. This increase in IL-10 secretion was comparable for the isotype control (33.03% ± 36.05) and could be partially but significantly blocked by anti-CD1a (16.80% ± 24.28), suggesting that IL-10 secretion of Treg clones upon anti-CD3/anti-CD28 co-stimulation is at least in part

CD1a-dependent. Reducing the co-stimulation concentration to 20ng/ml highly reduced CD1a-unspecific IL-10 secretion in the K562-EV control condition (1.45% ± 2.22) while still inducing a significant increase in IL-10 secretion (10.67-79.80%, 9.47% ± 27.08). A further reduction of anti-CD3/anti-CD28 co-stimulation to 2ng/ml reduced IL-10 secretion drastically, but IL-10 secretion was still increased upon CD1a stimulation (2.55% ± 2.46) compared to the control (0.60% ± 0.69). These data confirm previous results (Fig. 2.3, B) that anti-CD3/anti-CD28 co-stimulation during CD1a stimulation has the potential to aid Treg secretion of IL-10, but that non-specific IL-10 secretion is also increased.

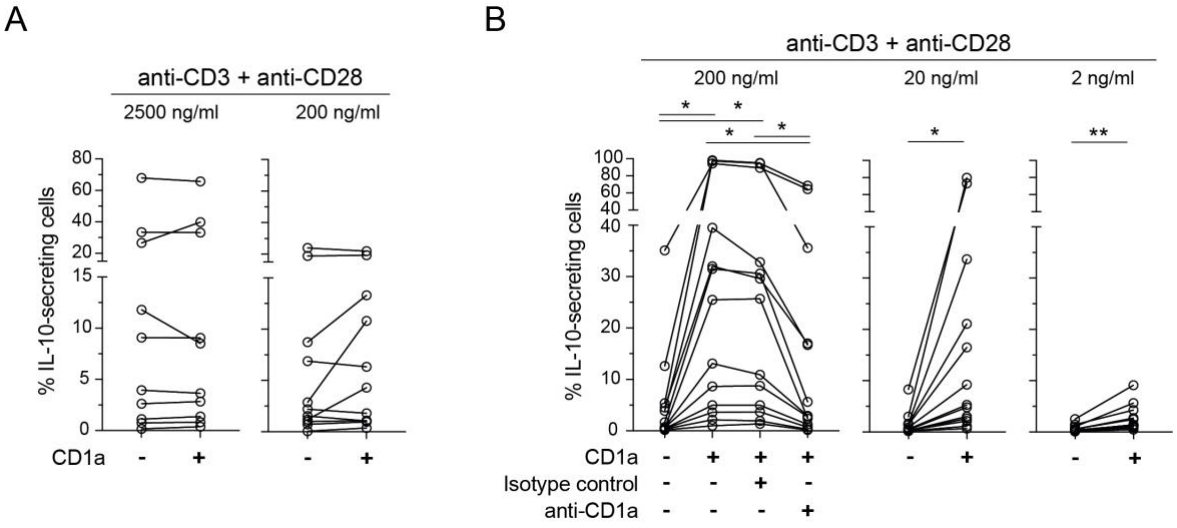

Fig. 2.20 Effect of anti-CD3/anti-CD28 co-stimulation on CD1a-mediated IL-10 secretion by Treg clones.

IL-10 secretion by Treg clones upon CD1a stimulation in the presence of IL-2 and varying concentrations of anti-CD3 and anti-CD28. Secretion of IL-10 by Tregs was determined by IL-10 secretion assay, gating on live $CD3^+CD4^+$ cells. Every data point represents a different Treg clone. Lines connect the same Treg clone for different conditions. **(A)** IL-10 secretion upon stimulation with CD1a-coated beads or empty beads as control, using 2500 or 200ng/ml anti-CD3 and anti-CD28 as co-stimulation. **(B)** IL-10 secretion upon co-culture with K562-CD1a cells or K562-EV cells as control in the presence and absence of anti-CD1a (clone HI149) or an isotype control. Anti-CD3 and anti-CD28 were added at 200, 20 or 2ng/ml during co-culture. (n=10-13 Treg clones; 1 experiment). *P < 0.05; **P < 0.01; ***P < 0.001; Two-sided paired t-test or RM One-way ANOVA with Tukey's correction for multiple comparisons.

To assess whether the observed increase in CD1a-unspecific IL-10 secretion upon co-stimulation with anti-CD3/anti-CD28 may be contributed to one or the other antibody, Treg clones were stimulated with K562-CD1a cells in the presence of anti-CD11a and 20ng/ml anti-CD3 or anti-CD28, respectively (Fig. 2.21, A). The addition of anti-CD28 induced comparable IL-10 secretion (0.97% ± 0.37 for K562-EV and 5.75% ± 1.87 for K562-CD1a) as co-stimulation with anti-CD11a alone (0.77% ± 0.31 for K562-EV and 5.05% ± 1.78 for K562-CD1a). In contrast, addition of anti-CD3 increased IL-10 secretion of Treg clones for both co-culture with K562-EV cells (1.73% ± 0.71) and K562-CD1a cells (28.80% ± 35.37). These data indicate that anti-CD3 co-stimulation is the dominant driving factor of non-specific IL-10 secretion of Treg clones.

In addition to antibodies, many cytokines are known to modulate IL-10 production and/or Treg function. IL-4 has been proposed to support suppressive immune responses of Tregs and enhance IL-10 production in Th1 cells[392-394]. IL-27, a member of the IL-12 cytokine family, has been demonstrated to promote IL-10 production by many different T cell types, including Tregs[405-407], and IL-21 induction *via* IL-27 has been shown to induce IL-10 production by Tr1 cells[395]. Additionally, TCR priming in the presence of IL-21 has been proposed to result in the accumulation of T cells with an IL-10-dependent immunosuppressive phenotype[395,396]. Although mostly known for reversing Treg suppressive function and inducing IFNγ production, IL-12 has also been proposed to promote Th1-like Tregs and prime CD4 and CD8 T cells for IL-10 production[408-411]. Although IL-7Rα (CD127) is expressed at low levels on Tregs rendering them largely insensitive to IL-7-mediated effects, several studies reported that IL-7 and IL-7R signalling can contribute to Foxp3 expression, Treg-mediated tolerance and Treg suppressive function[412,413]. Similarly, IL-15 can contribute to Foxp3 expression and Treg stability as well as Treg suppressive function[412,414]. Moreover, IL-33 can promote Treg activity in the gut

and *via* TLR and suppression of tumorigenicity 2 (ST2) signalling further promotes survival, proliferation and suppressive functionality of Tregs[412]. To investigate whether either or combinations of these cytokines could increase CD1a-mediated Treg clone secretion of IL-10, Treg clones were stimulated with K562-CD1a cells in the presence of anti-CD11a and IL-4, IL-7, IL-12, IL-15, IL-21, IL-27, or IL-33.

The addition of IL-4 and IL-21, IL-7, IL-15, IL-27, or IL-33 during CD1a stimulation of Treg clones with K562-CD1a resulted in comparable increases of IL-10 secretion (4.92% ± 1.44, 5.10% ± 1.31, 5.58% ± 1.38, 5.48% ± 1.45, 5.93% ± 1.83, respectively) as to co-stimulation with anti-CD11a only (5.05% ± 1.78) (Fig. 2.21, A). While addition of IL-12 increased IL-10 secretion upon CD1a stimulation to 9.60% ± 4.06, IL-10 secretion was also increased for the K562-EV control, leading to a similar fold-increase (7.6-fold) compared to co-stimulation with anti-CD11a only (6.5-fold). When adding a combination of IL-4, IL-7 and IL-33, IL-10 secretion by Treg clones was comparable to co-stimulation with anti-CD11a only (Fig. 2.21, B). The addition of IL-15 combined with IL-21 showed similar IL-10 secretion compared to anti-CD11a alone for 3 of 4 tested Treg clones. However, one clone showed highly increased non-specific IL-10 secretion (Fig. 2.21, B). When adding IL-12 combined with IL-27 or a combination of all tested cytokines, the same Treg clone showed drastically higher IL-10 secretion compared to the other tested Treg clones. Although IL-10 secretion was slightly increased in the other three Treg clones upon CD1a stimulation compared to anti-CD11a only, also higher non-specific IL-10 secretion could be observed. Paired with differential responses of different Treg clones, this resulted in a much lower average fold-increase in IL-10 secretion upon CD1a stimulation in the presence of IL-12 combined with IL-27 or a combination of all tested cytokines (1.5- and 1.4-fold, respectively) compared to co-stimulation with anti-CD11a only (6.6-fold) (Fig. 2.21, B). Taken together with previous results obtained for CD1a-mediated IL-10 secretion in

polyclonal Tregs (Fig. 2.4), these results suggest that co-stimulation with the here tested cytokines in addition to anti-CD11a does not significantly increase IL-10 secretion of Treg clones in a CD1a-dependent manner.

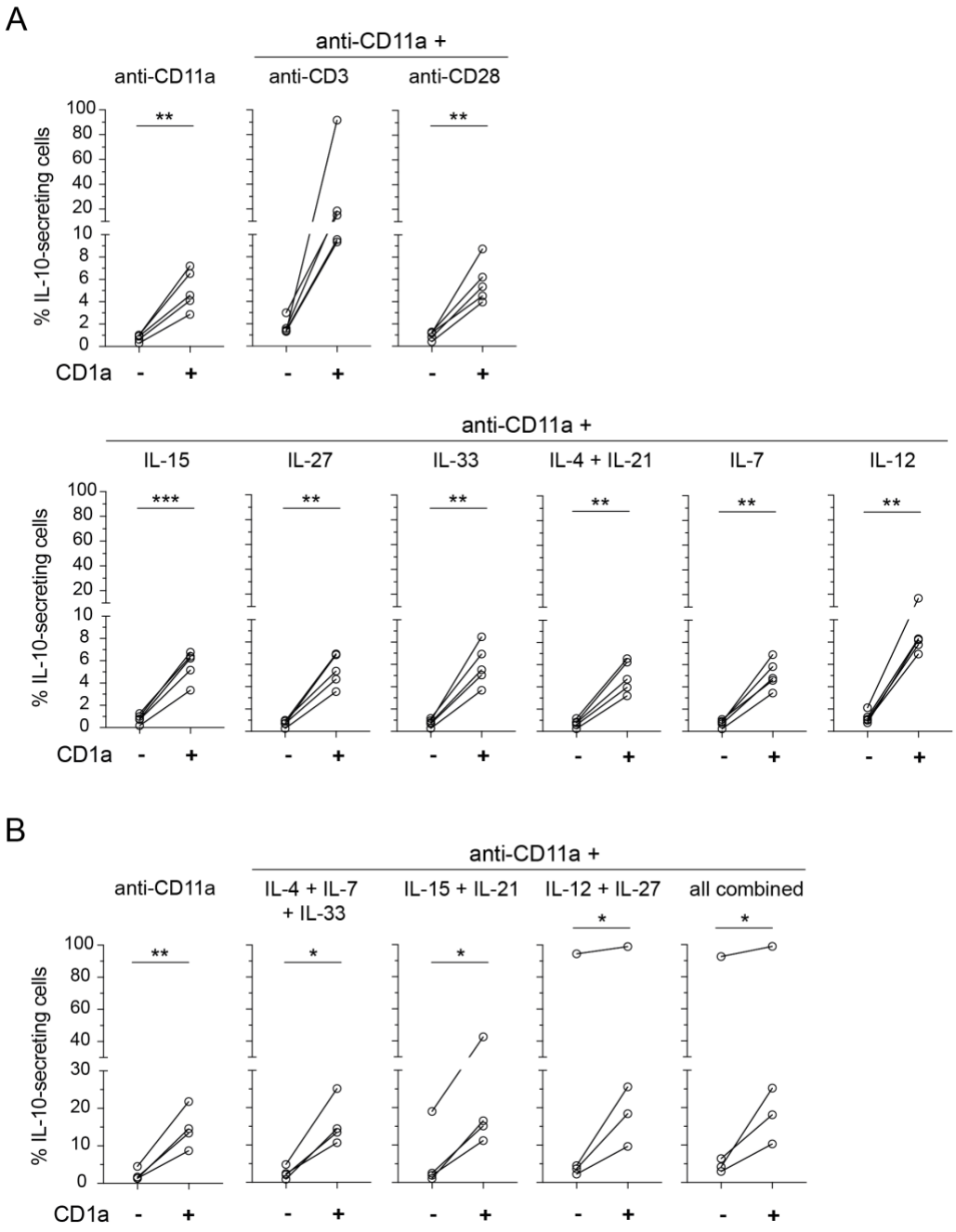

Fig. 2.21 Effect of different co-stimulations on CD1a-dependent IL-10 secretion by Treg clones. Treg clones were co-cultured with K56-CD1a cells or K562-EV cells as control, using IL-2 and anti-CD11a combined with different antibodies or cytokines as co-stimulation. Each data point represents a different Treg clone. Lines connect the same clone for different conditions. **(A)** IL-10 secretion of Treg clones upon co-stimulation with 2500ng/ml anti-CD11a combined with 20ng/ml of anti-CD3, anti-CD28, IL-4 and IL-21, IL-7, IL-12, IL-15, IL-27, or IL-33. (n=5 Treg clones; 1 experiment). **(B)** IL-10 secretion of Treg clones upon co-stimulation with 2500ng/ml anti-CD11a combined with 20ng/ml of IL-4, IL-7 and IL-33, or IL-15 and IL-21, or IL-12 and IL-27, or a combination of all. (n=4 Treg clones; 1 experiment). *P < 0.05; **P < 0.01; ***P < 0.001; Two-tailed paired t-test.

2.2.6.5 Secretion of LAP-TGF-β by CD1a-reactive Treg clones

Tregs can use the immunomodulatory cytokine TGF-β to exert their suppressive function[248]. To investigate whether CD1a-reactive Treg clones show a similar trend towards increased LAP-TGF-β secretion as observed for polyclonal CD1a-reactive Tregs (Fig. 2.11), CD1a stimulation using CD1a-coated beads was employed to study LAP-TGF-β secretion by Treg clones. Treg clones secreted very low levels of LAP-TGF-β in the presence of the empty bead control (0.56% ± 0.12) (Fig. 2.22). Stimulating Treg clones with CD1a-coated beads significantly reduced LAP-TGF-β secretion to 0.28% ± 0.15. However, LAP-TGF-β secretion was comparable between Treg clones stimulated with CD1a-coated beads in the presence of the isotype control (0.35% ± 0.27) or anti-CD1a antibody (0.35% ± 0.19). These data indicate that the Treg clones do not secrete LAP-TGF-β in a CD1a-dependent manner.

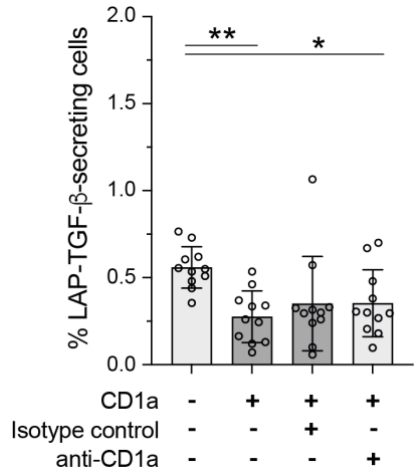

Fig. 2.22 LAP-TGF-β secretion of CD1a-stimulated Treg clones.

Treg clones were co-cultured with CD1a-coated beads or empty beads as control in the absence or presence of anti-CD1a antibody (clone HI149) or an isotype control. Treg clones were co-stimulated with IL-2 and anti-CD11a. Secretion of LAP-TGF-β was measured by secretion assay. Each data point represents a different Treg clone. (n=11 Treg clones; 2 independent experiments). *P < 0.05; **P < 0.01; ***P < 0.001; RM One-way ANOVA with Tukey's correction for multiple comparison (mean ± SD).

2.2.6.6 Secretion of skin inflammation-associated cytokines by CD1a-reactive Treg clones

To study Treg clone cytokine production and upregulation upon CD1a stimulation, levels of different cytokines were measured in the supernatant of Treg clones cultured in the presence or absence of K562 cells. Cytokine levels of prepared supernatants were kindly measured by Dr Yi-Ling Chen using LEGENDplex technology. In total, 12 cytokines were investigated: chemokine ligand 5 (CCL5; Rantes), GM-CSF, granzyme A, granzyme B, granulysin, IFNγ, IL-10, IL-17A, IL-22, TNFα, programmed death-ligand 1 (PD-L1) and perforin. Levels of IL-10, IL-22, TNFα and PD-L1 were below detection limit or only detectable at very low levels in ≤ 3 samples and were therefore excluded from further analysis. In the absence of K562 cells, Treg clones showed significantly higher levels of IFNγ, CCL5, perforin and granzyme B as upon co-cultured with K562 cells, irrespective of CD1a expression (Fig. 2.23, C, D, E, G). IL-17A levels were overall very low (≤ 0.05ng/ml), but Treg clones secreted increased levels in the presence of K562 cells (Fig. 2.23, B). Compared to Treg clones only (0.032ng/ml ± 0.03), IL-17A levels were slightly but not significantly higher for co-culture with K562-EV cells (0.032ng/ml ± 0.03) but significantly increased when K562-CD1a cells were present (0.043ng/ml ± 0.03) (Fig. 2.23, B). GM-CSF and IFNγ levels showed a non-significant trend toward increased levels upon CD1a stimulation (2.19ng/ml ± 3.19 and 1.29ng/ml ± 1.66, respectively) compared to the K562-EV control (0.98ng/ml ± 1.22 and 0.80ng/ml ± 0.65, respectively) (Fig. 2.23, A, C). Similarly, granzyme A levels were significantly increased upon co-culture with K562-CD1a cells (MFI: 28255 ± 16667) compared to the K562-EV control (MFI: 20512 ± 10460) (Fig. 2.23, F). In contrast, CCL5 showed a trend towards lower levels in the presence of K562-CD1a cells (0.14ng/ml ± 0.15) compared to K562-EV cells (0.27ng/ml ± 0.38) (Fig. 2.23, D). Levels of perforin, granzyme B and granulysin were comparable in the presence

or absence of CD1a stimulation (Fig. 2.23, E, G, H). These data indicate that CD1a-reactive Treg expression of cytokines other than IL-10 may also be modulated by CD1a stimulation.

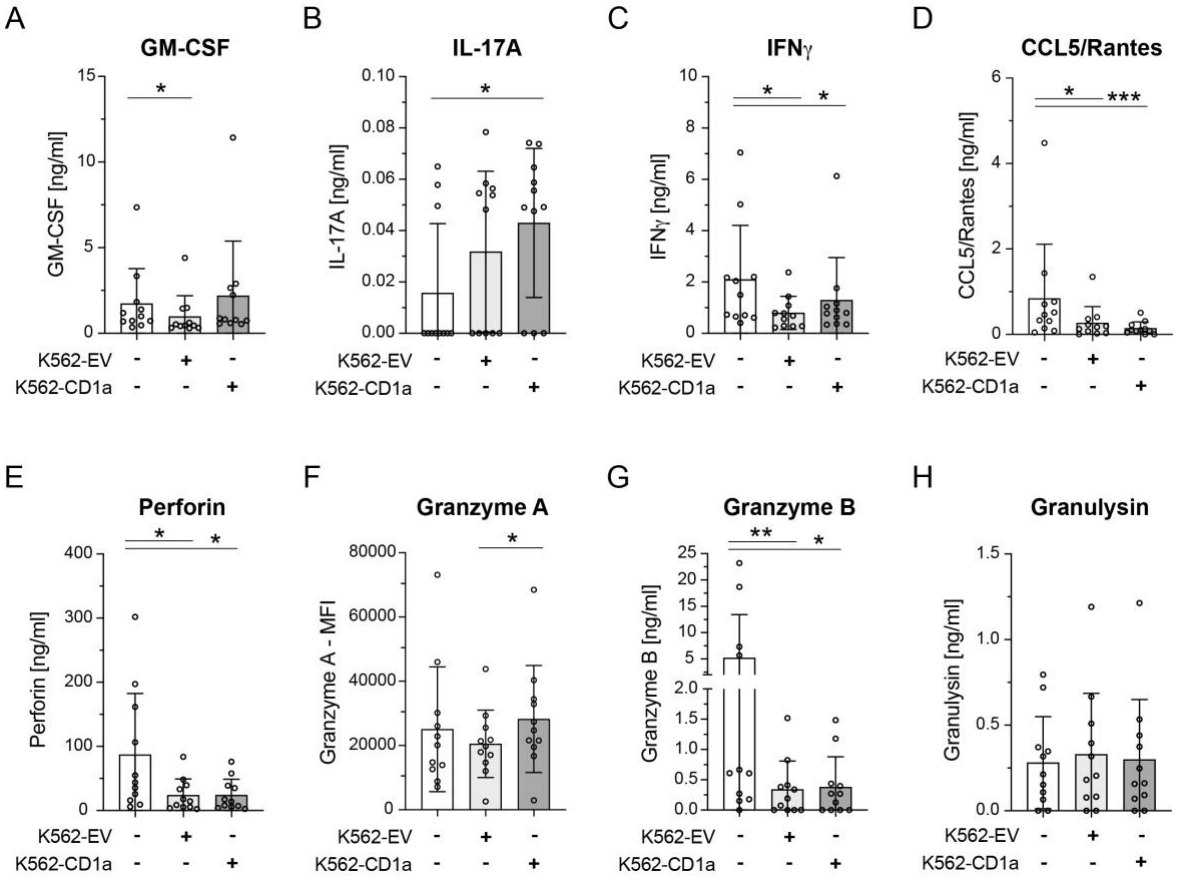

Fig. 2.23 Cytokine production of Treg clones in the absence or presence of K562 cells and CD1a stimulation.

Cytokine levels produced by Treg clones only and during co-culture with K562-EV and K562-CD1a cells were measured by LEGENDplex. Cells were co-stimulated with IL-2 and anti-CD11a and supernatants harvested after 24h. Levels of **(A)** GM-CSF, **(B)** IL-17A, **(C)** IFNγ, **(D)** CCL5, **(E)** perforin, **(F)** granzyme A, **(G)** granzyme B and **(H)** granulysin in culture supernatants. Granzyme A levels are given as MFI values as measured MFIs were higher than the detection limit and therefore quantification was not possible. All values below the respective detection limit were set to zero. IL-10, IL-22, TNFα and PD-L1 levels were below detection limit or only detectable at very low levels in ≤ 3 samples and were therefore excluded. Each data point represents a different Treg clone. (n=11 Treg clones; 1 experiment). *P < 0.05; **P < 0.01; ***P < 0.001; (A, C, E, F) RM One-way ANOVA with Tukey's correction for multiple comparison or (B, D, G, H) Friedman test with Dunn's correction for multiple comparison (mean ± SD).

To confirm these findings, to study the CD1a-dependency of GM-CSF, IL-17A and IFNγ production by Treg clones, and to extend the findings to additional cytokines relevant in skin inflammation, cytokine secretion assays for GM-CSF, IL-13, IL-17A, IL-22 and IFNγ were performed. Treg clones were stimulated with CD1a by co-culture with K562-CD1a cells in the absence or presence of anti-CD1a antibody or an isotype control, using K562-EV cells as control. Cells were co-stimulated with IL-2 and anti-CD11a. In contrast to polyclonal Tregs (Fig. 2.13), Treg clones secreted substantial levels of GM-CSF, IL-13 and IFNγ when co-cultured with K562-EV cells (5.66% ± 4.78, 11.40% ± 9.40 and 4.16% ± 2.57, respectively), which was further increased in the presence of CD1a (14.25% ± 11.31, 26.44% ± 22.90 and 8.08% ± 4.87, respectively) (Fig. 2.24). This increase was significant for IFNγ secretion. Secretion of GM-CSF and IFNγ was comparable or higher in the presence or absence of CD1a blocking antibody, indicating that the observed increase in secretion upon co-culture with K562-CD1a cells was independent of CD1a. In contrast, blocking of CD1a partially but significantly reduced IL-13 secretion (18.39% ± 17.12) compared to the isotype control (33.02% ± 29.53). Secretion of IL-17A and IL-22 were comparably low between CD1a stimulation (1.32% ± 1.04 and 0.75% ± 0.45, respectively) and control (1.23% ± 0.88 and 0.79% ± 0.62, respectively). Taken together, these results suggest that Treg clones may secrete IL-13, but not GM-CSF, IL-17A, IL-22 and IFNγ, in a CD1a-dependent manner.

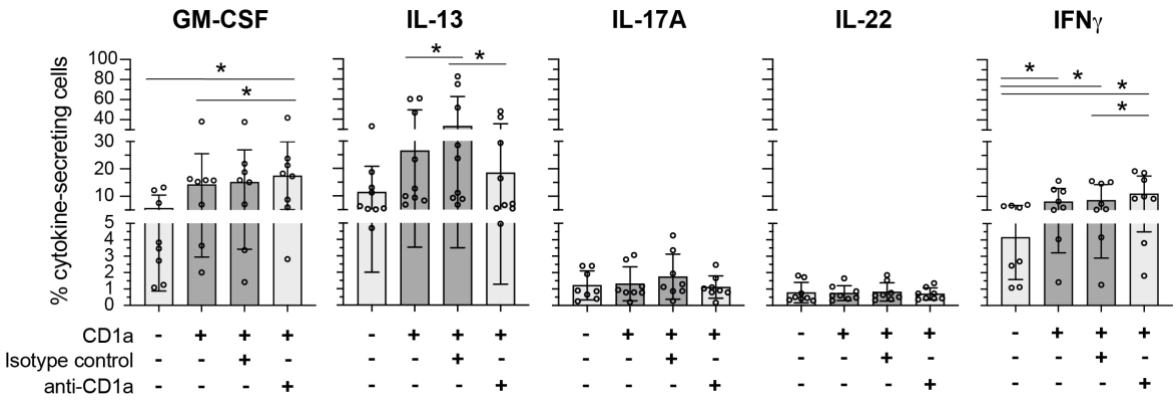

Fig. 2.24 Secretion of skin inflammation-associated cytokines by Treg clones.
Secretion of GM-CSF, IL-13, IL-17A, IL-22 and IFNγ by Treg clones upon CD1a stimulation with K562-CD1a cells or K562-EV cells as control in the presence or absence of anti-CD1a (clone HI149) or an isotype control. Cells were co-stimulated with IL-2 and anti-CD11a. Secretion was determined by cytokine secretion assays, gating on live $CD3^+CD4^+$ cells. (n=8 Treg clones; 2 independent experiments). *P < 0.05; **P < 0.01; ***P < 0.001; RM One-way ANOVA with Tukey's correction for multiple comparison (mean ± SD).

To assess whether Treg clones could be skewed towards a phenotype in which they produce higher levels of skin inflammation-associated cytokines, Treg clones were stimulated with CD1a in the presence of skewing cytokines. In addition to IL-2 and anti-CD11a, the following cytokines were added as co-stimulation: IL-1β and IL-12 for GM-CSF and IL-17A secretion assays, IL-4 and IL-33 for IL-13 secretion assays, IL-6 and TNFα for IL-22 secretion assays, and IL-12 and IL-18 for IFNγ secretion assays. Treg clones were stimulated with CD1a using K562-CD1a cells (Fig. 2.25, A) or CD1a-coated beads (Fig. 2.25, B), using K562-EV cells or empty beads as control, respectively. In response to K562 cell stimulation in the presence of skewing cytokines, Treg clones secreted GM-CSF, IL-13, IL-17A and IL-22 at comparable levels as Treg clones that were co-stimulated with IL-2 and anti-CD11a only (Fig. 2.24). In contrast, IFNγ secretion was highly upregulated from 4-8% (Fig. 2.24) to about 74% in the presence of IL-12 and IL-18 (Fig. 2.25, A, B). IFNγ secretion was comparable between CD1a stimulation and control as well as upon CD1a

blocking (Fig. 2.25, A), suggesting that this increase was not mediated by CD1a. GM-CSF secretion was slightly but significantly increased in Treg clones upon K562-CD1a stimulation (13.20% ± 12.97 compared to 8.66% ± 10.20 for K562-EV) (Fig. 2.25, A). Secretion of GM-CSF remained unchanged in the presence of the isotype control (13.74% ± 11.78) and was marginally but not significantly decreased upon CD1a blocking (11.36% ± 9.71), confirming previous results (Fig. 2.24) that GM-CSF secretion in Treg clones may be independent of CD1a. The trend towards increased CD1a-dependent secretion of IL-13 seen upon co-stimulation with IL-2 and anti-CD11a only (Fig. 2.24) was much lower and not significant in the presence of skewing cytokines (Fig. 2.25, A). When co-cultured with K562-EV cells, 18.71% ± 28.97 of Treg clones secreted IL-13 which was increased to 23.91% ± 31.43 in the presence of CD1a. This increase could be blocked by anti-CD1a antibody (15.38% ± 25.04). While IL-17A secretion of Treg clones was comparable between control and CD1a stimulation upon co-stimulation with IL-2 and anti-CD11a only (Fig. 2.24), the addition of skewing cytokines led to a CD1a-dependent increase in IL-17A secretion of Treg clones in the presence of K562-CD1a cells (Fig. 2.25, A). Treg clones secreted 1.02% ± 0.30 IL-17A when co-cultured with K562-EV cells, which was slightly but significantly increased in co-culture with K562-CD1a cells in the absence and presence of the isotype control to 1.30% ± 0.30 and 1.43% ± 0.50, respectively. Blocking of CD1a significantly reduced IL-17A secretion to 1.12% ± 0.35 (Fig. 2.25, A). Although IL-22 secretion was significantly increased upon CD1a stimulation, this increase was very minor, increasing IL-22 secretion from 0.54% ± 0.22 for the K562-EV control to 0.69% ± 0.23 for K562-CD1a. Treg clones were sorted based on IL-10 secretion, and therefore these observations are in line with results obtained from single-cell sequencing of CD1a-reactive Tregs (see Chapter 3) in which the frequency of the IL-10^{+}IL-22^{+} population was low (Fig. 3.8). Overall, Treg clone secretion levels for most cytokines were comparable between

stimulation with K562 cells (Fig. 2.25, A) and beads (Fig. 2.25, B). However, unlike stimulation with K562 cells, CD1a stimulation with CD1a-coated beads did not modulate cytokine secretion compared to empty beads for any cytokine or condition (Fig. 2.25, B).

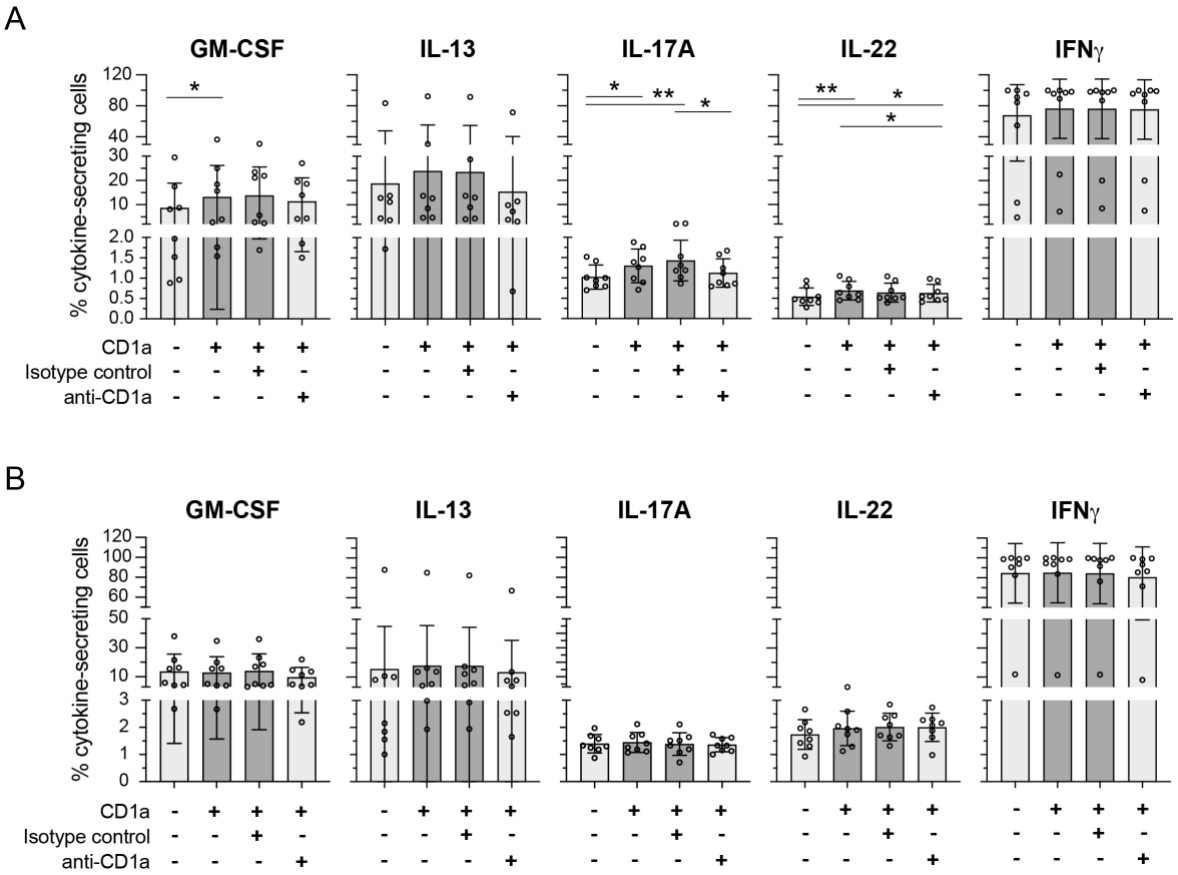

Fig. 2.25 Secretion of skin inflammation-associated cytokines by Treg clones in the presence of skewing cytokines.

Secretion of GM-CSF, IL-13, IL-17A, IL-22 and IFNγ by Treg clones upon CD1a stimulation. Tregs were stimulated with **(A)** K562-CD1a cells or **(B)** CD1a-coated beads in the presence and absence of anti-CD1a (clone HI149) or isotype control, using K562-EV cells or empty beads as control, respectively. IL-2 and anti-CD11a were used as co-stimulation in all conditions. The following cytokines were added as additional co-stimulation to the respective secretion assays: IL-1β and IL-12 for GM-CSF and IL-17A secretion assays, IL-4 and IL-33 for IL-13 secretion assays, IL-6 and TNFα for IL-22 secretion assays, and IL-12 and IL-18 for IFNγ secretion assays. Each data point represents a different Treg clone. (n=7-8 Treg clones; 2 independent experiments). *P < 0.05; **P < 0.01; ***P < 0.001; RM One-way ANOVA with Tukey's correction for multiple comparison (mean ± SD).

It should be noted that the cytokine secretion assays were performed so that secretion can be accurately quantified when ≤ 20% of cells secrete the measured cytokine. Detection of higher levels of cytokine secretion may not be accurate as high levels of cytokine secrete can result in paracrine binding.

2.2.6.7 TCR sequencing of CD1a-reactive Treg clones

CD1a-reactive effector T cells express α/β TCRs[150], but very few specific TCR sequences have been published[34,133,134,138]. As the Treg clones generated herein drifted from their original Treg phenotype, Treg clones are unlikely to present a viable therapeutic option for treatment of CD1a-mediated inflammation. However, there may be alternative approaches, such as the use of CD1a-reactive Treg TCRs with therapeutic potential, i.e. for TCR transduction of primary Tregs for the treatment of CD1a-mediated skin inflammation. To identify CD1a-reactive Treg clone TCRs, TCRα and TCRβ mRNA was amplified by polymerase chain reaction (PCR) and sequences were obtained by Sanger sequencing (see 6.11 TCR sequencing). For 25 Treg clones, both TCRα and TCRβ variable (V) and joining (J) regions could be identified. Combinations of TCRα V and J regions and TCRβ V and J regions of the different Treg clones are visualised in the chordDiagram in Fig. 2.26. All identified TCRα and TCRβ V and J regions, including isotypes, are listed in Table 2.1.

All Treg clones could be shown to express α/β TCRs (Table 2.1). Overall, Treg clones expressed highly variable α/β TCRs, but several V and J regions could be observed more frequently than others. Three or more Treg clones expressed the V regions TRAV2, TRAV13-1 and TRAV16 or the J regions TRAJ6 and TRAJ49. For TCRβ, the V region TRBV6-6 was expressed by 3 Treg clones and 5 Treg clones expressed the J regions TRBJ2-1 and TRBJ2-3. Although the expression of TCRαβ was highly variable between Treg clones, several pairs of Treg clones showed identical or very similar TCRαβ sequences.

The Treg clones 96-10-2G9 and 30-10-2G8, originating from different donors, both expressed TRAV13-1 (TRAV13-1*01 and TRAV13-1*02, respectively), TRBV20-1 (TRBV20-1*01 and TRBV20-1*02, respectively) and TRBJ-2*01, but differed in the expression of the TCRα J region (TRAJ37*02 and TRAJ10*01, respectively). The Treg clones 30-10-3D11 and 30-10-5E11, originating from the same donor, share the same TCRα V and J region (TRAV13-1*02, TRAJ6*01), but expressed different TCRβ sequences. Similarly, the Treg clones 32-10-1C5 and 32-10-2E9, originating from the same donor, share the same TCRα V and J region (TRAV8-3*01, TRAJ49*01), but the corresponding TCRβ sequences have not yet been successfully identified. These data indicate that although CD1a-reactive Tregs express a highly variable TCRαβ repertoire, specific TCRs may be enriched and shared between different donors.

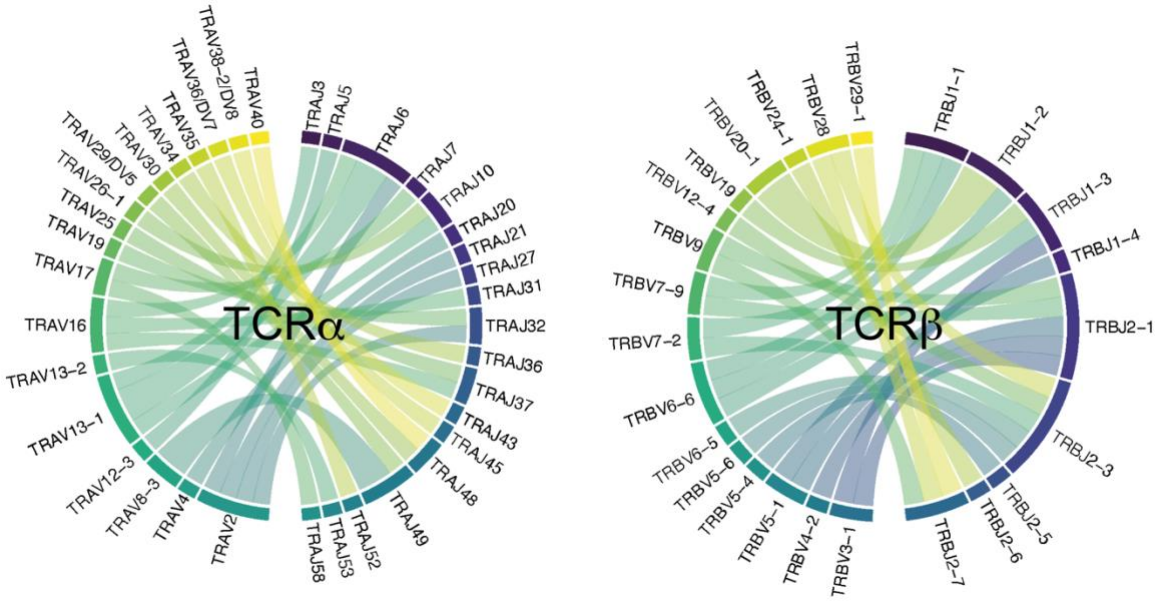

Fig. 2.26 CD1a-reactive IL-10-secreting Treg clones express a variety of α/β T cell receptors. TCRα and TCRβ variable (V) and joining (J) regions of CD1a-reactive IL-10-secreting Treg clones as determined by TCR sequencing. V and J regions of the same clone are linked by coloured lines. Only Treg clones for which both TCRα and TCRβ chain could be identified were included (n=25).

Table 2.1 TCRα and TCRβ V and J regions of CD1a-reactive Treg clones.

TCRα and TCRβ variable (V) and joining (J) regions of CD1a-reactive Treg clones were determined by TCR sequencing. For entries shown in grey, the isotype is not yet confirmed.

Donor	Clone	TRAV	TRAJ	TRBV	TRBJ
96	1B6	TRAV2*01	TRAJ6*01	TRBV5-1*01	TRBJ2-1*01
	1F6	TRAV16*01	TRAJ6*01	TRBV5-1*01	TRBJ1-4*01
	2G9	TRAV13-1*01	TRAJ37*02	TRBV20-1*01	TRBJ1-2*01
	3B2	TRAV19*01	TRAJ32*02	TRBV3-1*01	TRBJ2-1*01
	3E9	TRAV13-1*01	TRAJ3*01	TRBV9*01	TRBJ2-7*01
	3F2	TRAV36/DV7*04	TRAJ45*01	TRBV6-6*01	TRBJ1-2*01
	4B3	TRAV25*01	TRAJ37*02	TRBV6-6*01	TRBJ1-3*01
	4B10	TRAV17*01	TRAJ7*01	TRBV5-4*01	TRBJ2-5*01
	4C8	TRAV30*05	TRAJ48*01	TRBV4-2*01	TRBJ2-1*01
	4E8	TRAV34*01	TRAJ36*01	TRBV29-1*01	TRBJ2-7*01
	4G8	TRAV13-2*01	TRAJ53*01	TRBV7-9*01	TRBJ2-1*01
	5B7	TRAV2*01	TRAJ32*02	TRBV28*01	TRBJ2-7*01
	5C2	TRAV4*01	TRAJ20*01	TRBV12-4*01	TRBJ2-3*01
30	1B11	TRAV40*01	TRAJ48*01	TRBV19*01	TRBJ1-3*01
	1C8	TRAV2*01	TRAJ21*01	TRBV3-1*01	TRBJ1-3*01
	1D9	TRAV16*01	TRAJ37*02	TRBV7-2*01	TRBJ1-1*01
	1D10		TRAJ16*02		TRBJ2-7*01
	1F11	TRAV17*01	TRAJ58*01	TRBV7-2*01	TRBJ2-3*01
	2G8	TRAV13-1*02	TRAJ10*01	TRBV20-1*02	TRBJ1-2*01
	3D11	TRAV13-1*02	TRAJ6*01	TRBV7-9*03	TRBJ1-1*01
	4C4	TRAV26-1*02	TRAJ10*01		
	5D10	TRAV38-2/DV8*01	TRAJ43*01	TRBV6-6*01	TRBJ1-1*01
	5E11	TRAV13-1*02	TRAJ6*01	TRBV6-5*01	TRBJ2-3*01
32	1C5	TRAV8-3*01	TRAJ49*01		
	1E4	TRAV29/DV5*01	TRAJ49*01		
	1F9	TRAV12-3*01	TRAJ5*01	TRBV5-6*01	TRBJ2-3*01
	2C10	TRAV16*01	TRAJ31*01	TRBV28*01	TRBJ2-3*01
	2E9	TRAV8-3*01	TRAJ49*01		
	3F6	TRAV2*01	TRAJ27*01	TRBV24-1*01	TRBJ2-6*01
	4D2	TRAV35*02	TRAJ52*01	TRBV9*01	TRBJ2-1*01

2.2.7 CD1a-Klickmer staining of Tregs

CD1a-reactive effector T cells have been shown to bind to multiplexed CD1a[34,133-135,200]. However, not all CD1a-reactive T cells stain with multiplexed CD1a in flow cytometry analysis (unpublished data, Ogg Lab). To assess whether CD1a-reactive Tregs can stably bind to multiplexed CD1a and thereby be stained for flow cytometry analysis, CD1a obtained from the NIH Tetramer facility was multiplexed using Klickmer technology. Polyclonal Tregs and Treg clones were then stained for flow cytometry analysis with CD1a-Klickmers, using empty Klickmers as a control. 1.16% ± 0.33 of expanded polyclonal Tregs were able to bind to CD1a-Klickmer, which was significantly higher compared to the empty control (4.9-fold) (Fig. 2.27, A). Similarly, 3.15% ± 1.46 of each tested Treg clone was able to bind to CD1a-Tetramer, a significantly higher proportion compared to the empty control (3.6-fold) (Fig. 2.27, B).

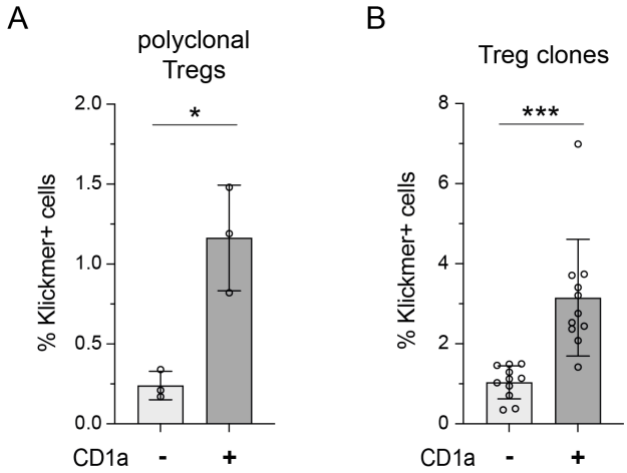

Fig. 2.27 A subpopulation of polyclonal Tregs and CD1a-reactive Treg clones stain with CD1a-Klickmers.

(A) Expanded polyclonal Tregs and **(B)** Treg clones were stained with CD1a-Klickmers (CD1a was obtained from the NIH Tetramer Core Facility) and analysed by flow cytometry. Polyclonal Tregs were gated on live $CD3^+CD4^+CD25^+CD127^{low}$ cells. Treg clones were gated on live $CD3^+CD4^+$ cells. (n=3 donors for polyclonal Tregs, n=11 for Treg clones; 1 experiment). *P < 0.05; **P < 0.01; ***P < 0.001; Two-tailed paired t-test (mean ± SD).

2.2.8 Effect of CD1a stimulation on CD1a-reactive Treg functionality

2.2.8.1 CD1a-mediated suppressive capacity of CD1a-reactive Tregs

Tregs suppress effector T cell proliferation and function by a variety of different mechanisms (see 1.3.1 Mechanisms of suppression). To investigate whether CD1a stimulation may increase the suppressive functionality of CD1a-reactive Tregs, polyclonal Tregs and Treg clones were stimulated with CD1a and their ability to inhibit autologous T cell proliferation was determined by suppression assay. Stimulating polyclonal Tregs with K562-CD1a cells overnight increased the suppression of $CD4^+$ and $CD8^+$ T cell proliferation by 1.1- to 2.1-fold, depending on PBMC:Treg ratio, compared to the K562-EV control (Fig. 2.28, A). The highest increase in suppression of $CD4^+$ and $CD8^+$ T cell proliferation by CD1a-stimulated Tregs could be observed at a PBMC:Treg ratio of 16:1 (1.8- and 2.0-fold, respectively). However, as K562-EV and K562-CD1a cells express different levels of TGF-β (Fig. 2.10) and therefore a contribution of differential cytokine production by K652 cells to the observed change in Treg suppressive function cannot be excluded, a cell-free bead assay was used to eliminate K562-dependent effects. When expanded polyclonal Tregs were pre-stimulated with CD1a-coated beads, no difference in the suppression of T cell proliferation compared to the empty bead control could be observed (Fig. 2.28, B).

As only a small subset of polyclonal Tregs express IL-10 in response to CD1a stimulation, it is plausible that CD1a-mediated suppressive effects may be overshadowed by CD1a-independent effects. Therefore, the effect of CD1a stimulation on the Treg suppression of T cell proliferation was studied using CD1a-reactive Treg clones. Three different Treg clones (30-10-1D10, 32-10-1C5 and 32-10-2C10) were pre-stimulated with CD1a-coated beads, using empty beads as control (Fig. 2.28, C). Two of three Treg clones showed a slightly higher suppressive capacity when pre-stimulated with CD1a compared to

the control. At a PBMC:Treg ratio of 8:1, Treg clones 32-10-1C5 and 32-10-2C10 showed 1.5- and 1.7-fold increased suppression when stimulated with CD1a compared to the control, respectively. In contrast, Treg clone 30-10-1D10 showed lower suppression of $CD4^+$ T cell proliferation when pre-stimulated with CD1a showing 0.8-fold suppression compared to the control. Taken together, these data indicate that the interaction of CD1a-reactive Tregs with CD1a may modulate their suppressive functionality and that different TCRs may differentially modulate CD1a-dependent Treg function.

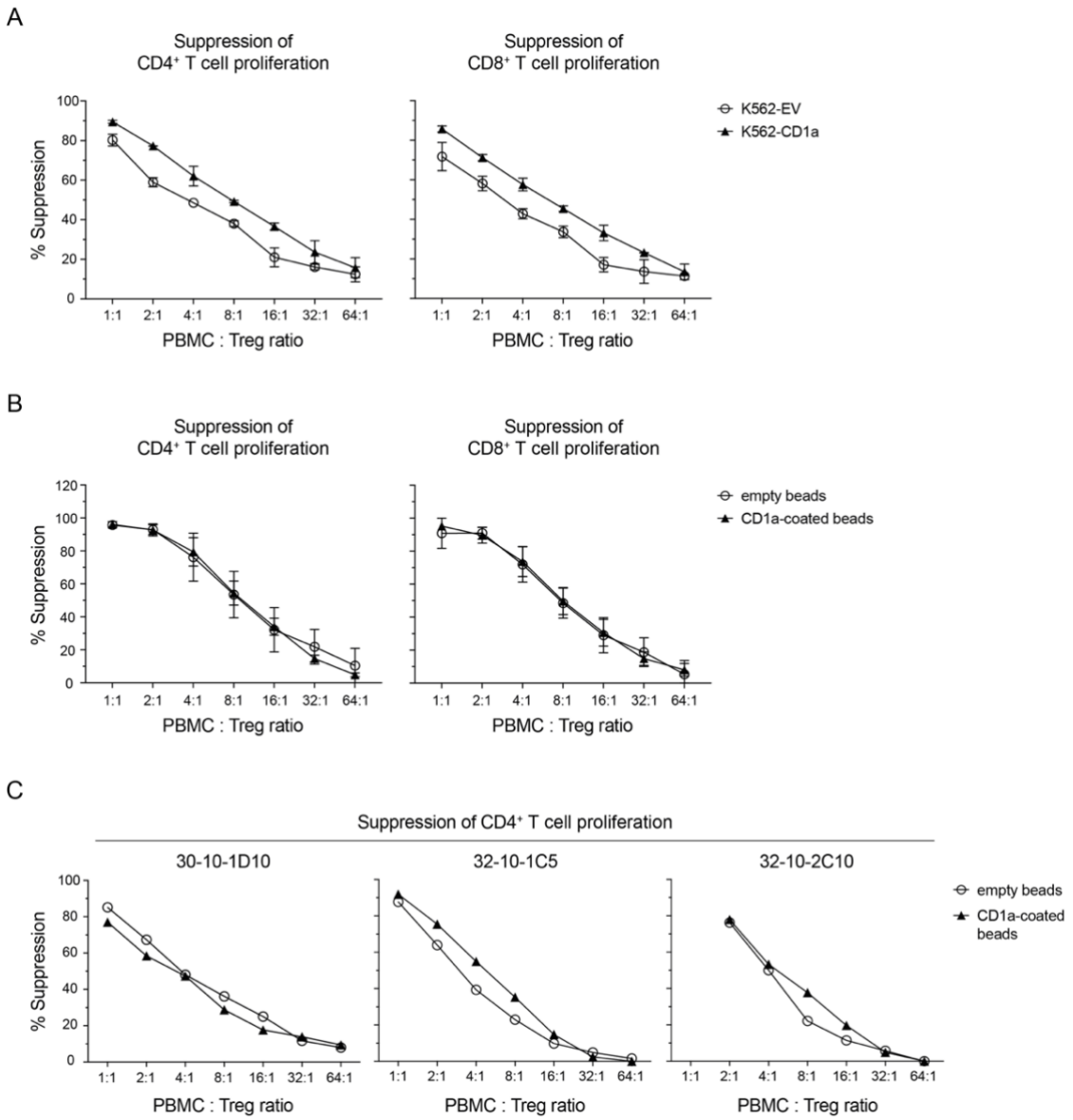

Fig. 2.28 Suppressive capacity of Tregs upon CD1a stimulation.

Suppression of $CD4^+$ and $CD8^+$ T cell proliferation by Tregs as determined by division index. Tregs were co-cultured with autologous PBMCs in the presence of anti-CD3/anti-CD28 microbeads (5:1 PBMC:bead ratio) and suppression was calculated relative $CD4^+$ and $CD8^+$ T cell proliferation in the absence of Tregs. **(A)** Expanded polyclonal Tregs were pre-incubated with irradiated K562-CD1a or K562-EV cells at a ratio of 2:1 overnight (IL-2 co-stimulation). Cell numbers were adjusted for Treg numbers before the suppression assay to obtain accurate PBMC:Treg ratios. (n=2 donors; 1 experiment). **(B)** Expanded polyclonal Tregs were pre-incubated with CD1a-coated beads or empty beads as a control at a ratio of 1:1 overnight (anti-CD11a and IL-2 co-stimulation). Beads were removed before the suppression assay. (n=4 donors; 2 independent experiments). **(C)** Treg clones were pre-incubated with CD1a-coated beads or empty beads as a control at a ratio of 1:1 for 6h (anti-CD11a and IL-2 co-stimulation). Beads were removed before the suppression assay (1 experiment).

2.2.8.2 CD1a-reactive Treg clones may inhibit CD8$^+$ T cell cytotoxic function

In addition to suppressing effector T cell proliferation, Tregs can also inhibit cytotoxic T cell function[289,290,415]. To investigate whether CD1a-reactive Tregs show an increased suppression of cytotoxic T cell function upon CD1a stimulation, Treg clones were co-cultured with CD8$^+$ cytotoxic T cell clones (kindly provided by Dr Yi-Ling Chen) and cytotoxic activity against K562 cells was measured by flow cytometry analysis of K562 cell death. Cytotoxicity was quantified by flow cytometry staining of K562 cells with Annexin V and CellTox reagent, thus including apoptotic and necrotic cells. The experimental hypothesis is schematically presented in Fig. 2.29.

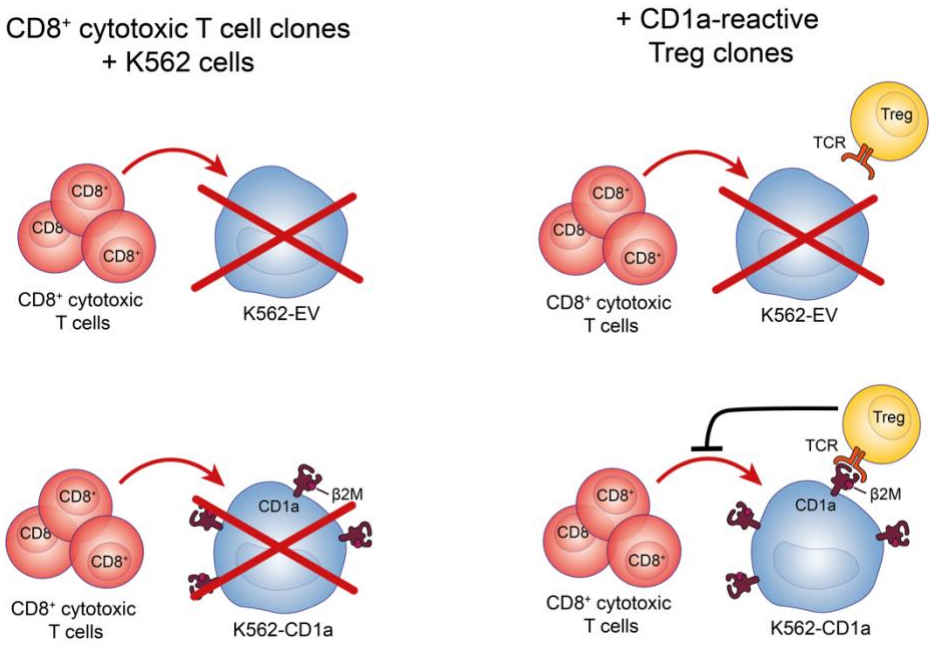

Fig. 2.29 Experimental hypothesis - CD1a-mediated inhibition of CD8$^+$ T cell cytotoxic function by CD1a-reactive Tregs.

CD8$^+$ T cell clones induce K562 cell death, irrespective of CD1a expression on K562 cells. Adding CD1a-reactive Treg clones to this system, no or minimal changes in K562 cell death are expected. However, when CD1a stimulation is present, CD1a-reactive Tregs may inhibit K562 cell death *via* inhibition of CD8$^+$ T cell clone cytotoxic activity.

$CD8^+$ cytotoxic T cell clones kill K562 cells regardless of the presence of CD1a on K562 cells. K562 cell death upon co-culture of K562 cells with $CD8^+$ cytotoxic T cell clones in the absence of Treg clones was used as baseline of the cytotoxic activity. Adding Treg clones to this system, CD1a stimulation may increase the ability of Treg clones to inhibit the cytotoxic activity of $CD8^+$ T cell clones. For this, Treg clones were pre-stimulated with anti-CD11a or anti-CD3/anti-CD28, followed by pre-incubation with K562-CD1a cells, using K562-EV cells as control. $CD8^+$ cytotoxic T cell clones were then added to the Treg-K562 co-culture together with co-stimulatory cytokines needed for $CD8^+$ T cell clone cytotoxic function (IL-12 and IL-18 for IFNγ-producing or IL-1β and IL-12 for GM-CSF-producing $CD8^+$ T cell clones). $CD8^+$ T cell clone cytotoxicity was then measured by flow cytometry analysis of K562 cell death.

In the absence of $CD8^+$ T cell and Treg clones, K562-CD1a cells showed a slightly higher percentage of $AnnexinV^+/CellTox^+$ cells compared to K562-EV cells (12.00% ± 0.28 compared to 8.13% ± 0.22) (Fig. 2.30, A). When K562 cells were co-cultured with $CD8^+$ T cell clones in the absence of Treg clones, 12-66% (18.58% ± 12.79) of K562-EV and 17-90% (30.13% ± 20.58) of K562-CD1a cells stained positive for $AnnexinV^+/CellTox^+$ (Fig. 2.30, A). To calculate suppression of cytotoxicity by Treg clones, K562 cell death in the presence of $CD8^+$ T cell clones and CD1a-reactive Treg clones was corrected for K562 only cell death and the baseline inhibition of each $CD8^+$ T cell clone respectively. In the presence of Treg clones pre-stimulated with anti-CD11a, cytotoxic activity of $CD8^+$ T cell clones was suppressed significantly by two of three tested Treg clones. In the presence of CD1a stimulation, Treg clones 96-10-1F6 and 96-10-4C8 reduced $CD8^+$ T cell clone cytotoxicity to 60.18% ± 20.11 and 54.31% ± 17.99 compared to the control, respectively (Fig. 2.30, B). While Treg clone 96-10-2G9 showed a similar trend, CD1a stimulation reduced cytotoxicity non-significantly to 76.03% ± 50.34 of the control (Fig. 2.30, B).

Anti-CD3 and anti-CD28 co-stimulation of Treg clones has shown increased activity of these clones in previous experiments (Fig. 2.20). To test whether co-stimulation with these antibodies may increase CD1a-mediated suppression of cytotoxic T cell activity by Tregs, Treg clones were pre-stimulated with anti-CD3 and anti-CD28 before CD1a stimulation and co-culture with $CD8^+$ cytotoxic T cell clones. One of three tested Treg clones, 96-10-4E8, was able to inhibit $CD8^+$ T cell clone cytotoxicity significantly in the presence of CD1a to 70.93% ± 6.49 compared to the control (Fig. 2.30, C). While Treg clones 96-10-3E9 and 96-10-3F2 showed a similar trend, CD1a stimulation reduced $CD8^+$ T cell clone cytotoxicity not significantly to 76.63% ± 3.36 and 86.35% ± 30.42 compared to the control (Fig. 2.30, C). Reduced CD1a-mediated inhibition of $CD8^+$ T cell clone cytotoxic activity compared to anti-CD11a co-stimulation (Fig. 2.30) may be explained by higher CD1a-independent Treg stimulation by anti-CD3/anti-CD28 co-stimulation observed in previous experiments (Fig. 2.20). It should further be noted that the inhibition of $CD8^+$ T cell clone cytotoxic activity was highly dependent on Treg clone feeding and $CD8^+$ T cell clone activity. Particularly upon repeated feeding, Treg clones showed reduced ability to suppress cytotoxicity by $CD8^+$ T cell clones. Nevertheless, these data suggest that CD1a-reactive Tregs may have the ability to suppress $CD8^+$ T cell cytotoxicity and that CD1a-mediated inhibition of cytotoxic T cell activity may be dependent on TCR as well as Treg activation status.

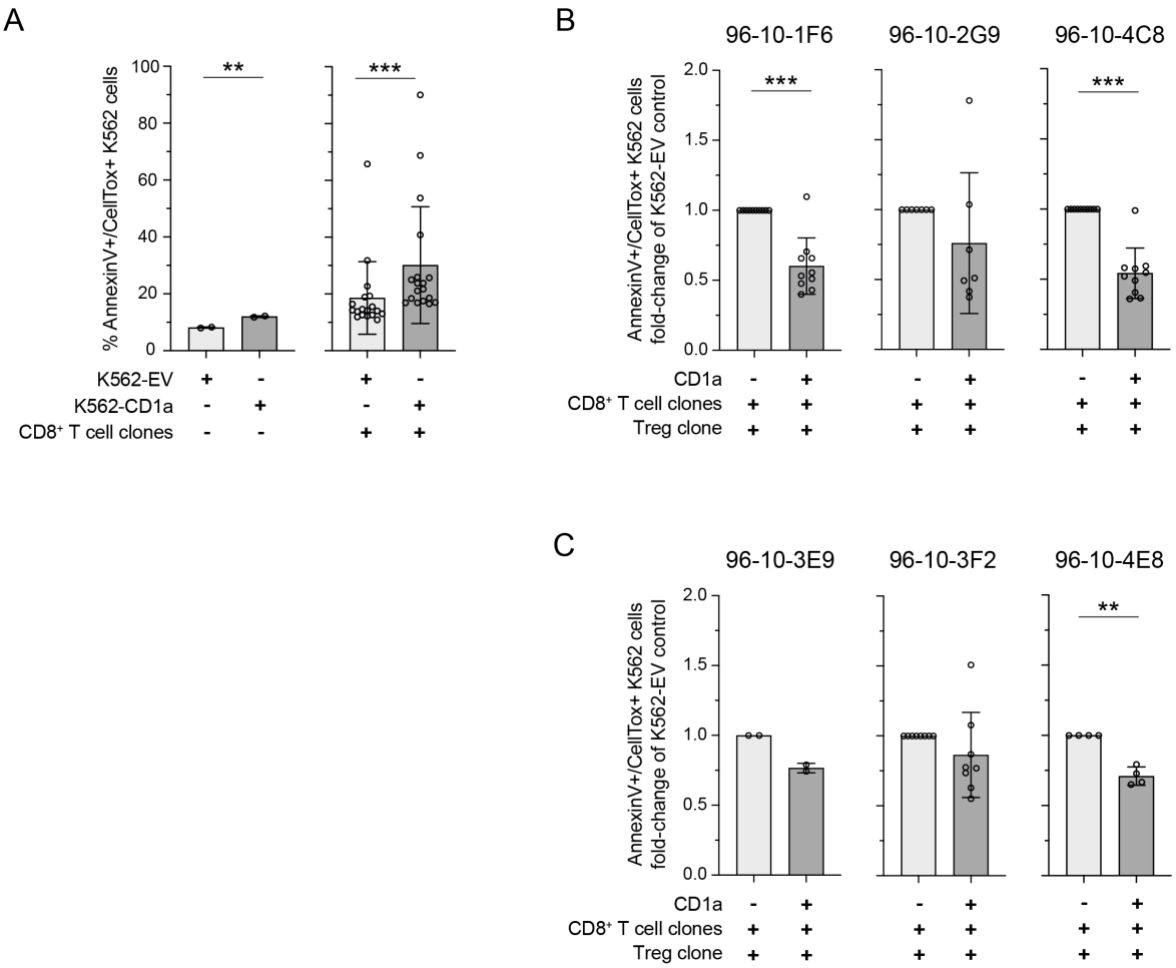

Fig. 2.30 CD1a-reactive Treg clones may inhibit CD8$^+$ T cell cytotoxic function.

Treg clones were pre-stimulated with **(B)** anti-CD11a or **(C)** anti-CD3 and anti-CD28 overnight, before pre-incubation with K562-CD1a or K562-EV cells for 4h. CD8$^+$ cytotoxic T cell clones were then added to the co-culture together with co-stimulatory cytokines for 2-3 days (IL-12 and IL-18 for IFNγ-producing or IL-1β and IL-12 for GM-CSF-producing CD8$^+$ T cell clones). Cytotoxic activity was determined by measuring K562 cell death using flow cytometry analysis of Annexin V and CellTox reagent staining. The percentage of AnnexinV$^+$/CellTox$^+$ K562 cells in the presence of CD8$^+$ T cell clones and absence of Treg clones served as baseline cytotoxic activity. Each dot represents a different CD8$^+$ T cell clone. **(A)** Percentage of AnnexinV$^+$/CellTox$^+$ K562 cells only (n=2) and in the presence of CD8$^+$ cytotoxic T cell clones (n=18). **(B, C)** AnnexinV$^+$/CellTox$^+$ K562 cells as fold-change of the K562-EV control for co-culture of K562 cells, CD8$^+$ T cell clones and CD1a-reactive Treg clones (corrected for cell death of K562 cells only and the baseline cytotoxic activity of each CD8$^+$ T cell clones). CD1a-reactive Treg clones were pre-stimulated with **(B)** anti-CD11a (96-10-1F6, 96-10-2G9, and 96-10-4C8) (n=7-10 CD8$^+$ cytotoxic T cell clones), or **(C)** anti-CD3 and anti-CD28 (96-10-3E9, 96-10-3F2, and 96-10-4E8) (n=2-8 CD8$^+$ cytotoxic T cell clones). ((A) 2 independent experiments or (B, C) 1 experiment). *P < 0.05; **P < 0.01; ***P < 0.001; Two-tailed paired t-test (mean ± SD).

2.3 Discussion

Skin Tregs play an important role in maintaining cutaneous immune homeostasis[28,307]. During skin inflammation and in skin inflammatory disease, Tregs often become dysfunctional and lose the ability to suppress aberrant immune responses[416,417]. CD1a-mediated immune responses play an important role in skin inflammation and skin diseases such as psoriasis (see 1.2.3 CD1a in skin inflammatory disease). While effector T cells can respond to CD1a and contribute to the exacerbation of skin diseases[6,167,174], it is unknown whether Tregs can engage with CD1a and modulate cutaneous immunity.

2.3.1 A subset of polyclonal Tregs functionally interacts with CD1a to secrete IL-10

Tregs exert their suppressive function through a variety of different cell-cell contact-dependent and -independent mechanisms[247,248]. One important suppressive mechanism is the generation and secretion of suppressive cytokines including IL-10 and TGF-β.

The data presented herein demonstrates that a subpopulation of polyclonal Tregs (~2%) secretes IL-10 in response to CD1a stimulation (Fig. 2.2, Fig. 2.6). IL-10 secretion could be blocked significantly but not completely by CD1a blocking antibodies when Tregs were stimulated with CD1a in an antigen-presenting cell system using K562 cells (Fig. 2.2). The here used K562-EV and K562-CD1a cells express very low levels of MHC class I and no MHC class II molecules[150] but many other proteins and molecules that may act as stimulatory factors for Tregs. Although K562 cells expressing the empty vector control or CD1a were generated from the same K562 cell line, K562-EV and K562-CD1a cells present several differences such as cell size and TGF-β production (Fig. 2.10). Because TGF-β is important for induction of Tregs, modulates Treg function *via* enhancing Foxp3 expression

and can promote T cell production of IL-10[281,282,418], it is possible that the higher TGF-β production of K562-CD1a cells may increase IL-10 secretion of Tregs independent of CD1a. However, the presence of recombinant TGF-β1 during CD1a stimulation decreased IL-10 secretion (Fig. 2.4). This indicates that differential TGF-β production by K562-EV and K562-CD1a cells may not influence CD1a-dependent IL-10 secretion of Tregs. Moreover, eliminating these factors by using a cell-free system in which Tregs are stimulated with CD1a-coated beads, Tregs secreted IL-10 to a comparable level in response to CD1a as for K562-CD1a stimulation. This increase in IL-10 secretion was entirely dependent on CD1a, as CD1a blocking abolished the effect (Fig. 2.6). These results indicate that a subpopulation of Tregs can functionally interact with CD1a to secrete IL-10 independent of additional APC-mediated stimulation.

In addition to IL-10 secretion, polyclonal Tregs also showed a trend towards CD1a-mediated secretion of LAP-TGF-β (Fig. 2.11). Interestingly, CD1a-dependent Treg secretion of LAP-TGF-β negatively correlated with secretion of IL-10. Different Treg subsets are known to employ different suppressive mechanisms[419,420], indicating that IL-10 secretion may present a key characteristic of CD1a-reactive Tregs. Due to lack of commercially available antibodies against active TGF-β, only secretion of the latent form of TGF-β was investigated and it remains unknown whether CD1a stimulation may induce increased levels of active TGF-β. Moreover, Tregs not only secrete TGF-β but can also express membrane-bound TGF-β. Whether surface expression of TGF-β is modulated by CD1a stimulation remains to be addressed.

Several skin inflammatory diseases are associated with infiltration of immune cells, including effector T cells, and increased levels of inflammatory cytokines[397,421]. In response to CD1a stimulation, CD1a-reactive effector T cells derived from peripheral blood and skin

have been shown to produce increased levels of cytokines associated with skin inflammation, including GM-CSF, IL-13, IL-17A, IL-22 and IFNγ [34,135,150,168]. Very few polyclonal Tregs (≤ 1%) were found to secrete these cytokines in the presence of K562 cells, and cytokine secretion was independent of CD1a (Fig. 2.13, A). When polyclonal Tregs were stimulated with CD1a-coated or empty beads, secretion of GM-CSF, IL-13 and IL-22 was increased to 2-5%, but cytokine secretion remained independent of CD1a (Fig. 2.13, B). Unspecific increases in cytokine secretion upon bead stimulation are also seen for effector T cells (unpublished data, Dr Yi-Ling Chen) and may result from CD1a-independent T cell activation due to bead-T cell interaction.

Direct binding of effector T cells to CD1a has been shown by CD1a-Tetramer staining of effector T cells and CD1a-reactive T cell clones[34,133-135,200]. Similarly, a subpopulation of polyclonal Tregs (approximately 1.2%) could be shown to bind to CD1a-Klickmers (Fig. 2.27, A), confirming direct interaction of a Treg subpopulation with CD1a.

Taken together, the here presented data demonstrates for the first time that a subpopulation of polyclonal Tregs can bind to and functionally interact with CD1a to secrete IL-10. While CD1a-reactive Tregs also show a trend towards CD1a-mediated secretion of LAP-TGF-β, they do not secrete skin inflammation-associated cytokines in a CD1a-dependent manner. Therefore, CD1a-reactive Tregs present an anti-inflammatory and suppressive phenotype and CD1a-mediated Treg function may at least partially rely on IL-10 secretion. Whether CD1a stimulation also modulates Treg secretion of other immunomodulatory cytokines or modulates other suppressive mechanisms, such as cell-cell contact-dependent suppression, remains to be addressed.

2.3.2 CD1a-reactive Treg clones drift from a Treg phenotype but retain the ability to secrete IL-10 in a CD1a-dependent manner

CD1a-reactive Tregs compose only a small subpopulation of peripheral Tregs (~2%) and thus studying the functional properties of these cells is challenging. The generation of CD1a-reactive Treg clones may overcome this obstacle. Due to very low polymorphism of CD1a, specific functionally active CD1a-restricted Treg clones may further have therapeutic potential to treat skin inflammation, as such Treg clones would be donor unrestricted.

Here, CD1a-reactive Treg clones were generated from IL-10-secreting CD1a-reactive Tregs. Although variable between different clones, several Treg clones showed expression of the Treg markers CD25 and Foxp3, while lacking CD127 expression, after the first round of expansion (Fig. 2.16). Additionally, most Treg clones expressed GITR and CLTA-4 (Fig. 2.17). However, Treg maker expression varied between different feedings and time points and Foxp3 expression steadily declined over repeated rounds of expansion (Fig. 2.17). Rapamycin and all-*trans* retinoic acid (ATRA) have been shown to (synergistically) promote Treg expansion, function, and stability[422-424]. The continuous loss of Treg markers by CD1a-reactive Treg clones could not be reversed by the addition of rapamycin and ATRA to the culture medium (data not shown). However, it is plausible that addition of ATRA and/or rapamycin may protect Treg lineage when added from the time of sorting. Independent of Treg marker loss, many Treg clones showed efficient suppression of T cell proliferation, although this suppressive capacity was also highly dependent on time point of testing and differed between Treg clones (Fig. 2.18). Independent of Treg phenotype, CD1a-reactive Treg clones retained the ability to secrete IL-10 in a CD1a-dependent manner over repeated rounds of expansion (Fig. 2.19). Unlike polyclonal Tregs, CD1a-reactive Treg clones secreted higher levels of IL-10 in the presence of K562-CD1a cells compared to

cell-free stimulation with CD1a-coated beads. Further, anti-CD3/anti-CD28 co-stimulation of Treg clones during CD1a stimulation led to CD1a-dependent secretion of IL-10 in the antigen-presenting cell system but increased secretion independent of CD1a in the cell-free system (Fig. 2.20). Taken together, these results may indicate that due to a lack in phenotypic and TCR diversity, CD1a-reactive Treg clones may require additional APC-mediated co-stimulatory factors to efficiently interact with CD1a.

Although all CD1a-reactive Treg clones were clonal (as determined by TCR sequencing), not all cells of the same clone responded equally to CD1a stimulation. For each CD1a-reactive Treg clone, an average of 5% and 8% of cells secreted IL-10 in response to IL-10 stimulation, depending on stimulation system (Fig. 2.19). Partial CD1a-reactive responses can also be observed for CD1a-reactive effector T cell clones (unpublished data, Dr Yi-Ling Chen). Possible reasons include drifting of the Treg phenotype in subpopulations, differing activation status between cells, and differential TCR expression. Similar reasons may explain that only a small proportion of each CD1a-reactive Treg clone bound to CD1a-Klickmer (approximately 3%) (Fig. 2.27, B). Additionally, although staining with multiplexed CD1a can identify T cells that are able to bind to CD1a[34,133-135,200], not all CD1a-reactive T cells can be stained with multiplexed CD1a and negative staining does not exclude CD1a reactivity (unpublished data, Ogg Lab). It may be that mixed lipid content of CD1a multimers contributes to this effect.

CD1a-reactive Treg clones also produced high levels of perforin, granzyme A and granzyme B (Fig. 2.23). Especially granzyme B and perforin play an important role in Treg-mediated cytotoxic activity but are also expressed by other cell types such as cytotoxic $CD8^+$ T cells[63,425]. In comparison to polyclonal Tregs, CD1a-reactive Treg clones secreted much higher levels of GM-CSF (9-14%), IL-13 (15-33%) and IFNγ (4-74%) (Fig. 2.24; Fig.

2.25). While secretion of LAP-TGF-β, GM-CSF and IFNγ was not dependent on CD1a stimulation, secretion of IL-13 was at least partially mediated by CD1a and additional co-stimulation with skewing cytokines further induced CD1a-mediated secretion of IL-17A. This CD1a-mediated secretion of IL-13 and IL-17A was not observed in the cell-free stimulation system. IL-13 is typically considered a pro-inflammatory cytokine, but several mouse studies suggest that Treg production of IL-13 may also have regulatory functions. Treg-derived IL-13 was proposed to be protective in an autoimmune encephalomyelitis model and was further shown to promote macrophage secretion of IL-10 and efferocytosis during resolution of inflammation[426,427]. Whether CD1a-mediated IL-13 secretion of Tregs may have protective functions remains to be investigated. However, changes in Treg phenotype can be observed in inflammatory environments such as psoriasis, where Tregs have been shown to produce high levels of IL-17A and IFNγ[428]. Therefore, secretion of high levels of IFNγ, GM-CSF and granulysin by CD1a-reactive Treg clones (Fig. 2.23; Fig. 2.24; Fig. 2.25) suggests that repeated unspecific stimulation during feeding may result in a phenotypic change towards a pro-inflammatory phenotype.

Taken together, the here presented data show that CD1a-reactive Treg clones retain their ability to secrete IL-10 upon CD1a stimulation. While maintaining some Treg-like features, CD1a-reactive Treg clones showed loss of Treg marker expression and phenotypic changes upon prolonged culture, shifting towards a more pro-inflammatory phenotype. Therefore, the CD1a-reactive Treg clones may not be suitable for therapeutic use but present a valuable tool to obtain specific CD1a-specific TCR sequences.

2.3.3 CD1a stimulation may modulate CD1a-reactive Treg function

Tregs are essential for immune homeostasis and suppression of excessive T cell responses and CD1a stimulation may modulate the suppressive functionality of CD1a-reactive Tregs.

Polyclonal Tregs stimulated with K562-CD1a cells showed higher suppression of T cell proliferation compared to Tregs co-cultured with K562-EV cells (Fig. 2.28, A). However, CD1a-mediated suppression was not observed when using the cell-free stimulation system, stimulating polyclonal Tregs with CD1a-coated beads (Fig. 2.28, B). K562-CD1a cells express higher levels of TGF-β compared to K562-EV cells (Fig. 2.10). Therefore, K562-produced TGF-β or other K562-mediated factors may have contributed to higher suppressive function of CD1a-reactive Tregs or directly modulated T cell proliferation. It is also possible that the sorted polyclonal Tregs do not require additional CD1a-dependent stimulation for all suppressive effects. As only a small percentage of polyclonal Tregs is CD1a-reactive, it is plausible that increased CD1a-mediated function of this population may be concealed by the generally high suppressive capacity of polyclonal Tregs. This issue can be circumvented by studying the CD1a-mediated suppressive functionality of CD1a-reactive Treg clones. Two of three tested CD1a-reactive Treg clones showed a CD1a-mediated increase in suppression of T cell proliferation, whereas one Treg clone showed a trend towards lower suppression upon CD1a stimulation (Fig. 2.28, C). Moreover, CD1a stimulation elevated CD1a-mediated Treg clone suppression of $CD8^+$ T cell cytotoxicity (Fig. 2.30). Most, but not all, CD1a-reactive Treg clones showed increased inhibition of $CD8^+$ T cell clone-mediated killing. Suppression of $CD8^+$ T cell clone cytotoxicity was not only dependent on CD1a-reactive Treg clone, but also $CD8^+$ T cell clone. Differences in inhibition of $CD8^+$ T cell clone cytotoxic activity may result from differences in T cell phenotype, strength of cytotoxic activity and mechanism of cytotoxicity. Moreover, $CD8^+$ T cell clones required the addition of co-stimulatory cytokines for efficient cytotoxic functionality (IL-12 and IL-18 for IFNγ-producing, and IL-12 and IL-1β for GM-CSF-producing clones). However, also CD1a-reactive Treg clones responded to these co-stimulatory cytokines, producing higher levels of IFNγ and GM-CSF

(Fig. 2.23). IL-12, which is increased in psoriasis[429], has been shown to increase IFNγ production by Tregs and induce a shift towards a Th1 phenotype, but IL-12-mediated effects on Treg suppressive function remain debated[410,430,431]. These results suggest that CD1a-reactive Treg clones may acquire a more pro-inflammatory phenotype under these conditions and suppressive functionality may be modulated by the environment. Additionally, Treg clones were shown to drift in their Treg phenotype, indicating that these results need to be treated with caution. Nevertheless, the here presented data suggest that the suppressive functionality of CD1a-reactive Treg clones may be modulated by CD1a stimulation, with most Treg clones showing an increase in suppressive capacity. Further, CD1a-mediated suppression varied between different CD1a-reactive Treg clones, indicating that diverse TCRs may interact with CD1a and that differential TCR-CD1a interaction may modulate CD1a-mediated Treg function

While not investigated here, blocking of CD1a would confirm CD1a-dependency of CD1a-mediated increases in Treg suppressive function. Insights into mechanisms of CD1a-mediated Treg suppression could be gained by spatially separating Tregs from $CD8^+$ cytotoxic T cell, i.e. using transwell plates, and blocking of IL-10 secretion, i.e. by anti-IL-10 antibodies. This would allow the differentiation between cell-cell contact dependent and humoral factor-mediated mechanisms as well as delineating the involvement of IL-10. Moreover, using the here identified CD1a-reactive TCRs to transduce primary Tregs would enable the study of CD1a-mediated modulation of Treg function while circumventing repeated expansion of Tregs and the thereby caused drifting of the Treg phenotype. If successful, these studies could be extended to CD1a-mediated inhibition of skin inflammation by CD1a-reactive Tregs in CD1a-transgenic mouse models. First clinical trials on adoptive Treg therapy using expanded polyclonal Tregs have shown promising results and pre-clinical studies showed superior treatment potential for antigen-specific

Tregs as well as Tregs transduced with specific TCRs[432-434]. Therefore, Tregs expressing a specific CD1a-reactive TCR known to inhibit inflammatory responses may present therapeutic potential for the treatment of skin inflammatory diseases.

2.3.4 CD1a-reactive Tregs respond to CD1a presenting skin-relevant lipids

CD1a can present a variety of lipids that are present in the skin, including LPC and SM[34,134,135]. LPC is generated *via* PLA_2-mediated cleavage of phosphatidylcholine, a major mammalian cell membrane component, and PLA_2 activity as well as LPC levels are increased in psoriatic skin[400-404]. SM, which is enriched in plasma membranes, may elicit differential CD1a-mediated T cell responses depending on carbon chain length and saturation[34,134]. While CD1a-Tetramers loaded with SM 18:1 efficiently bind to CD1a-reactive T cells, loading of CD1a with SM 24:0 partially and loading of CD1a with SM 24:1 completely inhibits Tetramer binding of CD1a-reactive T cells[134]. This differential effect on the ability of CD1a-reactive T cell TCRs to bind CD1a is proposed to result from lipid-induced rearrangement of the CD1a A' roof by SM 24:0 and SM 24:1. The herein presented data show that CD1a-reactive Tregs can bind to and functionally interact with LPC- and SM-loaded CD1a (Fig. 2.14). Stimulation with LPC-loaded CD1a increased IL-10 secretion of CD1a-reactive Tregs by up to 1.6-fold compared to unloaded CD1a containing endogenous lipids (Fig. 2.14, B, D). CD1a-reactive Tregs also secreted IL-10 in response to CD1a loaded with SM 18:1, SM 24:0 and SM 24:1 (Fig. 2.14, B, D). Similar to CD1a-reactive effector T cells, CD1a-reactive Tregs showed a higher response towards CD1a loaded with SM 18:1 compared to SM 24:0 and SM 24:1. However, while CD1a loaded with SM 18:1 stimulated CD1a-reactive Tregs stronger compared to the unloaded CD1a control, loading of CD1a with SM 24:0 or SM 24:1 showed comparable or only moderately lower induction of CD1a-mediated Treg responses compared to unloaded CD1a,

depending on stimulation system (Fig. 2.14, B, D). These findings contrast the partial or complete blocking of CD1a-Tetramer staining of CD1a-reactive effector T cells by loading of CD1a with SM 24:0 or SM 24:1, respectively[134]. However, the study did not investigate functional responses of CD1a-reactive effector T cells to SM-loaded CD1a. As lack of CD1a-Tetramer staining does not necessarily relate to a lack in functional interaction, the inhibition of CD1a-reactive effector T cell responses by SM 24:0 and SM 24:1 remains to be confirmed. In addition to lipids present during immune homeostasis, CD1a-reactive Tregs also secreted IL-10 in response to CD1a loaded with the plant-derived lipid urushiol (C15:2) (Fig. 2.14, D). Urushiol has been demonstrated to bind to CD1a, activate CD1a-mediated T cell responses and trigger CD1a-dependent skin inflammation[6].

Taken together, the presented data show that CD1a-reactive Tregs and CD1a-reactive effector T cells share the ability to bind to CD1a loaded with lipids such as LPC, SM 18:1 and urushiol. This may indicate that not only CD1a-reactive effector T cells but also CD1a-reactive Tregs may be involved in CD1a-mediated immune responses in the skin. On the contrary, Treg and effector T cells may interact differentially with CD1a loaded with SM 24:0 or SM 24:1. When bound to CD1a, SM 24:0 and SM 24:1 protrude further above the A' roof compared to SM 18:1 and induce remodelling of the CD1a binding cleft[134]. It is plausible that differences in CD1a-mediated responses to SM-loaded CD1a between Tregs and effector T cells may result from distinct TCR repertoires leading to different mechanisms of interaction or from partially different binding sites. In addition to the here identified TCR sequences of CD1a-reactive Tregs (Table 2.1), only few TCR sequences of CD1a-reactive T cells and crystal structures of CD1a-TCR interactions are published[34,133,134,138]. Single-cell TCR sequencing of CD1a-rective Tregs and effector T cells could provide further insights into differences between TCR repertoires that may shed light onto differences in CD1a-mediated responses.

2.3.5 CD1a-reactive Tregs express a variable α/β T cell receptor repertoire

Similar to the TCR-peptide-MHC model based on head group discrimination, CD1b and CD1d antigen recognition are thought to depend on the interaction of the TCR with CD1 and antigen[130,131]. In contrast, TCR recognition of many CD1a-presented antigens seems independent of antigen-binding by the TCR[90,133]. In this 'absence of interference' model, antigens lacking large headgroups do not protrude from the CD1a binding cleft, thereby leaving the TCR binding site free for CD1a-TCR interaction. Antigens with larger headgroups or those which are able to remodel the CD1a A' roof upon binding are thought to interfere with TCR-CD1a interaction and suppress CD1a-mediated immune responses[133,135]. Recent findings suggest that some CD1a-reactive T cell TCRs may also interact with some protruding antigens and not just the A' roof (unpublished data), comparable to head group discrimination seen for other CD1 and MHC molecules. CD1a-reactive effector T cells have been shown to express a variety of α/β T cell receptors[133,134,150]. Similarly, IL-10-secreting CD1a-reactive polyclonal Tregs were found be part of the α/β T cell receptor repertoire (Fig. 2.9).

The anti-CD1a antibody clone OKT6 has been shown to efficiently, and in most cases completely, inhibit CD1a-reactive effector T cell responses[34,135,150,166,168,200]. Interestingly, blocking of CD1a-mediated secretion of IL-10 by polyclonal Tregs with anti-CD1a antibody clone OKT6 showed only partial and not significant reduction of IL-10 secretion, while clone HI149 efficiently and completely inhibited CD1a-mediated Treg responses (Fig. 2.8). As anti-CD1a clone OKT6 was only used in one experiment, these findings need to be confirmed. Nevertheless, it is plausible that CD1a-reactive Treg TCRs may bind to different binding sites of the CD1a A' roof compared to CD1a-reactive effector T cell TCRs. However, both Tregs and effector T cells can bind to CD1a loaded with i.e. LPC and

SM 18:1 while showing differential responses to CD1a loaded with longer chain SMs (see 2.3.4 CD1a-reactive Tregs respond to CD1a presenting skin-relevant lipids). This may suggest that either TCR repertoires or TCR binding sites of CD1a-reactive Tregs and effector T cells may overlap, or that binding to different CD1a sites may result in differential T cell activation. It is further possible that CD1a-mediated T cell activation may depend on T cell subset and phenotype.

Very few specific TCR sequences of CD1a-reactive effector T cells have been published, but the TCR sequences of 5 different CD1a-reactive T cell clones indicate a variable expression of different α/β TCRs[34,133,134,138]. The here generated CD1a-reactive Treg clones similarly express highly variable α/β TCRs (Fig. 2.26). While several TCRα or TCRβ V or J regions are present in both CD1a-reactive Treg and effector T cell clones (TRAV12-3, TRAV26-1, TRAJ20, TRBV29-1 and TRBJ1-2), the number of known TCR sequences is too low to draw any conclusions on differences between the two TCR repertoires. Single-cell TCR sequencing of CD1a-rective Tregs and effector T cells could provide further insights into similarities or differences of CD1a-reactive Treg and effector T cell TCRs.

2.3.6 Implications of CD1a-reactive Tregs in skin immunity

CD1a-mediated immune responses, driven by CD1a-reactive effector T cells, play an important role in the pathogenesis of skin inflammation and skin diseases (see 1.2.3 CD1a in skin inflammatory disease). The results of this study, identifying a subpopulation of polyclonal Tregs that recognise and functionally interact with CD1a, suggest that CD1a may also contribute to skin immune homeostasis and modulate skin immunity though suppressive mechanisms. Unlike some CD1-reactive T cell populations (i.e. iNKT cells), CD1a-reactive T cells are do not present a semi-invariant or invariant population but express diverse TCRs[133,134,140-142,150,153,154] (see 2.2.6.7 TCR sequencing of CD1a-reactive Treg

clones). Nevertheless, many CD1a-reactive T cells can recognise the same lipids, like LPC[34] (Fig. 2.14). This diversity of the CD1a-reactive TCR repertoire may enable CD1a to balance CD1a-mediated immune responses. It is plausible that while many TCRs recognise CD1a presenting a variety of endogenous lipids leading to a general 'low' T cell stimulation, abundance of a specific lipid may unleash a much stronger CD1a-mediated T cell response. This may further be dependent on the CD1a-presenting cell type, with LCs that express high levels of CD1a triggering a broader immune response compared to i.e. dermal DCs.

Although CD1a-reactive Tregs can recognise similar CD1a-presented lipids as CD1a-reactive effector T cells, the functional response and thereby the implication for skin immunity may differ. In contrast to CD1a stimulation inducing pro-inflammatory responses in effector T cells (see 2.1.1 CD1a-reactive T cells), here presented data suggest a predominantly suppressive phenotype for CD1a-reactive Tregs. Interestingly, longer chain SMs have been shown to block CD1a-binding of effector T cells[134] but seem to elicit a suppressive immune response *via* CD1a-reactive Tregs (Fig. 2.14), suggesting that specific lipids may uniformly promote immune homeostasis while others, such as LPC, may elicit differential immune responses. Here presented data, showing reduced CD1a-reactive Treg clone responses in the cell-free system compared to antigen-presenting cell-mediated CD1a stimulation (Fig. 2.19), further indicates that CD1a-reactive Tregs may require strong activation signals for CD1a-mediated suppressive function. Therefore, in highly activating environments, CD1a-reactive Tregs may act as a protective 'self-regulation' mechanism to counteract excessive CD1a-mediated effector T cell responses. Additionally, once sufficiently stimulated, CD1a-reactive Tregs may further modulate immune responses by bystander suppression and by induction of 'infectious tolerance', i.e. *via* IL-10-mediated modulation of DC function.

During skin immune homeostasis, when the skin barrier is intact, many skin lipids such as sebum, exogenous antigens and environmental allergens are spatially separated from CD1a. When the skin barrier is breached, as commonly seen in skin inflammatory disease, these lipids can be presented by CD1a and elicit CD1a-mediated T cell responses. In healthy skin, T cells are spread out and activation signals as well as CD1a stimulation are limited. Therefore, it is plausible that CD1a-reactive Tregs may be as important for resolution of skin inflammation as in preservation of skin immune homeostasis. In inflammatory environments, as seen in skin inflammatory diseases, Tregs can become dysfunctional and acquire effector functions[416,417]. Elevated levels of inflammatory cytokines, such as IL-12 and IL-1β, during inflammatory conditions may further modulate Treg function by inducing non-specific IFNγ and GM-CSF production, as observed for CD1a-reactive Treg clones (Fig. 2.25). Additionally, due to barrier defects, CD1a antigens are enriched in these environments[400-404]. Thus, 'self-regulation' of CD1a-mediated immune responses may be perturbed by Treg dysfunction, leading to excessive CD1a-mediated effector T cell responses that exacerbate disease. Moreover, CD1a-mediated T cell responses play an important role in allergic responses in the skin[166-168]. CD1a-reactive Tregs responding to CD1a-presented urushiol (Fig. 2.14), a plant-derived lipid shown to trigger CD1a-dependent skin inflammation[6], suggests that CD1a-reactive Tregs may also be involved in resolving allergic immune responses.

The involvement of CD1a-mediated immune responses in skin inflammation and skin diseases (see 1.2.3 CD1a in skin inflammatory disease) makes CD1a-reactive T cells an interesting therapeutic target. Lipids that bind to CD1a and modulate CD1a-mediated T cell responses could easily be formulated into topical treatments, limiting systemic side effects. Although CD1a-reactive Tregs and effector T cells seem to respond to similar lipids, specific lipids that disturb CD1a-binding of effector T cells while eliciting CD1a-mediated

Treg suppression, i.e. longer chain SMs, may present valuable candidates for the treatment of skin inflammation. Although SM 24:1 has shown promising preliminary results in the here presented study, further evaluation of differential Treg and effector T cell responses are essential to verify its therapeutic potential. Moreover, CD1a-reactive Tregs created *via* transduction of specific TCRs that inhibit CD1a-mediated inflammatory responses could be used for Treg adoptive cell therapy. First clinical trials of adoptive Treg therapy using expanded polyclonal Tregs have shown promising results and pre-clinical studies further emphasize the potential of antigen-specific Tregs and TCR-specific Tregs[432-434]. Therefore, transduction of polyclonal Tregs with CD1a-reactive Treg-TCRs and subsequent adoptive Treg transfer may present a possible treatment for skin inflammation and skin disease.

Chapter 3 Single-cell analysis of CD1a-reactive regulatory T cells in health and psoriasis

3.1 Introduction and Aims

3.1.1 Psoriasis

Psoriasis is a chronic, immune-mediated inflammatory disease with an estimated global prevalence of 2-3%[435]. The disease is thought to result from a complex interplay between multiple genetic and environmental factors. Psoriasis has a strong genetic component, with 50-70% of psoriasis susceptibility resulting from genetic variation. The remaining disease risks are attributed to environmental effects, and environmental factors such as infection (e.g. streptococcal infection), medication (e.g. imiquimod, IFNα) or trauma can trigger or exacerbate psoriasis[182,436]. Over 40 genomic regions and more than 400 SNPs associated with psoriasis have been identified[437,438]. The major genetic determinant is the psoriasis susceptibility locus PSORS1 which maps to MHC on chromosome 6 and primarily comprises of genes involved in antigen presentation[439-445]. Human leukocyte antigen C (HLA-C) is considered the most likely causal susceptibility allele within PSORS1[444,445], and HLA-Cw6 has been shown to present T cell auto-antigens such as the psoriasis auto-antigen cathelicidin (LL-37)[446-448]. Additional association signals that are independent of HLA-Cw6 have been identified within MHC, mapping to HLA-A, HLA-B and HLA-DQA1, HLA-DQB1 and HLA-DRB1[449-454]. Large-scale association studies have further identified additional candidate genes, including genes involved in innate immunity pathways such as IFN signalling (including *TYK2*, *SOCS1*, *IFIH1*, *DDX58* and *RNF114*)[445,455-457] and nuclear factor 'kappa-light-chain-enhancer' of activated B-cells (NFκB) signalling (including *TNFAIP3*, *TNIP1*, *TYK2*, *REL* and *NFKBIA*)[444,445,458,459], and adaptive immunity pathways

such as antigen presentation (including *HLA-C* and *ERAP1*)[439-445,458] and Th17 cell activation (including *IL23R*, *IL23A*, *IL12B* and *TRAF3IP2*)[444,445,460-463].

Psoriasis is characterised by thickening and scaling of the epidermis resulting from increased proliferation of keratinocytes and can manifest as various phenotypes[464,465]. The most common type is psoriasis vulgaris, also known as plaque psoriasis, which most commonly affects elbows, knees, scalp, and trunk. Psoriasis vulgaris is characterized by well-defined erythematous plaques with loosely adherent silvery white scales. Guttate psoriasis, the second most common type of psoriasis, is characterized by small erythematous papules over the trunk and extremities. Pustular psoriasis presents with sterile pustules on an erythematous base; and erythrodermic psoriasis is a severe form of psoriasis that is characterised by widespread erythema involving the majority of the body surface area.

The formation of inflammatory plaques is characterised by the infiltration of inflammatory cells into the skin. Infiltrating cells include $CD4^+$ and $CD8^+$ T cells, innate lymphoid cells, macrophages, mast cells, neutrophils, NK cells and NKT cells[466-470]. Psoriasis pathogenesis is driven by the dysfunction of several immune cell subsets including Th1, Th2 and Th17 cells as well as Tregs, which results in the aberrant release of corresponding cytokines such as IFNγ, TNFα, IL-23 and IL-17 family members[421]. In addition to peptide-reactive T cells, also inflammatory CD1a-reactive T cell responses contribute to exacerbation of disease (see 1.2.3 CD1a in skin inflammatory disease).

IL-36 cytokines, members of the IL-1 family that are highly expressed in keratinocytes, play a key role in epithelial immune homeostasis[471,472]. While IL-36α, IL-36β and IL-36γ (hence IL-36) bind to IL-36 receptor (IL-36R) and activate pro-inflammatory responses *via* MAPK and NFκB, the IL-36R antagonist (IL-36Ra) blocks downstream signal transduction. IL-36 is elevated in psoriatic skin and was identified as an important driver of psoriasis that

activates DCs and promotes Th17 polarisation[472-477]. The gene encoding IL-36R (*IL1RL2*) has been identified as a susceptibility locus for psoriasis and loss-of-function mutations in *IL36RN* (encoding for IL-36Ra) are associated with generalised pustular psoriasis[475,478]. Moreover, IL-36R blockade can reverse the inflammatory phenotype in psoriatic skin, likely by disruption of keratinocyte activation[474]. IL-36 has further been shown to upregulate PLA_2G4D, which generates lipid antigens for presentation by CD1a. Through PLA_2G4D, IL-36 may thereby potentiate Th17 activity *via* CD1a-mediated T cell responses[174,473,474].

The transcription factor NFκB, which regulates a variety of immune pathways including cell proliferation, differentiation, and apoptosis, plays an important role in psoriasis pathogenesis. Elevated levels of activated NFκB are found in lesional skin and genetic variation of several NFκB pathway components is linked to disease[444,445,458,459,479]. Many cell types implicated in psoriasis, including Th17 cells, DCs and keratinocytes, depend on NFκB signalling for cytokine and chemokine production, and it has been hypothesised that NFκB may link altered keratinocyte and immune cell behaviour seen in psoriasis[480].

3.1.2 Regulatory T cells in psoriasis

3.1.2.1 Frequency and phenotype

Correlation between Treg frequency and disease severity remains disputed. Several studies have reported decreased Treg frequencies in peripheral blood of psoriatic patients; however, correlation to disease severity varied between cohorts[481-484]. In contrast, other studies showed no difference in circulating Treg frequency[485-488]. Moreover, Zhang *et al.* observed that patients with moderate-to-severe disease showed a higher frequency of Tregs, which correlated with psoriasis area severity index (PASI) scores, while patients with mild disease showed no change in Treg precentage compared to healthy controls[486]. For lesional skin,

most studies report an increased infiltration and frequency of Tregs compared to healthy skin[26,486,489-491]. Further, one study reported an increase in Treg frequency in chronic disease but a decrease in acute status[487], and differences between psoriasis types have been described[492]. Threfore, conflicting observations may result from differing disease states, biopsie sites and psoriasis types investigated.

3.1.2.2 Dysfunction

In most patients with psoriasis, Tregs isolated from skin lesions or peripheral blood are deficient in their ability to suppress effector T cell responses and proliferation[488,493,494] (Fig. 3.1), and Treg suppressive function may be partially restored after disease remission[493]. Further, Treg dysfunction was shown to be causal for effector T cell hyper-proliferation in CD18 (β2 integrin) knockout mice that present a psoriasiform phenotype[495]. Recent studies have identified several mechanisms through which Treg suppressive function might be impaired in psoriasis. Exposure of Tregs to high levels of IL-6 decreases Treg activity and enables effector T cells to escape from Treg suppression[496], indicating that the pro-inflammatory cytokine milieu in psoriasis lesions may contribute to impaired Treg suppressive function. MicroRNA (miR)-210, which inhibits expression of Foxp3, has been proposed to contribute to Treg dysfunction in psoriasis vulgaris, where $CD4^+$ T cells show increased miR-210 expression[497]. Overexpression of miR-210 was shown to reduce expression of the immunosuppressive cytokines IL-10 and TGF-β while increasing expression of the pro-inflammatory cytokines IL-17A and IFNγ. Circulating Tregs from patients with psoriasis show aberrant activation of the STAT3 pathway, induced by the pro-inflammatory cytokines IL-6, IL-21 and IL-23, and increased expression of pro-inflammatory cytokines including IL-17[498]. Interestingly, STAT3 is critical for Th17 cell differentiation *via* the expression of IL-23 receptor (IL-23R) and RORγt, both of which stabilize the Th17 phenotype that plays a crucial role in psoriasis pathogenesis[499]. Moreover,

the ectonucleases CD39 and CD73 modulate Treg numbers and function by converting adenosine triphosphate (ATP) to adenosine, which binds to the adenosine A2 receptor on Tregs[500,501]. In psoriasis vulgaris, Tregs show reduced expression of CD73 and inactivity of the CD73/adenosine monophosphate (AMP)-activated protein kinase (AMPK) pathway resulting in reduced suppressive function[502]. Further, ineffective homing of Tregs to inflamed tissues may also impact Treg functionality in psoriasis, as Tregs from patients with psoriasis show numerical, chemotactic, and functional impairment of $CCR5^+$ Tregs[503]. Taken together, these studies provide clear evidence for impaired suppressive function in both circulating and skin-resident lesional Tregs in psoriasis.

3.1.2.3 Th17/Treg balance

Th17 cells play an important role in immune responses to extracellular pathogens but are also implicated in the pathogenesis of inflammatory and autoimmune diseases[421,504-506]. In psoriasis, Th17 cells are hyper-activated and infiltrate into lesional skin[507], and the Th17-polarising cytokine IL-23 is elevated in psoriatic lesions[508,509]. The essential role of Th17 responses in psoriasis pathogenesis is further supported by the therapeutic efficiency of treatments blocking IL-17 and IL-23[510]. Several studies have reported an imbalance of the Th17/Treg ratio in patients with psoriasis[486,493,511]. This imbalance has been proposed to be regulated *via* the Notch1 signalling pathway[302]. Interestingly, neither Tregs from healthy controls nor psoriasis patients were able to control $CD4^+$ T cell-mediated IL-17 secretion[493].

3.1.2.4 Treg plasticity

Induced Tregs (pTregs and iTregs) and Th17 cells are in a constant competition for development, as they share the requirement for TGF-β for development from their common precursor, naïve T cells[512,513]. Upon *ex vivo* stimulation, Tregs from patients with severe psoriasis can differentiate to an IL-17A-producing phenotype which was linked to increased

levels of RORγt and loss of Foxp3[514]. This plasticity could be prevented by inhibition of histone/protein deacetylases. The histone deacetylase 1 (HDAC-1) is elevated in psoriatic skin[515], indicating that Treg plasticity and histone acetylation may be linked in psoriasis. IL-17A$^+$Foxp3$^+$CD4$^+$ cells have also been identified in psoriatic lesions[514]. Further, STAT3 can stabilise the Th17 phenotype through IL-23R and RORγt expression and thereby STAT3 hyper-activation in psoriasis may contribute to Treg plasticity[498,499].

Under inflammatory conditions, Tregs can produce pro-inflammatory cytokines such as IFNγ and IL-17A; however, while some studies suggest that these Tregs retain their suppressive phenotype, others report dysfunction and contribution to immunopathology[516]. Tregs from patients with psoriasis were reported to show a moderate, although not significant, increase in IFNγ production compared to healthy Tregs, while IL-22 production was unchanged[514]. Moreover, exposure of Tregs to IL-17A and IL-12, which are increased in psoriatic lesions[429,517], was shown to promote IFNγ production of Tregs[410,430,431,518]. IL-17A-mediated IFNγ production of Tregs was mediated *via* NFκB signalling[518], and IL-12 exposure led to a shift of Tregs towards a Th1 phenotype[410,430]. These studies indicate that Treg plasticity to produce other pro-inflammatory cytokines such as IFNγ may also play a role in skin inflammatory disease.

3.1.2.5 Therapeutics targeting Tregs in psoriasis

Many current or prospective psoriasis treatments modulate Treg frequency and/or functionality[417] (Fig. 3.1). Several treatments increase Treg numbers, including anti-TNFα, the folic acid analogue methotrexate, vitamin D, retinoids such as acitretin, and phototherapy (narrowband ultraviolet (UV)B, bath-psoralen UVA)[481,485,519-524]. Many psoriasis treatments have further been shown to (partially) rescue Treg suppressive function, i.e. methotrexate, phototherapy and the pan-protein kinase C (pan-PKC) inhibitor

sotrastaurin[485,502,524,525]. Moreover, anti-IL-17A and anti-IL-23 have been proposed to increase Treg frequency and *via* inhibition of Th2 and Th17 responses may also aid in restoring the Th17/Treg balance[526,527]. The restoration of Treg function in psoriasis may have a broad impact on pathogenesis and specific targeting of Tregs to increase functionality may provide an effective treatment.

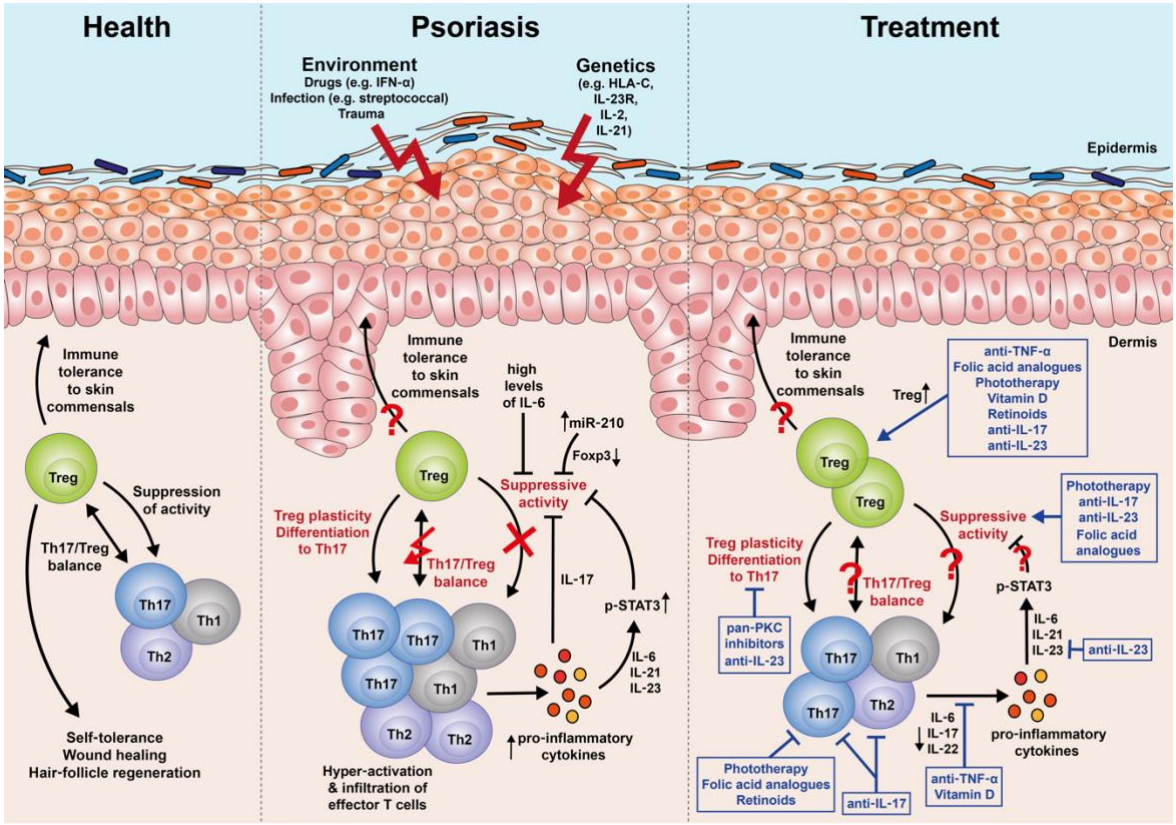

Fig. 3.1 Role of Tregs in psoriasis and impact of treatment on Treg phenotype and function. Psoriasis results from an interplay of genetic and environmental factors. Infiltration and hyper-activation of effector T cells lead to increased expression of pro-inflammatory cytokines and an impaired balance between Tregs and effector T cells. The pro-inflammatory milieu together with high levels of miRNA-210 cause impaired Treg suppressive functionality, and psoriatic Tregs show plasticity towards a Th17 phenotype. Several current and prospective psoriasis treatments have direct or indirect effects on Treg phenotype and frequency, can rescue Treg suppressive functionality and/or may restore Th17/Treg balance. Image reprinted with permission from Nussbaum *et al.* 2021, BJD[417].

3.1.3 Hypothesis and aims

Psoriasis is a T cell-mediated skin inflammatory disease in which CD1a-mediated T cell responses, including the secretion of inflammatory cytokines such as IL-17A, IL-22 and IFNγ, have been shown to contribute to exacerbation of disease (see 1.2.3 CD1a in skin inflammatory disease). Our studies presented in the previous chapter show that Tregs can functionally interact with CD1a to secrete IL-10 (see Chapter 2). Aiming to further elucidate the phenotype of CD1a-reactive Tregs, single-cell gene and surface marker expression analysis were performed. While increasing evidence supports a role for Tregs in the control of skin inflammation (see 1.3.2 Tregs in the skin), Tregs from patients with psoriasis are commonly dysfunctional and may contribute to pathogenesis (see 3.1.2 Regulatory T cells in psoriasis). Psoriatic Tregs show plasticity towards a Th17 phenotype[514], and high levels of IL-12 and IL-17A in psoriatic lesions may further shift Tregs towards an IFNγ-producing phenotype[410,430,431,517,518]. Therefore, I hypothesised that CD1a-reactive Tregs from patients with psoriasis may show a similarly dysfunctional and/or plastic phenotype, thereby contributing to disease pathogenesis.

The aims of the project included:

- Investigate the frequency of circulating CD1a-reactive Tregs in individuals with psoriasis
- High-dimensional profiling of peripheral CD1a-reactive Tregs in health and psoriasis to elucidate the role of CD1a-reactive Tregs in skin inflammatory diseases

3.2 Results

3.2.1 *Ex vivo* analysis of CD1a-autoreactive Tregs in health and psoriasis

To assess whether polyclonal Tregs from patients with psoriasis can interact with CD1a, IL-10 secretion of polyclonal Tregs from patients with psoriasis (PS) and healthy controls (HC) was measured (for patient information see Table 6.1). For this, circulating $CD25^+$ cells were isolated from peripheral blood, rested, and stimulated with K562-CD1a cells, using IL-2 and anti-CD11a as co-stimulation. IL-10 secretion was measured by secretion assay, gating on $CD3^+CD4^+CD25^+CD127^{low}$ cells. Of gated Tregs, 87.99% ± 6.21 of psoriasis patient cells and 88.68% ± 3.66 of healthy control cells expressed Foxp3, as determined by flow cytometry staining. Tregs from HC and PS secreted comparable levels of IL-10 upon stimulation with the K562-EV control (0.36% ± 0.09 and 0.44% ± 0.16, respectively) (Fig. 3.2). IL-10 secretion was significantly increased to 1.92% ± 0.37 and 2.10% ± 0.63 in the presence of CD1a, respectively. A comparable IL-10 secretion was observed when the isotype control was present (1.67% ± 0.35 and 1.74% ± 0.38, respectively), while IL-10 secretion was inhibited to levels comparable to the K562-EV control in the presence of anti-CD1a antibody (0.42% ± 0.15 and 0.52% ± 0.14, respectively). These data suggest that polyclonal Tregs from patients with PS can interact with CD1a and that CD1a-dependent IL-10 secretion is comparable between Tregs from psoriatic patients and healthy controls.

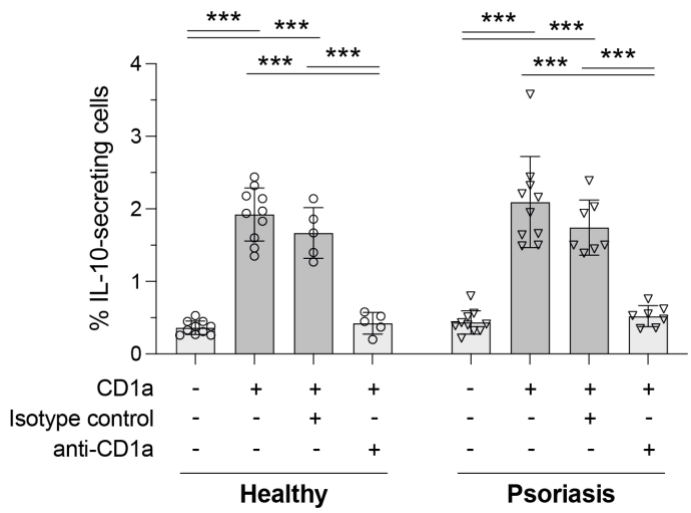

Fig. 3.2 CD1a-mediated IL-10 secretion of *ex vivo* polyclonal Tregs from psoriasis patients and healthy controls.

$CD25^+$ cells were isolated from peripheral blood of psoriasis patients or healthy controls and rested in Treg medium containing 200IU/ml IL-2 overnight. Cells were co-cultured with K562-CD1a cells or K562-EV cells as control in the absence or presence of anti-CD1a antibody (clone HI149) or an isotype control, in R10 medium supplemented with 200IU/ml IL-2 and 2.5µg/ml anti-CD11a. Secretion of IL-10 was determined by IL-10 secretion assay and Tregs were defined by gating on $CD3^+CD4^+CD25^+CD127^{low}$ cells. (n=5-10 donors; 3-4 independent experiments). *P < 0.05; **P < 0.01; ***P < 0.001; Two-way ANOVA with Tukey's and Šidák's correction for multiple comparison (mean ± SD).

To assess whether Tregs from psoriasis patients may secrete increased levels of the psoriasis-associated inflammatory cytokine IL-17A in response to CD1a stimulation compared to Tregs from healthy individuals, IL-17A secretion was assessed by secretion assay (Fig. 3.3). Tregs from both HC and PS showed a low baseline secretion of IL-17A (0.34% ± 0.21 and 0.32% ± 0.16, respectively), which did not change significantly in the presence of CD1a (0.29% ± 0.12 and 0.38% ± 0.23, respectively). These data suggest that psoriatic CD1a-reactive Tregs may not show a more Th17-like phenotype compared to healthy CD1a-reactive Tregs.

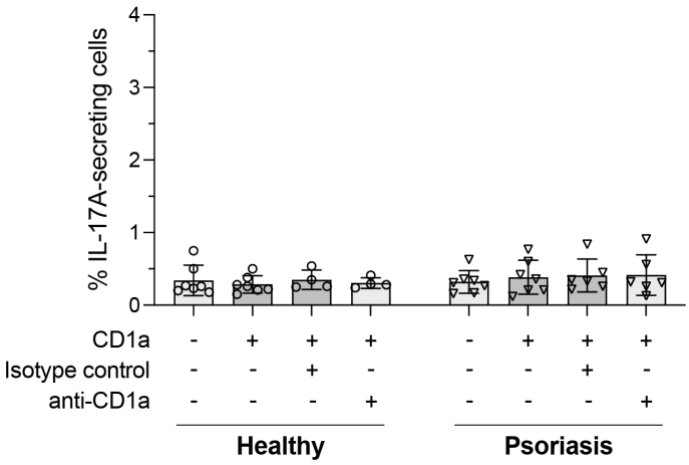

Fig. 3.3 CD1a-mediated IL-17A secretion of *ex vivo* polyclonal Tregs from psoriasis patients and healthy controls.

$CD25^+$ cells were isolated from peripheral blood of psoriasis patients or healthy controls and rested in Treg medium containing 200IU/ml IL-2 overnight. Cells were co-cultured with K562-CD1a cells or K562-EV cells as control in the absence and presence of anti-CD1a antibody (clone HI149) or an isotype control, in R10 medium supplemented with 200IU/ml IL-2 and 2.5µg/ml anti-CD11a. Secretion of IL-17A was determined by IL-17A secretion assay and Tregs were defined by gating on $CD3^+CD4^+CD25^+CD127^{low}$ cells. (n=4-7 donors; 2 independent experiments). ns > 0.05; *P < 0.05; Two-way ANOVA with Tukey's and Šidák's correction for multiple comparison (mean ± SD).

3.2.2 Single-cell analysis of CD1a-reactive Tregs

To gain a broader understanding of CD1a-reactive Tregs and study differences between these cells in health and psoriasis, single-cell sequencing of CD1a-reactive Tregs from healthy controls and patients with psoriasis was performed using the 10x Genomics platform. In the previous chapter, Tregs were shown to secrete IL-10 in response to CD1a stimulation (see Chapter 2). In psoriasis, Tregs show plasticity towards a Th17 phenotype[514], and high levels of IL-12 and IL-17A in psoriatic lesions may further cause Tregs to shift towards an IFNγ-producing phenotype[410,430,431,517,518]. Above, Treg secretion of IL-17A was shown to be independent of CD1a and comparable between HC and PS (Fig. 3.3). Next to IL-17A, CD1a-reactive T cells can also produce IL-22 and IFNγ, which is likely to be relevant to psoriasis pathogenesis[6,167,174]. Therefore, Tregs secreting IL-10, IFNγ and/or IL-22 in response to CD1a stimulation were investigated. For this, $CD25^+$ cells were isolated from peripheral blood of 3 healthy controls and 4 patients with psoriasis (for patient information see Table 6.1) and rested for 2 days. Cells were stimulated with CD1a using K562-CD1a cells in the presence of IL-2 and anti-CD11a and secretion assays for IL-10, IFNγ and IL-22 were performed. IL-10- and/or IFNγ-secreting Tregs (PE^+ and APC^+, respectively) were obtained by fluorescence-activated cell sorting (FACS) sorting, gating on $CD3^+CD4^+CD25^+CD127^{low}$ cells. The IL-22 detection antibody used was tagged with biotin and IL-22-secreting cells were identified post sequencing by TotalSeq-C antibody against biotin. IL-10 and IFNγ double-negative Tregs were sorted as stimulation control and unstimulated Tregs as negative control. In addition, IL-22- and/or IFNγ-secreting CD1a-reactive effector T cells (PE^+ and APC^+, respectively), IL-22 and IFNγ double-negative effector T cells and unstimulated effector T cells were sorted (Dr Yi-Ling Chen, Ogg Lab). Gene expression was determined by single-cell RNA sequencing

(scRNA-seq) and cell surface marker expression by TotalSeq-C antibody staining and cellular indexing of transcriptomes and epitopes by sequencing (CITE-seq). Bioinformatics analysis was performed by Dr Jeongmin Woo.

3.2.2.1 Identification of Treg cell subsets

Tregs are a heterogenous population that can be divided into different subpopulations with distinct phenotypes and functions. To cluster cell populations, Tregs and effector T cells (separated library sets from the same donors, Ogg Lab) were combined. As the herein studied Tregs are exclusively $CD4^+$, $CD8^+$ effector T cells were excluded from analysis based on cell surface protein and gene expression. Cell clusters were identified based on the weighted nearest neighbour (WNN) clustering algorithm in Seurat and visualised using Uniform Manifold Approximation and Projection (UMAP) analysis. A total of 15 clusters were identified (Fig. 3.4, A). Healthy and psoriasis samples were evenly distributed among all subsets (Fig. 3.4, B) and effector T cells and Tregs clustered separately (Fig. 3.4, B, C). However, while CD1a-reactive effector T cells clustered together (clusters 10 and 12), CD1a-reactive Tregs were distributed among all Treg clusters (Fig. 3.4, C, D).

Treg and effector T cell subpopulations were identified by gene expression obtained *via* scRNA-seq (Fig. 3.6) and cell surface marker expression obtained *via* CITE-seq (Fig. 3.7). Using previously defined markers for naïve and effector/memory Tregs, including CD45RA, CD45RO, CCR7, CD62L and HLA-DR[232,528-534], clusters 1 and 7 were termed naïve Tregs and clusters 0, 5 and 6 were termed effector/memory Tregs (Fig. 3.5). IL-10-secreting Tregs could be found throughout all Treg clusters but were enriched in clusters 6 and 7 (Fig. 3.5, C). The naïve Treg subpopulation was characterised by a $CD45RA^+CCR7^+CD62L^+HLA\text{-}DR^{low}$ phenotype (Fig. 3.5, B; Fig. 3.7), expressing high levels of CD27, CD38 and PD-L1 (Fig. 3.7). CD27 and CD38 are implicated in Treg

suppressive function and are present on highly suppressive Treg subsets[337-339,535], while the PD-L1/programmed cell death protein 1 (PD-1) axis plays an important role in Treg development and function[536]. Effector/memory Tregs were defined by expression of high levels of the memory marker CD45RO, the activated/memory marker CD147, as well as effector/memory and migration markers such as CCR4, CCR5 and CCR6[537-541] (Fig. 3.5, B; Fig. 3.7). This subpopulation further expressed high levels of several proteins involved in maintaining Treg stability and suppressive function, including tumor necrosis factor receptor 2 (TNFR2)[542-544] and CD39[252,545,546], and co-stimulatory molecules implicated in Treg activation and function, including CD28 and ICOS[547,548].

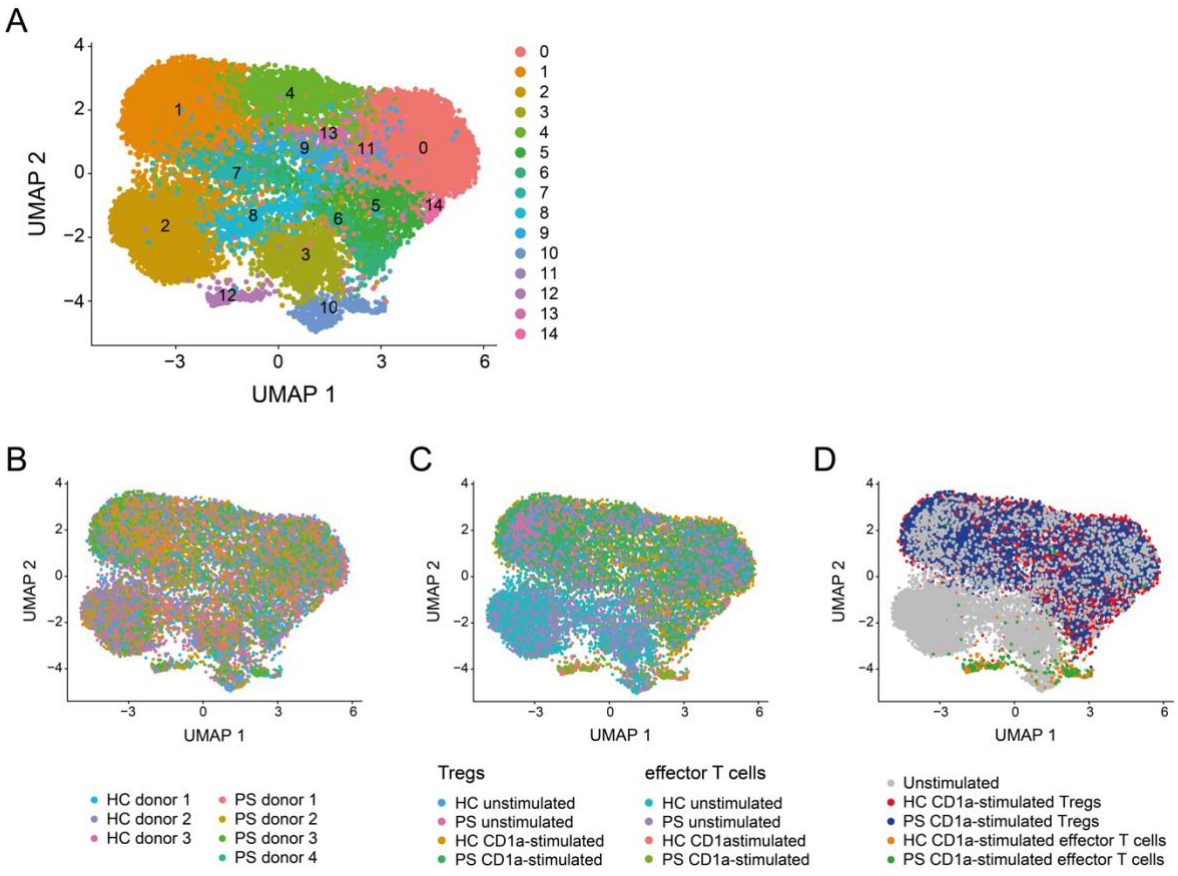

Fig. 3.4 Cell clustering of Tregs and CD4$^+$ effector T cells.

(A) Cell clusters within Tregs and CD4$^+$ effector T cells were identified based on WNN clustering algorithm in Seurat and visualised through UMAP analysis. **(B)** Distribution of healthy control (HC) and psoriasis (PS) samples within clusters. **(C, D)** Distribution of unstimulated and CD1a-stimulated Tregs and CD4$^+$ effector T cells within clusters.

Cluster 4 showed low to moderate expression of CD45RA and CD45RO but expressed high levels of several Treg function-associated proteins such as TIGIT (T cell immunoreceptor with Ig and ITIM domains)[549,550], GARP[551], CD27[337-339] and CD39[252,545,546] (Fig. 3.5, B; Fig. 3.7). These cells further expressed high levels of PD-1 and moderate levels of PD-L1, which are involved in Treg development and function[536], and high levels of CD49d, an integrin subunit that mediates interaction with ECM components and migration, and is constitutively expressed by many cell types including lymphocytes[552-554]. While CD49d is thought to be a marker of antigen-experienced T cells[555,556], recent publications suggest that CD49d$^+$ Tregs may show lower suppressive capacity compared to CD49d$^-$ Tregs[557] and the use of CD49d as a marker to exclude non-Tregs during Treg isolation[558]. However, although Foxp3 expression was higher in effector/memory Tregs, both the naïve Treg cluster and cluster 4 expressed Foxp3 (Fig. 3.5, B). This suggests that the here isolated peripheral Tregs may have encountered antigens before or that CD49d expression may be driven by antigen-independent mechanisms, i.e. TCR-independent cell activation. Due to its 'intermediate' and distinct phenotype, cluster 4 was analysed separately from naïve and effector/memory Tregs.

While cluster 9 showed only low expression of CD45RO, this subpopulation expressed high levels of C-X-C motif chemokine receptor 3 (CXCR3) and CCR5, suggesting an effector/memory phenotype[539,540] (Fig. 3.5, B; Fig. 3.7). Moreover, these cells expressed high levels of CD94, an NK cell receptor that is increased on T cells in psoriasis[559] and Tim-3, a Treg marker associated with suppression that is found infrequently on peripheral Tregs but is commonly expressed in peripheral tissue[550]. Due to the differential expression of CD45RO and CXCR3/CCR5 and a higher frequency of IL-22-secreting Tregs within this subpopulation (Fig. 3.5, C), cluster 9 was analysed separate from the effector/memory Treg population.

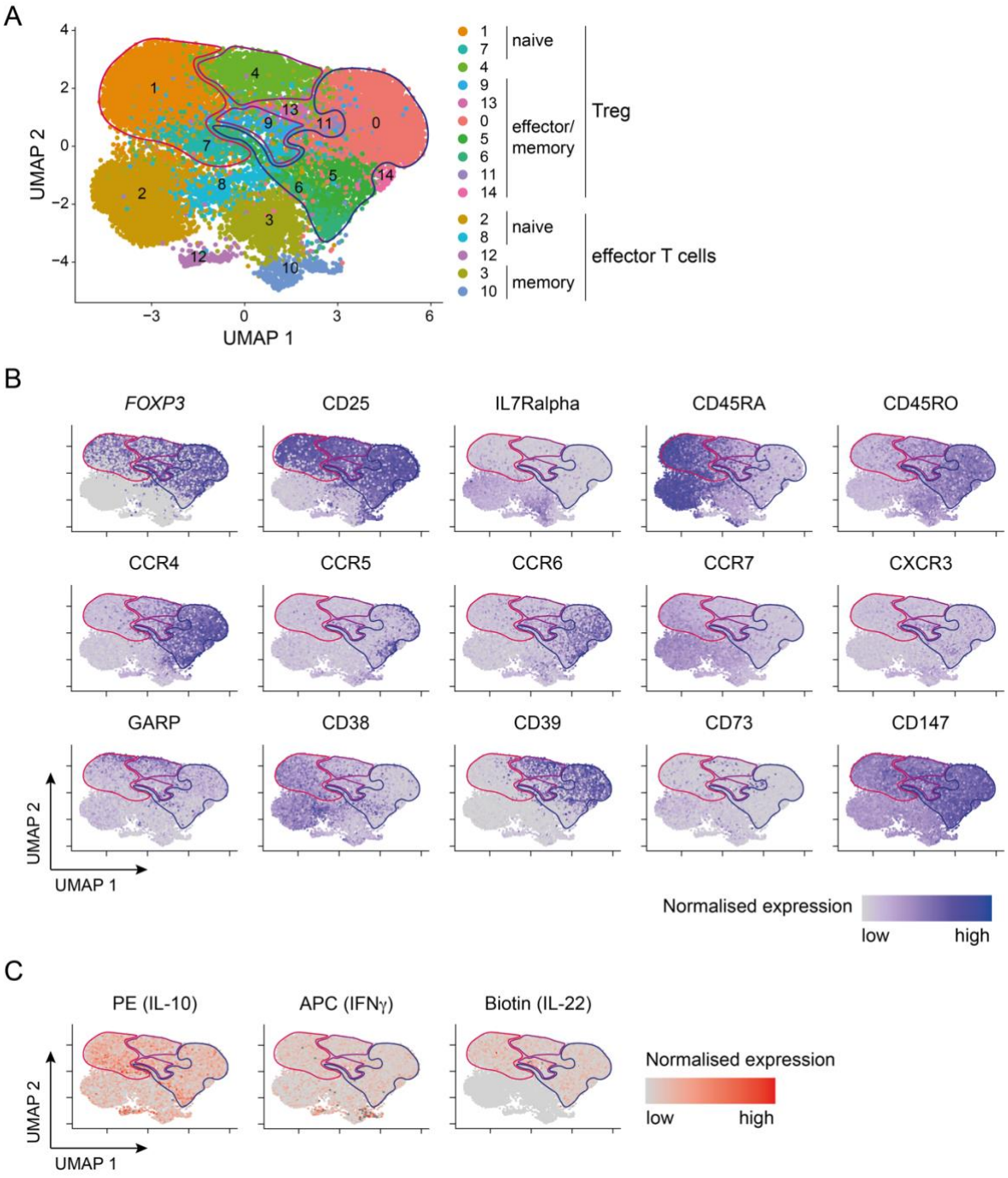

Fig. 3.5 Identification of Treg subsets and cell surface expression within Treg subpopulations. **(A)** UMAP plot showing clustering of Tregs and effector T cells, labelled based on naïve and memory marker expression. Encircled clusters represent Treg cell subsets that were further analysed for gene and cell surface marker expression. **(B)** Feature plots showing gene expression of Foxp3 and cell surface expression of CD25, IL7Ralpha (CD127), CD45RA, CD45RO, CCR4, CCR5, CCR6, CCR7, CXCR3, GARP, CD38, CD39, CD73 and CD147. **(C)** Feature plots showing staining with PE (IL-10 secretion for Tregs, IL-22 secretion for effector T cells), APC (IFNγ secretion for Tregs and effector T cells) and Biotin (IL-22 secretion for Tregs; no Biotin staining of effector T cells was performed).

While clusters 11 and 14 showed similar effector/memory marker expression to clusters 0, 5 and 6, they showed distinct expression patterns and were therefore not combined with the effector/memory Treg subpopulation. Cluster 11 showed high expression of CD73 (Fig. 3.5, B; Fig. 3.7), an ectonuclease that together with CD39 enables Tregs to convert ATP to immunosuppressive adenosine[252,545,546]. Cluster 14 showed particularly high expression of HLA-DR (Fig. 3.7), a marker for Treg activation that may also be associated with terminal differentiation[528]. Cluster 13, while only expressing moderate levels of CD45RO, expressed high levels of CD147 and was classified as an activated/memory Treg cluster (Fig. 3.5, B; Fig. 3.7). Unlike the effector/memory Treg clusters, this cluster expressed much lower levels of migration-associated chemokines. Due to low cell numbers (Table 6.18), these clusters were excluded from further analysis.

For most markers, surface protein expression correlated with gene expression. However, CD1a was upregulated on the cell surface within all CD1a-stimulated subpopulations (Fig. 3.7), but no gene expression of CD1a could be detected, indicating that Tregs and effector T cells may acquire CD1a protein from co-cultured K562-CD1a cells *via* trogocytosis (supported by unpublished data, Ogg Lab).

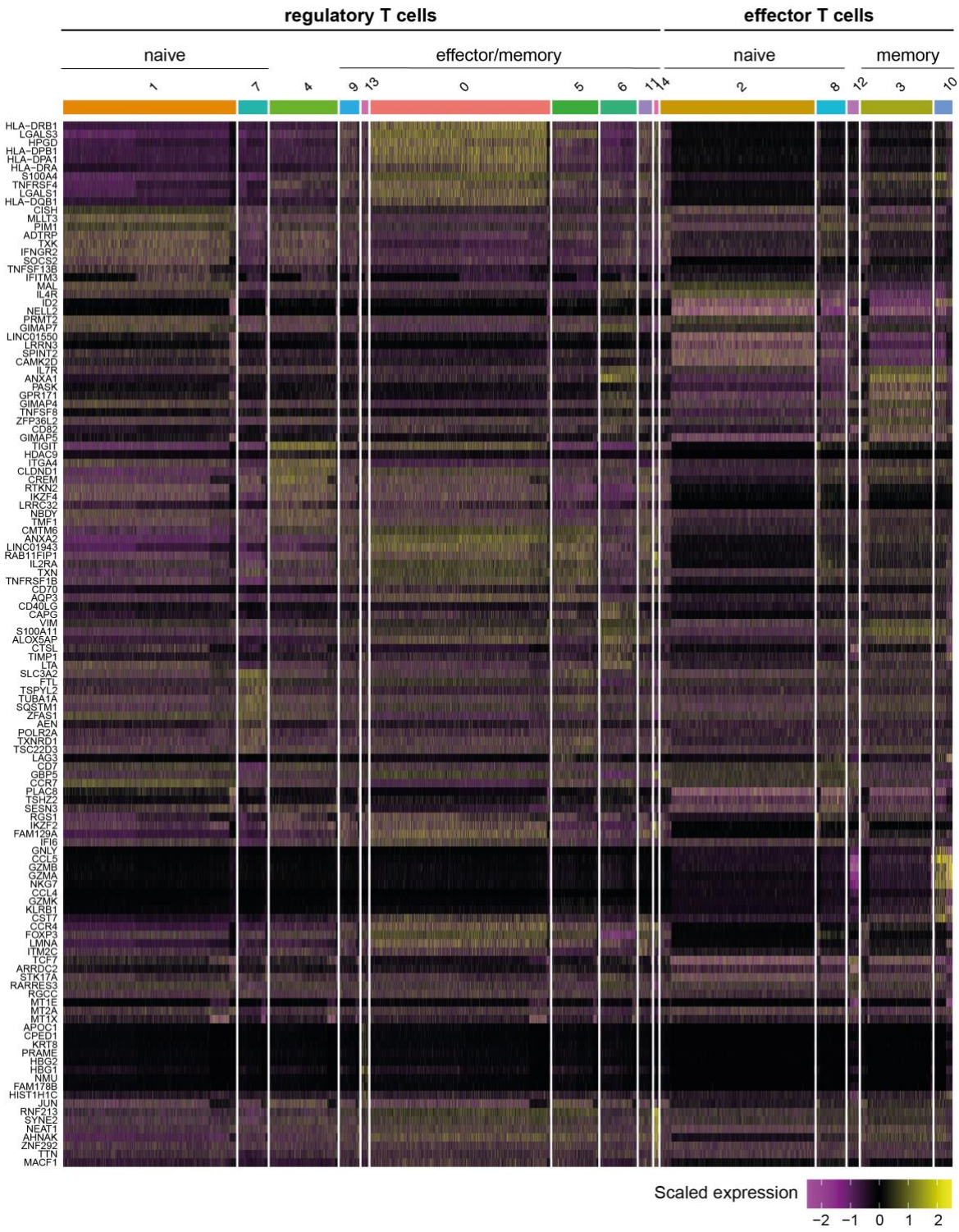

Fig. 3.6. Differential gene expression between cell clusters.

Heatmap showing the top 10 gene markers (by fold change; adj. p-values of < 0.05) for each subset, excluding ribosomal and mitochondrial genes. Gene expression is shown as scaled expression (normalised expression was centred on the overall median expression), fold-changes were calculated from normalised expression in a specific subset compared to the normalised expression in the other subsets.

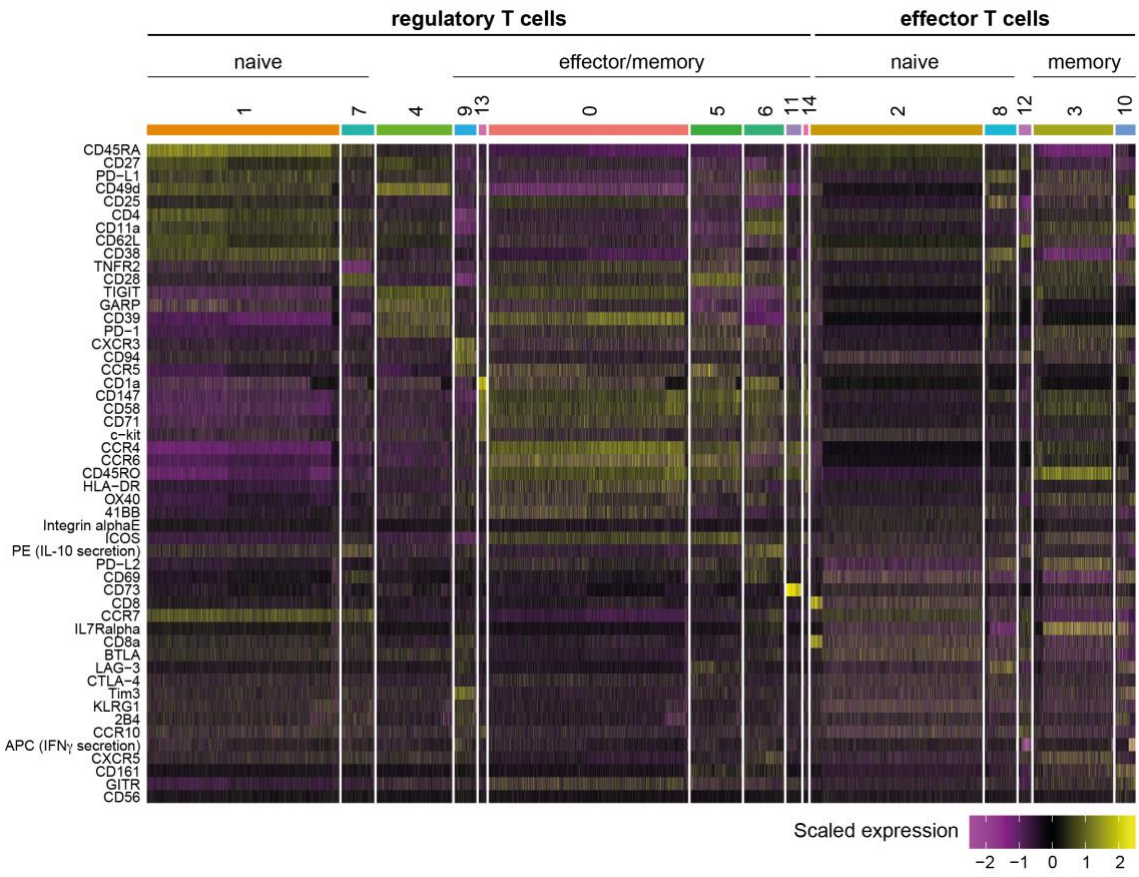

Fig. 3.7. Differential surface marker expression between cell clusters.

Heatmap showing differentially expressed CITE-Seq surface markers (by fold change; adj. p-value of < 0.05) for each subset. Marker expression is shown as scaled expression (normalised expression was centred on the overall median expression), fold-changes were calculated from normalised expression in a specific subset compared to the normalised expression in the other subsets.

3.2.2.2 Frequency of IL-10-, IFNγ-, and IL-22-secreting Tregs

To investigate the distribution of IL-10-, IFNγ-, and/or IL-22-secreting Tregs within healthy controls and psoriasis patients as well as between different Treg subpopulations, the frequency of different secreting populations (as percentage of all secreting cells within the respective subpopulation) were determined (Fig. 3.8). Overall, Tregs from PS showed lower frequencies of IFNγ- and higher frequencies of IL-10- and IL-22-secreting Tregs compared to HC. Naïve Tregs showed a slightly higher frequency of IL-10-secreting and lower frequency of IFNγ-secreting Tregs compared to effector/memory Tregs, but levels of

IL-22-secreting Tregs were comparable. In contrast, cluster 9 showed much higher frequencies of IL-22-secreting Tregs.

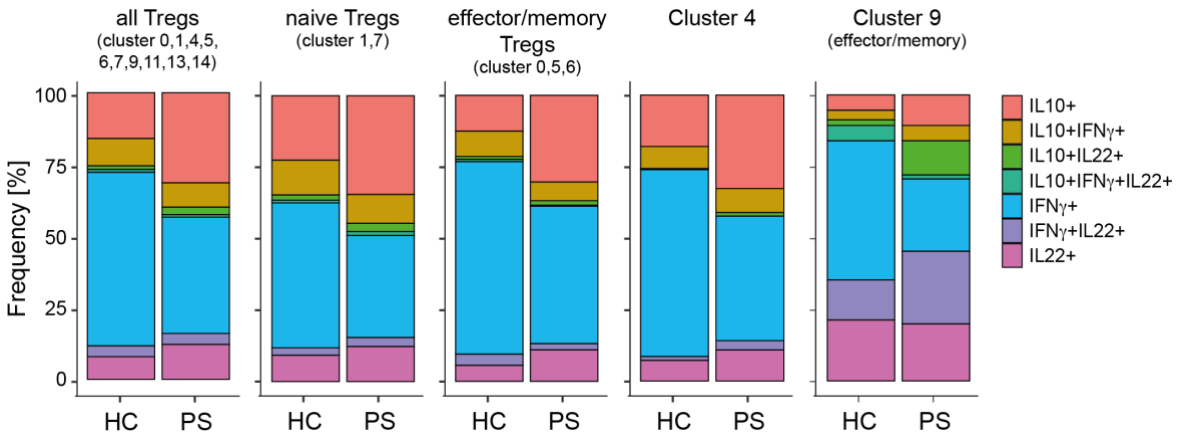

Fig. 3.8 Frequencies of IL-10-, IFNγ-, and IL-22-secreting Tregs.

Frequency (as percentage) of different populations of IL-10-, IFNγ- and/or IL-22-secreting Tregs, in all Tregs, naïve Tregs (cluster 1, 7), effector/memory Tregs (cluster 0, 5, 6), cluster 4 or cluster 9. Frequencies shown are relative to all IL-10-, IFNγ- and IL-22-secreting Tregs in the respective clusters.

3.2.2.3 Stimulation-induced changes in gene expression independent of CD1a reactivity

Several genes were differentially expressed in Tregs upon CD1a-stimulation but independent of IL-10, IFNγ or IL-22 secretion, and therefore may indicate (partially) altered activation pathways. As these genes were modulated independent of disease state, Tregs from HC and PS were pooled for analysis and visualisation (Fig. 3.9). Many genes that were differentially expressed upon stimulation are associated with cell cycle progression, stress response, and cell proliferation and differentiation. Moreover, most of these genes were similarly up- or down-modulated within all 4 compared groups, which contrasts differential gene expression of cytokine-secreting CD1a-reactive Tregs (Fig. 3.11; Fig. 3.12; Fig. 3.14;

Fig. 3.15). This further strengthens that these genes are likely modulated in a CD1a-independent manner.

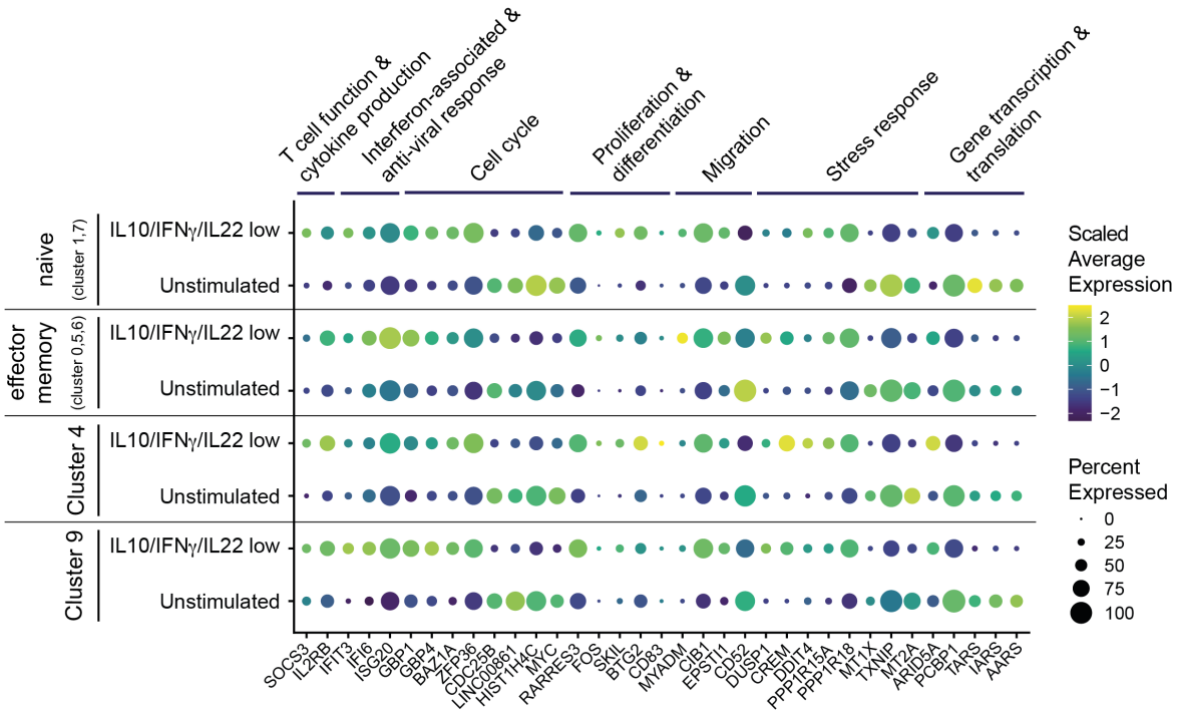

Fig. 3.9 Stimulation-mediated changes in Treg gene expression.

Gene expression dot plot showing genes differentially expressed (adj. p-value < 0.05; log2FC > 0.9) between CD1a-stimulated Tregs that secrete no or low levels of IL-10, IFNγ and IL-22 (IL10/IFNγ/IL22 low) and unstimulated Tregs. Genes that were differentially expressed in an IL-10-, IFNγ- or IL-22-secreting population in either of the shown groups were excluded and are shown in following figures.

3.2.2.4 Differential gene expression in Tregs from patients with psoriasis and healthy controls

Several genes were differentially expressed between Tregs from patients with psoriasis and healthy controls, independent of CD1a reactivity (Fig. 3.10). Many of these are known to be associated with psoriasis pathogenesis. The psoriasis susceptibility genes *RELB*[445], a member of the NFκB family, and *ERAP2*[455,560], which is involved in the processing of

MHC-I ligands[561], were expressed at lower levels in stimulated Tregs from individuals with PS compared to HC. Interferon-stimulated genes, including *IFI44L* and *RGS1*, have been reported to be upregulated in psoriasis lesions[562-564]. While *IFI44L* expression was upregulated, expression of *RGS1* was lower in Tregs from patients with PS compared to HC. As previous studies measured gene expression in whole skin biopsies, it is plausible that different cell types may show differential expression of *RGS1*. Tregs express higher levels of *RGS1, RGS9* and *RGS16* compared to naïve T cells, and expression is correlated to lower migratory capability[565]. Therefore, reduced expression of *RGS1* in Tregs from individuals with PS may support increased Treg cell migration and tissue infiltration. Moreover, Tregs from psoriasis patients showed higher expression of *OSM,* which is elevated in psoriasis lesions and plays a pro-inflammatory role in a mouse model of psoriasis-like skin inflammation[566,567].

Additionally, *NFKBIA* (encoding NFκB Inhibitor Alpha, IκBα) and *NFKB2* (encoding NFκB2) were expressed to a higher degree in HC compared to PS upon stimulation in all Treg subpopulations, independent of CD1a reactivity (Fig. 3.11, Fig. 3.12, Fig. 3.14, Fig. 3.15). IκBα is involved in the regulation of NFκB activity[568] and decreased expression of *NFKBIA* in Tregs from patients with PS fits with previously reported increased expression of NFκB in psoriasis, driving inflammation[479,480]. NFκB2 plays an important role in Treg homeostasis and deletion of *NFKB2* in Tregs results in impaired Treg function and inflammation in mouse models[569,570]. Thus, lower expression of *NFKB2* in Tregs from individuals with PS may add to Treg dysfunction in psoriasis.

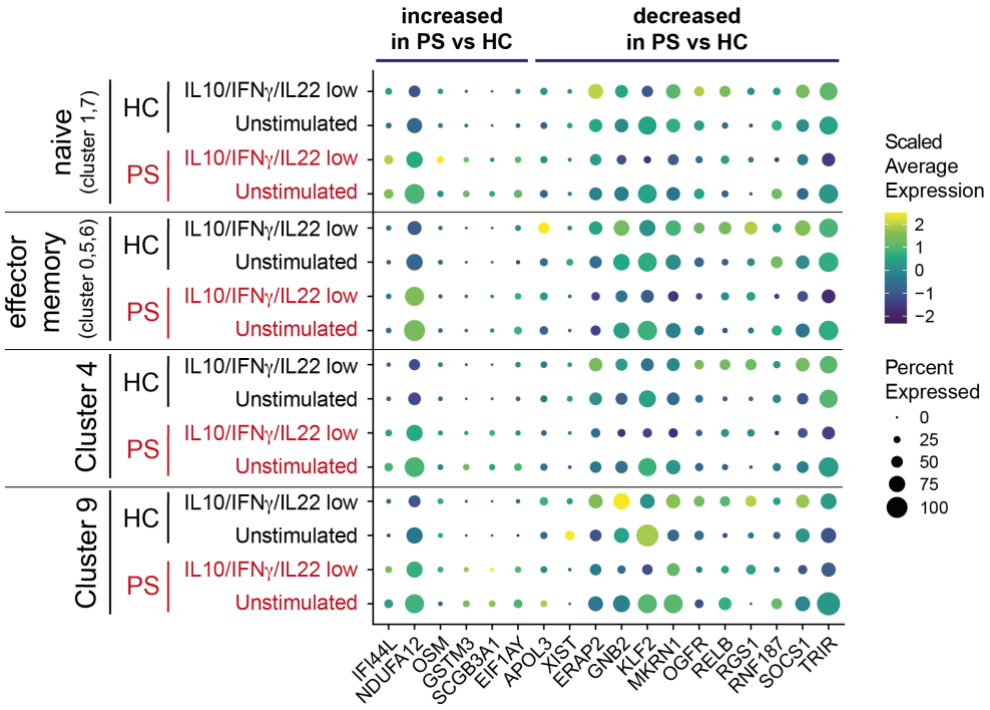

Fig. 3.10 Differential gene expression of Tregs from psoriasis patients and healthy controls. Gene expression dot plot of genes differentially expressed (adj. p-value < 0.05; log2FC > 0.5) between Tregs from PS and HC. Genes shown were differentially expressed in CD1a-stimulated Tregs that secrete no or low levels of IL-10, IFNγ and IL-22 (IL10/IFNγ/IL22 low) and/or in unstimulated Tregs. Genes that were differentially expressed in any IL-10-, IFNγ- or IL-22-secreting population are shown in following figures.

3.2.2.5 Analysis of gene and surface marker expression of CD1a-reactive Tregs in health and psoriasis

For differential gene and cell surface marker expression analysis, unstimulated Tregs, CD1a-stimulated Tregs that secrete no or low levels of IL-10, IFNγ and IL-22 (IL10/IFNγ/IL22 low Tregs), and CD1a-stimulated Tregs that secrete IL-10, IFNγ and/or IL-22 were compared, separating Treg populations secreting either or combinations of these cytokines.

3.2.2.5.1 Naïve Tregs

All naïve Tregs from patients with PS showed higher surface expression of CCR7 and lower surface expression of CCR5 and CXCR3 compared to HC (Fig. 3.11, B). It is possible that circulating naïve Tregs in patients with psoriasis may present a phenotype with poor tissue migratory capacity, which in turn could reduce naïve Treg activation and function.

Naïve Tregs secreting IL-10, IFNγ and/or IL-22 in response to CD1a stimulation showed overall similar Treg lineage and functional marker expression compared to CD1a-stimulated IL10/IFNγ/IL22 low Tregs (Fig. 3.11, A). While *GIMAP1*, *GIMAP7* and *EEF1B2* expression was increased in IL-10-secreting Tregs from HC compared to PS, *CTLA4* was expressed at a higher level in IFNγ-secreting Tregs from PS (Fig. 3.11, A). In other respects, gene expression patterns were comparable between Tregs that upregulated IL-10, IFNγ and/or IL-22 secretion upon CD1a-stimualtion and the stimulation control. IL-10-secreting Tregs showed reduced cell surface expression of CD25, TIGIT and TNFR2 (Fig. 3.11, B), indicating that induction of IL-10-secretion may negatively affect the Treg phenotype and may be independent of disease state in naïve Tregs[542-544,549,550]. However, these cells also upregulated expression of CD69, which is an activation marker that is further associated with suppressive functionality[571]. Further, IL-22-secreting Tregs from patients with PS showed high expression of CD11a (Fig. 3.11, B). CD11a can be induced by TCR engagement, and it is possible that CD1a-reactive IL-22-secreting Tregs from patients with PS may have previously been exposed to higher amounts of CD1a-presented antigens compared to HC.

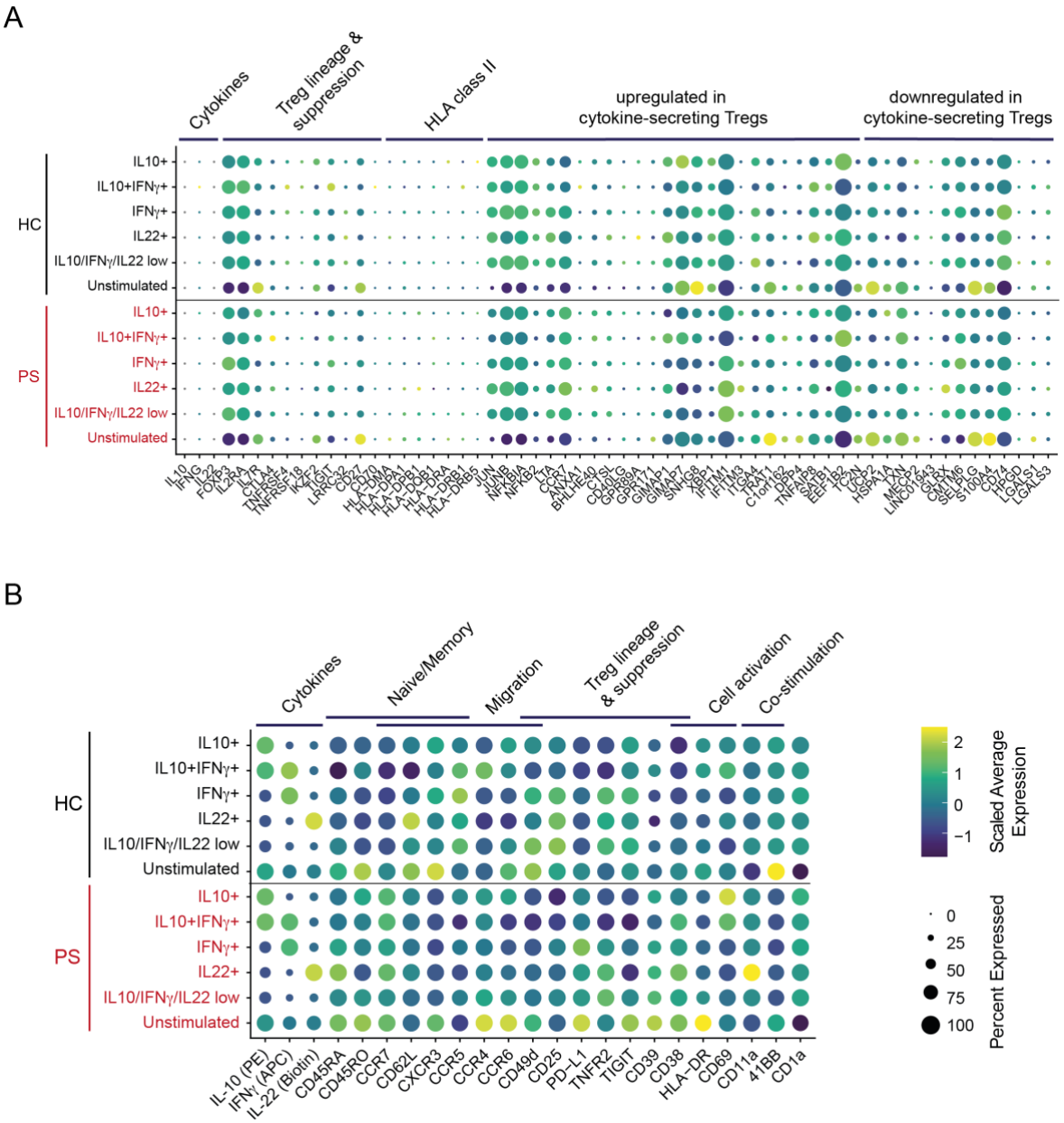

Fig. 3.11 Differential gene and surface protein expression in IL-10-, IFNγ-, and IL-22-secreting CD1a-reactive naïve Tregs.

(A) Gene expression and **(B)** surface protein expression dot plots for naïve Tregs (cluster 1, 7), showing expression of Tregs from HC and PS separately. Differential expression analysis was performed between unstimulated Tregs, CD1a-stimulated Tregs that secrete no or low levels of IL-10, IFNγ and IL-22 (IL10/IFNγ/IL22 low), and CD1a-stimulated Tregs that secrete IL-10, IFNγ and/or IL-22 ($IL10^+$, $IL10^+IFN\gamma^+$, $IFN\gamma^+$, $IL22^+$). Genes and cell surface markers shown were differentially expressed (gene expression: adj. p-value < 0.05; log2FC > 1) or selected genes and surface markers of interest within either naïve Tregs, effector/memory Tregs, cluster 4 or cluster 9.

3.2.2.5.2 Effector/memory Tregs

Within the effector/memory Treg subpopulation, Tregs that secreted IL-10 in response to CD1a stimulation ($IL10^+$ and $IL10^+IFN\gamma^+$) showed distinct gene and cell surface marker expression patterns (Fig. 3.12; Fig. 3.13). CD1a-reactive IL-10-secreting Tregs downregulated the expression of Treg lineage markers such as *FOXP3* and CD25 (gene and surface expression), while upregulating *IL7R*. In addition, many markers associated with Treg function and suppressive capacity were downregulated in these cells, including *CTLA4*[572], *TNFRSF4* (encoding TNF receptor superfamily member 4/OX40)[547], *TNFRSF18* (GITR)[573], *IKZF2* (encoding IKAROS family zinc finger 2; Helios)[574], *TIGIT* (gene and cell surface expression)[549,550], *LRRC32* (encoding LLRC32/GARP)[551] and *CD27*[337-339]. OX40 and CD27 further play a role in limiting the differentiation of Tregs to a Th17 phenotype, and Tregs lacking OX40 and CD27 signalling expressed high levels of IL-17A and were impaired in their ability to control skin inflammation[575]. In psoriatic skin, CD27 expression was further inversely correlated to Treg production of IL-17[575], which may hint towards CD1a-mediated stimulation promoting Treg differentiation into a Th phenotype. Unlike IL-22- and IFNγ-secreting Tregs, IL-10-secreting Tregs further showed an increase in naïve and central/memory Treg makers[232,528-534], including CD45RA, CCR7 (gene expression in HC and PS, surface expression only in PS) and CD62L (in PS), while HLA-DR expression was decreased (Fig. 3.12, A, B; Fig. 3.13, C). Further, IL-10-secreting Tregs expressed higher cell surface levels of CD49d, which is increased upon antigen stimulation but has also been proposed to mark less suppressive Tregs or even non-Treg cells[555-558]. These data suggest that CD1a-reactive IL-10-secreting Tregs may shift towards a more naïve to central/memory phenotype and may at least partially lose their Treg and suppressive phenotype.

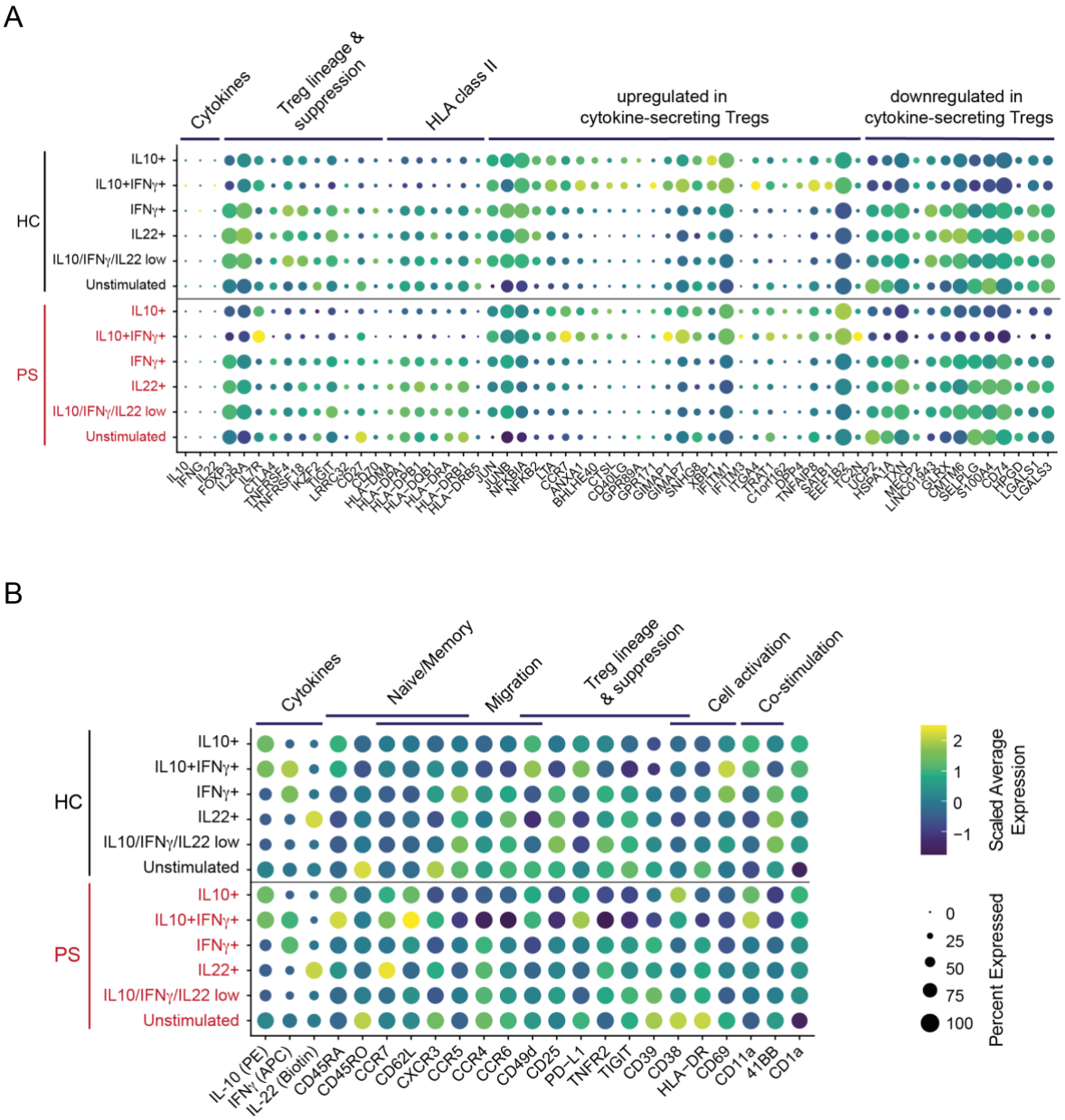

Fig. 3.12 Differential gene and surface protein expression in IL-10-, IFNγ-, and IL-22-secreting CD1a-reactive effector/memory Tregs.

(A) Gene expression and **(B)** surface protein expression dot plots for effector/memory Tregs (cluster 0, 5, 6), showing expression of Tregs from HC and PS separately. Differential expression analysis was performed between unstimulated Tregs, CD1a-stimulated Tregs that secrete no or low levels of IL-10, IFNγ and IL-22 (IL10/IFNγ/IL22 low), and CD1a-stimulated Tregs that secrete IL-10, IFNγ and/or IL-22 ($IL10^+$, $IL10^+IFN\gamma^+$, $IFN\gamma^+$, $IL22^+$). Genes and surface markers shown were differentially expressed (gene expression: adj. p-value < 0.05; log2FC > 1) or selected genes and surface markers of interest within either naïve Tregs, effector/memory Tregs, cluster 4 or cluster 9.

Several genes further suggest (partial) loss of suppressive functionality in CD1a-stimulated IL-10-secreting Tregs. MECP2 (methyl CpG binding protein 2) is a transcriptional repressor that is crucial for maintenance of Foxp3 expression during inflammation and Treg-specific deletion causes spontaneous immune activation and failure to protect against autoimmunity in mice[576]. Further, *MECP2* expression is reduced in PBMCs from patients with psoriasis[577]. Similarly, *MECP2* expression was downregulated in IL-10-secreting Tregs from PS compared to HC (Fig. 3.13, A, B) and therefore may contribute to loss of Treg lineage stability and enhance Treg dysfunction in psoriasis. Unlike most other gene expression changes seen in IL-10-secreting Tregs, *MECP2* was also downregulated in IFNγ-secreting Tregs in both HC and PS, which may hint towards MECP2 playing a broader role in Treg dysfunction, independent of IL-10 secretion. HPGD (15-Hydroxyprostaglandin Dehydrogenase) has been shown to be important in suppression of conventional T cells to maintain adipose tissue homeostasis[578], and Galectin 1 (encoded by *LGALS1*) is an anti-inflammatory protein that is highly expressed in Tregs[579,580]. Galectin 1 antagonises T cell TCR signalling and blocking of galectin 1 binding has been shown to reduce Treg suppressive functionality. In CD1a-reactive IL-10-secreting effector/memory Tregs, *HPGD* and *LGALS1* expression were decreased (Fig. 3.13, A, B), which may augment loss of Treg function. Although most gene expression changes in CD1a-reactive IL-10-secreting Tregs suggest a more inflammatory and less suppressive phenotype, increased expression of *ANXA1* (encoding Annexin 1) may indicate that these cells retain some anti-inflammatory and suppressive properties. Annexin 1 is an anti-inflammatory protein that may also be involved in Treg suppressive function[581,582].

Several genes indicated in effector differentiation and T cell polarisation were modulated in CD1a-stimulated IL-10-secreting Tregs. Foxp3 acts as a repressor of the DNA-binding protein SATB1 (Special AT-Rich Sequence Binding Protein 1), and lacking SATB1

repression leads to Treg effector differentiation and loss of Treg functionality[583]. Similarly, absence of P-Selectin Glycoprotein Ligand 1 (PSGL-1; encoded by *SELPLG*) promotes effector T cell differentiation, PSGL-1-deficiency impairs T cell recruitment to inflamed skin, and PSGL-1-deficient Tregs show reduced suppressive functionality[584-586]. *S100A4* (encoding S100 calcium binding protein A4), which is increased in psoriasis, is involved in T cell activation and polarisation to a Th2 phenotype[587-589]. Moreover, expression of the mitochondrial transporter protein UCP2 (Uncoupling Protein 2) is reduced in lesional psoriatic skin and inhibition of *UCP2* promotes terminal differentiation of $CD8^+$ T cells into short-lived effector cells[590,591]. Therefore, increased gene expression of *SATB1* and decreased expression of *SELPLG*, *S100A4* and *UCP2* by CD1a-reactive IL-10-secreting Tregs (Fig. 3.13, A, B) may indicate a polarisation of these Tregs towards a more effector-like phenotype.

In addition to changes seen in all IL-10-secreting effector/memory Tregs, IL-10-secreting Tregs from patients with PS (especially $IL10^+IFN\gamma^+$) showed higher upregulation of CD45RA, CCR7 (gene and surface protein expression) and CD62L in response to CD1a stimulation (Fig. 3.12; Fig. 3.13), suggesting that Tregs from patients with psoriasis may more readily shift towards a naïve to central/memory phenotype compared to HC[232,528-534]. Further, *IL7R* expression was increased in $IL10^+IFN\gamma^+$ Tregs. Expression of CD127 (encoded by *IL7R*) on $CD8^+$ T cells is related to a central/memory phenotype[592], however, whether this is also true for Tregs, or whether CD127 expression on Tregs is mainly associated with Treg activation[593], is not known. Interestingly, *ex vivo* skin Tregs have been shown to express CD127[593], which may indicate that $IL10^+IFN\gamma^+$ Tregs from patients with PS may be enriched for re-circulating skin Tregs. Moreover, several other genes were increased in $IL10^+IFN\gamma^+$ Tregs from individuals with PS (i.e. *IFITM3*, *GIMAP1*, *TC2N*), while others were increased in $IL10^+IFN\gamma^+$ Tregs from HC (i.e. *GPR171*, *TNFAIP8*) (Fig.

3.12, A). This may indicate that differences in Treg activation status and previous priming of CD1a-reactive Tregs in the skin may influence CD1a-mediated changes in Treg phenotype.

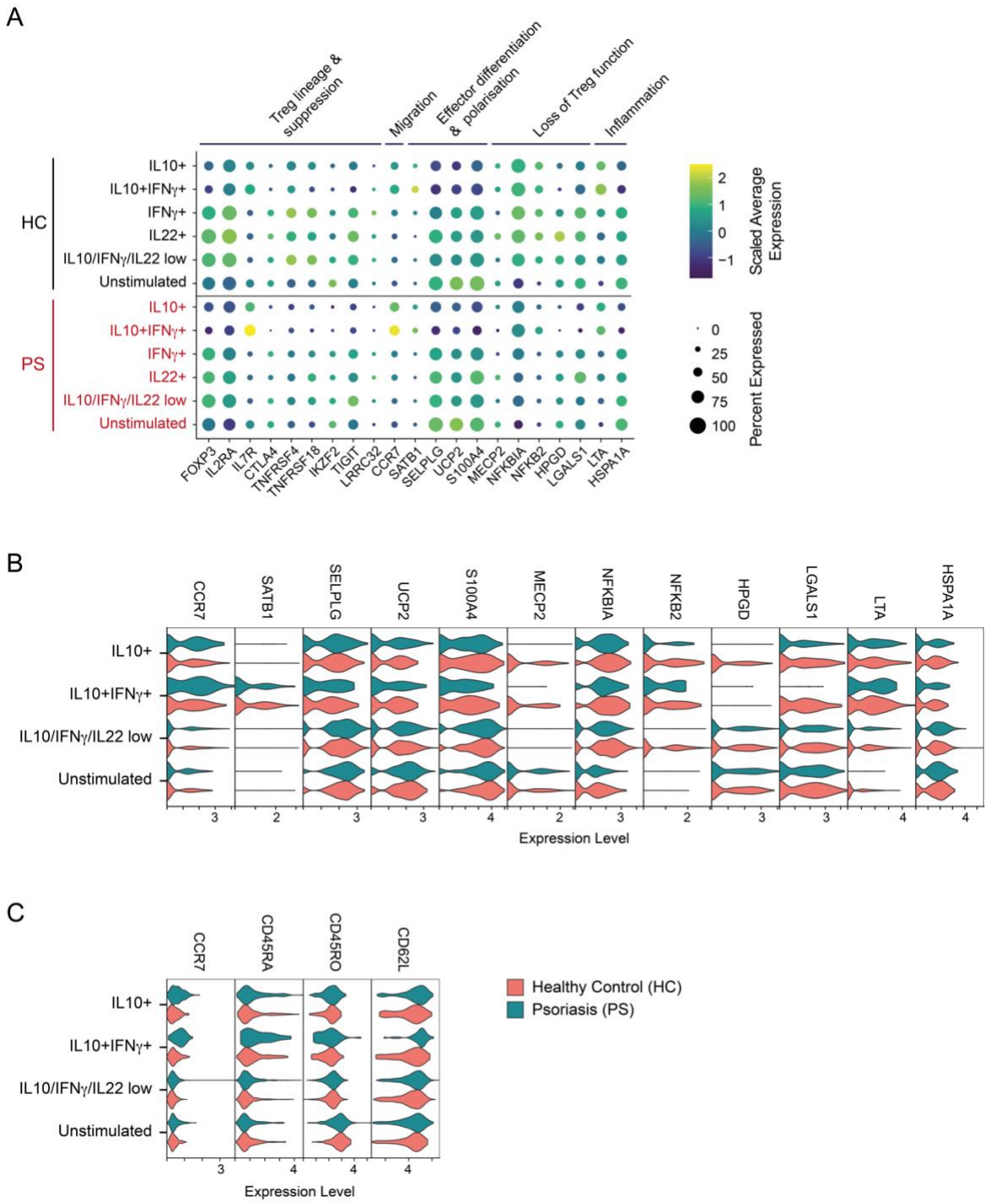

Fig. 3.13 IL-10-secreting CD1a-reactive effector/memory Tregs shift towards a central/memory phenotype and downregulate Treg lineage and suppressive markers.

(A) Gene expression dot plots and **(B, C)** violin plots of **(B)** gene expression and **(C)** surface protein expression of markers associated with Treg lineage and suppressive function in effector/memory Tregs (cluster 0, 5, 6). Expression of Tregs from HC and PS are shown separately for unstimulated Tregs, CD1a-stimulated Tregs that secrete no or low levels of IL-10, IFNγ and IL-22 (IL10/IFNγ/IL22 low), and CD1a-stimulated Tregs that secrete IL-10 ($IL10^+$) or IL-10 and IFNγ ($IL10^+IFN\gamma^+$).

3.2.2.5.3 Cluster 4

Within cluster 4, Tregs from patients with psoriasis showed lower expression of Treg lineage and functional markers upon CD1a stimulation compared to HC, including *FOXP3*, *IL2RA* (gene expression and CD25 surface expression), *TNFSR4*[547] and *TNFSR18*[573] (Fig. 3.14, A, B). Moreover, CD1a stimulation-induced IL-10 and IFNγ secretion was lower in Tregs from PS compared to HC (Fig. 3.14, B). These results may indicate that this Treg subpopulation, independent of CD1a-mediated modulation of Treg function, may be profoundly dysfunctional in patients with psoriasis. Cluster 4 Tregs from PS showed increased expression of interferon-induced genes (*IFITM1* and *IFITM3*) and PS-derived IL-10-secreting Tregs expressed higher levels of *TIGIT* and *EEF1B2* (Fig. 3.14, A). In contrast, IL-10-secreting Tregs from PS showed reduced expression of *CMTM6*, which binds PD-L1 and maintains its cell surface expression thereby suppressing T cell activity[594]. Overall, IL-10- and IFNγ-secreting Tregs showed few changes in gene and surface protein expression, comparable to the naïve Treg subpopulation (Fig. 3.11).

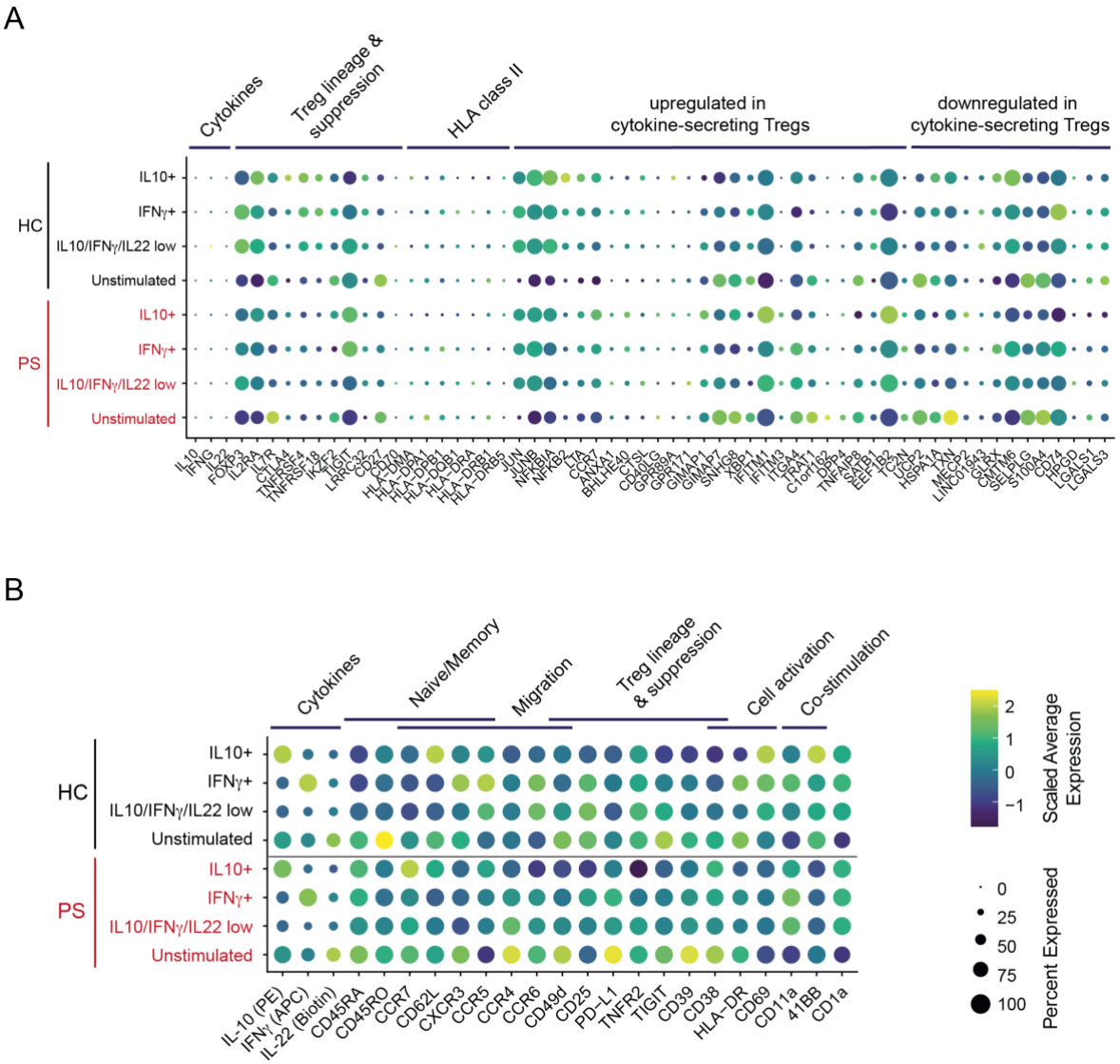

Fig. 3.14 Differential gene and surface protein expression in IL-10-, IFNγ-, and IL-22-secreting CD1a-reactive Tregs in cluster 4.

(A) Gene expression and **(B)** surface protein expression dot plots for Tregs in cluster 4, showing expression of Tregs from HC and PS separately. Differential expression analysis was performed between unstimulated Tregs, CD1a-stimulated Tregs that secrete no or low levels of IL-10, IFNγ and IL-22 (IL10/IFNγ/IL22 low), and CD1a-stimulated Tregs that secrete IL-10 or IFNγ ($IL10^+$, $IFN\gamma^+$). Genes and surface markers shown were differentially expressed (gene expression: adj. p-value < 0.05; log2FC > 1) or selected genes and surface markers of interest within either naïve Tregs, effector/memory Tregs, cluster 4 or cluster 9.

3.2.2.5.4 Cluster 9

For cluster 9, the cell numbers within populations were not high enough to separate HC and PS, thus HC and PS data were analysed combined. Cluster 9 contained effector/memory-like Tregs that express high levels of CXCR3 and CCR5[539,540], and was enriched for Tregs secreting IL-22 in response to CD1a stimulation (Fig. 3.5; Fig. 3.8). Similar to the effector/memory subpopulation, Treg lineage and functional markers were downregulated in IL-10-secreting Tregs in cluster 9 (Fig. 3.15). Moreover, CD1a-reactive IL10$^+$ Tregs showed similar gene expression changes as the corresponding population from the effector/memory subpopulation (Fig. 3.12), suggesting a similar loss of Treg phenotype.

While IL10$^+$IL22$^+$ Tregs showed similar changes in Treg lineage and functional markers as IL10$^+$ Tregs, they increased HLA class II gene expression, which may indicate a more activated phenotype[528] (Fig. 3.15). Gene and surface marker expression were otherwise comparable to IL22$^+$ Tregs and IL10/IFNγ/IL22 low Tregs. In contrast, IL22$^+$ Tregs retained the expression of Treg lineage and functional markers, and general gene and cell surface marker expression closely resembled that of IL10/IFNγ/IL22 low Tregs (Fig. 3.15). This suggests that IL-22-secreting Tregs, in particular those that do not upregulate and secrete IL-10, may retain their functional phenotype. However, taken together with only minor gene expression changes seen for IL-22- and IFNγ-secreting Tregs in all subpopulations analysed, it is also plausible that the observed IL-22 and IFNγ secretion may be a result of general Treg stimulation rather than mediated by the interaction with CD1a.

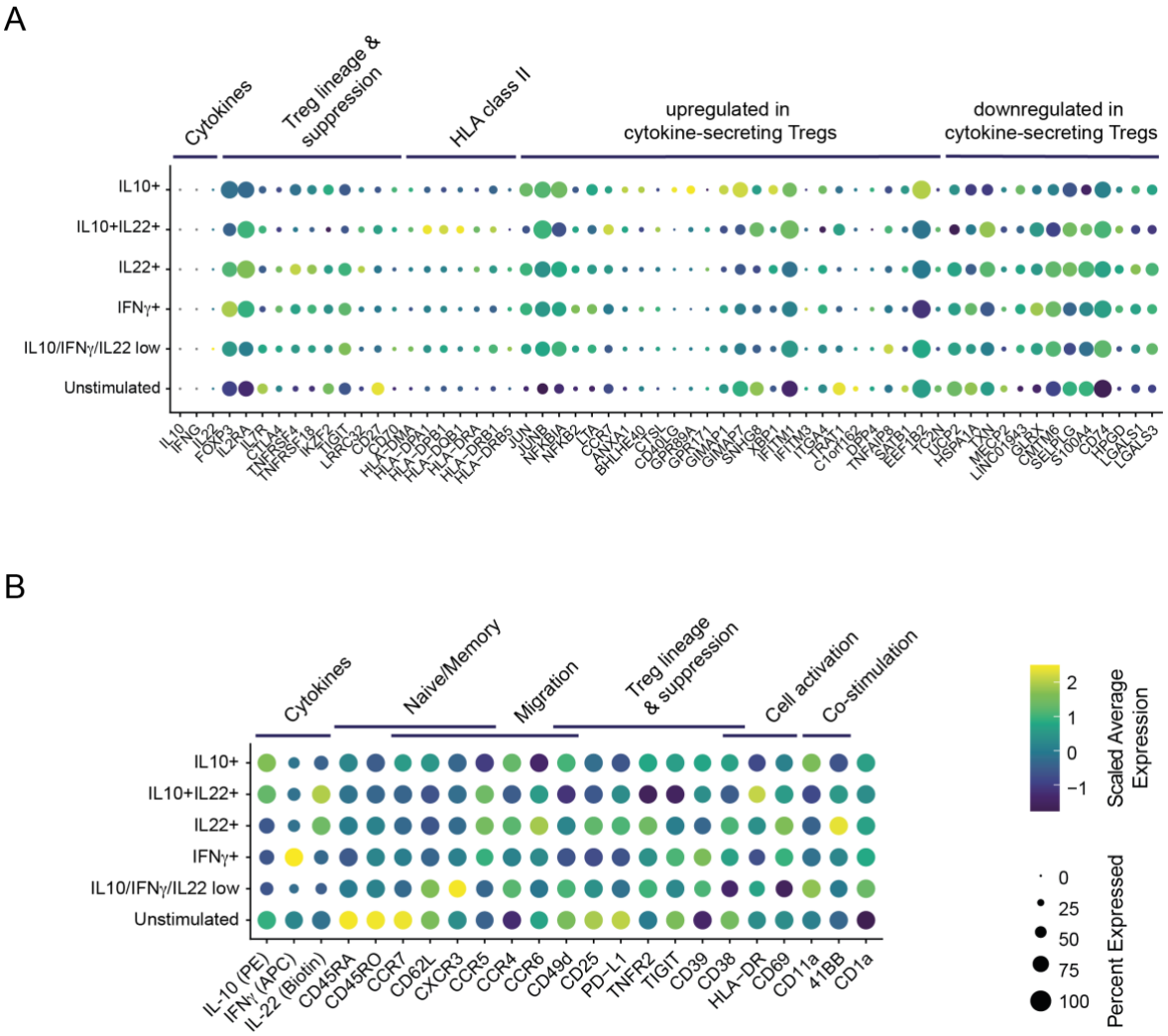

Fig. 3.15 Differential gene and surface protein expression in IL-10-, IFNγ-, and IL-22-secreting CD1a-reactive Tregs in cluster 9.

(A) Gene expression and **(B)** surface protein expression dot plots for effector/memory-like Tregs in in cluster 9, showing expression of Tregs from HC and PS combined. Differential expression analysis was performed between unstimulated Tregs, CD1a-stimulated Tregs that secrete no or low levels of IL-10, IFNγ and IL-22 (IL10/IFNγ/IL22 low), and CD1a-stimulated Tregs that secrete IL-10, IFNγ and/or IL-22 ($IL10^+$, $IFN\gamma^+$, $IL10^+IL22^+$, $IL22^+$). Genes and surface markers shown were differentially expressed (gene expression: adj. p-value < 0.05; log2FC > 1) or selected genes and surface markers of interest within either naïve Tregs, effector/memory Tregs, cluster 4 or cluster 9.

3.3 Discussion

CD1a-mediated T cell responses play an important role in the exacerbation of skin inflammatory diseases such as psoriasis (see 1.2.3 CD1a in skin inflammatory disease) and our studies presented in the previous chapter demonstrate that also Tregs can functionally interact with CD1a (see Chapter 2). The data presented here gives further insights into the phenotype of CD1a-reactive Tregs and indications for their role in skin inflammatory disease. *Ex vivo* analysis of Tregs showed that a comparable percentage of Tregs from patients with psoriasis and healthy controls secreted IL-10 in a CD1a-dependent manner (Fig. 3.2). This suggests that CD1a-reactive Treg frequency may be unaffected in psoriasis. However, in single-cell sequencing samples, a higher frequency of IL-10-secreting and lower frequency of IFNγ-secreting CD1a-stimulated Tregs could be observed in PS compared to HC (Fig. 3.8). In psoriasis, Tregs commonly display dysfunction and plasticity (see 3.1.2 Regulatory T cells in psoriasis) and therefore different Treg subsets may be more prevalent in peripheral blood compared to HC, possibly leading to enrichment of CD1a-reactive IL-10-secreting Tregs. Similar to expanded polyclonal Tregs (Fig. 2.13), *ex vivo* Tregs from PS or HC did not secrete increased levels of IL-17A in response to CD1a stimulation (Fig. 3.3). Whether CD1a-reactive Tregs from patients with psoriasis more readily secrete IL-17A in response to general stimulation compared to HC and show Th17 plasticity, as seen for Tregs in psoriasis[514], remains to be addressed.

Single-cell sequencing of Tregs secreting IL-10, IL-22 and/or IFNγ upon CD1a stimulation revealed that while naïve Tregs show only minor changes in gene and surface marker expression upon CD1a engagement, effector/memory Tregs that secrete IL-10 in response to CD1a stimulation shift towards a naïve to central/memory and likely less suppressive phenotype (Fig. 3.13). Skin harbours predominately effector/memory Tregs[26] and the

majority of CD1a-reactive T cells are thought to be of a memory phenotype (unpublished data, Ogg Lab). This may explain why CD1a-mediated modulation of Treg phenotype and function observed herein was more profound in effector/memory Tregs compared to naïve Tregs.

In contrast to IL-10-secreting Tregs, only minor changes could be observed in gene and surface protein expression of IL-22- and IFNγ-secreting Tregs throughout all Treg subpopulations. Expanded polyclonal Tregs showed low levels of IL-22 and IFNγ secretion (Fig. 2.13), whereas CD1a-reactive Treg clones were able to secrete high levels of IFNγ in a CD1a-independent manner (Fig. 2.24). It is plausible that secretion of IL-22 and IFNγ resulted from CD1a-independent stimulation of Tregs, i.e. through stimulatory factors present on K562 cells. Further, upregulation of CD49d, a marker of antigen-experienced T cells[555,556], in effector/memory Tregs secreting IL-10 but not in those secreting IL-22 and/or IFNγ (Fig. 3.12) may indicate that neither IL-22- nor IFNγ-secreting Tregs interacted with CD1a-presented antigens.

Effector/memory T cells migrate to peripheral tissues and display immediate effector functions, whereas central/memory T cells primarily migrate between peripheral blood and secondary lymphoid tissues and are important for reactive memory[595,596]. It is possible that IL-10-secreting CD1a-reactive Tregs may adopt a central/memory phenotype upon CD1a engagement to re-circulate to lymph nodes. However, it is also plausible that CD1a interaction may modulate CD1a-reactive Tregs to a less suppressive phenotype, similar to CD1a-reactive T cells showing an inflammatory phenotype in skin inflammatory disease (see 1.2.3 CD1a in skin inflammatory disease). TCR engagement has been previously reported to cause downregulation of Foxp3 expression and may promote reprogramming of Tregs to a Th lineage, particularly in inflammatory settings[514,597,598]. Further, rescuing Foxp3

expression in Tregs during systemic inflammation was shown to normalise immune activation and reduce tissue inflammation[599].

CD1a-reactive IL-10-secreting effector/memory Tregs from PS showed higher upregulation of central/memory markers compared to HC (Fig. 3.13), suggesting that in psoriasis, CD1a-reactive Tregs may more readily shift towards a central/memory phenotype and enter re-circulation. Further, $IL10^{+}IFN\gamma^{+}$ effector/memory Tregs from PS upregulated *IL7R* expression (Fig. 3.13, A, B), a central/memory marker for $CD8^{+}$ T cells that is expressed on skin Tregs, which may indicate that circulating Tregs in psoriasis may be enriched for CD1a-reactive Tregs that used to reside in the skin[592,593].

The here presented data represents a snapshot of Treg gene and surface marker expression after *in vitro* CD1a stimulation of *ex vivo* Tregs. Therefore, it is possible that CD1a-mediated activation of Tregs leads to a temporary loss of Treg lineage and functionality, or the development of a prolonged inflammatory phenotype that contributes to the exacerbation of skin inflammation. The latter hypothesis is supported by the data in Chapter 2 where gradual loss of Treg phenotype and functionality and gain of inflammatory cytokine expression by CD1a-reactive Treg clones was elevated in the presence of inflammatory cytokines (see 2.2.6 CD1a-reactive IL-10-secreting Treg clones).

In psoriasis, CD1a-expressing DC subsets infiltrate and accumulate in the skin[177-179] and disruption of the skin barrier further facilitates CD1a-mediated presentation of exogenous antigens. Increased exposure of CD1a-reactive Tregs to CD1a and resulting phenotypic modulation towards a central/memory and less suppressive phenotype may therefore exacerbate disease by inefficient suppression of effector T cell inflammatory responses. While the here presented data give first insights into the phenotype of CD1a-reactive Tregs, further studies are needed to elucidate the functional role of CD1a-reactive Tregs in health

and psoriasis. Possible approaches could be the transduction of CD1a-reactive Treg-TCRs into primary Tregs and investigation of CD1a-mediated Treg functional responses, and the use of CD1a-transgenic mouse models for psoriasis. In addition, trajectory analyses would help define inter-relationships between cell subsets and whether these are altered in the setting of psoriasis - these studies are underway. Lesional and non-lesional skin single-cell Treg analyses would also help define how the cells relate to tissue-resident and migratory populations. Moreover, single-cell TCR analysis of CD1a-reactive Tregs could illuminate additional differences between CD1a-reactive Tregs in health and psoriasis. The findings have implications for the therapeutic use of primary Tregs in psoriasis and like Chapter 2, point more towards the use of TCR transduction approaches and/or strategies to stabilise Treg phenotype and function.

Chapter 4 CD1a-mediated impact of short- and medium-chain fatty acids on skin immunity

4.1 Introduction and Aims

4.1.1 Dendritic Cells

DCs are professional APCs that are crucial in the initiation and modulation of adaptive immune responses. Through pattern recognition receptors (PRRs), DCs can recognise and capture self- and non-self antigens. DC activation through pathogen-associated molecular patterns (PAMPs) or danger-associated molecular patterns (DAMPs) leads to antigen uptake and migration to the draining lymph nodes. Subsequent presentation of processed antigens to antigen-specific adaptive immune cells such as naïve T cells leads to induction of immunity or tolerance. Human DCs are functionally and phenotypically heterogenous. A number of DC subsets have been described, including conventional DCs (cDCs), plasmacytoid DCs (pDCs), moDCs and LCs and single-cell studies are defining further heterogeneity[53,600-602]. While the primary function of cDCs is the priming of naïve T cells, pDCs specialise in the production of type I interferons thereby promoting $CD4^+$ T cell polarisation into Th1 cells and activation of $CD8^+$ T cells and NK cells[603]. MoDCs are composed of a variety of subsets with different functions, including a heterogenous subset of inflammatory DCs and a subset of TNF and inducible nitric oxide synthase (iNOS)-producing DCs known as TIP-DCs[600,601]. LCs are characterised by the expression of the C-type lectin Langerin and CD1a. They largely reside in the epidermis where they prime $CD8^+$ T_{RM} cell responses and play an important role in immunosurveillance[7,8,604].

The use of primary DCs as an experimental model is limited by low numbers present in peripheral blood (1-2% of PBMCs). To study DCs *in vitro*, circulating monocytes can be

differentiated to moDCs in the presence of GM-CSF and low levels of IL-4. These moDCs present an immature phenotype characterised by lack of CD14 expression, high levels of CD11c, expression of the C-type lectin DC-SIGN (dendritic cell-specific intracellular adhesion molecules (ICAM)-3 grabbing non-integrin), MHC class I and class II molecules as well as expression of CD1a, CD1b and CD1c[605-607].

4.1.1.1 Dendritic cells in the skin

Skin DCs migrate to skin draining lymph nodes where they present cutaneous antigens to initiate adaptive immune responses. During steady state and inflammation, they further shape the immune response by interacting with skin-resident and infiltrating immune cells. In healthy skin, LCs reside within the epidermis where they play a crucial role in immunosurveillance and tissue homeostasis[604]. When activated during inflammation, LCs elongate their dendrites reaching to the stratum corneum where they survey foreign antigens and have the capacity to migrate to local lymph nodes[10,608-610]. They are continuously replaced from a local pool of precursors that is established during early development; but after major depletion, may also be replenished from a blood population of myeloid precursors[611-616]. The main DC subsets present in the dermis include $CD14^+CD1a^-$ DCs, $CD14^-CD1a^+$ DCs and 6-Sulpho $LacNAc^+$ DCs[617,618]. LCs and $CD1a^+$ DCs can induce Th1, Th2 and Th17 responses[619-622] and further influence skin immunity through lipid antigen presentation *via* CD1a expression (see 1.2 Lipid antigen presentation and CD1a). $CD14^+CD1a^-$ DCs have a variety of functions, including modulation of B cell responses, skewing of $CD4^+$ T cells to a T-helper phenotype, and induction of Treg differentiation[7,623,624]. During skin inflammation, pDCs and inflammatory DCs are recruited to the skin[625]. Further, a $CD1a^+$ DC subset co-expressing BDCA-2 and intermediate levels of CD123 has been shown to infiltrate into the skin upon acute sterile skin inflammation[180]. Different skin inflammatory diseases are characterised by the presence of different

inflammatory DC subsets. While psoriatic skin harbours TIP-DCs and DCs producing IL-20 and IL-23[469,626], patients with atopic dermatitis show skin infiltration of inflammatory dendritic epithelial cells (IDECs)[177]. Moreover, CD1a-mediated T cell responses have been shown to exacerbate inflammation in several skin inflammatory diseases including AD, psoriasis, and contact dermatitis[6,14,167,174].

4.1.2 Fatty acids

FAs are comprised of a hydrocarbon chain with a terminal reactive carboxyl group. Based on the length of the hydrocarbon chain, they are classed into three groups: short-chain fatty acids (SCFAs) with 2-5 carbons, medium-chain fatty acids (MCFAs) with 6-12 carbons, and long-chain fatty acids (LCFAs) with 13-21 carbons. FAs play diverse roles in immunity, serving as an energy source, structural components, signalling molecules and precursors for bioactive lipid mediators. They exert their functions through a variety of mechanisms including regulation of enzyme activity by inhibiting HDACs[627-629], binding to nuclear hormone receptors such as PPAR[630], and activating G-protein-coupled receptors (GPCRs)[631]. Furthermore, FAs have been shown to act as ligands for CD1a and modulate CD1a-mediated immune responses[34,166] (see 1.2.2.1 CD1a lipid antigens).

4.1.2.1 Short-chain fatty acids in skin immunity

Commensal bacteria in the skin produce SCFAs through anaerobic fermentation[632]. Butyrate and propionate, but not acetate, have been demonstrated to modulate gene expression in *in vitro*-differentiated moDCs, inhibiting the secretion of pro-inflammatory chemokines and cytokines such as IL-6 and IL-12p40[633]. In line with these anti-inflammatory properties, butyrate was shown to ameliorate inflammation in models of skin inflammation. In a mouse model for contact hypersensitivity (CHS), sodium butyrate (SB) increased the number of Tregs in the skin by converting $CD4^+$ non-Treg cells into Tregs in a HDAC-dependent

manner and thereby reduced CHS responses. A similar increase in Tregs upon SB treatment could be observed in human skin *ex vivo*[634]. Similarly, SB reduced imiquimod-induced inflammation in a mouse model of psoriasis and restored impaired Treg function in *in vitro* cultures of human Tregs from patients with psoriasis[635]. Butyric acid (BA) from *S. epidermidis* has further been shown to reduce the pro-inflammatory cytokine IL-6 in mice exposed to UVB light[636]. In contrast to the observed anti-inflammatory properties of butyrate, SCFAs produced by *P. acnes*, a contributor to the skin inflammatory disorder acne vulgaris, have been demonstrated to activate an inflammatory response in human sebocytes by TLR activation *via* HDAC inhibition and by signalling through FA receptors[637]. In line with these results, *in vitro* keratinocytes have been shown to produce pro-inflammatory cytokines in response to butyrate[638]. In this study, topical treatment of mice with SCFAs showed a similar pro-inflammatory phenotype that was not observed when SCFAs were administered by intradermal injection[638]. Taken together, SCFAs show varying immunomodulatory effects that may be dependent on cell type and environment.

4.1.2.2 Medium-chain fatty acids in skin immunity

MCFAs are present only at low levels in the skin[33,639]. Several MCFAs like lauric acid have been shown to have direct antibacterial effects against a variety of pathogenic microbes including *Malassezia* and *S. aureus*[640,641], both of which are associated with skin diseases such as AD and psoriasis[642,643]. In an artificial skin model, capric acid and benzoic acid derivatives have been demonstrated to synergistically act against *S. aureus* and methicillin-resistant *S. aureus*[644]. While MCFAs are rare in the skin, they are abundant in foods such as coconut oil. In the context of the gut microenvironment, MCFAs have been shown to influence gut immunity *via* GPCRs, inducing a mostly pro-inflammatory phenotype[645]. In contrast, 4-phenylbutyrate derivatives like 6-phenylhexanoic acid seem to protect against ER stress-induced neuronal cell death[646]. Like SCFAs, MCFAs seem to have

varying immunomodulatory effects. However, the influence of MCFAs on skin immunity remains largely unknown.

4.1.2.3 Effect of fatty acids on CD1 expression and lipid antigen presentation

Several FAs of varying hydrocarbon chain length have been demonstrated to modulate CD1 expression. Human serum, in particular the polar fraction, has been shown to decrease expression of group 1 CD1 molecules during *in vitro* differentiation of moDCs and abrogate CD1c-mediated activation of a CD1c-restricted T cell line[75]. CD1 modulation was associated with PPARγ activation. While this study reported no change in CD1d expression or CD1d-restricted T cell clone activation[75], PPARγ-mediated increase in CD1d expression is commonly observed. FFAs derived from olive pollen have been shown to selectively upregulate CD1d expression in *in vitro*-generated moDCs at protein and transcriptional level in a PPARγ-dependent manner. CD1d upregulation was further shown to activate iNKT cells[76]. Several studies have demonstrated that PPARγ activation through PPARγ agonists leads to downregulation of CD1a and upregulation of CD1d on *in vitro*-generated moDCs[72-74] inducing iNKT cell expansion[73].

Several FAs with long hydrocarbon chains have been shown to reduce CD1a expression during moDC differentiation, including lysophosphatidic acid (C18:1)[75], α-lineloic acid (C18:3), eicosapentaenoic acid (C20:5), and decosahexanoic acid (C22:6)[647]. Moreover, the MCFA nonanoic acid (C9:0), but not sodium lauryl sulfate (C12:0), led to a decrease in $CD1a^+$ cells in human skin immunohistochemistry[648].

Modulation of CD1 expression has also been observed for SCFAs, in particular butyrate. Higher diversity in gut microbiota and higher levels of bacterial SCFAs in faeces were associated with lower expression of CD1a on *in vitro*-differentiated moDCs[203]. BA was shown to inhibit CD1a, CD1b and CD1d expression on *in vitro*-differentiated immature and

mature moDCs; co-culture of T cells with BA-treated moDCs seemed to not affect T cell proliferation, but skewed T cells to a Th2-like phenotype[201]. Further, SB has been shown to partially inhibit the acquisition of CD1a during *in vitro* differentiation of moDCs[202]. The effect was abolished when SB was added after differentiation, suggesting an inhibition of acquisition rather than downregulation of CD1a expression. SB also reduced CD1a at the transcriptional level, while CD1d transcription was increased. However, increase in CD1d transcription was not confirmed at protein level. In contrast to above discussed studies, SB could block TLR2 activation-induced CD1a expression, but inhibition of CD1a expression on moDCs seemed independent of PPARγ activation[202].

Taken together, these studies demonstrate that SCFAs, MCFAs, and LCFAs differentially modulate CD1 expression on moDCs. While group 1 CD1 molecules are inhibited, group 2 CD1d is upregulated. Several molecular mechanisms have been proposed for FA-mediated CD1 regulation: PPARγ activation, HDAC inhibition, and TLR2 activation. While HDAC inhibition, similar to butyrate treatment, has been demonstrated to affect *in vitro* moDC differentiation by preventing CD1a acquisition[79], HDAC inhibition has also been shown to partially inhibit CD1d expression and CD1d-dependent NKT cell responses[80]. Similarly, TLR2 activation, i.e. by mycobacterial lipids, induces CD1a, CD1b and CD1c, but not CD1d, expression on monocytes[77,78]. Therefore, CD1 expression may not be exclusively regulated by one of these proposed mechanisms but by a combination, which may further be dependent on the microenvironment and other cellular and molecular factors.

Several of the above discussed studies suggest a functional effect of CD1 modulation on T cell activation and reactivity. However, whether CD1a-mediated T cell responses may be modulated by CD1a inhibition *via* FAs remains unknown.

4.1.2.4 Potential of fatty acids as therapeutics for skin diseases

SCFAs have been shown to have predominantly anti-inflammatory properties (see 4.1.2.1 Short-chain fatty acids in skin immunity) and in most cases ameliorate inflammation in pre-clinical models of CHS and psoriasis[634,635,638]. While not much is known about the effects of SCFAs on skin diseases, pre-clinical studies support a role for SCFAs in the modulation of colonic function and inflammatory and metabolic processes[649].

The oral application of ϖ-3 and ϖ-6 polyunsaturated fatty acids (PUFAs) has been shown to alleviate skin inflammatory diseases such as psoriasis and AD[650]. α-linoleic acid, a ϖ-3 PUFAs that has been shown to inhibit CD1a expression on moDCs[647], improved psoriasis pathogenesis when applied topically as a linoleic acid-ceramide cream[424]. Natural oils contain varying amounts of different FAs, with many containing high levels of linoleic acid[651]. Topical application of several natural oils has been proposed to aid in restoring skin-barrier functions and alleviate skin inflammatory diseases, while others may act as skin irritants and further disrupt the skin barrier[651]. However, natural oils contain many different FAs which may act independent of each other or in synergy, and the therapeutically active components have not yet been identified.

Overall, very limited data are available on the therapeutic potential of FAs, especially SCFAs and MCFAs, in skin diseases. Whether modulation of CD1 and CD1-mediated immune responses contribute to the therapeutic effect seen for several FAs has not been addressed as of now. However, as CD1a is predominantly expressed in the skin and has been shown to exacerbate skin inflammatory diseases, the topical application of CD1a-inhibiting FAs has great therapeutic potential.

4.1.3 Hypothesis and aims

CD1a-mediated immune responses play an important role in skin inflammatory diseases (see 1.2.3 CD1a in skin inflammatory disease). Fatty acids such as the SCFA butyrate have been shown to modulate CD1 induction and reduce the expression of CD1a during moDC differentiation[201-203]. While the modulation of both CD1c and CD1d has been proposed to affect T cell activation[73,75,76], the impact of CD1a inhibition on CD1a-mediated immune responses has not been studied. Additionally, fatty acids have been demonstrated to bind to the CD1a binding groove and act as CD1a ligands[34,88,166]. Whether fatty acids shown to modulate CD1a expression may act as CD1a ligands remains unknown. Therefore, I hypothesised that butyrate and structurally related fatty acids may modulate CD1a-mediated T cell activation *via* modulation of CD1a expression.

The aims of the project included:

- Investigate the effects of different SCFAs on moDC differentiation and CD1 surface expression
- Identify CD1a-modulating candidate compounds among fatty acids and fatty acid-related compounds with structural similarity to butyrate
- Determine whether SCFAs or candidate compounds can bind to CD1a as ligands
- Study the dose-dependent effect of butyrate and candidate compounds on moDC differentiation and CD1 surface expression
- Evaluate the impact of CD1a modulation on CD1a-reactive T cell responses

4.2 Results

4.2.1 The short-chain fatty acid butyrate inhibits the acquisition of CD1a during moDC differentiation

4.2.1.1 Inhibition of CD1a expression on differentiating moDCs by short-chain fatty acids

The differentiation of monocytes to moDCs is accompanied by the upregulation of CD1a on the cell surface[605]. CD1a induction during moDC differentiation has been shown to be inhibited by the SCFA sodium butyrate (SB)[202]. To investigate the inhibitory potential of butyrate-related SCFAs on CD1a expression, moDCs were differentiated *in vitro* from circulating monocytes in the presence of the salts and acids of acetate, propionate, and butyrate. *In vitro*-generated moDCs showed high levels of CD1a expression on day 5 of differentiation (82.22% ± 13.87) (Fig. 4.1, A). SB and butyric acid (BA) significantly reduced CD1a expression compared to the non-treated control. Although the decrease in percentage of CD1a-positive cells was highly variable depending on donor (71.65% ± 26.20 and 62.70.64% ± 30.36 of non-treated control), the mean fluorescent intensity (MFI) was consistently decreased in all donors (46.28% ± 21.15 and 35.64% ± 24.91 of non-treated control) (Fig. 4.1, B, C). Further, treatment reduced the CD1a MFI of the CD1a-positive population compared to the non-treated control (Fig. 4.1, A, C). Sodium propionate treatment showed a significant but lower decrease in CD1a expression (MFI 65.23% ± 9.26 of non-treated control) (Fig. 4.1, B, C). Propionic acid showed a similar trend towards CD1a inhibition as sodium propionate (MFI 69.19% ± 10.55 of non-treated control) (Fig. 4.1, B, C). Neither sodium acetate nor acetic acid inhibited CD1a expression (Fig. 4.1). These results show that not only SB, but also BA effectively inhibits CD1a expression during moDC differentiation, while propionate seems to have a limited CD1a-modulatory effect.

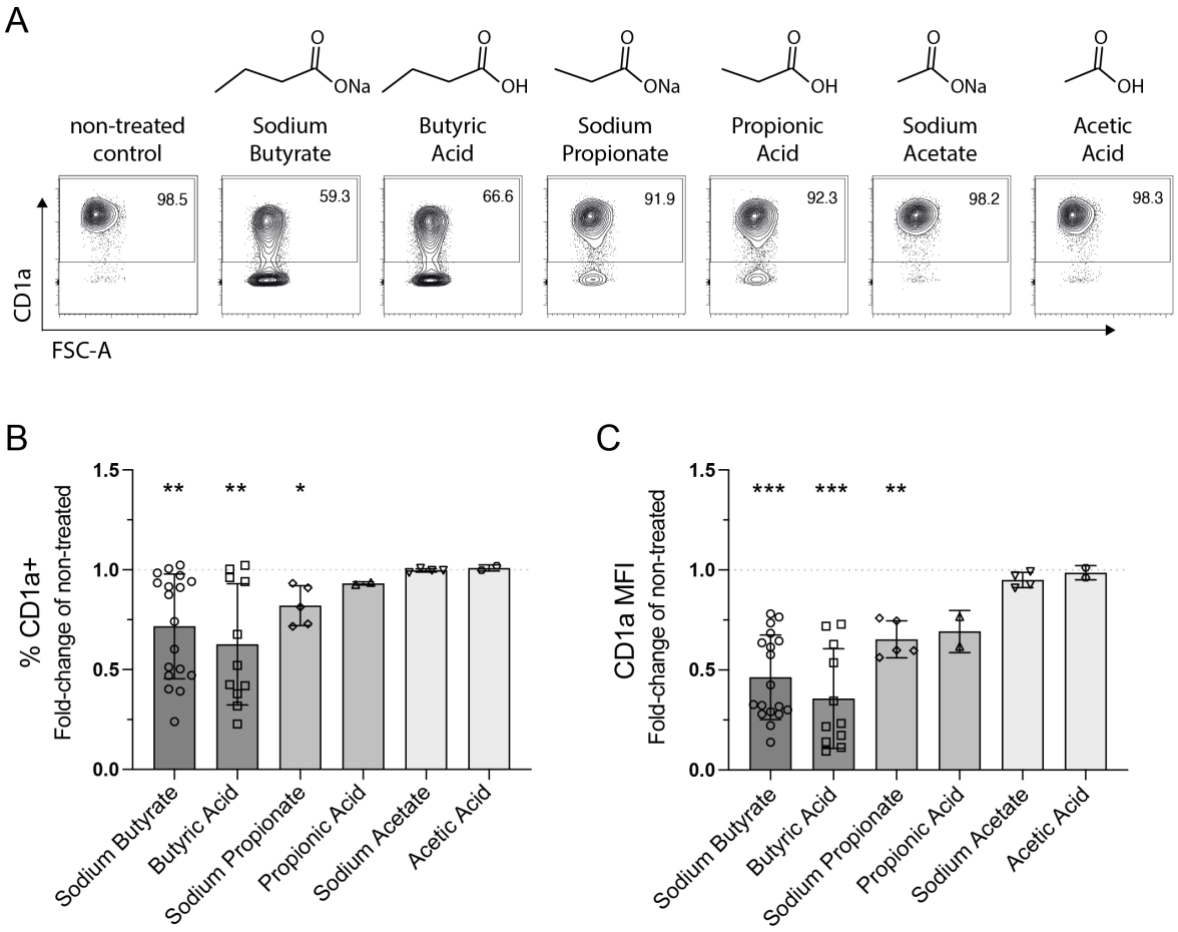

Fig. 4.1 Short-chain fatty acids decrease CD1a expression on differentiating moDCs.

Circulating $CD14^+$ monocytes were differentiated into immature moDCs in medium containing GM-CSF and IL-4. SCFAs were added from day 0 of differentiation at 250µM. Data shown is gated on live $CD14^-CD11c^+$ moDCs. **(A)** Representative FACS plots of CD1a expression on non-treated moDCs on day 5 of differentiation (gated on live $CD14^-CD11c^+$ cells). Numbers indicate percentages of $CD1a^+$ cells. **(B)** Percentage of CD1a-expressing cells as fold-change of the non-treated control. **(C)** CD1a MFI as fold-change of the non-treated control. (n=2-18 donors; 2 independent experiments for propionic acid and acetic acid, and ≥ 3 independent experiments for all other conditions). *P < 0.05; **P < 0.01; ***P < 0.001; RM Mixed-effects analysis with Dunnett's correction for multiple comparison (mean ± SD).

To determine whether butyrate downregulates CD1a expression or inhibits the acquisition of CD1a during moDC differentiation, as proposed by Nascimento *et al.*[202], butyrate was added either from the day 0 (d0) or day 3 (d3) of differentiation. Although the decrease in percentage of CD1a-positive cells was variable when butyrate was present throughout differentiation, the reduction in CD1a percentage was abrogated when butyrate was added from d3 (Fig. 4.2, A). The MFI of CD1a remained significantly reduced for both SB and BA when added from d3 (80.39% ± 14.51 and 75.20% ± 17.65 of non-treated control, respectively) but the inhibition of CD1a MFI was reduced approximately 2-fold compared to treatment from d0 (1.74- and 2.11-fold, respectively) (Fig. 4.2, B). In line with the findings from Nascimento *et al.*[202], these data suggest that both SB and BA inhibit the acquisition of CD1a during moDC differentiation rather than downregulating CD1a post induction of expression.

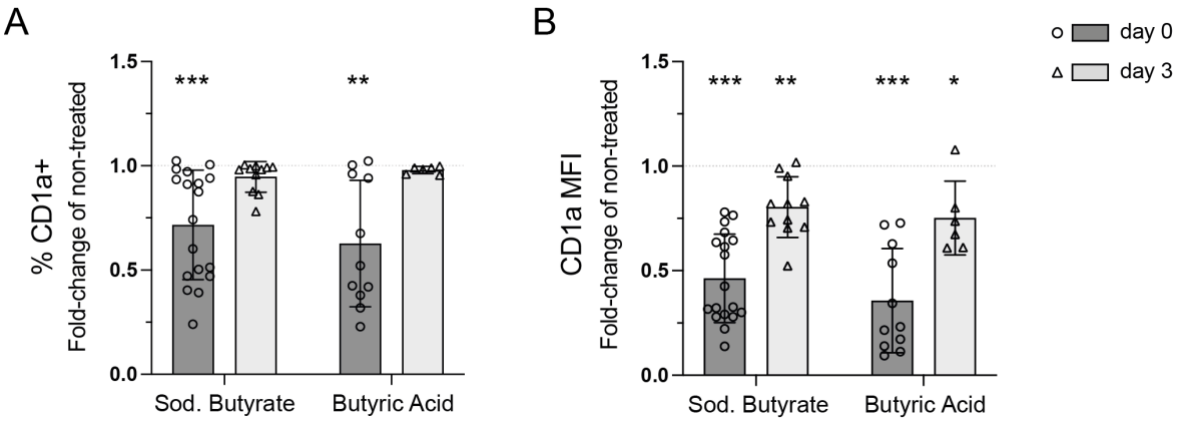

Fig. 4.2 Butyrate inhibits the acquisition of CD1a on moDCs during differentiation.
MoDCs were differentiated from circulating monocytes and treated with 250µM sodium butyrate or butyric acid from d0 or d3 of differentiation. **(A)** Percentage of CD1a-expressing cells as fold-change of the non-treated control. **(B)** CD1a MFI as fold-change of the non-treated control. (n ≥ 6 donors; ≥ 3 individual experiments). *P < 0.05; **P < 0.01; ***P < 0.001; RM Mixed-effects analysis with Dunnett's correction for multiple comparison (mean ± SD).

4.2.1.2 Effects of butyrate on moDC differentiation

To delineate whether the effect of butyrate on moDC differentiation is specific to CD1a or affects moDC differentiation more broadly, expression of moDC lineage markers, the co-stimulatory molecule CD86, and the other non-classical antigen presenting molecules CD1b, CD1c and CD1d were assessed by flow cytometry analysis. On day 5 of differentiation, non-treated moDCs had lost CD14 expression and gained the expression of CD11c and DC-SIGN (Fig. 4.3, A). Consistent with an immature phenotype[605-607,652], moDCs lacked the expression of DC-LAMP (dendritic cell lysosomal-associated membrane glycoprotein) and CD83, expressed high levels of HLA-DR (MHC class II) and HLA-ABC (MHC class I) while expressing moderate levels of the co-stimulatory molecule CD86 (Fig. 4.3, A). Upon treatment with SB or BA, the percentage of moDC-sized cells was slightly but not significantly reduced (97.85% ± 7.21 and 93.37% ± 17.86 of non-treated control, respectively; Fig. 4.3, B). and the percentage of $CD14^{-}CD11c^{+}$ cells was slightly, but significantly, increased (109.38% ± 14.80 and 102.10% ± 2.75 of non-treated control, respectively; Fig. 4.3, D). Taken together with unchanged viability (Fig. 4.3, C), this suggested no toxicity of SB or BA at 250µM. Although BA showed toxicity at this concentration in later experiments (Fig. 4.7; Fig. 4.11), the CD1a-modulating effect of BA was still observed at lower, non-toxic concentrations (Fig. 4.9; Fig. 4.10). While there was some donor variability, DC-SIGN (Fig. 4.3, E), DC-LAMP (Fig. 4.3, F), HLA-DR (Fig. 4.3, H) and CD86 (Fig. 4.3, J) expression did not change significantly upon treatment. However, moDCs showed a trend towards reduced expression of DC-SIGN and CD86 upon treatment with BA. In contrast, both SB and BA significantly downregulated HLA-ABC (Fig. 4.3, G) and CD83 (Fig. 4.3, I) expression.

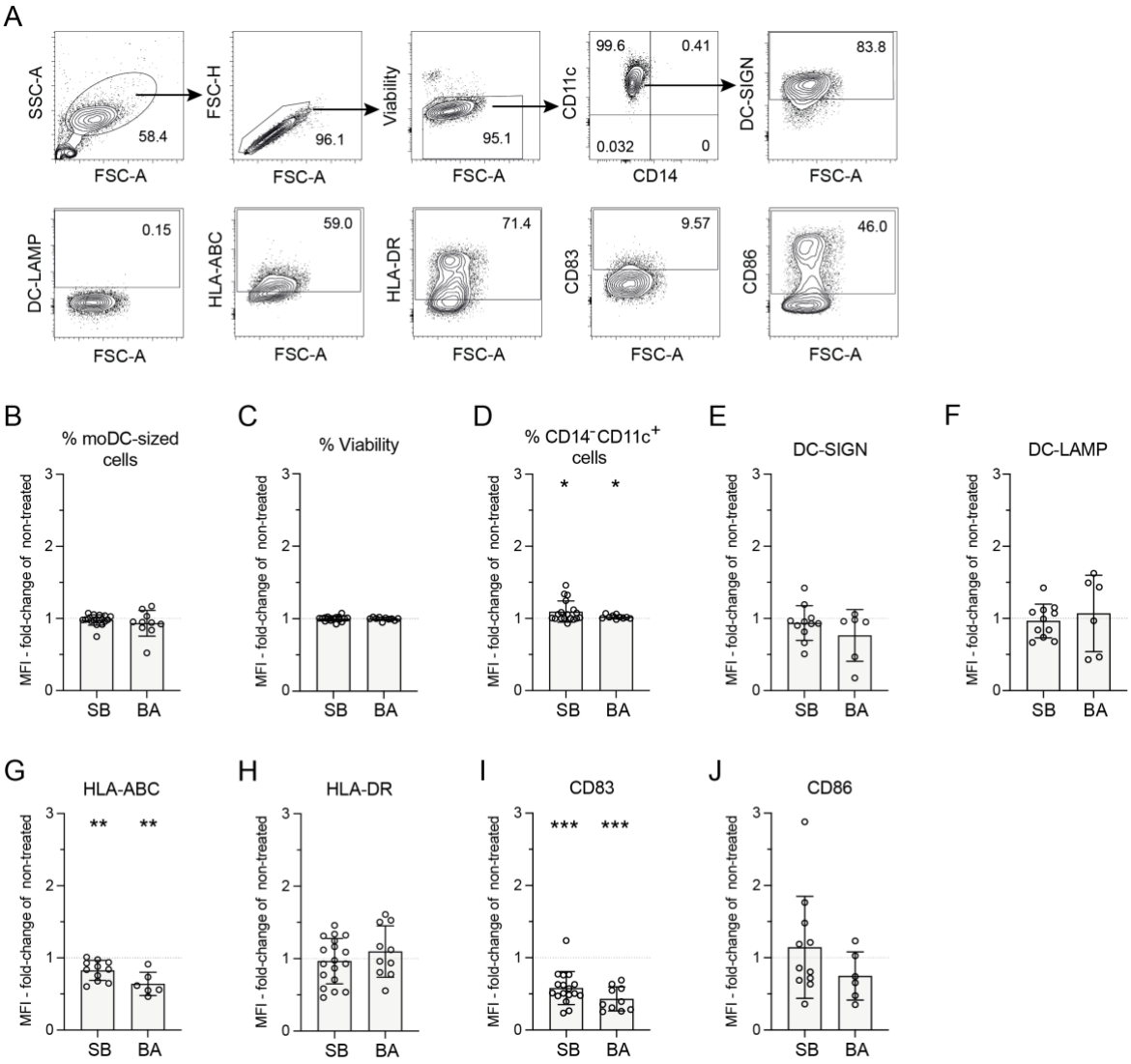

Fig. 4.3 Expression of lineage and activation markers on moDCs following differentiation in the presence of sodium butyrate or butyric acid.

MoDCs were differentiated from circulating monocytes in the presence of 250µM SB or BA. **(A)** Representative FACS plots for non-treated moDCs on d5 of differentiation. Arrows indicate gating on the parent population. Numbers present the percentage of cells in the indicated gates. **(B-D)** Percentage of **(B)** moDC-sized cells, **(C)** live cells (viability dye-negative cells of moDC-sized cells), **(D)** $CD14^{-}CD11c^{+}$ cells (gated on live cells) as fold-change of the non-treated control. **(E-J)** Expression levels (MFI) of **(E)** DC-SIGN, **(F)** DC-LAMP, **(G)** HLA-ABC, **(H)** HLA-DR, **(I)** CD83 and **(J)** CD86, as fold-change of the non-treated control. ($n \geq 6$ donors; ≥ 3 individual experiments). *$P < 0.05$; **$P < 0.01$; ***$P < 0.001$; RM Mixed-effects analysis with Dunnett's correction for multiple comparison (mean ± SD).

On non-treated moDCs, group 1 CD1 molecules – CD1a, CD1b and CD1c – were highly expressed (Fig. 4.4, A). SB and BA not only inhibited CD1a expression (46.28% ± 21.15 and 35.64% ± 24.91 of non-treated control), but also significantly decreased the expression of CD1b (45.32% ± 16.92 and 27.66% ± 17.24 of non-treated control) and CD1c (48.71% ± 18.13 and 28.61% ± 18.98 of non-treated control) (Fig. 4.4, B-D). For all three molecules, BA seemed to inhibit expression slightly more potently compared to SB (significant for CD1c; $P < 0.05$, unpaired t-test). CD1d expression was almost undetectable on non-treated moDCs (Fig. 4.4, A). The seen variation in fold-change expression of CD1d upon differentiation in the presence of butyrate compared to the non-treated control may therefore be attributed to this low expression (Fig. 4.4, E).

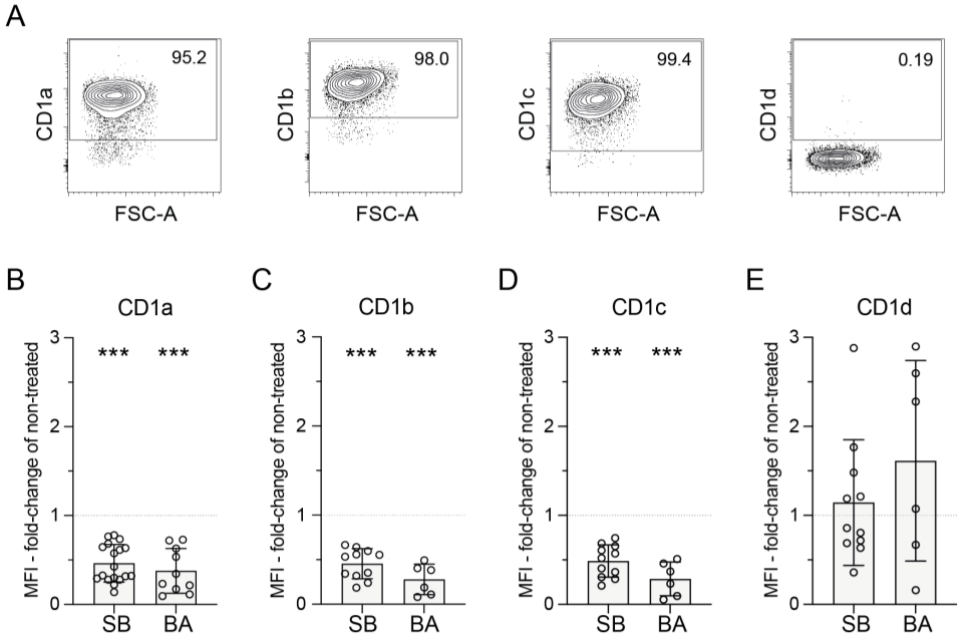

Fig. 4.4 Expression of CD1a, CD1b and CD1c is decreased on moDCs following differentiation in the presence of butyrate.

Circulating monocytes were differentiated into moDCs in the presence of 250µM SB or BA. **(A)** FACS plots representing the expression of CD1a, CD1b, CD1c and CD1d in non-treated moDCs. Numbers present the percentage of cells in the indicated gates. **(B-D)** Expression levels (MFI) of **(B)** CD1a, **(C)** CD1b, **(D)** CD1c and **(E)** CD1d as fold-change of the non-treated control. ($n \geq 6$ donors; ≥ 3 individual experiments). *$P < 0.05$; **$P < 0.01$; ***$P < 0.001$; RM Mixed-effects analysis with Dunnett's correction for multiple comparison (mean ± SD).

These results demonstrate that the effect of butyrate on moDC differentiation is not limited to the inhibition of CD1a acquisition. While affecting moDC differentiation only mildly, butyrate significantly inhibits the induction of CD1a, CD1b and CD1c expression.

4.2.1.3 Butyrate does not act as a ligand of CD1a

CD1a has been shown to bind and present headless antigens with short carbon chains such as FAs and squalene[34,88,166]. Stimulation of circulating CD1a-reactive T cells with K562-CD1a cells has previously been shown to elicit a CD1a-autoreactive response that can be measured i.e. by IFNγ ELISpot[150]. To assess whether SCFAs may act as CD1a ligands and thus alter the CD1a-autoreactive response of CD1a-reactive T cells, K562-CD1a cells were pulsed with SCFAs and their potential to activate circulating CD1a-reactive T cells was measured by IFNγ ELISpot.

When compared to the CD1a-autoreactive response, pulsing with SCFAs (acetic acid, sodium acetate, propionic acid, sodium propionate, butyric acid and sodium butyrate) did not significantly change IFNγ secretion of circulating T cells (Fig. 4.5). These data imply that SCFAs may not act as CD1a ligands.

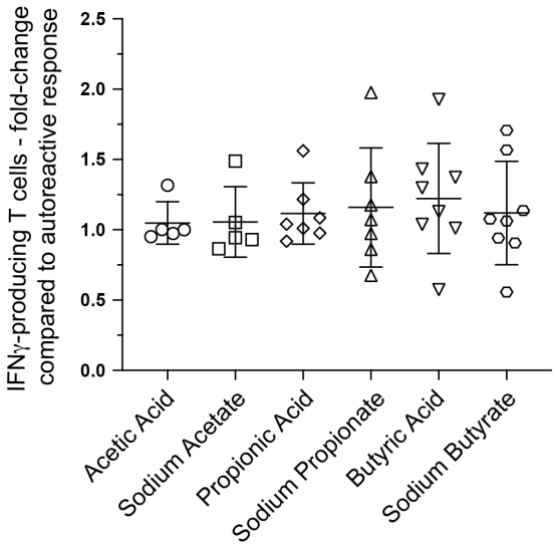

Fig. 4.5 CD1a reactivity of circulating T cells remains unchanged in response to K562-CD1a cells pulsed with short-chain fatty acids.

K562-CD1a cells were pulsed with 250µM acetic acid, sodium acetate, propionic acid, sodium propionate, butyric acid, or sodium butyrate. Pulsed K562-CD1a cells were co-cultured with T cells isolated from peripheral blood at a ratio of 1:3. IFNγ secretion was measured by ELISpot. Data is shown as fold-change of the CD1a-autoreactive response. ($n \geq 5$ donors; ≥ 3 individual experiments). *$P < 0.05$; **$P < 0.01$; ***$P < 0.001$; RM Mixed-effects analysis with Dunnett's correction for multiple comparison (mean ± SD).

To further strengthen the hypothesis that SCFAs cannot bind to CD1a, isoelectric focussing (IEF) was used to assess whether loading of CD1a with SCFAs changes the isoelectric point (pI) of CD1a. When the ligand in the CD1a binding groove is exchanged, the pI of CD1a may change. Change in pI is visible as band shift on an IEF gel. CD1a was incubated overnight with the different SCFAs or ganglioside GD3 (GD3) as positive control. GD3 displaced the endogenous lipids bound to CD1a as indicated by a shift in the bands on the IEF gel (Fig. 4.6, A). None of the SCFAs tested changed the pI of CD1a, suggesting that these SCFAs might not load onto CD1a (Fig. 4.6, A).

Pre-loading CD1a with GD3 is a common method for facilitating the exchange of endogenous CD1a ligands with target lipids[6,200]. GD3 seems to be more readily displaced

from the CD1a binding cleft compared to endogenous lipids due to which pre-loading of CD1a with GD3 can help CD1a ligands with lower affinity to load onto CD1a. CD1a pre-loaded with GD3 was incubated with the different SCFAs, and the subsequent IEF analysis showed no shift of the pI of CD1a loaded with either of the SCFAs (Fig. 4.6, B). Taken together, these data suggest that neither of the tested SCFAs act as a ligand of CD1a.

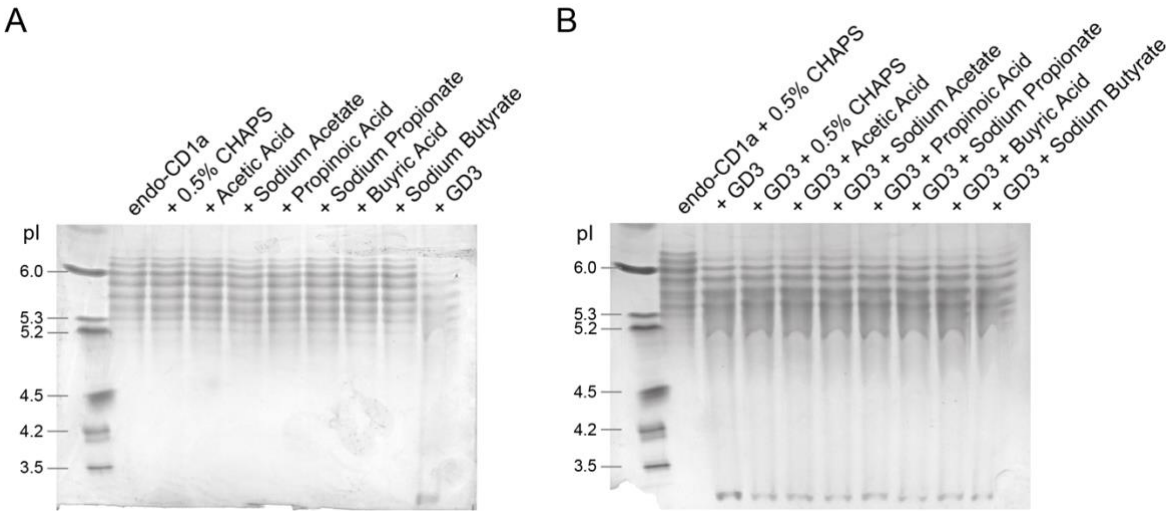

Fig. 4.6 Short-chain fatty acids do not change the isoelectric point of CD1a.
CD1a containing endogenous lipids (endo-CD1a) was incubated with acetate, propionate, or butyrate (acids and salts respectively) and run on an IEF gel to separate CD1a by isoelectric point (pI). SCFAs were dissolved in 0.5% CHAPS, which served as vehicle control. GD3 was used as positive control. **(A)** IEF gel of endo-CD1a incubated with SCFAs. **(B)** IEF gel of endo-CD1a pre-loaded GD3 before incubation with acetate, propionate, or butyrate (acids and salts respectively).

4.2.2 CD1a-modulating effects of fatty acids and fatty acid-related compounds with structural similarities to butyrate

CD1a-mediated immune responses have been shown to contribute to skin inflammatory diseases such as psoriasis and AD[6,167,174]. The inhibition of CD1a expression using chemical compounds that could be easily formulated into topical treatments therefore has great therapeutic potential. The data presented above suggest that not only butyrate but also propionate can partially inhibit CD1a acquisition during moDC differentiation (Fig. 4.1). To investigate if FAs and FA-related compounds with structural similarities to butyrate may act as more efficient CD1a inhibitors, monocytes were differentiated *in vitro* to moDCs in the presence or absence of 30 different FAs and FA-related compounds (see Table 6.10). SB and BA were included for comparison. MoDC differentiation and CD1a expression were analysed by flow cytometry.

Several tested compounds partially inhibited CD1a expression during moDC differentiation (Fig. 4.7). Based on inhibition of CD1a expression and considering the viability of treated moDCs, 4 candidates were chosen for validation and further investigation: 9-decenoic acid (9-DA), 8-hydroxyoctanoic acid (8-HOA), 6-phenylhexanoic acids (6-PHA) and 8-phenyloctanoic acid (8-POA) (marked in red in Fig. 4.7). Both 6-PHA and 9-DA strongly inhibited CD1a expression and moderately decreased HLA-DR expression. They showed no decrease in percentage of moDC-sized cells and $CD14^{-}CD11c^{+}$ cells, suggesting no effect on cell viability. 8-POA markedly reduced CD1a expression on moDCs when added from d0 or d3 of moDC differentiation. Although the compound decreased the percentage of moDC-sized cells and $CD14^{-}CD11c^{+}$ cells when added from d0, this decrease was not observed when added from d3. HLA-DR expression was moderately decreased by 8-POA. Due to the strong inhibition of CD1a expression when given from d0 or d3 of differentiation

and the possibility that lower concentrations may reduce toxicity while retaining the CD1a-inhibitory effect, the compound was chosen as a candidate for further investigation. 8-HOA showed effective inhibition of CD1a and DC-SIGN expression when added from d0 of moDC differentiation. The compound was chosen for further investigation as it showed a different pattern of effects in comparison to the other candidates and therefore may act through a different molecular mechanism. The structures of the candidate compounds and of several structurally related compounds that did not decrease CD1a expression are shown in Fig. 4.8.

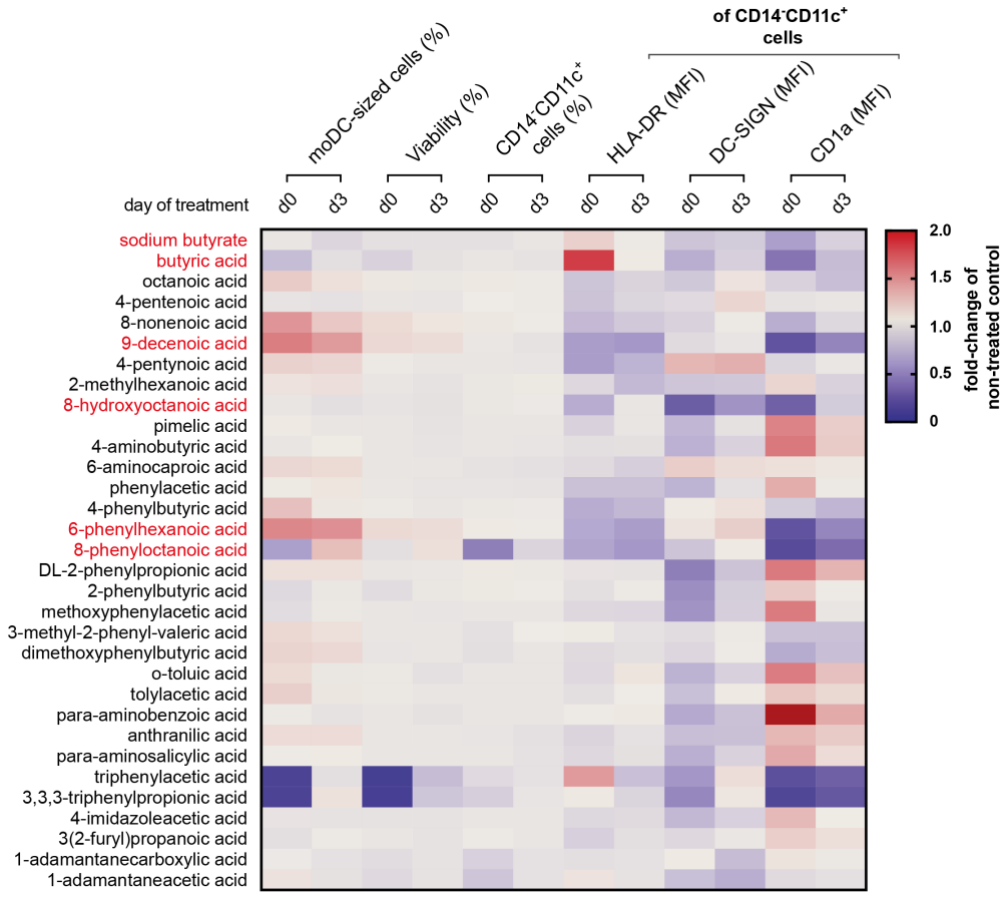

Fig. 4.7 Effects of fatty acids and fatty acid-related compounds with structural similarities to butyrate on moDC differentiation and CD1a expression.

Differentiating moDCs were treated with 250µM of the respective compounds from d0 or d3 of differentiation. Data is presented as fold-change of the non-treated control. Each data point represents the average of $n \geq 2$ donors; 2 independent experiments. Candidates for validation and further investigation are marked in red.

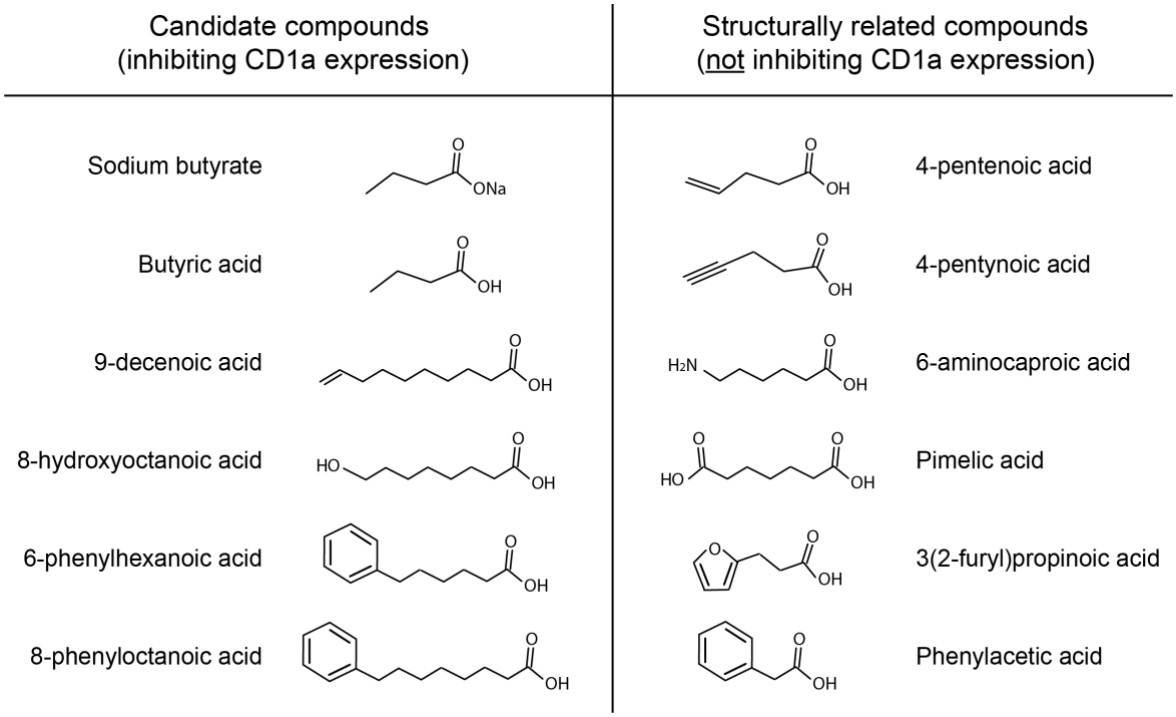

Fig. 4.8 Chemical structures of candidate compounds and structurally related compounds. Chemical structures of candidate compounds that inhibited CD1a expression during moDC differentiation and structurally related compounds that did not inhibit CD1a expression during moDC differentiation (see Fig. **4.7**).

The compounds were kindly provided by Prof Gurdyal S. Besra (University of Birmingham, UK). The experiments were performed under my supervision by Antonio Ji Xu during a research rotation. Data were analysed jointly.

4.2.3 Butyrate, 6-phenylhexanoic acid, 8-phenyloctanoic acid and 9-decenoic acid inhibit the acquisition of CD1a during moDC differentiation in a dose-dependent manner

4.2.3.1 Dose-dependent effects of butyrate and candidate compounds on CD1 acquisition during moDC differentiation

To validate the CD1a-inhibitory effect of the candidate compounds and to determine whether treatment with lower concentrations may still achieve the desired inhibition of CD1a expression, moDCs were differentiated in the presence of varying concentrations of the candidate compounds or butyrate. Monocytes were treated with concentrations between 7.81µM and 1000µM at d0 or d3 of moDC differentiation. Toxic concentrations were determined by ≥ 20% decrease in percentage and/or viability of moDC-sized cells and were excluded from analysis.

6-PHA, 8-POA and 9-DA could be confirmed to significantly inhibit acquisition of CD1a (MFI) on moDCs in a dose-dependent manner when added from d0 of differentiation (for 125µM: 33.86% ± 9.93, 23.02% ± 8.75 and 27.75% ± 8.01 of non-treated control, respectively) (Fig. 4.9, A). SB and BA showed a similar dose-dependency, but the overall inhibition of CD1a expression was not as pronounced (for 125µM: 68.83% ± 18.43 and 73.39% ± 7.49 of non-treated control, respectively) (Fig. 4.9, A). In line with previous results, CD1a expression was inhibited to a lesser extend when treatment was started from d3 of moDC differentiation with none of the compounds inhibiting CD1a expression (MFI) by more than 10% compared to the non-treated control at a concentration of 125µM (Fig. 4.9, B). 8-HOA could not be confirmed to inhibit CD1a expression (MFI for 125µM from d0: 105.38% ± 1.80 of non-treated control) (Fig. 4.9) and was therefore excluded from further analysis. Due to much higher inhibition of CD1a expression when the tested

compounds were present from d0 of moDC differentiation, the following analyses focus on this condition.

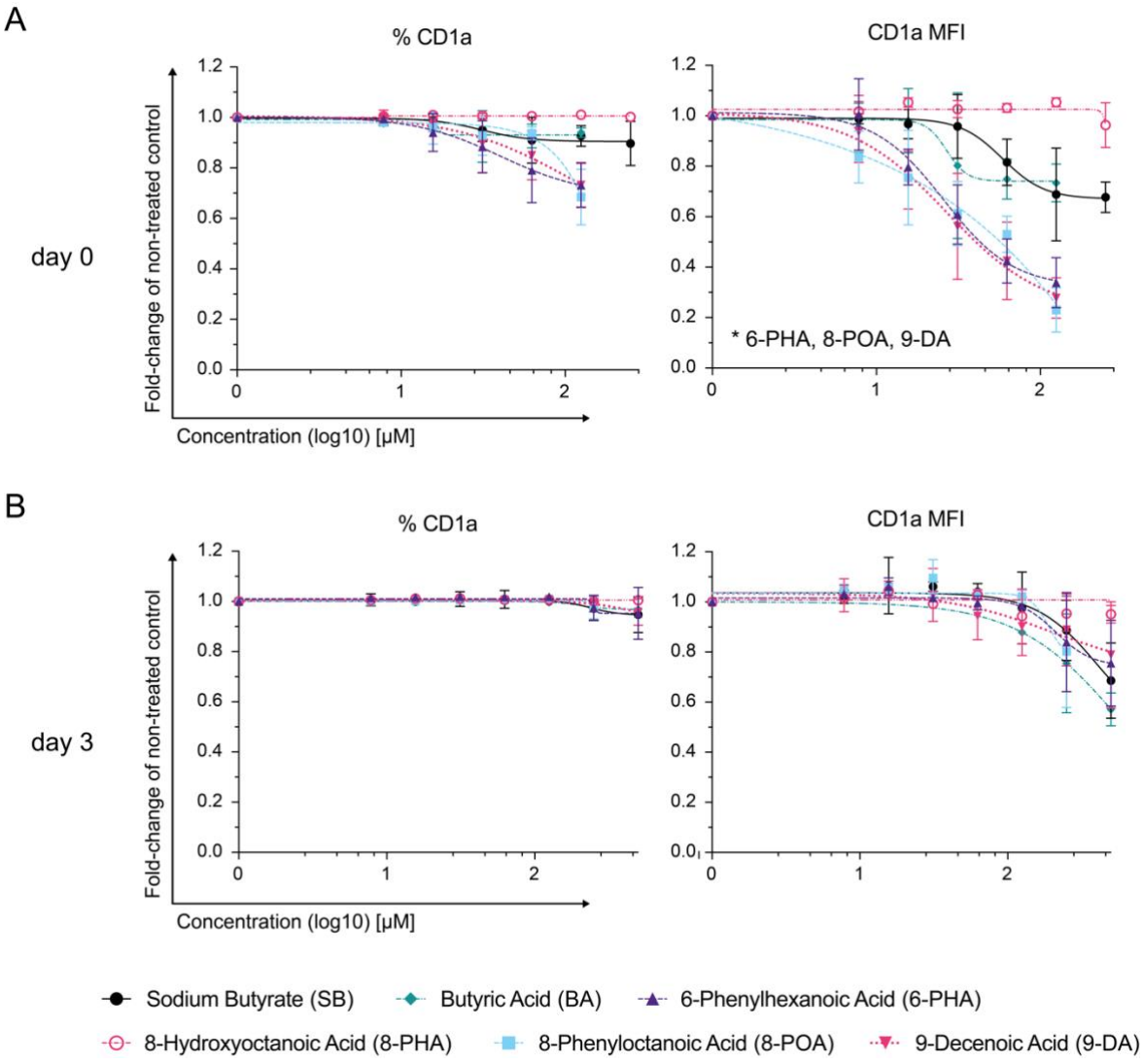

Fig. 4.9 Butyrate, 6-phenylhexanoic acid, 8-phenyloctanoic acid and 9-decenoic acid inhibit the acquisition of CD1a during moDC differentiation in a dose-dependent manner.

SB, BA, 6-PHA, 8-HOA, 8-POA or 9-DA were added to moDC differentiation at **(A)** d0 or **(B)** d3 of differentiation at concentrations of 7.81µM to 1000µM (2-fold serial dilution). Concentrations that led to ≥ 20% decrease in moDC-sized cells and/or viability compared to the non-treated control were excluded. Lines represent non-linear fits (four parameter variable slopes). (n=3 donors; ≥ 1 individual experiment). Statistics were calculated for (A) d0 treatment for 125µM and for (B) d3 treatment for 250µM. *P < 0.05; **P < 0.01; ***P < 0.001; (A) RM One-way ANOVA or (B) RM Mixed-effects analysis with Dunnett's correction for multiple comparison (mean ± SD).

6-PHA, 8-POA and 9-DA could also be shown to inhibit the expression of CD1b and CD1c (Fig. 4.10, A, B). Both CD1b and CD1c expression (MFI) were inhibited to a comparable degree at concentrations of 125 µM. Treatment with SB and BA reduced the expression of both CD1b and CD1c to approximately 71% (71.39% ± 9.21 and 71.95% ± 2.50) and 64% (62.49% ± 20.77 and 66.18% ± 20.77) of the non-treated control, respectively. 6-PHA and 9-DA showed a similar inhibition of CD1b and CD1c expression compared to butyrate, reducing the expression of both CD1b and CD1c to approximately 61% (59.67% ± 28.81 and 61.49% ± 23.49) and 64% (60.29% ± 21.79 and 66.69% ± 15.24) of the non-treated control, respectively. 8-POA showed a slightly higher impact on CD1b and CD1c expression, reducing expression of both molecules to approximately 47% (49.73% ± 26.87 and 44.97% ± 22.04) of the non-treated control.

CD1d expression (MFI) showed a non-significant increase in fold-change expression compared to the non-treated control for 6-PHA, 8-POA, and 9-DA (Fig. 4.10, C). The percentage of CD1d expression for non-treated moDCs in this data set was 11.74% ± 15.54 (ranging from 1-30%, depending on donor) and increased to 52.30% ± 27.86 for 6-PHA, 77.13% ± 16.65 for 8-POA, and 61.83% ± 17.27 for 9-DA at 125µM treatment. SB and BA showed no increase in percentage of CD1d expression (4.62% ± 2.86 and 10.50% ± 8.25 at 125µM, respectively), validating previous results. It is of note that the increased percentages of CD1d expression for all compounds resulted from relatively small whole-population shifts compared to the FMO and unlike CD1a, CD1b and CD1c expression did not result in a medium- to high-expressing population.

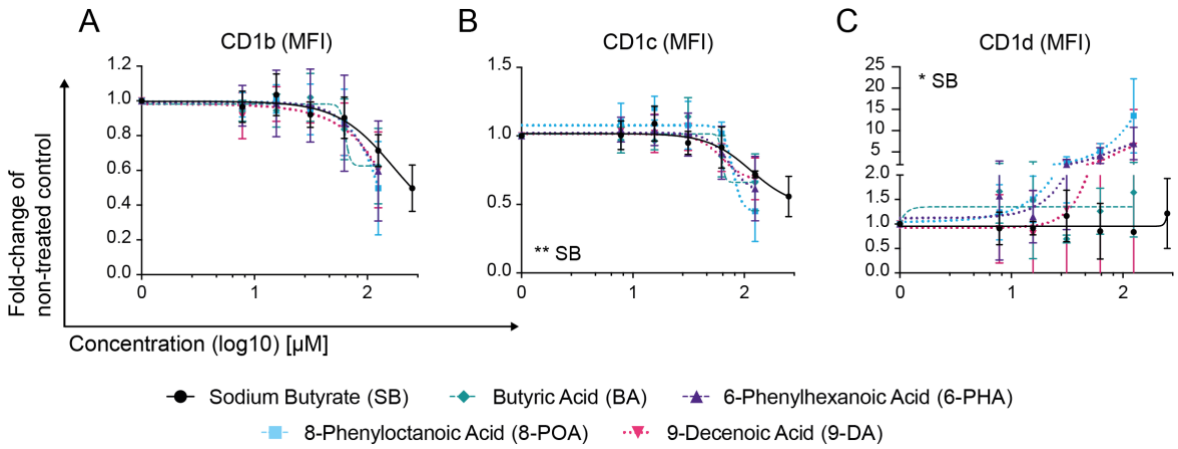

Fig. 4.10 Butyrate, 6-phenylhexanoic acid, 8-phenyloctanoic acid and 9-decenoic inhibit the acquisition CD1b and CD1c during moDC differentiation in a dose-dependent manner.
Circulating monocytes were differentiated in the presence of SB, BA, 6-PHA, 8-POA or 9-DA at concentrations ranging from 7.81µM to 1000µM (2-fold serial dilution). Concentrations that led to ≥ 20% decrease in moDC-sized cells and/or viability compared to the non-treated control were excluded from analysis. Expression (MFI) of **(A)** CD1b, **(B)** CD1c and **(C)** CD1c are shown as fold-change of the non-treated control. Lines represent non-linear fits (four parameter variable slopes). (n=3 donors; ≥ 1 individual experiment). Statistics were calculated for 125µM. *P < 0.05; **P < 0.01; ***P < 0.001; RM One-way ANOVA with Dunnett's correction for multiple comparison (mean ± SD).

To compare the 50% inhibitory concentration (IC50) of the different compounds on CD1a, CD1b and CD1c expression, nonlinear regression (log(inhibitor) vs. response – variable slope (four parameters)) was used to calculate IC50 values for each compound (Table 4.1). As all compounds show toxic effects at higher concentrations and therefore the bottom plateau needed for the exact calculation of IC50 values is missing for most samples, not all IC50 values could be determined with confidence. The calculated IC50 values for inhibition of CD1a acquisition during moDC differentiation were very similar for BA, 6-PHA and 9-DA with 26.81µM, 25.74µM and 26.98µM, respectively. The IC50 for SB was about 2-fold higher at 58.79µM. For SB, BA and 6-PHA, IC50 values for CD1b and CD1c expression were approximately 2- to 4-fold higher compared to the IC50 for CD1a expression. A similar approximately 2-fold lower IC50 compared to CD1a expression could

be seen for CD1c expression upon treatment with 9-DA. For 8-POA the IC50 for CD1a inhibition could not be calculated and for both 8-POA and 9-DA the IC50 values for CD1b could not be calculated with confidence and are very high (597.5µM and 1817µM, respectively). However, dose-dependent inhibition of CD1b and CD1c in Fig. 4.10 compared to the inhibition of CD1a in Fig. 4.9 (A) suggests that the IC50 for inhibiting CD1a compared to CD1b and CD1c may also be lower for 8-POA and 9-DA.

Table 4.1. IC50 for CD1a, CD1b and CD1c expression (MFI) on moDCs upon treatment with candidate compounds during differentiation.

50% inhibitory concentrations (IC50) were calculated based on non-linear fits (four parameter variable slope) to the dose-dependent inhibition of CD1a, CD1b and CD1c expression (MFI) following treatment with SB, BA, 6-PHA, 8-POA, or 9-DA from d0, as shown in Fig. **4.9** and Fig. **4.10**. (n.d. = not determined).

	SB	BA	6-PHA	8-POA	9-DA
CD1a	58.79 µM	26.81 µM	25.74 µM	n.d.	26.98 µM
CD1b	169.8 µM	63.74 µM	103.3 µM	597.5 µM	1817 µM
CD1c	114.5 µM	62.84 µM	73.64 µM	78.32 µM	62.76 µM

4.2.3.2 Effects of butyrate and candidate compounds on moDC differentiation

To assess the dose-dependent effect of butyrate and the candidate compounds on moDC differentiation, expression of moDC lineage markers and the co-stimulatory molecule CD86 was assessed by flow cytometry. All compounds showed toxic effects at higher concentrations (Fig. 4.11, A). To exclude toxic effects from analysis, concentrations at which the percentage of moDC-sized cells and/or viability was decreased by ≥ 20% were removed from further analysis. As seen in the primary screening experiment (Fig. 4.7), the compounds did not change the percentage of $CD14^{-}CD11c^{+}$ cells at non-toxic concentrations

(Fig. 4.11, A). The previously observed decrease in HLA-DR by SB, BA, 6-PHA and 9-DA (Fig. 4.7) could not be confirmed (Fig. 4.11, B). Unlike previous experiments, DC-SIGN expression (MFI) was reduced in a dose-dependent manner by SB and 9-DA (84.54% ± 2.90 and 58.27% ± 4.13 of the non-treated control at 125 µM, respectively). However, the percentage of DC-SIGN-expressing cells was not significantly reduced for either compound (99.11% ± 1.11 and 92.71% ± 5.83 DC-SIGN$^+$ cells compared to the non-treated control at 125µM, respectively) (Fig. 4.11, B). The other compounds showed only slight to moderate and no significant decrease in DC-SIGN expression (MFI ranging from 77-95% of non-treated control at 125µM) (Fig. 4.11, B). Neither HLA-ABC nor CD86 showed a significant change in expression upon treatment, but at higher concentrations HLA-ABC seemed to be slightly reduced and CD86 showed a slight dose-dependent increase in expression for all compounds. CD83 expression was dose-dependently downregulated upon treatment with all compounds (ranging from 42-68% of non-treated control at 125µM) (Fig. 4.11, B). 6-PHA, 8-POA and 9-DA showed a significant inhibition of CD83 at 125µM (55.16% ± 13.01, 42.11% ± 11.28, and 50.26% ± 9.77 of non-treated control, respectively). DC-LAMP was only decreased upon treatment with 9-DA (Fig. 4.11, B). However, as DC-LAMP expression was barely detectable on differentiated moDCs (Fig. 4.3, A) this observation may be an artefact of calculating the fold-change between two negative populations.

Taken together, all compounds reduced CD83 expression to a moderate degree in a dose-dependent manner and most compounds further showed a slight dose-dependent inhibition of DC-SIGN expression, which was more pronounced only for 9-DA.

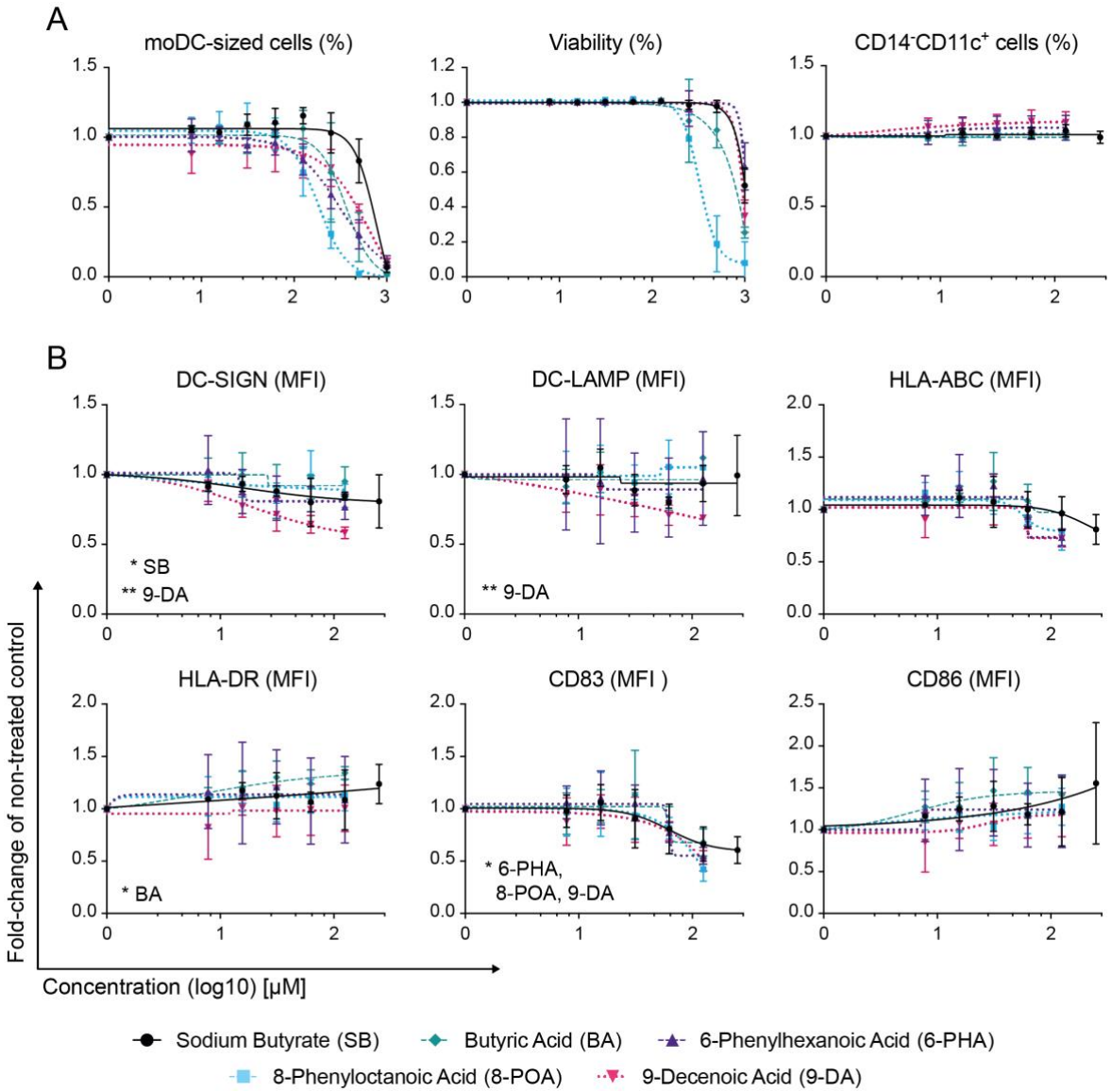

Fig. 4.11 Butyrate, 6-phenylhexanoic acid, 8-phenyloctanoic acid and 9-decenoic acid inhibit DC-SIGN and CD83 expression on moDCs in a dose-dependent manner.

SB, BA, 6-PHA, 8-POA or 9-DA were added to the culture medium from d0 of moDC differentiation at concentrations from 7.81µM to 1000µM (2-fold dilution series). All results are shown as fold-change of the non-treated control. Concentrations that led to ≥ 20% decrease in moDC-sized cells and/or viability compared to the non-treated control were excluded. **(A)** Dose-dependent effect of compounds on percentage of moDC-sized cells, viability (gated on moDC-sized cells) and $CD14^{-}CD11c^{+}$ cells (gated on live cells). **(B)** Dose-dependent effect of compounds on moDC expression (MFI) of DC-SIGN, DC-LAMP, HLA-ABC, HLA-DR, CD83 and CD86. Gated on live $CD14^{-}CD11c^{+}$ moDCs. Lines represent non-linear fits (four parameter variable slopes). (n=3 donors; ≥ 1 individual experiment). Statistics were calculated for 125µM. *P < 0.05; **P < 0.01; ***P < 0.001; RM One-way ANOVA with Dunnett's correction for multiple comparison (mean ± SD).

4.2.3.3 Candidate compounds do not act as CD1a ligands

CD1a has been shown to bind and present a variety of FAs[34,88,166]. The candidate compounds 6-PHA, 8-POA and 9-DA all contain a hydrocarbon chain with a terminal carboxyl group, classing them as FAs. To investigate whether these compounds may bind to CD1a as ligands, it was determined by IEF whether they may change the pI of CD1a. Post incubation with CD1a to allow for loading, none of the compounds showed a band shift compared to the respective vehicle control (Fig. 4.12, A). To confirm these results, CD1a was pre-loaded with GD3 before incubation with the candidate compounds. While GD3 loads onto CD1a as indicated by the band shift, neither of the tested compounds changed the pI of GD3-loaded CD1a (Fig. 4.12, B). Taken together, these data suggest that the tested compounds do not act as CD1a ligands.

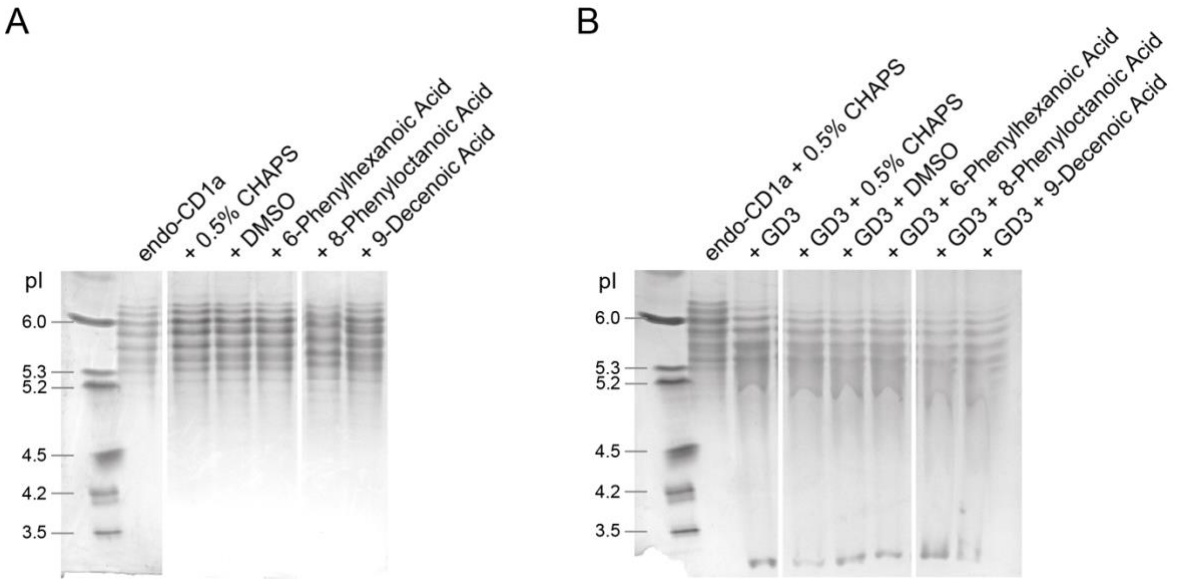

Fig. 4.12 Candidate compounds do not change the isoelectric point of CD1a.
CD1a containing endogenous lipids (endo-CD1a) was incubated with 6-PHA, 8-POA, or 9-DA and run on an IEF gel to separate CD1a by isoelectric point (pI). 8-POA was dissolved in DMSO, the other compounds in 0.5% CHAPS. DMSO or 0.5% CHAPS served as vehicle control. **(A)** IEF gel of endo-CD1a incubated with candidate compounds. **(B)** IEF gel of endo-CD1a pre-loaded GD3 before incubation with candidate compounds.

4.2.4 Inhibition of CD1a expression by butyrate, 6-phenylhexanoic acid, or 9-decenoic acid does not affect CD1a-mediated activation of T cell clones

The inhibition of CD1a acquisition during moDC differentiation has the potential to influence CD1a-mediated immune responses. To assess whether the reduction of CD1a expression by SB, BA, 6-PHA, or 9-DA could influence CD1a-mediated T cell activation, moDCs differentiated in the presence of these compounds were co-cultured with CD1a-reactive T cell clones (kindly provided by Dr Yi-Ling Chen). CD1a reactivity was measured by ELISA, quantifying IFNγ production of CD1a-reactive T cell clones. To exclude MHC-mediated effects on T cell activation, HLA-ABC and HLA-DR were blocked with antibodies before and during co-culture. Co-culturing moDCs and CD1a-reactive T cell clones at a ratio of 1:2, IFNγ production of CD1a-reactive T cell clones was comparable to the non-treated control for treatment with SB, 6-PHA, and 9-DA (Fig. 4.13, A). A slight but significant increase of IFNγ production (1.1-fold) could be observed upon co-culture with BA-treated moDCs (Fig. 4.13, A). CD1a reactivity of the T cell clones was confirmed by blocking moDCs with anti-CD1a antibody which reduced IFNγ production significantly (Fig. 4.13, B).

As the used CD1a-reactive T cell clones were highly reactive to CD1a stimulation, producing high amounts of IFNγ, lower effector-to-target ratios may be needed to show differences in CD1a stimulation. To test this, moDCs differentiated in the presence of SB or 9-DA were co-cultured with CD1a-reactive T cell clones at ratios of 1:2, 1:4 and 1:8 (Fig. 4.14, A) or 1:2, 1:50 and 1:100 (Fig. 4.14, C). CD1a reactivity of the T cell clones was confirmed by blocking moDCs with anti-CD1a antibody, which reduced IFNγ production significantly (Fig. 4.14, B, D). Even though CD1a-reactive T cell clones were sensitive to

CD1a stimulation even at effector-to-target ratio of 1:100 (Fig. 4.14, D), inhibition of CD1a expression by SB or 9-DA had no effect on IFNγ production (Fig. 4.14, A, C).

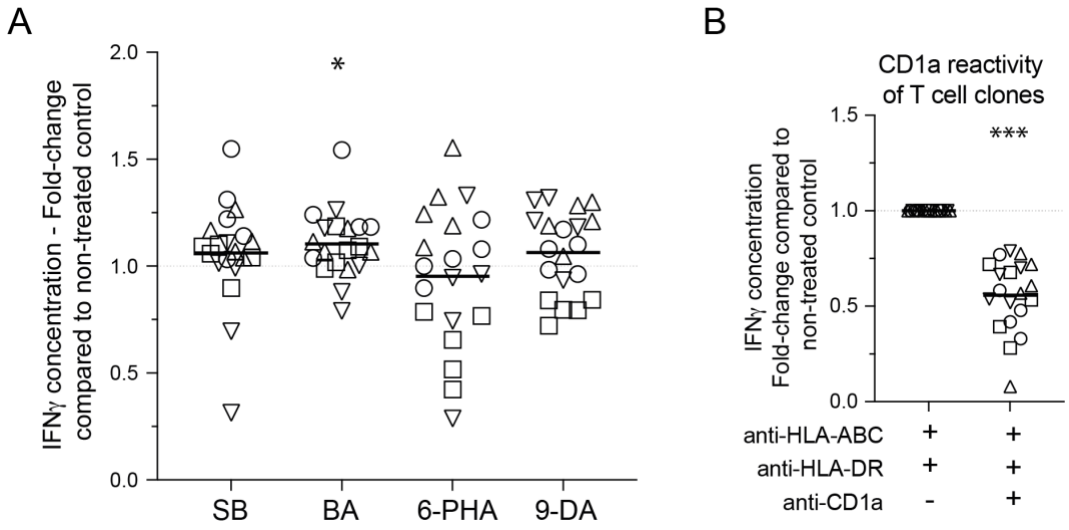

Fig. 4.13 IFNγ secretion of CD1a-reactive T cell clones is unchanged by decreased CD1a expression on moDCs resulting from treatment with butyrate, 6-phenylhexanoic acid and 9-decenoic acid.

MoDCs, blocked with anti-human HLA-ABC and HLA-DR antibodies, were co-cultured with CD1a-reactive T cell clones at a ratio of 1:2. CD1a reactivity of T cell clones was quantified by IFNγ ELISA. IFNγ concentration in the supernatant is shown as fold-change of the non-treated control. Each dot represents a different T cell clone; different shapes present different moDC donors. **(A)** IFNγ production of T cell clones upon co-culture with moDCs differentiated in the presence of 125µM SB, BA, 6-PHA, or 9-DA. **(B)** IFNγ production of T cell clones co-cultured with non-treated moDCs in the presence or absence of anti-CD1a antibody. (n=20 (4 moDC donors co-cultured with 5 T cell clones each); 2 individual experiments). *P < 0.05; **P < 0.01; ***P < 0.001; (A) RM One-way ANOVA with Dunnett's correction for multiple comparison; (B) Two-tailed paired t-test (mean).

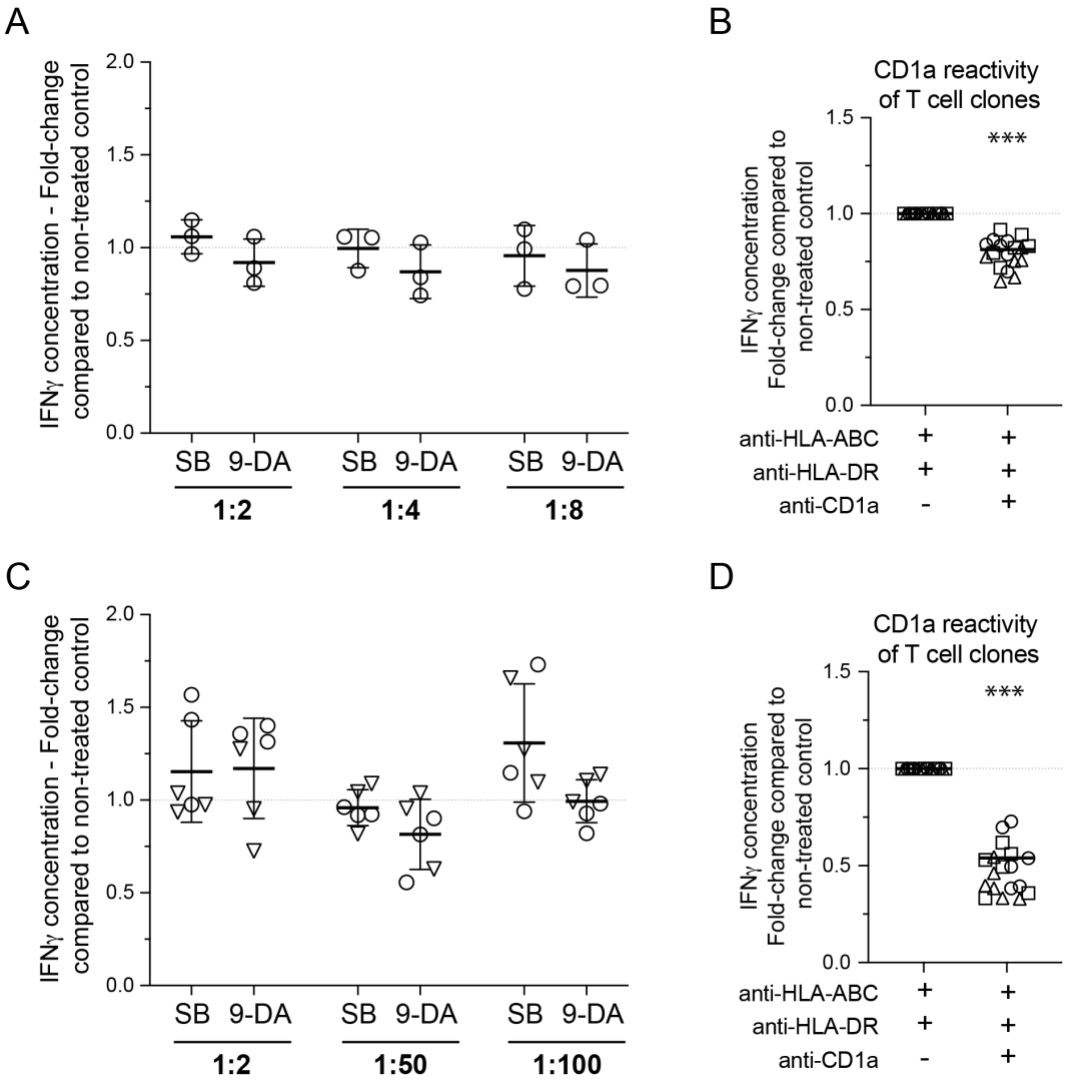

Fig. 4.14 IFNγ secretion of CD1a-reactive T cell clones is unchanged when co-cultured with varying effector-to-target ratios of moDCs treated with sodium butyrate or 9-decenoic acid. MoDCs, blocked with anti-human HLA-ABC and HLA-DR antibodies, were co-cultured with CD1a-reactive T cell clones at varying ratios. CD1a reactivity of T cell clones was quantified by IFNγ ELISA. IFNγ concentration in the supernatant is shown as fold-change of the non-treated control. Each dot represents a different T cell clone; different shapes present different moDC donors. **(A, C)** IFNγ production of T cell clones upon co-culture with moDCs differentiated in the presence of 125µM SB or 9-DA at ratios of **(A)** 1:2, 1:4 and 1:8 or **(C)** 1:2, 1:50 and 1:100 moDCs:T cell clones. **(B, D)** IFNγ production of T cell clones co-cultured with non-treated moDCs in the presence or absence of anti-CD1a antibody, corresponding to experiments shown in (A) and (B), respectively. ((A) n=3 (1 moDC donor co-cultured with 3 T cell clones); 1 experiment; (C) n=6 (2 moDC donors co-cultured with 3 T cell clones each); 1 experiment). *P < 0.05; **P < 0.01; ***P < 0.001; (A, C) RM One-way ANOVA with Dunnett's correction for multiple comparison; (B, D) Two-tailed paired t-test (mean ± SD).

4.3 Discussion

CD1a is predominantly expressed on DCs and LCs in the skin where it influences skin immunity by presenting lipid antigens[160]. CD1a-mediated immune responses play an important role in skin inflammation during allergic reactions and in skin inflammatory diseases[6,166-168,174]. The modulation of CD1a-mediated immune responses *via* alteration of CD1a expression may present great therapeutic potential for the treatment of CD1a-mediated inflammation. Several FAs show CD1-modulating properties[75,201,202,647,648] and their chemical properties allow their formulation into topical treatments which can be easily applied by patients without the need for interventions in professional medical settings. Topical rather than systemic treatment would further permit direct targeting of CD1a-expressing cells in the skin while limiting systemic side effects.

4.3.1 The short-chain fatty acid butyrate partially inhibits acquisition of group 1 CD1 molecules during moDC differentiation

The SCFA butyrate has been shown to inhibit the acquisition of CD1a during moDC differentiation[201,202] and has further been demonstrated to ameliorate inflammation in pre-clinical models of CHS and psoriasis[634,635]. The data presented here confirms the CD1a-inhibitory effect of butyrate during moDC differentiation. Butyrate treatment from d0 of differentiation inhibited CD1a surface expression levels consistently, although the reduction of the percentage of $CD1a^+$ cells was highly variable between donors (Fig. 4.1). When butyrate was added partway through differentiation (d3), CD1a expression per cell was still reduced, but to a smaller degree compared to treatment from d0. No change in percentage of CD1a-expressing moDCs was observed when butyrate was added from d3 (Fig. 4.2). These findings corroborate data by Nascimento *et al.* showing that butyrate inhibits CD1a acquisition during moDC differentiation rather than downregulating existing

CD1a expression[202]. Acute tissue inflammation is often associated with an infiltration and accumulation of monocytes[653,654] which can differentiate into moDCs and macrophages [653,655]. Therefore, the inhibition of CD1a acquisition may reduce moDC-mediated CD1a-dependent pro-inflammatory T cell responses. SCFAs of different hydrocarbon chain length have shown gradual immunomodulatory effects on moDCs (butyrate > propionate > acetate)[633]. In line with this, different SCFAs showed a similar gradual effect on CD1a surface expression on moDCs. While butyrate showed varying but efficient inhibition of CD1a expression, propionate showed only minor reduction of CD1a expression, whereas acetate had no effect on CD1a surface expression (Fig. 4.1).

Published studies suggest that butyrate also downregulates CD1b expression and may modulate the expression of CD1d[201,202], however little is known about the effects of butyrate on general moDC differentiation. The here presented data paints a more comprehensive picture of the effect of butyrate on differentiating moDCs in regard to lineage markers, co-stimulatory markers and CD1 expression (Fig. 4.3). Butyrate did not affect general moDC differentiation, with percentages of $CD14^{-}CD11c^{+}$ cells and expression levels of DC-SIGN and HLA-DR remaining comparable to non-treated moDCs. The co-stimulatory molecule CD86 was slightly but not significantly decreased upon treatment with BA, but not SB. HLA-ABC and the activation marker CD83 were reduced to a minor and moderate degree, respectively. Lack of DC-LAMP expression combined with no increase in MHC and co-stimulatory molecule expression suggests that butyrate-treated moDCs retain their immature and non-activated phenotype[605,656,657]. CD1a has been proposed to be downregulated on activated and matured moDCs[658], however, as butyrate-treated moDCs do not present an activated phenotype, butyrate does not seem to modulate CD1a expression *via* moDC activation. In addition to inhibiting the induction of CD1a, butyrate also decreased the surface expression of other group 1 CD1 molecules, CD1b and CD1c, in

differentiation moDCs (Fig. 4.4). CD1d surface expression showed a trend towards higher expression in some donors (Fig. 4.4). However, as CD1d expression was very low or absent on moDCs from most donors, very minor changes in expression relate to high fold-change differences compared to the control. Therefore, CD1d expression was likely not significantly affected by butyrate treatment. While Wang *et al.* reported a downregulation of CD1d in mature and immature BA-treated moDCs, the fluorescent intensity of CD1d expression reported was very low, especially in immature moDCs[201]. This indicates that, similar to our results, CD1d was not expressed on either non-treated nor butyrate-treated immature moDCs in their model. In contrast, Nacimento *et al.* observed an upregulation of CD1d transcription upon treatment with SB. However, they did not confirm whether this transcriptional change related to an increase in CD1d surface expression[202].

4.3.2 6-phenylhexanoic acid, 8-phenyloctanoic acid and 9-decenoic acid differentially modulate group 1 and group 2 CD1 molecule expression on differentiating moDCs

Overall, butyrate showed partial inhibition of CD1a expression, reducing mainly the expression level per cell but showing only limited and donor-dependent inhibition. To investigate whether butyrate-related compounds may be more effective at inhibiting CD1a and therefore may present better therapeutic candidates, 30 compounds were tested (Fig. 4.7). The tested compounds are FAs or FA-related with varying degrees of structural similarity to butyrate. Based on efficiency of CD1a modulation, four compounds were chosen for further investigation, three of which could be confirmed to inhibit CD1a expression: 6-phenylhexanoic acid (6-PHA), 8-phenyloctanoic acid (8-POA) and 9-decenoic acid (9-DA). While general moDC differentiation seemed mostly unchanged by treatment of differentiating moDCs with these compounds, 9-DA and SB decreased

DC-SIGN expression per cell but not the percentage of DC-SIGN$^+$ cells (Fig. 4.11). The decrease was minor for SB and not seen in previous experiments.

Like butyrate, 6-PHA, 8-POA and 9-DA seem to inhibit the acquisition of CD1a rather than downregulating existing CD1a, as inhibition was almost abolished when moDCs were treated from d3 of differentiation compared to d0 (Fig. 4.9). All candidate compounds and butyrate inhibited CD1a in a dose-dependent manner. Compared to butyrate, 6-PHA, 8-POA and 9-DA reduced CD1a expression 2- to 3-fold more efficiently, but with comparable IC50 values (Table 4.1). Furthermore, butyrate and the candidate compounds dose-dependently inhibited CD1b and CD1c expression (Fig. 4.10). Interestingly, dose-response curves for CD1b and CD1c were shifted to a higher concentration compared to CD1a, suggesting lower IC50 concentrations for the inhibition of CD1a compared to CD1b and CD1c. Where calculation was possible, IC50 calculations confirmed 2- to 4-fold lower IC50 values for CD1a inhibition compared to CD1b and CD1c inhibition (Table 4.1). In contrast to the inhibition of group 1 CD1 molecules, treatment with 6-PHA, 8-POA and 9-DA showed a trend towards increased CD1d expression, while SB and BA showed minor reduction or no change in CD1d expression, respectively (Fig. 4.10).

6-PHA, 8-POA and 9-DA are MCFAs, the former two containing phenyl groups at the end of the hydrocarbon chain opposite a terminal carboxyl group (Fig. 4.8). 8-HOA, a MCFA which contains a terminal hydroxyl group opposite the terminal carboxyl group (Fig. 4.8), showed CD1a-inhibiting effects in the initial screen (Fig. 4.7), but inhibition of CD1a acquisition could not be validated (Fig. 4.9). Therefore, all validated candidates and butyrate are composed of a carbon chain with a terminal hydrophobic carboxyl group at one end and a hydrophobic tail, with or without a double bond or a phenyl group at the other end. Compounds with polar headgroups at both sides of the carbon chain, short carbon chains or double bonds near the carboxyl group showed no CD1a inhibitory effects (Fig. 4.7; Fig.

4.8), suggesting that these chemical and/or structural properties may interfere with modulation of CD1a expression.

The surface expression of group 1 and group 2 CD1 molecules on DCs show distinct differences in kinetics and cellular mechanisms that control expression[78]. Studies by Wang *et al.* and Nascimento *et al.* suggest that butyrate modulates CD1 expression at the transcriptional level[201,202]. PPARγ activation, HDAC inhibition and TLR2 activation have all been shown to modulate both group 1 and group 2 CD1 molecule expression. While PPARγ activation has been shown to inhibit CD1a expression but upregulate CD1d expression[72-76], HDAC inhibition was shown to reduce expression of both CD1a and CD1d[79,80], and TLR2 activation can induce all group 1 CD1 molecules but not CD1d[77,78]. Upregulation of CD1d by 6-PHA, 8-POA and 9-DA suggests that these compounds may modulate CD1 expression *via* PPARγ activation. Considering varying reports on CD1 modulation by butyrate and other FAs (see 4.1.2.3 Effect of fatty acids on CD1 expression and lipid antigen presentation), it is plausible that butyrate and the candidate compounds may not modulate CD1 expression *via* a single molecular mechanism but through a combination of different mechanisms. Extending the here presented data by studying the effect of these compounds on CD1 expression on a transcriptional level and using PPARγ inhibitors, TLR2 inhibitors and investigating histone deacetylation could give further insights into specific mechanisms of action.

4.3.3 Short-chain fatty acids, 6-phenylhexanoic acid, 8-phenyloctanoic acid and 9-decenoic acid may not act as CD1a ligands

FAs like palmitoleic acid (C16:1) have been shown to bind to CD1a and serve as functional ligands[34,166]. The binding groove of CD1a is the smallest of the CD1 molecules accommodating carbon chains of up to 32-42 carbons[89]. The presented results suggest that

neither the SCFAs acetate, propionate, or butyrate, nor the candidate compounds 6-PHA, 8-POA, or 9-DA can bind to the CD1a binding cleft, as determined by IEF analysis (Fig. 4.5; Fig. 4.12) and CD1a-mediated T cell responses to pulsed K562-CD1a cells (Fig. 4.6). IEF analysis relies on change in the pI of CD1a after loading and there is a possibility that the binding of a new lipid, particularly if loaded inefficiently, may not change the pI enough to be visible on an IEF gel. As GD3 efficiently displaces endogenous lipids and binds to CD1a but can be removed more readily compared to endogenous lipids, pre-loading of CD1a with GD3 can enable easier loading of new lipids[6,200]. However, none of the tested compounds were able to displace GD3 from CD1a, reinforcing previous results that the tested compounds may not act as ligands for CD1a. To further strengthen the herein presented data, harsher CD1a loading methods that may more efficiently remove endogenous ligands from the binding cleft, such as prolonged 37°C incubation, and the addition of DMSO and/or various detergents to the loading buffer, could be tested. Interestingly, polyunsaturated FAs can inhibit CD1a expression but complexing of these FFAs has no reversing effect on CD1a inhibition, suggesting that CD1a modulation is not mediated by binding of the FFA to the CD1a binding cleft[647]. Together with the here presented results, these data imply that CD1a-modulating effects of the here tested compounds and other FAs may be independent of CD1a binding.

4.3.4 CD1a modulation by butyrate, 6-phenylhexanoic acid, 8-phenyloctanoic acid and 9-decenoic acid may not impact CD1a-mediated T cell responses

Little is known about the impact of CD1 modulation on DC-mediated T cell immune responses. Several studies suggest that changes in CD1c and CD1d expression can affect CD1c- and CD1d-restricted T cell responses[73-76]. However, it is unknown whether CD1a

inhibition on DCs impacts CD1a-mediated T cell activation. While 6-PHA, 8-POA and 9-DA inhibited CD1a expression more effectively than butyrate and decreased the CD1a MFI to 23-34% of the non-treated control, only approximately 30% of moDCs were negative for CD1a surface expression (Fig. 4.9). When co-culturing FA-treated moDCs with CD1a-reactive T cell clones, no change in CD1a-mediated IFNγ production could be observed compared to the non-treated control (Fig. 4.13). CD1a reactivity was verified by blocking CD1a with anti-CD1a antibody, which reduced IFNγ secretion significantly in all experiments. To exclude the possibility that a high effector-to-target ratio (1:2) may mask changes in CD1a-mediated T cell activation, lower effector-to-target ratios were tested. Clones retained CD1a reactivity even at ratios of as low as 1:100. However, only a trend towards a decreased CD1a-mediated T cell response could be observed for 9-DA at a ratio of 1:50 (Fig. 4.14). The reported lack in modulation of CD1a-mediated T cell responses by CD1a inhibition of moDCs treated with butyrate, 6-PHA, and 9-DA may be explained by incomplete inhibition of CD1a surface expression. CD1a is highly expressed on non-treated moDCs and even after inhibition of CD1a expression with 6-PHA, 8-POA and 9-DA the expression levels of CD1a were still relatively high. Therefore, more potent CD1a inhibition may be needed to influence CD1a-mediated immune responses. Furthermore, in the setting of LCs which express high levels of CD1a constitutively[7,65,66], the data herein suggest that SCFAs are unlikely to significantly modulate CD1a expression by mature LCs in order to sufficiently influence T cell responses. However, responses from DCs and LCs can vary; CD1a MFI reduction may affect LCs more strongly due to high density of CD1a, Langerin expression may play a role in CD1a presentation, and downstream pathways may be differentially affected in LCs and DCs. It will therefore be important to formally test this prediction.

Taken together, these results further give an indication that CD1a-mediated T cell stimulation is very sensitive and so reducing CD1a surface levels or the presence of fewer CD1a-presenting DCs may not be sufficient to reduce CD1a-reactive T cell activity in a clinical setting.

Chapter 5 Final Discussion

5.1 Implications of CD1a-reactive Tregs in health and psoriasis

Tregs are increasingly recognised to contribute to skin immunity and homeostasis (see 1.3.2 Tregs in the skin) and Tregs show impaired suppressive functionality in many skin inflammatory diseases[416]. However, it remains unstudied whether Tregs can recognise and interact with CD1a. The experiments presented in this thesis aimed to determine whether Tregs can functionally interact with CD1a and to investigate phenotypic and transcriptomic characteristics of CD1a-reactive Tregs in health and psoriasis.

Here, I demonstrate for the first time that Tregs can bind to and functionally interact with CD1a. A subpopulation of about 2% of polyclonal Tregs secreted IL-10 in a CD1a-dependent manner (Fig. 2.2; Fig. 2.6), and this was unchanged in patients with psoriasis (Fig. 3.2). It is possible that CD1a-reactive Tregs are composed of different subpopulations and CD1a stimulation may induce phenotypic changes independent of IL-10 secretion. Therefore, the here presented data may underestimate the frequency of CD1a-reactive Tregs. The presented data further demonstrates that CD1a-reactive Tregs can interact with CD1a loaded with skin-relevant lipids (Fig. 2.14), similar to other CD1a-reactive T cells[34,134,135]. However, CD1a-mediated responses to specific lipid antigens differed between Tregs and effector T cells. While binding of CD1a-reactive effector T cell to CD1a is blocked by SM 24:1[134], CD1a-mediated Treg responses were unaffected by loading of CD1a with this lipid antigen. Whether this differential CD1a-mediated antigen recognition results from distinct TCR repertoires and/or differential CD1a binding sites, or from distinct TCR-mediated intracellular signalling needs to be further investigated. CD1a-reactive T cells are thought to have a variable TCR$\alpha\beta$ repertoire[34,133,134,138] and here

presented TCR sequencing of CD1a-reactive Treg clones suggests that Tregs show a similarly variable expression of α/β TCRs rather than invariant TCRs (Fig. 2.26). Single-cell TCR repertoire analysis of CD1a-rective Tregs and effector T cells could provide additional insights into similarities or differences of TCR usages and CD1a-TCR interactions.

Expanded polyclonal CD1a-reactive Tregs showed no CD1a-dependent secretion of inflammatory cytokines (Fig. 2.13), suggesting an immunosuppressive phenotype. Moreover, several Tregs clones showed an increased suppressive functionality upon CD1a stimulation, suggesting that Treg functionality may be modulated by CD1a engagement (Fig. 2.28; Fig. 2.30). However, CD1a-reactive Treg clones progressively lost Treg lineage marker expression (Fig. 2.17) and gained the ability to secrete inflammatory cytokines (Fig. 2.24). This was further increased in the presence of skewing cytokines such as IL-12 (Fig. 2.25), which is increased in psoriatic lesions[429] and has been shown to induce Tregs to shift towards a Th1 phenotype and produce IFNγ[410,430,431]. Similarly, *ex vivo* single-cell sequencing revealed that upon CD1a-stimulation, IL-10-secreting CD1a-reactive Tregs downregulate the expression of Treg lineage and suppressive markers (Fig. 3.11; Fig. 3.12; Fig. 3.14; Fig. 3.15). Further, many genes associated with Treg function were differentially regulated in these cells, suggesting impaired suppressive capacity. In line with skin Tregs and CD1a-reactive T cells showing a memory phenotype[26] (unpublished data, Ogg Lab), this modulation of Treg phenotype was particularly strong in effector/memory CD1a-reactive IL-10-secreting Tregs (Fig. 3.13). Upon CD1a stimulation, these Tregs further shifted towards a central/memory phenotype. Whether these transcriptional and phenotypic changes are temporary, result in permanent Treg plasticity towards a Th phenotype, or enable CD1a-reactive Tregs to use different or even previously undefined pathways to exert their suppressive function remains to be addressed. Therefore, additional functional studies of CD1a-reactive Tregs, i.e. using TCR-transduced primary Tregs or

CD1a-transgenic mouse models, are needed to further elucidate the role of CD1a-mediated Treg responses.

CD1a-reactive IL-10-secreting Tregs from individuals with psoriasis showed a similar shift towards a central/memory phenotype and transcriptional and phenotypic changes indicating loss of Treg phenotype and function as healthy controls (Fig. 3.13). Functional experiments assessing CD1a-mediated Treg responses will be needed to determine whether CD1a-reactive Tregs show comparable functional phenotypes in health and psoriasis or whether general Treg dysfunction seen in psoriasis (see 3.1.2 Regulatory T cells in psoriasis) extends to CD1a-reactive Tregs.

In healthy skin, where Tregs and CD1a-expressing APCs are spatially separated, CD1a-reactive Tregs may only infrequently encounter and interact with CD1a, thus limiting CD1a-reactive Treg responses (Fig. 5.1). It is further plausible that low levels of CD1a stimulation, through limited numbers of CD1a-expressing cells and missing exogenous antigen stimulation, may induce distinct CD1a-mediated Treg responses compared to the highly stimulating environment of *in vitro* models. However, in psoriatic skin, many immune cells infiltrate and CD1a-expressing DC subsets and LCs accumulate in the skin[177-179], leading to increased CD1a stimulation (Fig. 5.1). Further, CD1a antigens are enriched in skin inflammatory environments[400-404] and disruption of the skin barrier permits the presentation of exogenous CD1a antigens. This may lead to an increase in CD1a-mediated activation of Tregs, resulting in (partial) loss of Treg phenotype and function. Impaired Treg suppressive function may in turn lead to increased effector T cell proliferation and production of inflammatory cytokines, thereby exacerbating disease.

Interestingly, it was recently shown that CD1a preferentially captures very long chain fatty acid (VLCFA) sphingolipids, in particular SM 24:1, which block TCR binding of

CD1a-reactive effector T cells[134]. In contrast, the here presented data demonstrate that CD1a-reactive Tregs can functionally interact with CD1a loaded with such longer chain SMs (Fig. 2.14). VLCFA-SMs are enriched in the skin[659,660], and it is therefore plausible that in healthy skin CD1a can activate CD1a-reactive Tregs more efficiently than effector T cells. During skin inflammation however, accumulation of CD1a-presenting APCs[177-179] and increased variety and abundance of CD1a lipid antigens[400-404] result in a shift in CD1a antigen presentation that in turn may cause CD1a-mediated activation of both CD1a-reactive Tregs and effector T cells. When Treg responses are additionally dysfunctional, as commonly observed in skin inflammatory disease[416], CD1a-reactive effector T cell responses may dominate over CD1a-reactive Treg responses.

5.1.1 Future directions

Tregs are crucial to maintain immune homeostasis, and their dysfunction can cause severe autoimmune and inflammatory diseases[204-207]. It is therefore important to further investigate the functional role of CD1a-reactive Tregs to assess whether the observed changes in Treg phenotype are of transient nature and whether these changes go in hand with reduced suppressive functionality. The transduction of here identified CD1a-reactive TCRs into primary Tregs may aid in assessing Treg suppressive functionality, either by suppression assays in the presence or absence of CD1a blocking antibodies or by evaluating suppression of cytotoxic T cell function. Additionally, TCR-transduced Tregs could be used for adoptive Treg transfer experiments to investigate the functional response of CD1a-reactive Tregs in CD1a-transgenic mouse models.

Although only a small subpopulation of approximately 2% of expanded Tregs showed CD1a reactivity as measured by IL-10 secretion (Fig. 2.2; Fig. 3.2), it is possible that a higher frequency of Tregs may interact with CD1a. Investigating Treg production of other

immunosuppressive cytokines as well as expression of Treg activation markers in response to CD1a may add to the here presented findings. Moreover, the expression of CD1a on specific APCs in the skin may facilitate spatial proximity of CD1a-reactive Tregs and effector T cells, thus potentially providing a regulatory mechanism for CD1a-mediated effector T cell activation. Further, CD1a expression by skin-resident APCs may lead to an enrichment of CD1a-reactive Tregs in the skin compared to the periphery. Therefore, analysis of CD1a-reactive Treg frequency in the skin may provide additional insights.

The here presented single-cell sequencing analysis provides novel insights into the phenotype of CD1a-reactive Tregs and more comprehensive analysis is ongoing. Transcriptional network analysis may give further insights into the mechanisms driving the differences between different subpopulations and between CD1a-reactive Tregs in health and psoriasis. Moreover, trajectory analysis may elucidate the timings of IL-10, IL-22 and IFNγ secretion and help elucidate whether CD1a-reactive Tregs secreting different cytokines present distinct subpopulations. Such analysis also offers the opportunity to compare transcriptional changes in early and late activation states. The analysis of CD1a-reactive Tregs that show transcriptional upregulation of IL-10, IL-22 and/or IFNγ while not (yet) secreting the respective cytokine may help to further decipher changes early after Treg activation.

As tissue-resident Tregs differ from their counterparts in the periphery[301-305], the integration of publicly available skin Treg single-cell sequencing data sets will be important to elucidate similarities and differences between CD1a-reactive Tregs from peripheral blood and those residing in the skin. Spatial analysis of human or mouse skin may further give insights into the spatial proximity of CD1a-expressing APCs and Tregs within the skin. Moreover, it would be important to address how CD1a-reactive Tregs behave in the skin environment, as

here presented experiments were performed using highly stimulating *in vitro* assays. Studying CD1a-transgenic mouse models may elucidate the functional phenotype of CD1a-reactive Tregs in a more physiological environment and may also be used to study the functional role of CD1a-reactive Tregs in skin inflammation models.

CD1a-reactive Tregs may present a valuable target for skin inflammatory diseases, but more research is needed to further characterise this newly identified Treg subpopulation. Depending on the functional phenotype of CD1a-reactive Tregs, it may be beneficial to block or enhance CD1a-mediated Treg responses. The here presented findings suggest that the use of primary CD1a-reactive Tregs for therapeutic purposes may risk drifting to pro-inflammatory phenotypes, and so may require modifications to maintain regulatory function, for example through *Foxp3* transduction[599]. As an additional strategy, TCR editing of primary Tregs may allow focussing of a large Treg population to specific relevant antigens and tissues, such as the skin. The modulation of lipid availability for presentation by CD1a may further provide a therapeutic tool to differentially target CD1a-reactive Tregs and effector T cells.

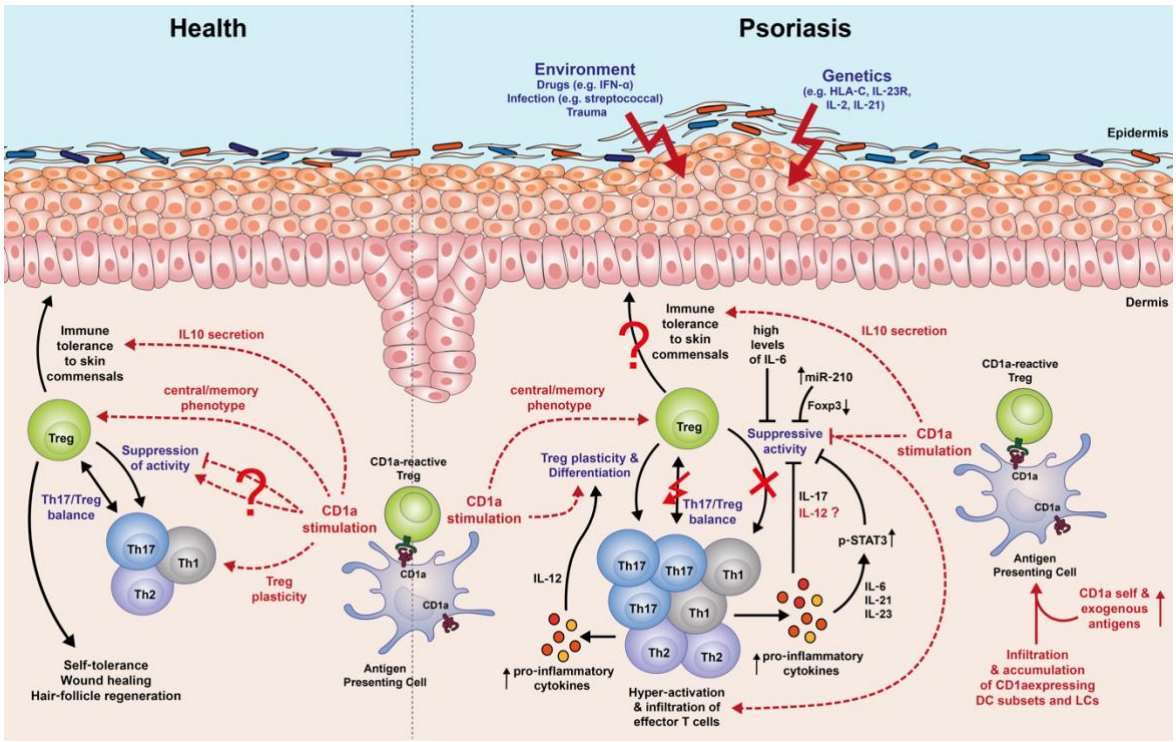

Fig. 5.1 Proposed model for CD1a-mediated modulation of Treg phenotype and function.
Tregs are important for skin immunity and homeostasis. In response to CD1a stimulation, Tregs can secrete the immunosuppressive cytokine IL-10 and may show CD1a-mediated increased suppressive capacity. However, IL-10-secreting CD1a-reactive effector/memory Tregs also undergo transcriptional and phenotypic changes that indicate (partial) loss of Treg phenotype and function. In addition, these Tregs shift towards a central/memory phenotype upon CD1a engagement. In healthy skin, CD1a-reactive Treg responses may be limited by spatial separation of CD1a-expressing antigen-presenting cells and Tregs. Low levels of CD1a stimulation, due to limited number of CD1a-expressing cells and missing exogenous antigen stimulation, may further elicit distinct CD1a-mediated Treg responses. In contrast, in psoriatic skin, CD1a-expressing DC subsets and LCs accumulate and CD1a antigens including exogenous antigens are enriched, resulting in increased CD1a stimulation. This may lead to an increase in CD1a-mediated Treg activation causing elevated loss of Treg phenotype and function as well as increased Treg plasticity towards Th phenotypes. Treg plasticity and dysfunction are further amplified by high levels of pro-inflammatory cytokines in psoriatic lesions, and subsequent reduction in the suppression of effector T cell responses further exacerbates disease. Adapted from Nussbaum *et al.* 2021, BJD[417].

5.2 Modulation of CD1a expression by butyrate and related fatty acids

CD1a-mediated T cell responses present an intriguing therapeutic target for treatment of skin inflammatory diseases, and lipid antigens that modulate CD1a-mediated immune responses can easily be formulated into skin preparations. FAs such as the SCFA butyrate have been shown to modulate CD1a expression in moDCs[201-203] and therefore may have therapeutic potential to inhibit CD1a-mediated immune responses. In mouse models missing CD1a expression, SCFAs have been shown to increase Treg numbers in the skin[634] and reduce imiquimod-induced inflammation in a model of psoriasis[635]. Further, SCFAs have been shown to restore impaired Treg function *in vitro*[635]. The experiments presented in this thesis aimed to investigate the effect of SCFAs and related molecules on moDC differentiation and CD1 expression as well as to determine the therapeutic potential of SCFAs and related molecules to modulate CD1a-mediated T cell responses. Butyrate and several structurally related FAs (6-phenylhexanoic acid, 8-phenyloctanoic acid and 9-decenoic acid) could be shown to inhibit acquisition of CD1a, CD1b and CD1c during *in vitro* moDC differentiation, while not affecting general moDC differentiation (Fig. 4.9; Fig. 4.10; Fig. 4.11). However, DCs and LCs can express high levels of CD1a[7,65,66] and CD1a cell surface expression was only partially inhibited by the tested compounds (Fig. 4.9). Although several FAs are CD1a ligands[34,88,166], neither SCFAs nor related FAs changed the isoelectric point of CD1a, indicating that they may not act as CD1a ligands (Fig. 4.6; Fig. 4.12). Moreover, CD1a-mediated effector T cell responses were unchanged upon co-culture with FA-treated moDCs (Fig. 4.13; Fig. 4.14), suggesting that SCFAs and related compounds cannot modulate CD1a expression sufficiently to influence CD1a-mediated T cell responses.

While blocking of CD1a expression presents a viable therapeutic option, CD1a also plays a role in maintaining skin immune homeostasis[150,367] and inhibition of CD1a expression will need to be investigated for any safety signals. A SNP causing CD1a deficiency has been associated with susceptibility to tuberculosis[158,159], but limited data are available on the clinical presentation of patients with CD1a deficiency. While it is possible that targeting of CD1a expression may not cause major side effects, more targeted approaches to modulate CD1a-mediated inflammatory responses may present safer and achievable alternatives. A promising approach is the modulation of CD1a-mediated T cell responses *via* lipid antigens that bind to CD1a and regulate CD1a-TCR interactions, through 'absence of interference' or CD1a conformational changes. Differential recognition of distinct lipid antigens by CD1a-reactive Tregs and effector T cells may further allow the specific targeting of either or both Tregs and effector T cells.

Chapter 6 Materials and Methods

6.1 Patients and samples

All study participants gave fully informed written consent. Blood samples from healthy adult donors or individuals with psoriasis were collected in the WIMM (University of Oxford, Oxford, UK) under Human Tissue Act (HTA) licence number 12433 or in the Department of Dermatology, Churchill Hospital (Radcliffe Hospitals NHS Trust, Oxford, UK) under local ethics approval (14/SC/0106, NRES). Leukocyte cones were obtained from the NHSBT Oxford Blood Donor Centre (customer nr. T266). Samples were stored anonymously and in compliance with HTA standards.

For donor information for '3.2.1 *Ex vivo* analysis of CD1a-autoreactive Tregs in health and psoriasis' and '3.2.2 Single-cell analysis of CD1a-reactive Tregs' see Table 6.1.

Table 6.1 Psoriasis patient and healthy control information.
PASI, psoriasis area and severity index

	Characteristic	Psoriasis Patients	Healthy Controls
***ex vivo* analysis of CD1a-autoreactive Tregs in health and psoriasis**	Number of samples	10	10
	Age (mean ± SD)	52.00 ± 17.26	50.60 ± 17.98
	Sex (nr.)		
	Female	2	8
	Male	8	2
	PASI score (mean ± SD)	4.80 ± 2.62	-
10x	Number of samples	4	3
	Age (mean ± SD)	39.25 ± 13.05	29.33 ± 2.52
	Sex (nr.)		
	Female	1	2
	Male	3	1
	PASI score (mean ± SD)	3.75 ± 1.89	-

6.2 Reagents and antibodies

6.2.1 Media and buffers

Table 6.2 Cell culture media.

DMSO, dimethyl sulphoxide; FBS, fetal bovine serum; HEPES, N-2-hydroxyethylpiperazine-N-2-ethane sulfonic acid; NEAA, non-essential amino acids

Media	Components	Supplier
R10 medium	RPMI-1640 medium	MilliporeSigma or Life Technologies
	FBS (10%)	MilliporeSigma
	L-glutamine [2mM]	Life Technologies
	Penicillin [100U/ml]	Life Technologies
	Streptomycin [100µg/ml]	Life Technologies
	HEPES [10mM]	Life Technologies
	Sodium pyruvate [1mM]	Life Technologies
	NEAA (1x)	Life Technologies
	β-mercaptoethanol [50µM]	Life Technologies
T cell medium	RPMI-1640 medium	MilliporeSigma or Life Technologies
	Human AB serum (10%)	MilliporeSigma
	L-glutamine [2mM]	Life Technologies
	Penicillin [100U/ml]	Life Technologies
	Streptomycin [100µg/ml]	Life Technologies
	HEPES [10mM]	Life Technologies
	Sodium pyruvate [1mM]	Life Technologies
	NEAA (1x)	Life Technologies
	β-mercaptoethanol [50µM]	Life Technologies
Treg medium	RPMI-1640 medium	MilliporeSigma or Life Technologies
	Human AB serum (10%)	Pan-Biotech UK Ltd
	L-glutamine [2mM]	Life Technologies
	Penicillin [100U/ml]	Life Technologies
	Streptomycin [100µg/ml]	Life Technologies
	Sodium pyruvate [1mM]	Life Technologies
Freezing solution	FBS	MilliporeSigma
	DMSO (10%)	MilliporeSigma
Freezing solution (Psoriasis samples and corresponding controls)	Cryostor CS10	Stemcell Technologies

Table 6.3 Buffers.

EDTA, ethylenediaminetetraacetic acid; FBS, fetal calf serum; PBS, phosphate-buffered saline.

Buffer	Components	Supplier
MACS buffer	PBS	OXOID
	0.5% FBS	MilliporeSigma
	EDTA [2 mM]	Invitrogen
Flow cytometry fixation buffer	PBS	ThermoFisher Scientific
	4% formaldehyde solution	ThermoFisher Scientific
ELISA wash buffer	PBS	ThermoFisher Scientific
	0.05% Tween20	VWR International

6.2.2 Flow cytometry antibodies

Cells were labelled according to the antibody panels described below and with Fixable Viability Dyes (BioLegend).

Table 6.4 Treg flow cytometry antibodies.

	Target	Clone	Fluoro-chrome	Dilution	Supplier
Treg FACS sorting	CD3	OKT3	PE	1:100	BioLegend, 317308
	CD4	OKT4	FITC	1:100	BioLegend, 317408
	CD25	M-A251	APC	1:50	BioLegend, 356110
	CD127	A019D5	PE/Cy7	1:50	BioLegend, 351320
Treg clone FACS sorting	CD3	SK7	BV785	1:100	BioLegend, 344842
	CD4	OKT4	FITC	1:100	BioLegend, 317408
	CD25	M-A251	APC	1:50	BioLegend, 356110
	CD127	A019D5	PE/Cy7	1:50	BioLegend, 351320
	IL-10 secretion	-	PE	1:10	Miltenyi Biotec
Treg panel (1)	CD3	SK7	BV785	1:100	BioLegend, 344842
	CD4	OKT4	FITC	1:100	BioLegend, 317408
	CD25	M-A251	APC	1:100	BioLegend, 356110
	CD127	A019D5	PE/Cy7	1:100	BioLegend, 351320
	Foxp3	206D	PE	1:50	BioLegend, 320108
Treg panel (2)	CD3	SK7	BV785	1:100	BioLegend, 344842
	CD4	OKT4	FITC	1:100	BioLegend, 317408
	CD25	M-A251	APC	1:100	BioLegend, 356110
	CD127	A019D5	PE/Cy7	1:100	BioLegend, 351320
	Foxp3	206D	PE	1:50	BioLegend, 320108
	CTLA-4 (intracellular)	BNI3	BV605	1:100	BioLegend, 369610
	GITR	108-17	PerCP/ Cy5.5	1:50	BioLegend, 371218

Treg panel (3)	CD3	SK7	BV785	1:100	BioLegend, 344842
	CD4	OKT4	BV650	1:100	BioLegend, 317436
	CD25	M-A251	BV421	1:100	BioLegend, 356114
	CD127	A019D5	AF700	1:100	BioLegend, 351344
	TCR$\alpha\beta$	IP26	APC/Cy7	1:50-1:100	BioLegend, 306728
	TCR$\gamma\delta$	B1	PE/Cy7	1:50-1:100	BioLegend, 331222
	Foxp3	206D	PE	1:50	BioLegend, 320108
Secretion assay (1)	CD3	SK7	BV785	1:100	BioLegend, 344842
	CD4	OKT4	BV650	1:100	BioLegend, 317436
	CD25	M-A251	BV421	1:100	BioLegend, 356114
	CD127	A019D5	PE/Cy7	1:100	BioLegend, 351320
	Secretion	-	PE	1:10	Miltenyi Biotec
	Secretion	-	APC	1:10	Miltenyi Biotec
	CFSE/GFP	-	Green/GFP	5µM	BioLegend
Secretion assay (2)	CD3	SK7	BV785	1:100	BioLegend, 344842
	CD4	OKT4	BV650	1:100	BioLegend, 317436
	CD25	M-A251	BV421	1:100	BioLegend, 356114
	CD127	A019D5	AF700	1:100	BioLegend, 351344
	TCR$\alpha\beta$	IP26	APC/Cy7	1:100	BioLegend, 306728
	TCR$\gamma\delta$	B1	PE/Cy7	1:100	BioLegend, 331222
	Secretion	-	PE	1:10	Miltenyi Biotec
	Secretion	-	APC	1:10	Miltenyi Biotec
	CFSE/GFP	-	Green/GFP	5µM	BioLegend
Secretion assay (3) – 10x	CD3	SK9	AF700	1:100	BioLegend, 344822
	CD4	OKT4	BV785	1:100	BioLegend, 317441
	CD25	M-A251	BV421	1:100	BioLegend, 356114
	CD127	A019D5	PE/Cy7	1:100	BioLegend, 351320
	Secretion IL-10		PE	1:100	Miltenyi Biotec
	Secretion IFNγ	-	APC	1:10	Miltenyi Biotec
	Secretion IL-22	-	(Biotin)	1:10	Miltenyi Biotec
	CFSE	-	Green	5µM	BioLegend
Suppression assay	CD3	SK7	BV785	1:100	BioLegend, 344842
	CD4	OKT4	FITC	1:100	BioLegend, 317408
	CD8	SK1	APC	1:100	BioLegend, 344722
	Tag-it Violet	-	Violet	1µM	BioLegend
Suppression assay (K562 co-culture)	CD3	SK9	AF700	1:100	BioLegend, 344822
	CD4	OKT4	BV650	1:100	BioLegend, 317436
	CD8	SK1	PerCP/ Cy5.5	1:100	BioLegend, 344710
	CD25	M-A251	BV785	1:100	BioLegend, 356140
	CD127	A019D5	PE/Cy7	1:100	BioLegend, 351320
	Foxp3	206D	PE/Dazzle	1:50	BioLegend, 320126
	CellTrace Red	-	Red	5µM	ThermoFisher Scientific
	CFSE	-	Green	5µM	BioLegend
	Tag-it Violet	-	Violet	1µM	BioLegend
	CD4	OKT4	BV650	1:100	BioLegend, 317436

Cytotoxicity assay	CD8	SK1	PerCP/ Cy5.5	1:100	BioLegend, 344710
	Annexin V	-	APC	1:50	BioLegend, 640941
	CellTox reagent	-	Green	1x	Promega
	Tag-it Violet	-	Violet	5µM	BioLegend
Klickmer staining	CD3	UCHT1	BV785	1:100	BioLegend, 300472
	CD4	OKT4	BV650	1:100	BioLegend, 317436
	CD25	M-A251	BV421	1:100	BioLegend, 356114
	CD127	A019D5	PE/Cy7	1:100	BioLegend, 351320
	Klickmer	-	APC	1:4	Immudex
Isotype controls	Mouse IgG1	MOPC-21	PE	1:33	BioLegend, 400140
	Mouse IgG2a	MOPC-173	BV605	1:67	BioLegend, 400269
	Mouse IgG1	MOPC-21	PE/Dazzle	1:125	BioLegend, 400175

Table 6.5 MoDC flow cytometry antibodies.

	Target	Clone	Fluorochrome	Dilution	Supplier
Fatty acid screening panel	CD1a	HI149	PerCP/Cy5.5	1:100	BioLegend, 300130
	CD11c	3.9	BV421	1:100	BioLegend, 301628
	CD14	M5E2	PE	1:100	BioLegend, 301806
	DC-SIGN	9E9A8	APC	1:100	BioLegend, 330108
	HLA-DR	L243	FITC	1:100	BioLegend, 307604
MoDC (1)	CD1a	HI149	BV421	1:100	BioLegend, 300128
	CD11c	Bu15	PerCP	1:100	BioLegend, 337234
	CD14	63D3	APC-H7	1:100	BioLegend, 367107
	CD40	5C3	BV650	1:100	BioLegend, 334337
	CD80	L307.4	BV711	1:100	BD, 740801
	CD83	HB15e	PE/Cy7	1:100	BioLegend, 305325
	HLA-DR	L243	FITC	1:100	BioLegend, 307604
	Langerin	10E2	PE	1:100	BioLegend, 352204
	PDL-1	29E.2A3	APC	1:200	BioLegend, 329708
MoDC (2)	CD1a	HI149	AF700	1:100	BioLegend, 300120
	CD1b	SN13 (K5-1B8)	FITC	1:100	BioLegend, 329106
	CD1c	L161	BV785	1:100	BioLegend, 331544
	CD1d	51.1	PE/Cy7	1:100	BioLegend, 350310
	CD11c	B-ly6	BUV395	1:100	BD, 563787
	CD14	M5E2	BV605	1:100	BioLegend, 301834
	CD69	FN50	BUV563	1:100	BD, 748764
	CD83	HB15e	BUV737	1:100	BD, 612823
	CD86	IT2.2	PE/Dazzle	1:400	BioLegend, 305434
	DC-LAMP	31B	APC	1:100	Invitrogen, 17-2089-41
	DC-SIGN	9E9A8	PerCP/Cy5.5	1:100	BioLegend, 330110
	HLA-ABC	W6/32	PB	1:1000	BioLegend, 311418
	HLA-DR	L243	BV650	1:100	BioLegend, 307650
	Langerin	10E2	PE	1:100	BioLegend, 352204

MoDC (3) - fatty acid validation & dose-response	CD1a	HI149	AF700	1:100	BioLegend, 300120
	CD1b	SN13 (K5-1B8)	FITC	1:100	BioLegend, 329106
	CD1c	L161	BV785	1:100	BioLegend, 331544
	CD1d	51.1	PE/Cy7	1:100	BioLegend, 350310
	CD11c	B-ly6	BUV395	1:100	BD, 563787
	CD14	M5E2	BV605	1:100	BioLegend, 301834
	CD83	HB15e	BUV737	1:100	BD, 612823
	CD86	IT2.2	PE/Dazzle	1:400	BioLegend, 305434
	DC-LAMP	31B	APC	1:100	Invitrogen, 17-2089-41
	DC-SIGN	9E9A8	PerCP/Cy5.5	1:100	BioLegend, 330110
	HLA-ABC	G46-2.6	BUV563	1:100	BD, 741378
	HLA-DR	L243	BV650	1:100	BioLegend, 307650
	Langerin	10E2	PE	1:100	BioLegend, 352204

6.2.3 Blocking antibodies

Table 6.6 Blocking antibodies and isotype controls.

	Target	Clone	Final blocking concentration	Supplier
anti-human	CD1a	HI149	10µg/ml	BioLegend, 300102
	CD1a	OKT6	10µg/ml	Purified in-house
	CD1a	SK9	10µg/ml	BioLegend, 344902
	HLA-ABC	W6/32	10µg/ml	BioLegend, 311441
	HLA-DR	L243	10µg/ml	BioLegend, 307666
Isotype controls	Mouse IgG1	MOPC-21	10µg/ml	BioLegend, 400197
	Mouse IgG2a	MOPC-173	10µg/ml	BioLegend, 400224
	Mouse IgG2b	MG2b-57	10µg/ml	BioLegend, 401202

6.2.4 Recombinant proteins and co-stimulation reagents

Table 6.7 Recombinant proteins and co-stimulation reagents.

rh, recombinant human.

Cytokine	Supplier
anti-human CD3 (clone HIT3a)	BioLegend, 300314
anti-human CD3 (clone OKT3)	BioLegend, 317326
anti-human CD28 (clone CD28.2)	BioLegend, 302934
anti-human CD11a (clone HI111)	BioLegend, 301234
anti-human CD137 (clone 4B4-1)	BioLegend, 309841
rhGM-CSF	BioLegend, 572905
rhIL-1β	BioLegend, 579408
rhIL-2	BioLegend, 589108
rhIL-4	BioLegend, 574008
rhIL-6	BioLegend, 570808
rhIL-7	BioLegend, 581904
rhIL-12	BioLegend, 573006
rhIL-15	BioLegend, 570308
rhIL-18	BioLegend, 592106
rhIL-21	BioLegend, 571202
rhIL-27	BioLegend, 589202
rhIL-33	BioLegend, 581808
rhTGF-β1	BioLegend, 781804
rhTNFα	BioLegend, 570108

6.2.5 Lipids and fatty acids

Table 6.8 Lipids.

CHAPS, 3-[(3-cholamidopropyl) dimethylammonio]-1-propanesulfonate hydrate; PBS, phosphate-buffered saline.

Lipid	Solvent	Supplier
18:1 Lyso PC (1-oleoyl-2-hydroxy-sn-glycero-3-phosphocholine)	0.5% CHAPS (in PBS)	Avanti, 845875
18:1 SM (d18:1/18:1(9Z)) (N-oleoyl-D-erythro-shpingosylphosphorylcholine)	0.5% CHAPS (in PBS)	Avanti, 860587
24:0 SM (N-lignoceroyl-D-erythro-sphingosylphosphorylcholine)	0.5% CHAPS (in PBS)	Avanti, 860592
24:1 SM (N-nervonoyl-D-erythro-sphingosylphosphorylcholine)	0.5% CHAPS (in PBS)	Avanti, 860593
Urushiol (C15:2) (3-(8Z,11Z-Pentadecadienyl)-1,2-benzenediol)	DMSO	PhytoLab, PHL80181

Table 6.9 Fatty acids.

CHAPS, 3-[(3-cholamidopropyl) dimethylammonio]-1-propanesulfonate hydrate; PBS, phosphate-buffered saline.

Lipid	Solvent	Supplier
Sodium butyrate (≥ 98.5%)	PBS / 0.5% CHAPS in PBS	Sigma-Aldrich
Butyric acid (≥ 99%)	PBS / 0.5% CHAPS in PBS	Sigma-Aldrich
Acetic acid (≥ 99%)	PBS / 0.5% CHAPS in PBS	Sigma-Aldrich
Sodium acetate (≥ 99%)	PBS / 0.5% CHAPS in PBS	Sigma-Aldrich
Propionic acid (≥ 99%)	PBS / 0.5% CHAPS in PBS	Sigma-Aldrich
Sodium propionate (≥ 99%)	PBS / 0.5% CHAPS in PBS	Sigma-Aldrich
8-phenyloctanoic acid	DMSO	ChemCruz
6-phenylhexanoic acid (98%)	PBS / 0.5% CHAPS in PBS	Sigma-Aldrich
8-hydroxyoctanoic acid (98%)	PBS / 0.5% CHAPS in PBS	Sigma-Aldrich
9-decenoic acid	PBS / 0.5% CHAPS in PBS	Sigma-Aldrich

Table 6.10 Fatty acids structurally related to butyrate.

Compounds were kindly provided by Prof Gurdyal S. Besra (University of Birmingham, UK).

1-adamantaneacetic acid	4-pentynoic acid	DL-2-phenylpropionic acid
1-adamantanecarboxylic acid	4-phenylbutyric acid	methoxyphenylacetic acid
2-methylhexanoic acid	6-aminocaproic acid	o-toluic acid
2-phenylbutyric acid	6-phenylhexanoic acid	octanoic acid
3-methyl-2-phenyl-valeric acid	8-hydroxyoctanoic acid	para-aminobenzoic acid
3,3,3-triphenylpropionic acid	8-nonenoic acid	para-aminosalicylic acid
3(2-furyl)propanoic acid	8-phenyloctanoic acid	phenylacetic acid
4-aminobutyric acid	9-decenoic acid	pimelic acid
4-imidazoleacetic acid	anthranilic acid	tolylacetic acid
4-pentenoic acid	dimethoxyphenylbutyric acid	triphenylacetic acid

6.3 CD1a

The here used CD1a was generated in-house by purification of CD1a from HEK293T cells stably transfected with CD1a (kindly provided by Demin Li; purified by Jessica Ng and Dr Yi-Ling Chen). For CD1a-Klickmer staining (see 6.10 CD1a-Klickmer staining), CD1a obtained from the NIH Tetramer Core Facility was used. Both versions of CD1a are very similar in structure but have minor differences in CD1a sequence[661,662], as highlighted below.

CD1a sequence - Demin Li

PLSFHV**T**WIASFYNHSWKQNLVSGWLSDLQTHTWDSNSSTIVFL**C**PWSRGNFSNEEWKELETLF
RIRTIRSFEGIRRYAHELQFEYPFEIQVTGGCELHSGKVSGSFLQLAYQGSDFVSFQNNSWLPYPV
AGNMAKHFCKVLNQNQHENDITHNLLSDTCPRFILGLLDAGKAHLQRQVKPEAWLSHGPSPGPG
HLQLVCHVSGFYPKPVWVMWMRGEQEQQGTQRGDILPSADGTWYLRATLEVAAGEAADLSCRV
KHSSLEGQDIVLYWEHHSSDP

CD1a sequence - NIH

LKEPLSFHV**I**WIASFYNHSWKQNLVSGWLSDLQTHTWDSNSSTIVFL**W**PWSRGNFSNEEWKELE
TLFRIRTIRSFEGIRRYAHELQFEYPFEIQVTGGCELHSGKVSGSFLQLAYQGSDFVSFQNNSWLP
YPVAGNMAKHFCKVLNQNQHENDITHNLLSDTCPRFILGLLDAGKAHLQRQVKPEAWLSHGPSP
GPGHLQLVCHVSGFYPKPVWVMWMRGEQEQQGTQRGDILPSADGTWYLRATLEVAAGEAADL
SCRVKHSSLEGQDIVLYWEHHSSVVDTTAPSAQL

6.3.1 CD1a biotinylation

CD1a was biotinylated with BirA Biotin-Protein Ligase kit buffers (Avidity) and 2.5µg BirA ligase (abcam) per 10nmol CD1a. Post biotinylation, BirA was removed by Pierce Glutathione Spin Columns (ThermoFisher Scientific). Remaining salts and substrates were removed by washing with phosphate buffered saline (PBS) using 30kDa Vivaspin columns (Sartorius).

6.3.2 CD1a antigen loading

CD1a was incubated with the respective antigen at > 100-fold antigen excess overnight at room temperature (RT). For a list of antigens and respective solvents, see '6.2.5 Lipids and fatty acids'. CD1a loaded with the respective solvents was used as control. Antigen-loaded CD1a was stored at 4°C and used within 1 week.

6.4 Cell isolation and culture

6.4.1 K562 cell culture

K562 cells, a myelogenous leukaemia cell line, modified to constitutively express CD1a (K562-CD1a) or an empty vector control (K562-EV) have been described by de Jong *et al.*[150] (gift from Prof Branch Moody, Harvard). Subsequently, the K562 cells were transduced to stably expressing GFP. K562 cells were cultured in R10 medium supplemented with 200µg/ml geneticin (G418; Life Technologies) and split every 2-3 days, depending on confluency and growth rate. Before co-culture experiments, K562 cells were cultured in the absence of geneticin for one or more days.

6.4.2 Isolation of immune cells from human blood

PBMCs were isolated by density gradient centrifugation. Heparinised blood or leukocyte cones were diluted 1:1 and 1:15 with RPMI-1640 medium, respectively. Diluted samples were layered on top of Lymphoprep density gradient solution (Stemcell Technologies) and centrifuged for 20min at 800g with the breaks off. The PBMC layer was collected and washed twice with R10 medium, spinning at 600g for 10min and 400g for 5min, and resuspended in R10 medium until further use. Alternatively, SepMate PBMC Isolation Tubes (Stemcell Technologies) were used. Diluted samples were layered on top of Lymphoprep solution and centrifuged for 10min at 1200g. PBMCs were collected and

washed twice with R10 medium, spinning at 800g for 8min and 300g for 5min, and resuspended in R10 medium until further use.

6.4.3 Isolation of immune cell subsets by MACS

$CD3^+$ T cells, $CD14^+$ monocytes and $CD25^+$ cells were isolated from PBMCs by magnetic-activated cell sorting (MACS) using CD3, CD14 or CD25 II MACS MircoBeads, respectively. PBMCs were resuspended in 80µl (for CD3 and CD14) or 90µl (for CD25) MACS buffer per 10^7 cells. 20µl (for CD3 or CD14) or 10µl (for CD25) MicroBeads per 10^7 cells were added and cell suspensions were incubated for 15min at 4°C. Cells were washed by adding MACS buffer (>2ml per 10^7 cells) and centrifugation at 300g for 10min. Cells were resuspended in 500µl MACS buffer per 10^7 cells. LS columns were placed on a MACS magnet and pre-rinsed with 3ml MACS buffer. Cell suspensions were passed through LS columns and columns were washed 3x with 3ml MACS buffer. Columns were removed from the magnet, placed onto a collection tube, and magnetically labelled cells were flushed out by adding 5ml MACS buffer onto the column and applying a plunger. The eluted cells were washed twice with R10 medium and resuspended in R10 medium until further use.

6.4.4 T cell culture

$CD3^+$ T cells, isolated from peripheral blood by MACS separation, were cultured in 48-well plates at a density of $2x10^6$ cells/well using T cell medium supplemented with 200IU/ml IL-2.

6.4.5 Treg isolation and expansion

6.4.5.1 Treg isolation

Tregs were isolated from PBMCs by MACS separation of $CD25^+$ cells and subsequent FACS sorting of $CD3^+CD4^+CD25^+CD127^{low/-}$ cells. MACS-isolated $CD25^+$ cells were incubated with 20% human FcR Blocking Reagent (Miltenyi Biotec) diluted in MACS buffer for 10min at 4°C before staining with cell surface anti-human antibodies (Table 6.4). FACS sorting was performed using the SH800S or MA900 cell sorters (Sony). The gating strategy is depicted in Fig. 6.1. In brief, forward and side scatter area and height were used to gate on $CD25^+$ cells and exclude doublets. Dead cells were excluded by gating on fixable viability dye-negative cells. Live cells were selected for $CD3^+CD4^+$ cells, followed by gating on $CD25^+CD127^{low/-}$ cells. Sorted Tregs were collected in Treg medium supplemented with 1,000IU/ml IL-2. Post sorting, the cells were washed with Treg medium supplemented with 1,000IU/ml IL-2 before use.

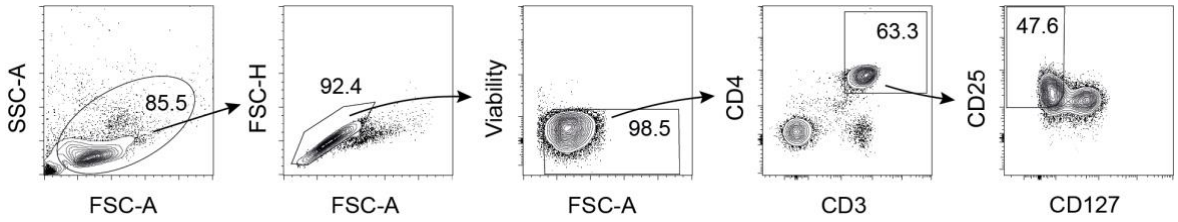

Fig. 6.1 FACS sorting strategy to isolate Tregs.
Flow cytometry gating strategy for Tregs using the cell surface markers CD3, CD4, CD25 and CD127. Tregs were defined as single live $CD3^+CD4^+CD25^+CD127^{low/-}$ cells. Arrows indicate gating on the parent population. Numbers indicate the percentage of cells in or next to the respective gate.

6.4.5.2 Treg expansion

FACS-sorted Tregs were plated at 100,000 cells per 96-round-bottom well in Treg medium supplemented with 1,000IU/ml IL-2. Dynabeads Human T-Activator CD3/28 beads (αCD3/αCD28 beads; ThermoFisher Scientific) were added at a bead:Treg ratio of 3:1. The cells were split 1:2 every 1-2 days starting from day 3-4 of expansion, using Treg medium supplemented with 1,000IU/ml IL-2. On day 7 of expansion, αCD3/αCD28 beads were removed and Tregs were resuspended in fresh Treg medium supplemented with 1,000IU/ml IL-2 and αCD3/αCD28 beads at a 1:1 bead:Treg ratio. Tregs were plated into 24-well plates at 1-2x10^6 cells/well. Tregs were split every 1-2 days, supplementing with fresh Treg medium containing 1,000IU/ml IL-2. On day 12-14 of expansion, αCD3/αCD28 beads were removed and Tregs were rested for 1-2 days in Treg medium supplemented with 200IU/ml IL-2 before use. Alternatively, Tregs were frozen on day 7 or 10 of expansion. Once thawed, Tregs were re-stimulated with αCD3/αCD28 beads at a 1:1 bead:Treg ratio for 3 days in Treg medium containing 1,000IU/ml IL-2. Beads were removed and cells rested in Treg medium supplemented with 200IU/ml IL-2 for 1 day before use.

6.4.6 Generation and culture of CD1a-reactive Treg clones

Tregs from healthy donors were isolated and expanded for 7 days (see 6.4.5.1 Treg isolation and 6.4.5.2 Treg expansion). αCD3/αCD28 beads were removed and Tregs were rested in Treg medium supplemented with 200IU/ml IL-2 overnight. Tregs were stimulated with CD1a using CD1a-coated beads (see 6.5.2 Cell-free stimulation system) at a ratio of 1:1 Treg:bead in 96-round-bottom wells using R10 medium supplemented with 20-200IU/ml IL-2 and 2.5µg/ml anti-CD11a for 4-6h. CD1a used for stimulation contained either endogenous lipids (for donor 30 and 32), or was loaded with LPC (for donor 96; see 6.3.2 CD1a antigen loading). Post CD1a stimulation, an IL-10 secretion assay was performed (see

6.7.2 Secretion Assay) and cells were stained for secretion of IL-10 and Treg lineage markers (Table 6.2). $CD3^+CD4^+CD25^+CD127^{low/-}$ cells that stained positive for IL-10 secretion were single-cell FACS sorted (Fig. 2.15) into 96-round-bottom plates containing Treg medium supplemented with 1,000IU/ml IL-2. Treg clones were expanded using irradiated feeder cells and Treg medium containing 1,000IU/ml IL-2. Feeders were prepared from two irradiated B cell lines (CP and DG; $0.2x10^6$ cells/ml each) and irradiated PBMCs from two donors ($1x10^6$ cells/ml each). The feeding mix was supplemented with 1,000IU/ml IL-2, 50ng/ml anti-CD3 (clone OKT3; BioLegend) and 1x phytohemagglutinin-L (PHA-L, Life Technologies). Immediately after sorting, 100µl feeders were added to each well. To half of Treg clones from donor 96, 500 beads/well αCD3/αCD28 beads were added as additional stimulation. During expansion, Treg clones were split using Treg medium containing 1000IU/ml IL-2. Treg clones were re-stimulated every 2-4 weeks using 5-10ml feeders per $1x10^6$ Tregs.

6.4.7 Monocyte-derived dendritic cell differentiation

MoDCs were differentiated from circulating $CD14^+$ monocytes. For this, $CD14^+$ monocytes were cultured in R10 medium supplemented with 100ng/ml GM-CSF and 10-20ng/ml IL-4 for 4-6 days. Cells were cultured in non-treated flat-bottom plates (ThermoFisher Scientific) at $1x10^6$ cells/well in 24-well plates, $0.6x10^6$ cells/well in 48-well plates or $0.17x10^6$ cells/well in 96-well plates. Half of the medium was replaced with fresh R10 medium containing 100ng/ml GM-CSF and 10-20ng/ml IL-4 on day 2-3 of differentiation. Differentiation and cell surface marker expression were assessed by flow cytometry analysis of moDC markers (Table 6.5).

6.5 CD1a stimulation systems

6.5.1 Antigen-presenting cell system using K562 cells

K562-CD1a cells express only low levels of HLA class I and no cell surface HLA-DR; therefore, they present a suitable model to study the role of CD1a in a donor-independent manner. To load K562-expressed CD1a with antigens of interest, K562 cells were plated into 24-well plates at 1-1.5x10^6 cells/well in R10 medium. The respective dissolved antigens were added to the culture and incubated for 16-24h. K562 cells were washed 3x with R10 medium before use. For CD1a blocking experiments, K562 cells were pre-incubated for 1h with 20µg/ml anti-CD1a or the respective isotype control (Table 6.6). The final concentration of blocking antibodies and isotype controls during K562 co-culture experiments was 10µg/ml. To differentiate between K562 and target cells in flow cytometry analysis, K562 cells were either stained with Proliferation and Cell Tracking Dyes (BioLegend) before use, or K562 cells stably expressing GFP were used.

6.5.2 Cell-free stimulation system using CD1a-coated beads

CD1a-coated beads were used to study CD1a stimulation in the absence of other APC-mediated stimulatory factors. For this, PureProteome Streptavidin Magnetic Beads (Millipore) were washed twice with MACS buffer and resuspended in 100µl MACS buffer containing 0.05-0.32mg/ml biotinylated CD1a (see 6.3.1 CD1a biotinylation) per 10^6 beads. Beads were incubated rotating overnight at 4°C. After washing 3x with MACS buffer, beads were resuspended at 1-2x10^6 beads/ml in R10 medium. For CD1a blocking, anti-CD1a antibody or isotype control (Table 6.6) were added at 20µg/ml and beads were incubated rotating overnight at 4°C. The final concentration of blocking antibodies and isotype controls during bead stimulation experiments was 10µg/ml. Beads were stored at 4°C and used within 2 days of CD1a-coating.

6.6 CD1a stimulation of Tregs

6.6.1 CD1a stimulation of Tregs for gene expression analysis

Tregs were co-cultured with CD1a-coated beads, using empty beads as control, at a 1:1 ratio in R10 medium containing 200IU/ml IL-2 and 2.5µg/ml anti-CD11a. Cells were harvested after 2h and 4h incubation, beads were removed, and cells were lysed for gene expression analysis (see 6.7 Analysis of gene expression).

6.6.2 CD1a stimulation of Tregs for secretion assays

Tregs were either stimulated with K562-CD1a cells or CD1a-coated beads (see 6.5 CD1a stimulation systems). Unless otherwise indicated, R10 medium containing 200IU/ml IL-2 and 2.5µg/ml anti-CD11a was used. Tregs were stimulated for 4-6h, upon which they were harvested, washed with R10 medium, and used for secretion assays (see 6.7.2 Secretion Assay). For K562 cell stimulation, K562 cells were plated to confluently cover the well surface area ($0.25x10^6$ and $0.5x10^6$ cells for 96- and 48-flat bottom wells, respectively). For 96-flat bottom wells, $0.1x10^6$ Tregs were added to each well; for 48-wells, up to $1x10^6$ Tregs were added per well. For bead stimulation, empty or CD1a-coated beads were added to Tregs at a ratio of 1:1 in 96-round-bottom plates ($0.1\text{-}0.2x10^6$ Tregs/well).

For secretion assays in the presence of skewing cytokines, R10 culture medium containing 200IU/ml IL-2 and 2.5µg/ml anti-CD11a was further supplemented with the following cytokines: 5ng/ml IL-1β and IL-12 for GM-CSF and IL-17A secretion assays, 20ng/ml IL-4 and IL-33 for IL-13 secretion assays, 5ng/ml IL-6 and TNFα for IL-22 secretion assays, and 5ng/ml IL-12 and IL-18 for IFNγ secretion assays.

6.6.3 CD1a stimulation of Tregs for LEGENDplex

Supernatants were obtained from Treg clones that were either cultured alone or in the presence of K562-EV or K562-CD1a cells. Cells were cultured in 96-flat-bottom wells ($0.1x10^6$ Tregs/well and $0.25x10^6$ K562 cells/well) using R10 medium containing 200IU/ml IL-2 and 2.5µg/ml anti-CD11a. Supernatants were harvested after 24h and stored at -80°C until use.

6.6.4 CD1a stimulation of Tregs for suppression assays

Tregs were pre-stimulated with K562 cells or beads for 6-24h before the suppression assay. For K562 cell stimulation, Tregs were co-cultured with irradiated K562-EV or K562-CD1a cells at a ratio of 2:1 Treg:K562 in 48-well plates using Treg medium supplemented with 200IU/ml IL-2. Treg numbers were quantified by counting Treg-sized cells, excluding larger K562 cells. For pre-stimulation with beads, Tregs were cultured with empty or CD1a-coated beads at a ratio of 1:1 Treg:bead in 96-round-bottom wells in Treg medium containing 200IU/ml IL-2 and 2.5µg/ml anti-CD11a. Beads were removed before the suppression assay. To quantify Treg suppressive capacity, Tregs were co-cultured with autologous PBMCs and suppression was calculated based on inhibition of $CD4^+$ and $CD8^+$ T cell proliferation as described in '6.9.1 Suppression Assay'.

6.7 Analysis of protein expression

6.7.1 Flow cytometry

For cell surface staining, cells were washed once with MACS buffer and stained with fixable viability dye and flow cytometry antibodies (see 6.2.2 Flow cytometry antibodies) for 15-30min at 4°C. After washing 3x with MACS buffer, labelled cells were fixed with FACS

fixation buffer for 10 min at RT. Cells were washed and resuspended in MACS buffer for flow cytometry analysis. Intracellular staining was performed using the Foxp3/Transcription Factor Staining Buffer Set (eBioscience Inc.). After staining for cell surface markers, the cells were incubated with fixation/permeabilization solution for 30min to 24h at 4°C, after which they were washed 3x with permeabilization buffer. The cells were incubated with 2% mouse and 2% rat serum (ThermoFisher Scientific) diluted in permeabilization buffer for 15min at RT. Intracellular staining antibodies were added and incubated for 30min at RT. Labelled cells were washed 3x with permeabilization buffer and resuspended in MACS buffer for flow cytometry analysis. For Annexin V staining, cells were stained with flow cytometry antibodies diluted in Annexin V Binding Buffer (BioLegend) for 15min at RT and analysed by flow cytometry within 1h of staining without fixation. Data was acquired on the following machines: Attune NxT Flow Cytometer (ThermoFisher Scientific), LSRFortessa Cell Analyzer (BD), LSRFortessa X-20 Cell Analyzer (BD) or LSRFortessa X-50 Cell Analyzer (BD). Single-stain compensation beads (UltraComp eBeads, Invitrogen) and Veri-Cells PBMCs (BioLegend) were used for compensation. Flow cytometry data was analysed using FlowJo version 10 (BD).

6.7.2 Secretion Assay

6.7.2.1 Secretion Assay for GM-CSF, IL-10, IL-13, IL-17A, IL-22 and IFNγ

Secretion assays were performed using Human Secretion Assay Detection Kits (Miltenyi Biotec) according to manufacturer's instructions. Cells were transferred to 96-round-bottom deep-well plates, washed with MACS buffer, and resuspended in 20µl MACS buffer containing 2µl catch reagent. After 5min incubation on ice, 0.8-1ml warm R10 medium supplemented with 20IU/ml IL-2 was added to each sample. For GM-CSF, IL-13 and IL-22, 2µl/sample biotin-conjugated detection antibody was added. The samples were incubated

for 45min at 37°C, rotating the plate 3x every 5min. Following the incubation, cells were washed with MACS buffer and stained with 20µl diluted flow cytometry staining antibodies (see 6.2.2 Flow cytometry antibodies) containing 2µl/sample PE- or APC-conjugated detection antibody (for IL-10, IL-17A and IFNγ) or 0.4µl/sample anti-biotin-PE (for GM-CSF, IL-13 and IL-22) for 15min at 4°C. Samples were washed twice using MACS buffer, fixed with FACS fixation buffer for 10min at RT, and washed again with MACS buffer before flow cytometry analysis.

To ensure sufficient dilution of cells and availability of catch and detection reagents for higher cell numbers, volumes were scaled up for the generation of CD1a-reactive Treg clones and 10x single-cell sequencing sample preparation. The secretion step was performed in 15ml falcons using 10ml R10 medium supplemented with 20IU/ml IL-2 per sample. Additionally, 5-fold higher volumes of catch and detection reagents as well as flow cytometry staining antibodies were used.

6.7.2.2 LAP-TGF-β Secretion Assay

As latent TGF-β (LAP-TGF-β) secretion assays are not commercially available, a home-made kit based on Wawrzyniak *et al.*[663] was created. The assay was performed in 96-round-bottom deep-well plates. For biotinylation of the cell surface, cells were washed twice with PBS and incubated with 1 mg/ml biotin (EZ-Link Sulfo-NHS-LC-Biotin, ThermoFisher Scientific) diluted in PBS for 30min at RT. To stop the biotinylation reaction, cells were washed twice with 100mM glycine (SLS) diluted in PBS, followed by a PBS wash. Streptavidin-tagged LAP-TGF-β antibody (clone TW7-7H4; BioLegend) was used as catch antibody. The antibody was tagged with streptavidin using the Streptavidin Conjugation Kit – Lightning-Link (abcam) according to manufacturer's instructions. Cells were incubated with streptavidin-LAP-TGF-β at 10µg/ml diluted in MACS buffer for 20min

on ice. To each sample, 0.8-1ml R10 medium supplemented with 20IU/ml IL-2 were added and the samples incubated for 45min at 37°C, rotating the plate 3x every 5min. LAP-TGF-β PE-conjugated flow cytometry antibody (clone TW4-6H10; BioLegend) was used as detection antibody. For flow cytometry staining, cells were incubated with the LAP-TGF-β detection antibody (at 5µg/ml) and flow cytometry antibodies (see 6.2.2 Flow cytometry antibodies) for 15min at 4°C. After washing twice with MACS buffer, the samples were fixed with FACS fixation buffer for 10min at RT. Fixed cells were washed once with MACS buffer before flow cytometry analysis.

6.7.3 Enzyme-linked Immunosorbent Assay (ELISA)

Cell culture supernatants were either analysed shortly after collection (stored at 4°C) or frozen at -80°C until analysis. LAP-TGF-β1 concentrations were determined using the TGF-β1 Human ELISA Kit (Invitrogen) and IFNγ concentrations either by the Human IFNγ ELISA Kit (Invitrogen) or the Human IFNγ ELISA MAX Deluxe Set (BioLegend). For LAP-TGF-β1, supernatants were used undiluted or 1:2-diluted. For IFNγ, supernatants were diluted 1:5 to 1:800. ELISAs were performed according to manufacturer's instructions, using 96-half well ELISA plates (Corning). The horseradish peroxidase (HRP) reaction was stopped using 2N H_2SO_4 (Sigma-Aldrich) or BioFx 450nm liquid stop solution (Surmodics). Absorbance was measured at 450 nm with a reference wavelength of 570 nm on the CLARIOstar plate reader (BMG Labtech). For each sample, the reference wavelength value was subtracted from the value measured at 450nm. Then, averaged blank control values were subtracted for each sample. Concentrations were determined by standard curve interpolation (sigmoidal 4-parameter logistic) using GraphPad Prism software (version 9; GraphPad Software).

6.7.4 LEGENDplex

LEGENDplex assay (BioLegend) was kindly performed by Dr Yi-Ling Chen according to manufacturer's instructions, measuring levels of CCL5, GM-CSF, granzyme A, granzyme B, granulysin, IFNγ, IL-10, IL-17A, IL-22, TNFα, PD-L1 and perforin. Supernatants were diluted 1:10 before analysis. Concentrations were determined by standard curve interpolation using the LEGENDplex data analysis software (BioLegend). Concentrations below the lowest standard were set to 0.

6.7.5 ELISpot

To measure IFNγ production by ELISpot (enzyme-linked immune absorbent spot), cells of interest were cultured for 16-24h in PVDF ELISpot plates (Millipore), which were used according to manufacturer's instructions. The plates were developed using the Human IFNγ ELISpot BASIC (ALP) kit (MABTECH) and the AP Conjugated Substrate Kit (Bio-Rad) as per manufacturer's instructions. ELISpot plates were analysed on AID iSpot ELISpot reader (AID Autoimmun Diagnostika) using the ELISpot7.0s software.

6.8 Analysis of gene expression

6.8.1 mRNA extraction and cDNA generation

mRNA extraction was performed using the TurboCapture96 mRNA kit (Qiagen) according to manufacturer's instructions. Cells were lysed in TCL buffer containing 2% β-mercaptoethanol (Sigma-Aldrich) or 2μM Bond-Breaker TCEP Solution (ThermoFisher Scientific). Lysed samples were transferred to TurboCapture plates, incubated on an orbital shaker at 150rpm for 90min, and the plates washed 3x with TCW buffer. For complementary deoxyribonucleic acid (cDNA) synthesis, M-MLV Reverse Transcriptase (Invitrogen) was

used (Table 6.11). cDNA was diluted 1:3 with nuclease-free water (Invitrogen) and stored at -20°C until use.

Table 6.11 cDNA synthesis.

Component	Volume [µl] per sample
Nuclease-free water	10
5x First strand buffer	4
DTT [0.1M]	2
dNTP [10mM each] (Qiagen)	1
Random Hexamer Primers [0.4µg/ml] (Qiagen)	1
RNAseOUT (Invitrogen)	1
M-MLV Reverse Transcriptase [200U/µl]	1

Time	Temperature
10min	30°C
60min	42°C
15min	70°C

6.8.2 RT-qPCR

Gene expression was quantified by reverse transcription quantitative real-time polymerase chain reaction (RT-qPCR) using 384-well plates, using Taqman Gene Expression Master Mix and Taqman probes (all Applied Biosystems). RT-qPCR was performed in triplicates as shown in Table 6.12 using the QuantStudio 7 Flex System (ThermoFisher Scientific). The following Taqman probes were used: *CD2* (Hs01040179_g1), *GAPDH* (Hs03929097_g1), *IL10* (Hs00961622_m1), *TGFB1* (Hs00998133_m1). *CD2* was used as housekeeping gene for gene expression of T cells and *GAPDH* was used as housekeeping gene for gene expression of K562 cell. Cycle threshold (C_t) values over 34 were excluded from analysis.

Table 6.12 RT-qPCR.

Component	Volume [µl] per sample
cDNA (1:3 diluted)	1
2x Taqman Gene Expression Master Mix	5
Taqman Probe	0.5
Nuclease-free water (Invitrogen)	3.5

Time	Temperature
2min	50°C
10min	95°C
Repeat 40x	
15sec	95°C
1min	60°C

6.9 Analysis of Treg suppressive functionality

6.9.1 Suppression Assay

Tregs were co-cultured with autologous PBMCs and suppression was calculated based on inhibition of $CD4^+$ and $CD8^+$ T cell proliferation. Frozen PBMCs were thawed and rested overnight in R10 medium before use. Proliferation was measured using Tag-it Violet Proliferation and Cell Tracking Dye (BioLegend). PBMCs were stained with 1µM Tag-it Violet as per manufacturer's instructions and washed 3x with R10 medium. PBMCs and Tregs were co-cultured in 96-round-bottom plates using Treg medium for 3 days. Each co-culture contained 100,000 PBMCs and Tregs were added at ratios of 1:1, 2:1, 4:1, 8:1, 16:1, 32:1 and 64:1. To each well, 20,000 αCD3/αCD28 beads (ratio of 1:5 bead:PBMC) were added. PBMCs cultured without Tregs were used to determine baseline proliferation. For analysis, cells were stained for flow cytometry with fixable viability dye and flow cytometry antibodies (see 6.2.2 Flow cytometry antibodies). PBMCs were identified by Tag-it Violet staining and division indices (DIs) of $CD4^+$ and $CD8^+$ T cells (gated on $CD3^+CD4^+$ and $CD3^+CD8^+$ T cells, respectively) were obtained using the FlowJo Proliferation Tool (FlowJo version 10). Percentage of Treg suppression was calculated using the following formula:

$$\%\, Suppression = 100 - \frac{Division\ Index\ of\ PBMCs/Treg\ co\text{-}culture}{Division\ Index\ of\ PBMCs\ only} * 100$$

6.9.2 Quantification of cytotoxic T cell activity

Cytotoxic activity of $CD8^+$ T cell clones was determined by their ability to induce K562 cell death. Cell death was measured by flow cytometry analysis, calculating the percentage of Annexin V (BioLegend) and CellTox reagent (Promega) double-positive K562 cells. To

distinguish K562 cells from other cells present in the culture, K562 cells were stained with 5µM Tag-it Violet Proliferation and Cell Tracking Dye (BioLegend) according to manufacturer's instructions prior to co-cultures. $CD8^+$ cytotoxic T cell clones were kindly provided by Dr Yi-Ling Chen. These clones were single-cell sorted for GM-CSF or IFNγ production upon CD1a stimulation and expanded using irradiated feeder cells (B cell lines and PBMCs, supplemented with anti-CD3 and PHA-L) and IL-2. Detailed methodology will be described in an upcoming publication. The here used clones were selected based on their ability to kill K562 cells regardless of the presence of CD1a. To study the effect of Treg clones on the cytotoxic activity of $CD8^+$ T cell clones, Treg clones were pre-stimulated overnight with 2.5µg/ml anti-CD11a or 2.5µg/ml anti-CD3 and anti-CD28 (each) in Treg medium containing 1000IU/ml IL-2. After washing 3x with R10 medium to remove stimulation antibodies, Treg clones were pre-incubated with K562-EV or K562-CD1a cells for 4h in R10 medium containing 200IU/ml IL-2 (100,000 Treg clones with 150,000 K562 cells per 96-flat-bottom well). $CD8^+$ T cell clones were added (100,000/well) together with co-stimulatory cytokines (1-5ng/ml of IL-12 and IL-18 for IFNγ-producing, or IL-1β and IL-12 for GM-CSF-producing $CD8^+$ T cell clones). Co-cultures were incubated for 2-3 days, upon which cells were harvested and stained for flow cytometry analysis of K562 cell death. K562 cells cultured alone or in the presence of $CD8^+$ T cell clones were used as control and to determine baseline cytotoxic activity, respectively.

6.10 CD1a-Klickmer staining

Cell binding to CD1a was determined using Klickmer technology (Immudex). For this, Klickmers were incubated with biotinylated CD1a monomers (obtained from the NIH Tetramer Core Facility) at a ratio of 5 CD1a molecules per dextran for 30min at RT. Klickmers loaded with PBS were used as negative control. For CD1a-Klickmer staining,

cells were washed with PBS and resuspended in 10µl flow cytometry staining buffer (eBioscience) containing 5% human TruStain FcX (BioLegend) and incubated for 5min at RT. 2.5µl CD1a-conjugated Klickmer were added, mixed, and incubated for 30min at RT. To each sample, 0.5µl anti-CD3 (clone OKT3; BioLegend) were added, the suspension mixed and incubated for 10min at RT. Cell surface antibodies were stained by adding 13µl 2x flow cytometry antibodies (see 6.2.2 Flow cytometry antibodies). The cells were incubated for 15min at 4°C and washed twice with flow cytometry staining buffer. After fixing with FACS fixation buffer for 10min at RT, cells were resuspended in flow cytometry staining buffer for flow cytometry analysis.

6.11 TCR sequencing

TCR sequencing was performed modified from a method published by Napolitani *et al.*[664]. mRNA was either obtained by TurboCapture (Qiagen; see 6.5.1 mRNA extraction and cDNA generation), or by RNA extraction using the RNeasy Mini kit (Qiagen) according to manufacturer's instructions. cDNA synthesis was either performed directly in TurboCapture plates or using 100-200ng RNA (as determined by Nanodrop One, ThermoFisher Scientific). cDNA synthesis was performed using template-switch reverse transcription with SMARTScribe Reverse Transcriptase (Clontech). The used primers TRAC and BCR1 target the constant regions of the *Trac* and *Trbc* genes. TSO is a template-switch oligo described by Kapteyn *et al.*[665]. Amplification of the TCR sequences was achieved through two rounds of nested PCR with Phusion High-Fidelity PCR Master Mix (New England BioLabs). After the first PCR, the obtained DNA was purified with 0.9x Mag-bind beads (Omega Bio-tek) according to manufacturer's instructions. For the second PCR, TCRα and TCRβ sequences were amplified independently, and amplified DNA was purified with 0.8x Mag-bind beads. The protocols for cDNA synthesis and PCR amplification are shown in Table 6.13, Table

6.14 and Table 6.15. Primer sequences are shown in Table 6.16. Amplified and purified DNA was sequenced using ACR3 tail and BCR3 tail primers by Sanger Sequencing *via* the MRC WIMM Sequencing facility.

Table 6.13 cDNA synthesis for TCR sequencing.

Component	Volume [µl] per sample
RNA (100-200ng)	1
TRAC [40µM]	0.5
BCR1 [40µM]	0.5
TSO [10µM]	0.5
Nuclease-free Water	2

Time	Temperature
3min	70°C

Component	Volume [µl] per sample
5x First strand buffer	2
DTT [20mM]	1
dNTP [10mM each]	1
RNAseOUT (Invitrogen)	0.5
SMARTScribe Reverse Transcriptase	1

Time	Temperature
75min	42°C
15min	70°C

Table 6.14 1st PCR for TCR sequencing.

Component	Volume [µl] per sample
cDNA	1
First PCR Fwd primer [10µM]	1
ACR2 [10µM]	1
BCR2 [10µM]	1
Phusion PCR Master Mix	10
DMSO	0.6
Nuclease-free Water	5.4

Time	Temperature
30sec	98°C
Repeat 18x	
20sec	98°C
20sec	67°C
1min	72°C
5min	72°C

Table 6.15 2nd PCR for TCR sequencing.

TCRα

Component	Volume [µl] per sample
DNA from 1st PCR (purified)	4
Second PCR Fwd primer [10µM]	1
ACR3 tail [10µM]	1
Phusion PCR Master Mix	10
DMSO	0.6
Nuclease-free Water	3.4

Time	Temperature
30sec	98°C
Repeat 25x	
20sec	98°C
20sec	67°C
1min	72°C
5min	72°C

TCRβ

Component	Volume [µl] per sample
DNA from 1st PCR (purified)	4
Second PCR Fwd primer [10µM]	1
BCR3 tail [10µM]	1
Phusion PCR Master Mix	10
DMSO	0.6
Nuclease-free Water	3.4

Table 6.16 Primer sequences for TCR sequencing.

Primers ordered from Invitrogen.

Primer	Sequence (5' to 3')
TRAC	TCAGCTGGACCACAGCCGCAG
BC1R	CAGTATCTGGAGTCATTGA
TSO	AAGCAGTGGTATCAACGCAGAGTGGCCATTACGGCCrGrGrG
AC2R	TACACGGCAGGGTCAGGGT
BC2R	TGCTTCTGATGGCTCAAACAC
First PCR Fwd	CACGACGCTCTTCCGATCTATTGACCCCAGTGGTATCAACGCAGAGTAC
BC3R tail	TGGAGTTCAGACGTGTGCTCTTCCGATCTACACSTTKTTCAGGTCCTC
AC3R tail	TGGAGTTCAGACGTGTGCTCTTCCGATCTGGGTCAGGGTTCTGGATAT
Second PCR Fwd	CACTCTTTCCCTACACGACGCTCTTCCGATC

6.12 10x single-cell sequencing

Single-cell sequencing was performed using the 10x genomics platform and according to manufacturer's instructions. PBMCs were isolated from peripheral blood of healthy donors and psoriasis patients (see 6.1 Patients and samples). $CD25^+$ cells were obtained by MACS separation (see 6.4.2 Isolation of immune cells from human blood) and rested for 2 days in Treg medium containing 200IU/ml IL-2. Cells were stimulated for 6h with K562-CD1a cells in R10 medium containing 200IU/ml IL-2 and 2.5µg/ml anti-CD11a (see 6.6.2 CD1a stimulation of Tregs for secretion assays). IL-10, IFNγ and IL-22 secretion assay was performed as described in '6.7.2 Secretion Assay'. Before staining with flow cytometry cell surface antibodies, samples were tagged with unique hashing antibodies. Hashtag-labelled cells were stained with flow cytometry antibodies for Treg markers and IL-10 and IFNγ secretion (Table 6.4), and subsequently stained with TotalSeq-C cell surface antibodies (BioLegend; Table 6.17). For FACS sorting, Tregs were gated as live $CD3^+CD4^+CD25^+CD127^{low/-}$ cells. CD1a-reactive IL-10- and IFNγ-secreting Tregs were sorted, using K562-EV cell-stimulated cells as baseline for gating of IL-10 and IFNγ secretion. Unstimulated Tregs and CD1a-stimulated Tregs negative for IL-10 and IFNγ secretion were sorted as controls. Cell partitioning and library preparation were performed by Dr Prathiba Kurupati and Dr Yi-Ling Chen according to manufacturer's instructions. Libraries were sequenced by Novogenes.

Table 6.17 List of TotalSeq-C cell surface antibodies.

Cell surface marker	Sequence	Cell surface marker	Sequence
Allophycocyanin (APC)	TTAACCGTCTCCCTT	CD137	CAGTAAGTTCGGGAC
Biotin	CGGTATATCAACAGA	CD147	CTTACGATTAAGAGC
CCR10	ATCTGTATGTCACAG	CD152	ATGGTTCACGTAATC
CD1a	GATCGTGTTGTGTTA	CD161	GTACGCAGTCCTTCT
CD1c	GAGCTACTTCACTCG	CD183	GCGATGGTAGATTAT
CD4	GAGGTTAGTGATGGA	CD194	AGCTTACCTGCACGA
CD8	GCGCAACTTGATGAT	CD195	CCAAAGTAAGAGCCA
CD8a	GCTGCGCTTTCCATT	CD196	GATCCCTTTGTCACT
CD11a	TATATCCTTGTGAGC	CD197	AGTTCAGTCAACCGA
CD25	TTTGTCCTGTACGCC	CD244	TCGCTTGGATGGTAG
CD27	GCACTCCTGCATGTA	CD272	GTTATTGGACTAAGG
CD28	TGAGAACGACCCTAA	CD273	TCAACGCTTGGCTAG
CD38	TGTACCCGCTTGTGA	CD274	GTTGTCCGACAATAC
CD39	TTACCTGGTATCCGT	CD278	CGCGCACCCATTAAA
CD45RA	TCAATCCTTCCGCTT	CD279	ACAGCGCCGTATTTA
CD45RO	CTCCGAATCATGTTG	CD294	TGTTTACGAGAGCCC
CD49d	CCATTCAACTTCCGG	CD366	TGTCCTACCCAACTT
CD56	TCCTTTCCTGATAGG	CXCR5	AATTCAACCGTCGCC
CD58	GTTCCTATGGACGAC	CXCR6	GACAGTCGATGCAAC
CD62L	GTCCCTGCAACTTGA	GARP	AGGTATGGTAGAGTA
CD69	GTCTCTTGGCTTAAA	GITR	ACCTTTCGACACTCG
CD71	CCGTGTTCCTCATTA	HLA-DR	AATAGCGAGCAAGTA
CD73	CAGTTCCTCAGTTCG	KLRG1	GTAGTAGGCTAGACC
CD85j	CCTTGTGAGGCTATG	LAG-3	CATTTGTCTGCCGGT
CD94	CTTTCCGGTCCTACA	OX40	AACCCACCGTTGTTA
CD103	GACCTCATTGTGAAT	Phycoerythrin (PE)	TGACCAGTTCCGCAT
CD117	AGACTAATAGCTGAC	TIGIT	TTGCTTACCGCCAGA
CD127	GTGTGTTGTCCTATG	TNFR2	GCGCAACTCCTTGTA

6.12.1 Bioinformatic analysis

Bioinformatics analysis was performed by Dr Jeongmin Woo. The Cell Ranger toolkit (version 6.0.1; 10x Genomics) was used to process raw scRNA-seq data, map cDNA libraries against the GRChg38 human reference genome and generate a feature count matrix. The hashed feature count matrix was demultiplexed using Seurat R toolkit[666] (version 4), filtering out hashtag-negative cells, defined as cells below the 99th percentile of a fitted negative binomial distribution per hashtag, and cells positive for multiple hashtags. Cells

were kept if they expressed a single hashtag, expressed > 200 and < 4,000 detected genes and > 1% and < 15% mitochondrial genes. Mitochondrial and ribosomal genes that were expressed in < 10 cells were removed from the final count matrix. The Seurat R toolkit[666] (version 4) was used for scRNA-seq analysis, including normalisation, scaling, transformation, clustering, dimensionality reduction, differential expression analysis and data visualisation. For RNA sequencing data, 5,459 genes, the union of the top 2,000 variable genes within each donor, were used to integrate data from different libraries. Total number of unique molecular identifier count per cell, percentage of mitochondrial features and individual donor effects were regressed out during library merging. Pre-processing and principal component (PC) analysis (PCA) was performed separately for RNA sequencing and cell surface antibody data (obtained by CITE-seq). Elbow plots and Jackstraw permutation tests were used to determine significant PCs (p-value < 0.01). Clustering analysis was performed with the weighted nearest neighbour (WNN) algorithm[667] using the first 20 PCs from the RNA sequencing data and the first 15 PCs from the cell surface antibody data. Cells were clustered using the Smart Local Moving (SLM) algorithm with a resolution of 0.6 and clustering was visualised using the Uniform Manifold Approximation and Projection (UMAP) algorithm. A table of cell numbers within clusters (or subpopulations) is shown in Table 6.18. Differential gene expression analysis was performed with the Seurat R toolkit[666] (version 4) using the MAST algorithm[668], treating cellular gene detection rate as covariant, and the FindMarkers function. Infrequently expressed genes were filtered out using default parameters. Differential cell surface marker expression was performed with the Seurat R toolkit[666] (version 4) using Wilcoxon rank-sum tests. Genes and cell surface markers were considered differentially expressed if the adjusted p-value was < 0.05. The results were corrected for multiple-testing using the Benjamini-Hochberg procedure.

Table 6.18 Cell numbers within clusters and subpopulations.

HC, healthy control; PS, psoriasis; Teff, effector T cells, Tregs, regulatory T cells.

		CD1a-stimulated Tregs IL10+/IFNγ-/IL22-	CD1a-stimulated Tregs IL10+/IFNγ+/IL22-	CD1a-stimulated Tregs IL10+/IFNγ-/IL22+	CD1a-stimulated Tregs IL10+/IFNγ+/IL22+	CD1a-stimulated Tregs IL10-/IFNγ+/IL22-	CD1a-stimulated Tregs IL10-/IFNγ-/IL22+	CD1a-stimulated Tregs IL10-/IFNγ+/IL22+	CD1a-stimulated Tregs IL10-/IFNγ-/IL22-	Unstimulated Tregs IL10-/IFNγ-/IL22-	CD1a-stimulated Teff IL22-/IFNγ+	CD1a-stimulated Teff IL22+/IFNγ-	CD1a-stimulated Teff IL22+/IFNγ+	CD1a-stimulated Teff IL22-/IFNγ-	Unstimulated Teff IL22-/IFNγ-
naïve Tregs (cluster 1,7)	HC	187	101	15	8	421	77	21	820	160	0	0	0	0	105
	PS	258	75	22	10	267	92	23	1035	274	0	0	1	0	74
effector/ memory Tregs (cluster 0,5,6)	HC	147	104	12	9	792	66	45	1518	248	2	2	4	1	29
	PS	157	34	8	2	249	57	11	1454	234	1	3	6	2	54
Cluster 4	HC	42	18	1	0	153	17	3	395	71	0	0	0	0	19
	PS	51	13	2	0	68	17	5	378	92	0	0	0	0	16
Cluster 9	HC	8	5	3	8	73	32	21	46	18	0	0	0	0	12
	PS	8	4	9	1	19	15	19	44	10	1	0	0	0	20
Cluster 11	HC	7	6	0	0	52	4	3	106	19	0	0	0	0	2
	PS	1	1	0	0	11	2	0	38	9	0	0	0	0	5
Cluster 13	HC	10	5	1	0	22	1	0	34	0	0	0	0	0	0
	PS	7	1	0	0	5	4	0	44	0	2	1	0	0	0
Cluster 14	HC	1	0	0	0	10	2	2	23	5	0	1	0	0	3
	PS	1	1	0	0	4	0	1	16	10	0	0	0	0	5
Cluster 2	HC	8	0	0	1	20	2	0	53	11	1	0	1	0	1715
	PS	9	3	1	0	19	4	2	69	14	0	1	1	2	1176
Cluster 3	HC	6	4	1	0	22	2	0	40	16	5	2	3	1	673
	PS	3	2	1	0	11	0	0	43	17	5	6	6	0	571
Cluster 8	HC	1	0	0	0	17	2	0	24	2	1	0	2	0	258
	PS	0	1	0	0	2	3	0	24	4	1	0	0	0	237
Cluster 10	HC	1	0	0	0	3	0	0	4	1	21	6	16	5	134
	PS	2	0	0	0	0	1	0	5	2	31	20	22	7	82
Cluster 12	HC	0	0	1	0	4	1	1	5	1	13	15	36	4	18
	PS	0	0	0	0	0	0	0	6	3	5	37	64	5	7

6.13 MoDC treatment with fatty acids

MoDCs were differentiated for 5 days from circulating $CD14^+$ monocytes (see 6.4.7 Monocyte-derived dendritic cell differentiation). SCFAs or FAs structurally related to butyrate (Table 6.9; Table 6.10) were added to the culture medium at indicated concentrations on day 0 and day 3 or only on day 3 of differentiation. SCFAs were dissolved in PBS, compounds structurally related to butyrate (Table 6.10) were dissolved in DMSO (Sigma-Aldrich), and candidate compounds were dissolved in PBS or DMSO as indicated (Table 6.9). FAs were sonicated for 20min at 60°C (FB15047 sonicator, Fisherbrand) before use. MoDC lineage and expression of markers of interest were analysed by flow cytometry (Table 6.5).

6.14 Co-culture systems for analysis of fatty acid-induced modulation of CD1a-mediated T cell responses

6.14.1 K562 and T cell co-culture for IFNγ ELISpot

K562 cells, plated at 10^6 cells/well in 48-well plates, were pulsed with SCFAs by overnight culture in R10 medium containing 250µM of the respective SCFA (dissolved in PBS; Table 6.9). K562 cells were washed 3x with R10 medium before co-culture. $CD3^+$ T cells were isolated from peripheral blood (see 6.4.3 Isolation of immune cell subsets by MACS) and cultured in T cell medium containing 200IU/ml IL-2 for 2 days, and in R10 medium overnight before co-culture. For IFNγ ELISpots, K562 cells and T cells were co-cultured for 16-24h at a ratio of 1:3 (25,000 K562 cells and 75,000 T cells) in coated ELISpot plates. Wells containing T cells only were used as baseline IFNγ secretion. ELISpots were performed as described in '6.7.5 ELISpot'.

6.14.2 MoDC and $CD8^+$ T cell clone co-culture for ELISA

MoDCs were differentiated for 4 days from circulating $CD14^+$ monocytes (see 6.4.7 Monocyte-derived dendritic cell differentiation). MoDCs were treated with 125µM of the respective compounds (dissolved in PBS or DMSO; Table 6.9). from day 0 of differentiation, refreshing treatment on day 2. On day 4 of differentiation, moDCs were harvested and incubated for 1h with 20µg/ml anti-HLA-ABC, anti-HLA-DR and anti-CD1a (clone HI149) or the respective isotype controls (Table 6.6) in R10 medium. Pre-blocked moDCs were co-cultured with CD1a-reactive $CD8^+$ cytotoxic T cell clones, which were kindly provided by Dr Yi-Ling Chen. $CD8^+$ cytotoxic T cell clones were single-cell sorted for GM-CSF or IFNγ production upon CD1a stimulation and expanded using irradiated feeder cells (B cell lines and PBMCs, supplemented with anti-CD3 and PHA-L) and IL-2. Detailed methodology will be described in an upcoming publication. The here used clones were selected based on their ability to secrete IFNγ in a CD1a-dependent manner. Co-culture was performed in 96-flat-bottom plates at ratios of 1:2-1:100 moDCs:$CD8^+$ T cell clones (1,000-50,000 moDCs and 100,000 $CD8^+$ T cell clones per well). 200IU/ml IL-2 and 1-10ng/ml IL-12 and IL-18 were added to the co-culture. The final concentration of blocking antibodies was 10µg/ml. Supernatants were harvested after 24h co-culture and stored at -80°C until use. ELISAs were performed as described in '6.7.3 Enzyme-linked Immunosorbent Assay (ELISA)'.

6.15 Isoelectric focussing (IEF) analysis

Isoelectric points (pI) were analysed by IEF using Novex pH 3-7 IEF protein gels (Invitrogen) and the pH 3-7 buffer kit (Invitrogen) according to manufacturer's instructions. IEF marker 3-10 (Invitrogen) served as pI ladder. IEF gels were loaded with CD1a and run

for 1h at 100V, 1h at 200V, and 30min at 500V. Gels were fixed with fixing solution containing 12% (w/v) trichloroacetic acid and 3.5% (w/v) 5-sulfosalicylic acid. (Sigma-Aldrich) and stained using SimplyBlue SafeStain (Invitrogen). After de-staining with deionised water, gels were recorded using the iBright Imaging System (ThermoFisher Scientific).

6.16 Statistical analysis

One-way ANOVA or Mixed-effects tests with Tukey's or Dunnett's post hoc multiple comparison tests, two-way ANOVA with Tukey's and Šidák's post hoc multiple comparison tests, two-tailed paired t-tests or non-parametric Friedman tests with Dunn's correction for multiple comparison were performed using GraphPad Prism version 9 (GraphPad Software), as indicated in figure legends.

Chapter 7 References

1 Nestle FO, Di Meglio P, Qin JZ, Nickoloff BJ. Skin immune sentinels in health and disease. *Nat Rev Immunol* 2009; **9**:679-91.

2 Pasparakis M, Haase I, Nestle FO. Mechanisms regulating skin immunity and inflammation. *Nat Rev Immunol* 2014; **14**:289-301.

3 Kabashima K, Honda T, Ginhoux F, Egawa G. The immunological anatomy of the skin. *Nat Rev Immunol* 2019; **19**:19-30.

4 Silk JD, Salio M, Brown J *et al.* Structural and functional aspects of lipid binding by CD1 molecules. *Annu Rev Cell Dev Biol* 2008; **24**:369-95.

5 Van Rhijn I, Godfrey DI, Rossjohn J, Moody DB. Lipid and small-molecule display by CD1 and MR1. *Nat Rev Immunol* 2015; **15**:643-54.

6 Kim JH, Hu Y, Yongqing T *et al.* CD1a on Langerhans cells controls inflammatory skin disease. *Nat Immunol* 2016; **17**:1159-66.

7 Klechevsky E, Morita R, Liu M *et al.* Functional specializations of human epidermal Langerhans cells and CD14+ dermal dendritic cells. *Immunity* 2008; **29**:497-510.

8 Romano E, Cotari JW, Barreira da Silva R *et al.* Human Langerhans cells use an IL-15R-alpha/IL-15/pSTAT5-dependent mechanism to break T-cell tolerance against the self-differentiation tumor antigen WT1. *Blood* 2012; **119**:5182-90.

9 Seneschal J, Clark RA, Gehad A *et al.* Human epidermal Langerhans cells maintain immune homeostasis in skin by activating skin resident regulatory T cells. *Immunity* 2012; **36**:873-84.

10 Kubo A, Nagao K, Yokouchi M *et al.* External antigen uptake by Langerhans cells with reorganization of epidermal tight junction barriers. *J Exp Med* 2009; **206**:2937-46.

11 Bruggen MC, Bauer WM, Reininger B *et al.* In Situ Mapping of Innate Lymphoid Cells in Human Skin: Evidence for Remarkable Differences between Normal and Inflamed Skin. *J Invest Dermatol* 2016; **136**:2396-405.

12 Salimi M, Ogg G. Innate lymphoid cells and the skin. *BMC Dermatol* 2014; **14**:18.

13 Villanova F, Flutter B, Tosi I *et al.* Characterization of innate lymphoid cells in human skin and blood demonstrates increase of NKp44+ ILC3 in psoriasis. *J Invest Dermatol* 2014; **134**:984-91.

14 Hardman CS, Chen YL, Salimi M *et al.* CD1a presentation of endogenous antigens by group 2 innate lymphoid cells. *Sci Immunol* 2017; **2**:eaan5918-eaan18.

15 Kim BS, Siracusa MC, Saenz SA *et al.* TSLP elicits IL-33-independent innate lymphoid cell responses to promote skin inflammation. *Sci Transl Med* 2013; **5**:170ra16.

16 Pantelyushin S, Haak S, Ingold B *et al.* Rorgammat+ innate lymphocytes and gammadelta T cells initiate psoriasiform plaque formation in mice. *J Clin Invest* 2012; **122**:2252-6.

17 Salimi M, Barlow JL, Saunders SP *et al.* A role for IL-25 and IL-33-driven type-2 innate lymphoid cells in atopic dermatitis. *J Exp Med* 2013; **210**:2939-50.

18 Vantourout P, Hayday A. Six-of-the-best: unique contributions of gammadelta T cells to immunology. *Nat Rev Immunol* 2013; **13**:88-100.

19 Becher B, Pantelyushin S. Hiding under the skin: Interleukin-17-producing γδ T cells go under the skin? *Nat Med* 2012; **18**:1748-50.

20 Cai Y, Shen X, Ding C *et al.* Pivotal role of dermal IL-17-producing gammadelta T cells in skin inflammation. *Immunity* 2011; **35**:596-610.

21 Gray EE, Ramirez-Valle F, Xu Y *et al.* Deficiency in IL-17-committed Vgamma4(+) gammadelta T cells in a spontaneous Sox13-mutant CD45.1(+) congenic mouse substrain provides protection from dermatitis. *Nat Immunol* 2013; **14**:584-92.

22 Laggner U, Di Meglio P, Perera GK *et al.* Identification of a novel proinflammatory human skin-homing Vgamma9Vdelta2 T cell subset with a potential role in psoriasis. *J Immunol* 2011; **187**:2783-93.

23 Carmi-Levy I, Homey B, Soumelis V. A modular view of cytokine networks in atopic dermatitis. *Clin Rev Allergy Immunol* 2011; **41**:245-53.

24 Nagao K, Kobayashi T, Moro K *et al.* Stress-induced production of chemokines by hair follicles regulates the trafficking of dendritic cells in skin. *Nat Immunol* 2012; **13**:744-52.

25 Paus R, Ito N, Takigawa M, Ito T. The hair follicle and immune privilege. *J Investig Dermatol Symp Proc* 2003; **8**:188-94.

26 Sanchez Rodriguez R, Pauli ML, Neuhaus IM *et al.* Memory regulatory T cells reside in human skin. *J Clin Invest* 2014; **124**:1027-36.

27 Ali N, Zirak B, Rodriguez RS *et al.* Regulatory T Cells in Skin Facilitate Epithelial Stem Cell Differentiation. *Cell* 2017; **169**:1119-29 e11.

28 Ali N, Rosenblum MD. Regulatory T cells in skin. *Immunology* 2017; **152**:372-81.

29 Nosbaum A, Prevel N, Truong HA *et al.* Cutting Edge: Regulatory T Cells Facilitate Cutaneous Wound Healing. *J Immunol* 2016; **196**:2010-14.

30 Park CO, Kupper TS. The emerging role of resident memory T cells in protective immunity and inflammatory disease. *Nat Med* 2015; **21**:688-97.

31 Adachi T, Kobayashi T, Sugihara E *et al.* Hair follicle-derived IL-7 and IL-15 mediate skin-resident memory T cell homeostasis and lymphoma. *Nat Med* 2015; **21**:1272-9.

32 Bibel DJ, Aly R, Shinefield HR. Antimicrobial activity of sphingosines. *J Invest Dermatol* 1992; **98**:269-73.

33 van Smeden J, Janssens M, Gooris GS, Bouwstra JA. The important role of stratum corneum lipids for the cutaneous barrier function. *Biochim Biophys Acta* 2014; **1841**:295-313.

34 de Jong A, Cheng TY, Huang S *et al.* CD1a-autoreactive T cells recognize natural skin oils that function as headless antigens. *Nat Immunol* 2014; **15**:177-85.

35 Di Nardo A, Wertz P, Giannetti A, Seidenari S. Ceramide and cholesterol composition of the skin of patients with atopic dermatitis. *Acta Derm Venereol* 1998; **78**:27-30.

36 Motta S, Monti M, Sesana S *et al.* Ceramide composition of the psoriatic scale. *Biochim Biophys Acta* 1993; **1182**:147-51.

37 Camera E, Ludovici M, Galante M *et al.* Comprehensive analysis of the major lipid classes in sebum by rapid resolution high-performance liquid chromatography and electrospray mass spectrometry. *J Lipid Res* 2010; **51**:3377-88.

38 Kendall AC, Nicolaou A. Bioactive lipid mediators in skin inflammation and immunity. *Prog Lipid Res* 2013; **52**:141-64.

39 Nicolaides N, Wells GC. On the biogenesis of the free fatty acids in human skin surface fat. *J Invest Dermatol* 1957; **29**:423-33.

40 Belkaid Y, Tamoutounour S. The influence of skin microorganisms on cutaneous immunity. *Nat Rev Immunol* 2016; **16**:353-66.

41 Byrd AL, Belkaid Y, Segre JA. The human skin microbiome. *Nat Rev Microbiol* 2018; **16**:143-55.

42 Linehan JL, Harrison OJ, Han SJ *et al.* Non-classical Immunity Controls Microbiota Impact on Skin Immunity and Tissue Repair. *Cell* 2018; **172**:784-96 e18.

43 Tamoutounour S, Han SJ, Deckers J *et al.* Keratinocyte-intrinsic MHCII expression controls microbiota-induced Th1 cell responses. *Proc Natl Acad Sci U S A* 2019; **116**:23643-52.

44 Lai Y, Di Nardo A, Nakatsuji T *et al.* Commensal bacteria regulate Toll-like receptor 3-dependent inflammation after skin injury. *Nat Med* 2009; **15**:1377-82.

45 Naik S, Bouladoux N, Linehan JL *et al.* Commensal–dendritic-cell interaction specifies a unique protective skin immune signature. *Nature* 2015; **520**:104-08.

46 Naik S, Bouladoux N, Wilhelm C *et al.* Compartmentalized control of skin immunity by resident commensals. *Science* 2012; **337**:1115-9.

47 Geoghegan JA, Irvine AD, Foster TJ. Staphylococcus aureus and Atopic Dermatitis: A Complex and Evolving Relationship. *Trends Microbiol* 2018; **26**:484-97.

48 Nakamura Y, Oscherwitz J, Cease KB *et al.* Staphylococcus delta-toxin induces allergic skin disease by activating mast cells. *Nature* 2013; **503**:397-401.

49 Wolf K, Muller R, Borgmann S *et al.* Amoeboid shape change and contact guidance: T-lymphocyte crawling through fibrillar collagen is independent of matrix remodeling by MMPs and other proteases. *Blood* 2003; **102**:3262-9.

50 Cruz MS, Diamond A, Russell A, Jameson JM. Human αβ and γδ T cells in skin immunity and disease. *Front Immunol* 2018; **9**:1304.

51 Ginhoux F, Collin MP, Bogunovic M *et al.* Blood-derived dermal langerin+ dendritic cells survey the skin in the steady state. *J Exp Med* 2007; **204**:3133-46.

52 Grimbaldeston MA, Simpson A, Finlay-Jones JJ, Hart PH. The effect of ultraviolet radiation exposure on the prevalence of mast cells in human skin. *Br J Dermatol* 2003; **148**:300-6.

53 Haniffa M, Gunawan M, Jardine L. Human skin dendritic cells in health and disease. *J Dermatol Sci* 2015; **77**:85-92.

54 Tong PL, Roediger B, Kolesnikoff N *et al.* The skin immune atlas: three-dimensional analysis of cutaneous leukocyte subsets by multiphoton microscopy. *J Invest Dermatol* 2015; **135**:84-93.

55 Weber-Matthiesen K, Sterry W. Organization of the monocyte/macrophage system of normal human skin. *J Invest Dermatol* 1990; **95**:83-9.

56 Weber A, Knop J, Maurer M. Pattern analysis of human cutaneous mast cell populations by total body surface mapping. *Br J Dermatol* 2003; **148**:224-8.

57 Tomura M, Honda T, Tanizaki H *et al.* Activated regulatory T cells are the major T cell type emigrating from the skin during a cutaneous immune response in mice. *J Clin Invest* 2010; **120**:883-93.

58 Natsuaki Y, Egawa G, Nakamizo S *et al.* Perivascular leukocyte clusters are essential for efficient activation of effector T cells in the skin. *Nat Immunol* 2014; **15**:1064-9.

59 Daniel PT, Kroidl A, Cayeux S *et al.* Costimulatory signals through B7.1/CD28 prevent T cell apoptosis during target cell lysis. *Journal of immunology (Baltimore, Md. : 1950)* 1997; **159**:3808-15.

60 Dudeck J, Medyukhina A, Frobel J *et al.* Mast cells acquire MHCII from dendritic cells during skin inflammation. *J Exp Med* 2017; **214**:3791-811.

61 Kashem SW, Riedl MS, Yao C *et al.* Nociceptive Sensory Fibers Drive Interleukin-23 Production from CD301b+ Dermal Dendritic Cells and Drive Protective Cutaneous Immunity. *Immunity* 2015; **43**:515-26.

62 Riol-Blanco L, Ordovas-Montanes J, Perro M *et al.* Nociceptive sensory neurons drive interleukin-23-mediated psoriasiform skin inflammation. *Nature* 2014; **510**:157-61.

63 Murphy KM, Weaver C. *Janeway's immunobiology*, 9th edition edn.: New York, NY : Garland Science/Taylor & Francis Group, LLC, [2017]. 2017.

64 Mori L, Lepore M, De Libero G. The Immunology of CD1- and MR1-Restricted T Cells. *Annu Rev Immunol* 2016; **34**:479-510.

65 Dougan SK, Kaser A, Blumberg RS. CD1 Expression on Antigen-Presenting Cells. *Curr Top Microbiol Immunol* 2007; **314**:113-41.

66 Salio M, Cerundolo V. Regulation of Lipid Specific and Vitamin Specific Non-MHC Restricted T Cells by Antigen Presenting Cells and Their Therapeutic Potentials. *Front Immunol* 2015; **6**:388.

67 Exley M, Garcia J, Wilson SB *et al.* CD1d structure and regulation on human thymocytes, peripheral blood T cells, B cells and monocytes. *Immunology* 2000; **100**:37-47.

68 Gumperz JE. The ins and outs of CD1 molecules: bringing lipids under immunological surveillance. *Traffic* 2006; **7**:2-13.

69 Salio M, Silk JD, Cerundolo V. Recent advances in processing and presentation of CD1 bound lipid antigens. *Curr Opin Immunol* 2010; **22**:81-8.

70 Cao X, Sugita M, Van Der Wel N *et al.* CD1 molecules efficiently present antigen in immature dendritic cells and traffic independently of MHC class II during dendritic cell maturation. *J Immunol* 2002; **169**:4770-7.

71 Porcelli S, Morita CT, Brenner MB. CD1b restricts the response of human CD4-8- T lymphocytes to a microbial antigen. *Nature* 1992; **360**:593-7.

72 Nencioni A, Grünebach F, Zobywlaski A *et al.* Dendritic Cell Immunogenicity Is Regulated by Peroxisome Proliferator-Activated Receptor γ. *The Journal of Immunology* 2002; **169**:1228-35.

73 Szatmari I, Gogolak P, Im JS *et al.* Activation of PPARγ Specifies a Dendritic Cell Subtype Capable of Enhanced Induction of iNKT Cell Expansion. *Immunity* 2004; **21**:95-106.

74 Szatmari I, Pap A, Ruhl R *et al.* PPARgamma controls CD1d expression by turning on retinoic acid synthesis in developing human dendritic cells. *J Exp Med* 2006; **203**:2351-62.

75 Leslie DS, Dascher CC, Cembrola K *et al.* Serum lipids regulate dendritic cell CD1 expression and function. *Immunology* 2008; **125**:289-301.

76 Abós-Gracia B, del Moral MG, López-Relaño J *et al.* Olea europaea pollen lipids activate invariant natural killer T cells by upregulating CD1d expression on dendritic cells. *Journal of Allergy and Clinical Immunology* 2013; **131**:1393-99.e5.

77 Roura-Mir C, Wang L, Cheng TY *et al.* Mycobacterium tuberculosis regulates CD1 antigen presentation pathways through TLR-2. *J Immunol* 2005; **175**:1758-66.

78 Moody DB. TLR gateways to CD1 function. *Nat Immunol* 2006; **7**:811-7.

79 Nencioni A, Beck J, Werth D *et al.* Histone deacetylase inhibitors affect dendritic cell differentiation and immunogenicity. *Clin Cancer Res* 2007; **13**:3933-41.

80 Tiper IV, Webb TJ. Histone deacetylase inhibitors enhance CD1d-dependent NKT cell responses to lymphoma. *Cancer Immunol Immunother* 2016; **65**:1411-21.

81 Kelly H, Mandraju R, Coelho-dos-Reis JG, Tsuji M. Effects of HIV-1-induced CD1c and CD1d modulation and endogenous lipid presentation on CD1c-restricted T-cell activation. *BMC Immunol* 2013; **14**:4.

82 Cho S, Knox KS, Kohli LM *et al.* Impaired cell surface expression of human CD1d by the formation of an HIV-1 Nef/CD1d complex. *Virology* 2005; **337**:242-52.

83 Shinya E, Owaki A, Shimizu M *et al.* Endogenously expressed HIV-1 nef down-regulates antigen-presenting molecules, not only class I MHC but also CD1a, in immature dendritic cells. *Virology* 2004; **326**:79-89.

84 Shinya E, Shimizu M, Owaki A *et al.* Hemopoietic cell kinase (Hck) and p21-activated kinase 2 (PAK2) are involved in the down-regulation of CD1a lipid antigen presentation by HIV-1 Nef in dendritic cells. *Virology* 2016; **487**:285-95.

85 Zeng Z, Castano AR, Segelke BW *et al.* Crystal structure of mouse CD1: An MHC-like fold with a large hydrophobic binding groove. *Science* 1997; **277**:339-45.

86 Gadola SD, Zaccai NR, Harlos K *et al.* Structure of human CD1b with bound ligands at 2.3 A, a maze for alkyl chains. *Nat Immunol* 2002; **3**:721-6.

87 Koch M, Stronge VS, Shepherd D *et al.* The crystal structure of human CD1d with and without alpha-galactosylceramide. *Nat Immunol* 2005; **6**:819-26.

88 Le Nours J, Shahine A, Gras S. Molecular features of lipid-based antigen presentation by group 1 CD1 molecules. *Semin Cell Dev Biol* 2018; **84**:48-57.

89 Zajonc DM, Elsliger MA, Teyton L, Wilson IA. Crystal structure of CD1a in complex with a sulfatide self antigen at a resolution of 2.15 A. *Nat Immunol* 2003; **4**:808-15.

90 Moody DB, Cotton RN. Four pathways of CD1 antigen presentation to T cells. *Curr Opin Immunol* 2017; **46**:127-33.

91 Joyce S, Woods AS, Yewdell JW *et al.* Natural ligand of mouse CD1d1: cellular glycosylphosphatidylinositol. *Science* 1998; **279**:1541-4.

92 Park JJ, Kang SJ, De Silva AD *et al.* Lipid-protein interactions: biosynthetic assembly of CD1 with lipids in the endoplasmic reticulum is evolutionarily conserved. *Proc Natl Acad Sci U S A* 2004; **101**:1022-6.

93 Sugita M, Porcelli SA, Brenner MB. Assembly and retention of CD1b heavy chains in the endoplasmic reticulum. *J Immunol* 1997; **159**:2358-65.

94 Manolova V, Kistowska M, Paoletti S *et al.* Functional CD1a is stabilized by exogenous lipids. *Eur J Immunol* 2006; **36**:1083-92.

95 Jackman RM, Stenger S, Lee A *et al.* The Tyrosine-Containing Cytoplasmic Tail of CD1b Is Essential for Its Efficient Presentation of Bacterial Lipid Antigens. *Immunity* 1998; **8**:341-51.

96 Jayawardena-Wolf J, Benlagha K, Chiu Y-H *et al.* CD1d Endosomal Trafficking Is Independently Regulated by an Intrinsic CD1d-Encoded Tyrosine Motif and by the Invariant Chain. *Immunity* 2001; **15**:897-908.

97 Sugita M, Grant EP, van Donselaar E *et al.* Separate pathways for antigen presentation by CD1 molecules. *Immunity* 1999; **11**:743-52.

98 Ernst WA, Maher J, Cho S *et al.* Molecular interaction of CD1b with lipoglycan antigens. *Immunity* 1998; **8**:331-40.

99 Spada FM, Koezuka Y, Porcelli SA. CD1d-restricted recognition of synthetic glycolipid antigens by human natural killer T cells. *J Exp Med* 1998; **188**:1529-34.

100 Sugita M, van Der Wel N, Rogers RA *et al.* CD1c molecules broadly survey the endocytic system. *Proc Natl Acad Sci U S A* 2000; **97**:8445-50.

101 Moody DB, Briken V, Cheng TY *et al.* Lipid length controls antigen entry into endosomal and nonendosomal pathways for CD1b presentation. *Nat Immunol* 2002; **3**:435-42.

102 Relloso M, Cheng TY, Im JS *et al.* pH-dependent interdomain tethers of CD1b regulate its antigen capture. *Immunity* 2008; **28**:774-86.

103 Bai L, Sagiv Y, Liu Y *et al.* Lysosomal recycling terminates CD1d-mediated presentation of short and polyunsaturated variants of the NKT cell lipid antigen alphaGalCer. *Proc Natl Acad Sci U S A* 2009; **106**:10254-9.

104 Sloma I, Zilber MT, Vasselon T *et al.* Regulation of CD1a surface expression and antigen presentation by invariant chain and lipid rafts. *J Immunol* 2008; **180**:980-7.

105 Salamero J, Bausinger H, Mommaas AM *et al.* CD1a molecules traffic through the early recycling endosomal pathway in human Langerhans cells. *J Invest Dermatol* 2001; **116**:401-8.

106 Mukherjee S, Soe TT, Maxfield FR. Endocytic sorting of lipid analogues differing solely in the chemistry of their hydrophobic tails. *J Cell Biol* 1999; **144**:1271-84.

107 Prigozy TI, Naidenko O, Qasba P *et al.* Glycolipid antigen processing for presentation by CD1d molecules. *Science* 2001; **291**:664-7.

108 Kang SJ, Cresswell P. Saposins facilitate CD1d-restricted presentation of an exogenous lipid antigen to T cells. *Nat Immunol* 2004; **5**:175-81.

109 de la Salle H, Mariotti S, Angenieux C *et al.* Assistance of microbial glycolipid antigen processing by CD1e. *Science* 2005; **310**:1321-4.

110 Angenieux C, Fraisier V, Maitre B *et al.* The cellular pathway of CD1e in immature and maturing dendritic cells. *Traffic* 2005; **6**:286-302.

111 Ly D, Moody DB. The CD1 size problem: Lipid antigens, ligands, and scaffolds. *Cell Mol Life Sci* 2014; **71**:3069-79.

112 Jahng A, Maricic I, Aguilera C *et al.* Prevention of autoimmunity by targeting a distinct, noninvariant CD1d-reactive T cell population reactive to sulfatide. *J Exp Med* 2004; **199**:947-57.

113 Shamshiev A, Gober HJ, Donda A *et al.* Presentation of the same glycolipid by different CD1 molecules. *J Exp Med* 2002; **195**:1013-21.

114 Bagchi S, Li S, Wang CR. CD1b-autoreactive T cells recognize phospholipid antigens and contribute to antitumor immunity against a CD1b(+) T cell lymphoma. *Oncoimmunology* 2016; **5**:e1213932.

115 Fox LM, Cox DG, Lockridge JL *et al.* Recognition of lyso-phospholipids by human natural killer T lymphocytes. *PLoS Biol* 2009; **7**:e1000228.

116 Haig NA, Guan Z, Li D *et al.* Identification of self-lipids presented by CD1c and CD1d proteins. *J Biol Chem* 2011; **286**:37692-701.

117 Wun KS, Reijneveld JF, Cheng TY *et al.* T cell autoreactivity directed toward CD1c itself rather than toward carried self lipids. *Nat Immunol* 2018; **19**:397-406.

118 Shamshiev A, Donda A, Prigozy TI *et al.* The αβ T Cell Response to Self-Glycolipids Shows a Novel Mechanism of CD1b Loading and a Requirement for Complex Oligosaccharides. *Immunity* 2000; **13**:255-64.

119 Shamshiev A, Donda A, Carena I *et al.* Self glycolipids as T-cell autoantigens. *Eur J Immunol* 1999; **29**:1667-75.

120 Wu DY, Segal NH, Sidobre S *et al.* Cross-presentation of disialoganglioside GD3 to natural killer T cells. *J Exp Med* 2003; **198**:173-81.

121 Moody DB, Young DC, Cheng TY *et al.* T cell activation by lipopeptide antigens. *Science* 2004; **303**:527-31.

122 Young DC, Kasmar A, Moraski G *et al.* Synthesis of dideoxymycobactin antigens presented by CD1a reveals T cell fine specificity for natural lipopeptide structures. *J Biol Chem* 2009; **284**:25087-96.

123 Beckman EM, Porcelli SA, Morita CT *et al.* Recognition of a lipid antigen by CD1-restricted alpha beta+ T cells. *Nature* 1994; **372**:691-4.

124 Layre E, Collmann A, Bastian M *et al.* Mycolic acids constitute a scaffold for mycobacterial lipid antigens stimulating CD1-restricted T cells. *Chem Biol* 2009; **16**:82-92.

125 Moody DB, Reinhold BB, Guy MR *et al.* Structural requirements for glycolipid antigen recognition by CD1b-restricted T cells. *Science* 1997; **278**:283-6.

126 Moody DB, Ulrichs T, Muhlecker W *et al.* CD1c-mediated T-cell recognition of isoprenoid glycolipids in Mycobacterium tuberculosis infection. *Nature* 2000; **404**:884-8.

127 Albacker LA, Chaudhary V, Chang YJ *et al.* Invariant natural killer T cells recognize a fungal glycosphingolipid that can induce airway hyperreactivity. *Nat Med* 2013; **19**:1297-304.

128 Kawano T, Cui J, Koezuka Y *et al.* CD1d-restricted and TCR-mediated activation of valpha14 NKT cells by glycosylceramides. *Science* 1997; **278**:1626-9.

129 Wieland Brown LC, Penaranda C, Kashyap PC *et al.* Production of alpha-galactosylceramide by a prominent member of the human gut microbiota. *PLoS Biol* 2013; **11**:e1001610.

130 Gras S, Van Rhijn I, Shahine A *et al.* T cell receptor recognition of CD1b presenting a mycobacterial glycolipid. *Nat Commun* 2016; **7**:13257.

131 Borg NA, Wun KS, Kjer-Nielsen L *et al.* CD1d-lipid-antigen recognition by the semi-invariant NKT T-cell receptor. *Nature* 2007; **448**:44-9.

132 Mansour S, Tocheva AS, Cave-Ayland C *et al.* Cholesteryl esters stabilize human CD1c conformations for recognition by self-reactive T cells. *Proc Natl Acad Sci U S A* 2016; **113**:E1266-75.

133 Birkinshaw RW, Pellicci DG, Cheng TY *et al.* alphabeta T cell antigen receptor recognition of CD1a presenting self lipid ligands. *Nat Immunol* 2015; **16**:258-66.

134 Cotton RN, Wegrecki M, Cheng TY *et al.* CD1a selectively captures endogenous cellular lipids that broadly block T cell response. *J Exp Med* 2021; **218**:e20202699.

135 Cotton RN, Cheng TY, Wegrecki M *et al.* Human skin is colonized by T cells that recognize CD1a independently of lipid. *J Clin Invest* 2021; **131**:e140706.

136 Cotton RN, Shahine A, Rossjohn J, Moody DB. Lipids hide or step aside for CD1-autoreactive T cell receptors. *Curr Opin Immunol* 2018; **52**:93-99.

137 Faure F, Jitsukawa S, Miossec C, Hercend T. CD1c as a target recognition structure for human T lymphocytes: analysis with peripheral blood gamma/delta cells. *Eur J Immunol* 1990; **20**:703-6.

138 Porcelli S, Brenner MB, Greenstein JL *et al.* Recognition of cluster of differentiation 1 antigens by human CD4-CD8-cytolytic T lymphocytes. *Nature* 1989; **341**:447-50.

139 Spada FM, Grant EP, Peters PJ *et al.* Self-recognition of CD1 by gamma/delta T cells: implications for innate immunity. *J Exp Med* 2000; **191**:937-48.

140 Salio M, Silk JD, Jones EY, Cerundolo V. Biology of CD1- and MR1-restricted T cells. *Annu Rev Immunol* 2014; **32**:323-66.

141 Dellabona P, Padovan E, Casorati G *et al.* An invariant V alpha 24-J alpha Q/V beta 11 T cell receptor is expressed in all individuals by clonally expanded CD4-8- T cells. *J Exp Med* 1994; **180**:1171-6.

142 Porcelli S, Yockey CE, Brenner MB, Balk SP. Analysis of T cell antigen receptor (TCR) expression by human peripheral blood CD4-8- alpha/beta T cells demonstrates preferential use of several V beta genes and an invariant TCR alpha chain. *J Exp Med* 1993; **178**:1-16.

143 Brennan PJ, Brigl M, Brenner MB. Invariant natural killer T cells: An innate activation scheme linked to diverse effector functions. *Nat Rev Immunol* 2013; **13**:101-17.

144 Brigl M, Tatituri RV, Watts GF *et al.* Innate and cytokine-driven signals, rather than microbial antigens, dominate in natural killer T cell activation during microbial infection. *J Exp Med* 2011; **208**:1163-77.

145 Fujii S, Shimizu K, Smith C *et al.* Activation of natural killer T cells by alpha-galactosylceramide rapidly induces the full maturation of dendritic cells in vivo and thereby acts as an adjuvant for combined CD4 and CD8 T cell immunity to a coadministered protein. *J Exp Med* 2003; **198**:267-79.

146 Galli G, Pittoni P, Tonti E *et al.* Invariant NKT cells sustain specific B cell responses and memory. *Proc Natl Acad Sci U S A* 2007; **104**:3984-9.

147 Hermans IF, Silk JD, Gileadi U *et al.* NKT cells enhance CD4+ and CD8+ T cell responses to soluble antigen in vivo through direct interaction with dendritic cells. *J Immunol* 2003; **171**:5140-7.

148 Silk JD, Hermans IF, Gileadi U *et al.* Utilizing the adjuvant properties of CD1d-dependent NK T cells in T cell-mediated immunotherapy. *J Clin Invest* 2004; **114**:1800-11.

149 Fuss IJ, Joshi B, Yang Z *et al.* IL-13Ralpha2-bearing, type II NKT cells reactive to sulfatide self-antigen populate the mucosa of ulcerative colitis. *Gut* 2014; **63**:1728-36.

150 de Jong A, Pena-Cruz V, Cheng TY *et al.* CD1a-autoreactive T cells are a normal component of the human alphabeta T cell repertoire. *Nat Immunol* 2010; **11**:1102-9.

151 de Lalla C, Lepore M, Piccolo FM *et al.* High-frequency and adaptive-like dynamics of human CD1 self-reactive T cells. *Eur J Immunol* 2011; **41**:602-10.

152 Lepore M, de Lalla C, Gundimeda SR *et al.* A novel self-lipid antigen targets human T cells against CD1c(+) leukemias. *J Exp Med* 2014; **211**:1363-77.

153 Kasmar AG, van Rhijn I, Cheng TY *et al.* CD1b tetramers bind alphabeta T cell receptors to identify a mycobacterial glycolipid-reactive T cell repertoire in humans. *J Exp Med* 2011; **208**:1741-7.

154 Van Rhijn I, Kasmar A, de Jong A *et al.* A conserved human T cell population targets mycobacterial antigens presented by CD1b. *Nat Immunol* 2013; **14**:706-13.

155 Ly D, Kasmar AG, Cheng TY *et al.* CD1c tetramers detect ex vivo T cell responses to processed phosphomycoketide antigens. *J Exp Med* 2013; **210**:729-41.

156 Matsunaga I, Bhatt A, Young DC *et al.* Mycobacterium tuberculosis pks12 produces a novel polyketide presented by CD1c to T cells. *J Exp Med* 2004; **200**:1559-69.

157 Cerny D, Thi Le DH, The TD *et al.* Complete human CD1a deficiency on Langerhans cells due to a rare point mutation in the coding sequence. *J Allergy Clin Immunol* 2016; **138**:1709-12 e11.

158 Seshadri C, Thuong NT, Yen NT *et al.* A polymorphism in human CD1A is associated with susceptibility to tuberculosis. *Genes Immun* 2014; **15**:195-8.

159 Seshadri C, Shenoy M, Wells RD *et al.* Human CD1a deficiency is common and genetically regulated. *J Immunol* 2013; **191**:1586-93.

160 Mizumoto N, Takashima A. CD1a and langerin: acting as more than Langerhans cell markers. *J Clin Invest* 2004; **113**:658-60.

161 Res P, Blom B, Hori T *et al.* Downregulation of CD1 marks acquisition of functional maturation of human thymocytes and defines a control point in late stages of human T cell development. *J Exp Med* 1997; **185**:141-51.

162 West JA, Olsen SL, Mitchell JM *et al.* Polyclonal T-cells express CD1a in Langerhans cell histiocytosis (LCH) lesions. *PLoS One* 2014; **9**:e109586.

163 Cernadas M, Cavallari M, Watts G *et al.* Early recycling compartment trafficking of CD1a is essential for its intersection and presentation of lipid antigens. *J Immunol* 2010; **184**:1235-41.

164 Zajonc DM, Crispin MD, Bowden TA *et al.* Molecular mechanism of lipopeptide presentation by CD1a. *Immunity* 2005; **22**:209-19.

165 Park JS, Kim JH. Role of non-classical T cells in skin immunity. *Mol Immunol* 2018; **103**:286-92.

166 Bourgeois EA, Subramaniam S, Cheng TY *et al.* Bee venom processes human skin lipids for presentation by CD1a. *J Exp Med* 2015; **212**:149-63.

167 Jarrett R, Salio M, Lloyd-Lavery A *et al.* Filaggrin inhibits generation of CD1a neolipid antigens by house dust mite-derived phospholipase. *Sci Transl Med* 2016; **8**:325ra18.

168 Subramaniam S, Aslam A, Misbah SA *et al.* Elevated and cross-responsive CD1a-reactive T cells in bee and wasp venom allergic individuals. *Eur J Immunol* 2016; **46**:242-52.

169 Agea E, Russano A, Bistoni O *et al.* Human CD1-restricted T cell recognition of lipids from pollens. *J Exp Med* 2005; **202**:295-308.

170 Fithian E, Kung P, Goldstein G *et al.* Reactivity of Langerhans cells with hybridoma antibody. *Proc Natl Acad Sci U S A* 1981; **78**:2541-4.

171 Ruco LP, Uccini S, Baroni CD. The Langerhans' cells. *Allergy* 1989; **44 Suppl 9**:27-30.

172 Jarrett R, Ogg G. Lipid-specific T cells and the skin. *Br J Dermatol* 2016; **175 Suppl 2**:19-25.

173 Van Rhijn I, Ly D, Moody DB. CD1a, CD1b, and CD1c in immunity against mycobacteria. *Adv Exp Med Biol* 2013; **783**:181-97.

174 Cheung KL, Jarrett R, Subramaniam S *et al.* Psoriatic T cells recognize neolipid antigens generated by mast cell phospholipase delivered by exosomes and presented by CD1a. *J Exp Med* 2016; **213**:2399-412.

175 Belkaid Y, Naik S. Compartmentalized and systemic control of tissue immunity by commensals. *Nat Immunol* 2013; **14**:646-53.

176 Baurecht H, Ruhlemann MC, Rodriguez E *et al.* Epidermal lipid composition, barrier integrity, and eczematous inflammation are associated with skin microbiome configuration. *J Allergy Clin Immunol* 2018; **141**:1668-76 e16.

177 Wollenberg A, Kraft S, Hanau D, Bieber T. Immunomorphological and Ultrastructural Characterization of Langerhans Cells and a Novel, Inflammatory Dendritic Epidermal Cell (IDEC) Population in Lesional Skin of Atopic Eczema. *J Invest Dermatol* 1996; **106**:446-53.

178 Langeveld-Wildschut EG, Bruijnzeel PL, Mudde GC *et al.* Clinical and immunologic variables in skin of patients with atopic eczema and either positive or negative atopy patch test reactions. *J Allergy Clin Immunol* 2000; **105**:1008-16.

179 He H, Bissonnette R, Wu J *et al.* Tape strips detect distinct immune and barrier profiles in atopic dermatitis and psoriasis. *J Allergy Clin Immunol* 2021; **147**:199-212.

180 Chen YL, Gomes T, Hardman CS *et al.* Re-evaluation of human BDCA-2+ DC during acute sterile skin inflammation. *J Exp Med* 2020; **217**.

181 Fahlen A, Engstrand L, Baker BS *et al.* Comparison of bacterial microbiota in skin biopsies from normal and psoriatic skin. *Arch Dermatol Res* 2012; **304**:15-22.

182 Fry L, Baker BS. Triggering psoriasis: the role of infections and medications. *Clin Dermatol* 2007; **25**:606-15.

183 Gao Z, Tseng CH, Strober BE *et al.* Substantial alterations of the cutaneous bacterial biota in psoriatic lesions. *PLoS One* 2008; **3**:e2719.

184 Gros E, Bussmann C, Bieber T *et al.* Expression of chemokines and chemokine receptors in lesional and nonlesional upper skin of patients with atopic dermatitis. *J Allergy Clin Immunol* 2009; **124**:753-60 e1.

185 Leung DY. Role of IgE in atopic dermatitis. *Curr Opin Immunol* 1993; **5**:956-62.

186 Palmer CN, Irvine AD, Terron-Kwiatkowski A *et al.* Common loss-of-function variants of the epidermal barrier protein filaggrin are a major predisposing factor for atopic dermatitis. *Nat Genet* 2006; **38**:441-6.

187 Zheng Y, Danilenko DM, Valdez P *et al.* Interleukin-22, a T(H)17 cytokine, mediates IL-23-induced dermal inflammation and acanthosis. *Nature* 2007; **445**:648-51.

188 Ansari MN, Nicolaides N, Fu HC. Fatty acid composition of the living layer and stratum corneum lipids of human sole skin epidermis. *Lipids* 1970; **5**:838-45.

189 Gong JQ, Lin L, Lin T *et al.* Skin colonization by Staphylococcus aureus in patients with eczema and atopic dermatitis and relevant combined topical therapy: a double-blind multicentre randomized controlled trial. *Br J Dermatol* 2006; **155**:680-7.

190 Moody DB, Suliman S. CD1: From Molecules to Diseases. *F1000Res* 2017; **6**:1909.

191 Fujii S, Shimizu K, Okamoto Y *et al.* NKT cells as an ideal anti-tumor immunotherapeutic. *Front Immunol* 2013; **4**:409.

192 Kharkwal SS, Arora P, Porcelli SA. Glycolipid activators of invariant NKT cells as vaccine adjuvants. *Immunogenetics* 2016; **68**:597-610.

193 Motohashi S, Nagato K, Kunii N *et al.* A phase I-II study of alpha-galactosylceramide-pulsed IL-2/GM-CSF-cultured peripheral blood mononuclear cells in patients with advanced and recurrent non-small cell lung cancer. *J Immunol* 2009; **182**:2492-501.

194 Schneiders FL, Scheper RJ, von Blomberg BME *et al.* Clinical experience with α-galactosylceramide (KRN7000) in patients with advanced cancer and chronic hepatitis B/C infection. *Clin Immunol* 2011; **140**:130-41.

195 Tefit JN, Crabe S, Orlandini B *et al.* Efficacy of ABX196, a new NKT agonist, in prophylactic human vaccination. *Vaccine* 2014; **32**:6138-45.

196 Zhao J, Siddiqui S, Shang S *et al.* Mycolic acid-specific T cells protect against Mycobacterium tuberculosis infection in a humanized transgenic mouse model. *Elife* 2015; **4**:e08525.

197 Dascher CC, Hiromatsu K, Xiong X *et al.* Immunization with a mycobacterial lipid vaccine improves pulmonary pathology in the guinea pig model of tuberculosis. *Int Immunol* 2003; **15**:915-25.

198 Larrouy-Maumus G, Layre E, Clark S *et al.* Protective efficacy of a lipid antigen vaccine in a guinea pig model of tuberculosis. *Vaccine* 2017; **35**:1395-402.

199 Kawasaki N, Rillahan CD, Cheng TY *et al.* Targeted delivery of mycobacterial antigens to human dendritic cells via Siglec-7 induces robust T cell activation. *J Immunol* 2014; **193**:1560-6.

200 Nicolai S, Wegrecki M, Cheng TY *et al.* Human T cell response to CD1a and contact dermatitis allergens in botanical extracts and commercial skin care products. *Sci Immunol* 2020; **5**:eaax5430.

201 Wang B, Morinobu A, Horiuchi M *et al.* Butyrate inhibits functional differentiation of human monocyte-derived dendritic cells. *Cell Immunol* 2008; **253**:54-58.

202 Nascimento CR, Freire-de-Lima CG, da Silva de Oliveira A *et al.* The short chain fatty acid sodium butyrate regulates the induction of CD1a in developing dendritic cells. *Immunobiology* 2011; **216**:275-84.

203 Radojević D, Tomić S, Mihajlović D *et al.* Fecal microbiota composition associates with the capacity of human peripheral blood monocytes to differentiate into immunogenic dendritic cells in vitro. *Gut Microbes* 2021; **13**:1-20.

204 Sakaguchi S, Yamaguchi T, Nomura T, Ono M. Regulatory T cells and immune tolerance. *Cell* 2008; **133**:775-87.

205 Fontenot JD, Gavin MA, Rudensky AY. Foxp3 programs the development and function of CD4+CD25+ regulatory T cells. *Nat Immunol* 2003; **4**:330-6.

206 Hori S, Nomura T, Sakaguchi S. Control of regulatory T cell development by the transcription factor Foxp3. *Science* 2003; **299**:1057-61.

207 Sakaguchi S, Ono M, Setoguchi R *et al.* Foxp3+ CD25+ CD4+ natural regulatory T cells in dominant self-tolerance and autoimmune disease. *Immunol Rev* 2006; **212**:8-27.

208 Hsieh CS, Lee HM, Lio CWJ. Selection of regulatory T cells in the thymus. *Nat Rev Immunol* 2012; **12**:157-67.

209 Josefowicz SZ, Lu LF, Rudensky AY. Regulatory T cells: mechanisms of differentiation and function. *Annu Rev Immunol* 2012; **30**:531-64.

210 Abbas AK, Benoist C, Bluestone JA *et al.* Regulatory T cells: recommendations to simplify the nomenclature. *Nat Immunol* 2013; **14**:307-08.

211 Kanamori M, Nakatsukasa H, Okada M *et al.* Induced Regulatory T Cells: Their Development, Stability, and Applications. *Trends Immunol* 2016; **37**:803-11.

212 Ohkura N, Hamaguchi M, Morikawa H *et al.* T cell receptor stimulation-induced epigenetic changes and Foxp3 expression are independent and complementary events required for Treg cell development. *Immunity* 2012; **37**:785-99.

213 Ohkura N, Sakaguchi S. Transcriptional and epigenetic basis of Treg cell development and function: its genetic anomalies or variations in autoimmune diseases. *Cell Res* 2020; **30**:1-10.

214 Polansky JK, Kretschmer K, Freyer J *et al.* DNA methylation controls Foxp3 gene expression. *Eur J Immunol* 2008; **38**:1654-63.

215 Josefowicz SZ, Niec RE, Kim HY *et al.* Extrathymically generated regulatory T cells control mucosal TH2 inflammation. *Nature* 2012; **482**:395-99.

216 Schlenner SM, Weigmann B, Ruan Q *et al.* Smad3 binding to the foxp3 enhancer is dispensable for the development of regulatory T cells with the exception of the gut. *J Exp Med* 2012; **209**:1529-35.

217 Zheng Y, Josefowicz S, Chaudhry A *et al.* Role of conserved non-coding DNA elements in the Foxp3 gene in regulatory T-cell fate. *Nature* 2010; **463**:808-12.

218 Miyao T, Floess S, Setoguchi R *et al.* Plasticity of Foxp3(+) T cells reflects promiscuous Foxp3 expression in conventional T cells but not reprogramming of regulatory T cells. *Immunity* 2012; **36**:262-75.

219 Thornton AM, Korty PE, Tran DQ *et al.* Expression of Helios, an Ikaros transcription factor family member, differentiates thymic-derived from peripherally induced Foxp3+ T regulatory cells. *J Immunol* 2010; **184**:3433-41.

220 Weiss JM, Bilate AM, Gobert M *et al.* Neuropilin 1 is expressed on thymus-derived natural regulatory T cells, but not mucosa-generated induced Foxp3+ T reg cells. *J Exp Med* 2012; **209**:1723-42.

221 Yadav M, Louvet C, Davini D *et al.* Neuropilin-1 distinguishes natural and inducible regulatory T cells among regulatory T cell subsets in vivo. *J Exp Med* 2012; **209**:1713-22.

222 Akimova T, Beier UH, Wang L *et al.* Helios expression is a marker of T cell activation and proliferation. *PLoS One* 2011; **6**:e24226.

223 Gottschalk RA, Corse E, Allison JP. Expression of Helios in peripherally induced Foxp3+ regulatory T cells. *J Immunol* 2012; **188**:976-80.

224 Petzold C, Steinbronn N, Gereke M *et al.* Fluorochrome-based definition of naturally occurring Foxp3(+) regulatory T cells of intra- and extrathymic origin. *Eur J Immunol* 2014; **44**:3632-45.

225 Szurek E, Cebula A, Wojciech L *et al.* Differences in Expression Level of Helios and Neuropilin-1 Do Not Distinguish Thymus-Derived from Extrathymically-Induced CD4+Foxp3+ Regulatory T Cells. *PLoS One* 2015; **10**:e0141161.

226 Wang J, Ioan-Facsinay A, van der Voort EI *et al.* Transient expression of FOXP3 in human activated nonregulatory CD4+ T cells. *Eur J Immunol* 2007; **37**:129-38.

227 Read S, Malmstrom V, Powrie F. Cytotoxic T lymphocyte-associated antigen 4 plays an essential role in the function of CD25(+)CD4(+) regulatory cells that control intestinal inflammation. *J Exp Med* 2000; **192**:295-302.

228 Takahashi T, Tagami T, Yamazaki S *et al.* Immunologic self-tolerance maintained by CD25(+)CD4(+) regulatory T cells constitutively expressing cytotoxic T lymphocyte-associated antigen 4. *J Exp Med* 2000; **192**:303-10.

229 McHugh RS, Whitters MJ, Piccirillo CA *et al.* CD4(+)CD25(+) immunoregulatory T cells: gene expression analysis reveals a functional role for the glucocorticoid-induced TNF receptor. *Immunity* 2002; **16**:311-23.

230 Chen W, Jin W, Hardegen N *et al.* Conversion of peripheral CD4+CD25- naive T cells to CD4+CD25+ regulatory T cells by TGF-beta induction of transcription factor Foxp3. *J Exp Med* 2003; **198**:1875-86.

231 Fisson S, Darrasse-Jeze G, Litvinova E *et al.* Continuous activation of autoreactive CD4+ CD25+ regulatory T cells in the steady state. *J Exp Med* 2003; **198**:737-46.

232 Miyara M, Yoshioka Y, Kitoh A *et al.* Functional delineation and differentiation dynamics of human CD4+ T cells expressing the FoxP3 transcription factor. *Immunity* 2009; **30**:899-911.

233 Thornton AM, Shevach EM. Suppressor effector function of CD4+CD25+ immunoregulatory T cells is antigen nonspecific. *J Immunol* 2000; **164**:183-90.

234 Beissert S, Schwarz A, Schwarz T. Regulatory T cells. *J Invest Dermatol* 2006; **126**:15-24.

235 Sharma A, Rudra D. Emerging Functions of Regulatory T Cells in Tissue Homeostasis. *Front Immunol* 2018; **9**:883.

236 Grant CR, Liberal R, Mieli-Vergani G *et al.* Regulatory T-cells in autoimmune diseases: Challenges, controversies and-yet-unanswered questions. *Autoimmun Rev* 2015; **14**:105-16.

237 Martín-Orozco E, Norte-Muñoz M, Martínez-García J. Regulatory T cells in allergy and asthma. *Front Pediatr* 2017; **5**:117.

238 Dombrowski Y, O'Hagan T, Dittmer M *et al.* Regulatory T cells promote myelin regeneration in the central nervous system. *Nat Neurosci* 2017; **20**:674-80.

239 Aluvihare VR, Kallikourdis M, Betz AG. Regulatory T cells mediate maternal tolerance to the fetus. *Nat Immunol* 2004; **5**:266-71.

240 Feuerer M, Herrero L, Cipolletta D *et al.* Lean, but not obese, fat is enriched for a unique population of regulatory T cells that affect metabolic parameters. *Nat Med* 2009; **15**:930-9.

241 Hansson GK, Hermansson A. The immune system in atherosclerosis. *Nat Immunol* 2011; **12**:204-12.

242 Godfrey VL, Wilkinson JE, Rinchik EM, Russell LB. Fatal lymphoreticular disease in the scurfy (sf) mouse requires T cells that mature in a sf thymic environment: potential model for thymic education. *Proc Natl Acad Sci U S A* 1991; **88**:5528-32.

243 Bacchetta R, Barzaghi F, Roncarolo MG. From IPEX syndrome to FOXP3 mutation: a lesson on immune dysregulation. *Ann N Y Acad Sci* 2018; **1417**:5-22.

244 Powell BR, Buist NR, Stenzel P. An X-linked syndrome of diarrhea, polyendocrinopathy, and fatal infection in infancy. *J Pediatr* 1982; **100**:731-7.

245 Malek TR, Castro I. Interleukin-2 Receptor Signaling: At the Interface between Tolerance and Immunity. *Immunity* 2010; **33**:153-65.

246 Walker LSK, Sansom DM. The emerging role of CTLA4 as a cell-extrinsic regulator of T cell responses. *Nat Rev Immunol* 2011; **11**:852-63.

247 Sakaguchi S, Wing K, Onishi Y *et al.* Regulatory T cells: how do they suppress immune responses? *Int Immunol* 2009; **21**:1105-11.

248 Schmidt A, Oberle N, Krammer PH. Molecular mechanisms of Treg-mediated T cell suppression. *Front Immunol* 2012; **3**:51.

249 Cao X, Cai SF, Fehniger TA *et al.* Granzyme B and perforin are important for regulatory T cell-mediated suppression of tumor clearance. *Immunity* 2007; **27**:635-46.

250 Gondek DC, Lu LF, Quezada SA *et al.* Cutting edge: contact-mediated suppression by CD4+CD25+ regulatory cells involves a granzyme B-dependent, perforin-independent mechanism. *J Immunol* 2005; **174**:1783-6.

251 Paust S, Lu L, McCarty N, Cantor H. Engagement of B7 on effector T cells by regulatory T cells prevents autoimmune disease. *Proc Natl Acad Sci U S A* 2004; **101**:10398-403.

252 Deaglio S, Dwyer KM, Gao W *et al.* Adenosine generation catalyzed by CD39 and CD73 expressed on regulatory T cells mediates immune suppression. *J Exp Med* 2007; **204**:1257-65.

253 Onishi Y, Fehervari Z, Yamaguchi T, Sakaguchi S. Foxp3+ natural regulatory T cells preferentially form aggregates on dendritic cells in vitro and actively inhibit their maturation. *Proc Natl Acad Sci U S A* 2008; **105**:10113-8.

254 Wing JB, Ise W, Kurosaki T, Sakaguchi S. Regulatory T cells control antigen-specific expansion of Tfh cell number and humoral immune responses via the coreceptor CTLA-4. *Immunity* 2014; **41**:1013-25.

255 Wing K, Onishi Y, Prieto-Martin P *et al.* CTLA-4 control over Foxp3+ regulatory T cell function. *Science* 2008; **322**:271-5.

256 Qureshi OS, Zheng Y, Nakamura K *et al.* Trans-endocytosis of CD80 and CD86: a molecular basis for the cell-extrinsic function of CTLA-4. *Science* 2011; **332**:600-3.

257 Fontenot JD, Rasmussen JP, Gavin MA, Rudensky AY. A function for interleukin 2 in Foxp3-expressing regulatory T cells. *Nat Immunol* 2005; **6**:1142-51.

258 Setoguchi R, Hori S, Takahashi T, Sakaguchi S. Homeostatic maintenance of natural Foxp3(+) CD25(+) CD4(+) regulatory T cells by interleukin (IL)-2 and induction of autoimmune disease by IL-2 neutralization. *J Exp Med* 2005; **201**:723-35.

259 Pandiyan P, Zheng L, Ishihara S *et al.* CD4+CD25+Foxp3+ regulatory T cells induce cytokine deprivation-mediated apoptosis of effector CD4+ T cells. *Nat Immunol* 2007; **8**:1353-62.

260 Sitrin J, Ring A, Garcia KC *et al.* Regulatory T cells control NK cells in an insulitic lesion by depriving them of IL-2. *J Exp Med* 2013; **210**:1153-65.

261 Moore KW, de Waal Malefyt R, Coffman RL, O'Garra A. Interleukin-10 and the interleukin-10 receptor. *Annu Rev Immunol* 2001; **19**:683-765.

262 O'Garra A, Vieira P. TH1 cells control themselves by producing interleukin-10. *Nat Rev Immunol* 2007; **7**:425-28.

263 Vieira P, de Waal-Malefyt R, Dang MN *et al.* Isolation and expression of human cytokine synthesis inhibitory factor cDNA clones: homology to Epstein-Barr virus open reading frame BCRFI. *Proc Natl Acad Sci U S A* 1991; **88**:1172-6.

264 Walter MR. The molecular basis of IL-10 function: From receptor structure to the onset of signaling. *Curr Top Microbiol Immunol* 2014; **380**:191-212.

265 Zdanov A, Schalk-Hihi C, Wlodawer A. Crystal structure of human interleukin-10 at 1.6 A resolution and a model of a complex with its soluble receptor. *Protein Sci* 1996; **5**:1955-62.

266 Kotenko SV, Krause CD, Izotova LS *et al.* Identification and functional characterization of a second chain of the interleukin-10 receptor complex. *EMBO J* 1997; **16**:5894-903.

267 Liu Y, Wei SH, Ho AS *et al.* Expression cloning and characterization of a human IL-10 receptor. *J Immunol* 1994; **152**:1821-9.

268 Mittal SK, Roche PA. Suppression of antigen presentation by IL-10. *Curr Opin Immunol* 2015; **34**:22-27.

269 Akdis CA, Joss A, Akdis M *et al.* A molecular basis for T cell suppression by IL-10: CD28-associated IL-10 receptor inhibits CD28 tyrosine phosphorylation and phosphatidylinositol 3-kinase binding. *FASEB J* 2000; **14**:1666-8.

270 Oral HB, Kotenko SV, Yilmaz M *et al.* Regulation of T cells and cytokines by the interleukin-10 (IL-10)-family cytokines IL-19, IL-20, IL-22, IL-24 and IL-26. *Eur J Immunol* 2006; **36**:380-8.

271 Taylor A, Akdis M, Joss A *et al.* IL-10 inhibits CD28 and ICOS costimulations of T cells via src homology 2 domain-containing protein tyrosine phosphatase 1. *J Allergy Clin Immunol* 2007; **120**:76-83.

272 Murai M, Turovskaya O, Kim G *et al.* Interleukin 10 acts on regulatory T cells to maintain expression of the transcription factor Foxp3 and suppressive function in mice with colitis. *Nat Immunol* 2009; **10**:1178-84.

273 Rubtsov YP, Rasmussen JP, Chi EY *et al.* Regulatory T cell-derived interleukin-10 limits inflammation at environmental interfaces. *Immunity* 2008; **28**:546-58.

274 Sojka DK, Fowell DJ. Regulatory T cells inhibit acute IFN-gamma synthesis without blocking T-helper cell type 1 (Th1) differentiation via a compartmentalized requirement for IL-10. *Proc Natl Acad Sci U S A* 2011; **108**:18336-41.

275 Gleizes P-E, Munger JS, Nunes I *et al.* TGF-β Latency: Biological Significance and Mechanisms of Activation. *Stem Cells* 1997; **15**:190-97.

276 Munger JS, Harpel JG, Gleizes PE *et al.* Latent transforming growth factor-beta: structural features and mechanisms of activation. *Kidney Int* 1997; **51**:1376-82.

277 Shi M, Zhu J, Wang R *et al.* Latent TGF-β structure and activation. *Nature* 2011; **474**:343-49.

278 Stockis J, Colau D, Coulie PG, Lucas S. Membrane protein GARP is a receptor for latent TGF-beta on the surface of activated human Treg. *Eur J Immunol* 2009; **39**:3315-22.

279 Tran DQ, Andersson J, Wang R *et al.* GARP (LRRC32) is essential for the surface expression of latent TGF-beta on platelets and activated FOXP3+ regulatory T cells. *Proc Natl Acad Sci U S A* 2009; **106**:13445-50.

280 Wang R, Kozhaya L, Mercer F *et al.* Expression of GARP selectively identifies activated human FOXP3+ regulatory T cells. *Proc Natl Acad Sci U S A* 2009; **106**:13439-44.

281 Travis MA, Sheppard D. TGF-beta activation and function in immunity. *Annu Rev Immunol* 2014; **32**:51-82.

282 Batlle E, Massague J. Transforming Growth Factor-beta Signaling in Immunity and Cancer. *Immunity* 2019; **50**:924-40.

283 Hayashi H, Abdollah S, Qiu Y *et al.* The MAD-related protein Smad7 associates with the TGFbeta receptor and functions as an antagonist of TGFbeta signaling. *Cell* 1997; **89**:1165-73.

284 Massagué J. TGFβ signalling in context. *Nat Rev Mol Cell Biol* 2012; **13**:616-30.

285 Nakao A, Afrakhte M, Morén A *et al.* Identification of Smad7, a TGFbeta-inducible antagonist of TGF-beta signalling. *Nature* 1997; **389**:631-5.

286 Frimpong-Boateng K, van Rooijen N, Geiben-Lynn R. Regulatory T cells suppress natural killer cells during plasmid DNA vaccination in mice, blunting the CD8+ T cell immune response by the cytokine TGFbeta. *PLoS One* 2010; **5**:e12281.

287 Wahl SM, Wen J, Moutsopoulos NM. The kiss of death: interrupted by NK-cell close encounters of another kind. *Trends Immunol* 2006; **27**:161-4.

288 Ghiringhelli F, Ménard C, Terme M *et al.* CD4+CD25+ regulatory T cells inhibit natural killer cell functions in a transforming growth factor-beta-dependent manner. *J Exp Med* 2005; **202**:1075-85.

289 Mempel TR, Pittet MJ, Khazaie K *et al.* Regulatory T cells reversibly suppress cytotoxic T cell function independent of effector differentiation. *Immunity* 2006; **25**:129-41.

290 Chen ML, Pittet MJ, Gorelik L *et al.* Regulatory T cells suppress tumor-specific CD8 T cell cytotoxicity through TGF-beta signals in vivo. *Proc Natl Acad Sci U S A* 2005; **102**:419-24.

291 Gershon RK, Kondo K. Infectious immunological tolerance. *Immunology* 1971; **21**:903-14.

292 Tran DQ. TGF-beta: the sword, the wand, and the shield of FOXP3(+) regulatory T cells. *J Mol Cell Biol* 2012; **4**:29-37.

293 Marie JC, Liggitt D, Rudensky AY. Cellular mechanisms of fatal early-onset autoimmunity in mice with the T cell-specific targeting of transforming growth factor-beta receptor. *Immunity* 2006; **25**:441-54.

294 Li MO, Sanjabi S, Flavell RA. Transforming growth factor-beta controls development, homeostasis, and tolerance of T cells by regulatory T cell-dependent and -independent mechanisms. *Immunity* 2006; **25**:455-71.

295 Gorelik L, Flavell RA. Abrogation of TGFbeta signaling in T cells leads to spontaneous T cell differentiation and autoimmune disease. *Immunity* 2000; **12**:171-81.

296 Kulkarni AB, Huh CG, Becker D *et al.* Transforming growth factor beta 1 null mutation in mice causes excessive inflammatory response and early death. *Proc Natl Acad Sci U S A* 1993; **90**:770-4.

297 Shull MM, Ormsby I, Kier AB *et al.* Targeted disruption of the mouse transforming growth factor-beta 1 gene results in multifocal inflammatory disease. *Nature* 1992; **359**:693-9.

298 Gutcher I, Donkor MK, Ma Q *et al.* Autocrine transforming growth factor-β1 promotes in vivo Th17 cell differentiation. *Immunity* 2011; **34**:396-408.

299 Marie JC, Letterio JJ, Gavin M, Rudensky AY. TGF-beta1 maintains suppressor function and Foxp3 expression in CD4+CD25+ regulatory T cells. *J Exp Med* 2005; **201**:1061-7.

300 Travis MA, Reizis B, Melton AC *et al.* Loss of integrin alpha(v)beta8 on dendritic cells causes autoimmunity and colitis in mice. *Nature* 2007; **449**:361-5.

301 DiSpirito JR, Zemmour D, Ramanan D *et al.* Molecular diversification of regulatory T cells in nonlymphoid tissues. *Sci Immunol* 2018; **3**:eaat5861.

302 Miragaia RJ, Gomes T, Chomka A *et al.* Single-Cell Transcriptomics of Regulatory T Cells Reveals Trajectories of Tissue Adaptation. *Immunity* 2019; **50**:493-504.e7.

303 Panduro M, Benoist C, Mathis D. Tissue Tregs. *Annu Rev Immunol* 2016; **34**:609-33.

304 Szabo PA, Levitin HM, Miron M *et al.* Single-cell transcriptomics of human T cells reveals tissue and activation signatures in health and disease. *Nat Commun* 2019; **10**:4706.

305 Whibley N, Tucci A, Powrie F. Regulatory T cell adaptation in the intestine and skin. *Nat Immunol* 2019; **20**:386-96.

306 Liston A, Gray DHD. Homeostatic control of regulatory T cell diversity. *Nat Rev Immunol* 2014; **14**:154-65.

307 Dudda JC, Perdue N, Bachtanian E, Campbell DJ. Foxp3+ regulatory T cells maintain immune homeostasis in the skin. *J Exp Med* 2008; **205**:1559-65.

308 Halabi-Tawil M, Ruemmele FM, Fraitag S *et al.* Cutaneous manifestations of immune dysregulation, polyendocrinopathy, enteropathy, X-linked (IPEX) syndrome. *Br J Dermatol* 2009; **160**:645-51.

309 Sather BD, Treuting P, Perdue N *et al.* Altering the distribution of Foxp3(+) regulatory T cells results in tissue-specific inflammatory disease. *J Exp Med* 2007; **204**:1335-47.

310 Suffia I, Reckling SK, Salay G, Belkaid Y. A role for CD103 in the retention of CD4+CD25+ Treg and control of Leishmania major infection. *J Immunol* 2005; **174**:5444-55.

311 Stephens LA, Mottet C, Mason D, Powrie F. Human CD4(+)CD25(+) thymocytes and peripheral T cells have immune suppressive activity in vitro. *Eur J Immunol* 2001; **31**:1247-54.

312 Dieckmann D, Plottner H, Berchtold S *et al.* Ex vivo isolation and characterization of CD4(+)CD25(+) T cells with regulatory properties from human blood. *J Exp Med* 2001; **193**:1303-10.

313 Levings MK, Sangregorio R, Roncarolo MG. Human cd25(+)cd4(+) t regulatory cells suppress naive and memory T cell proliferation and can be expanded in vitro without loss of function. *J Exp Med* 2001; **193**:1295-302.

314 Jonuleit H, Schmitt E, Stassen M *et al.* Identification and functional characterization of human CD4(+)CD25(+) T cells with regulatory properties isolated from peripheral blood. *J Exp Med* 2001; **193**:1285-94.

315 Taams LS, Smith J, Rustin MH *et al.* Human anergic/suppressive CD4(+)CD25(+) T cells: a highly differentiated and apoptosis-prone population. *Eur J Immunol* 2001; **31**:1122-31.

316 Fuhlbrigge RC, Kieffer JD, Armerding D, Kupper TS. Cutaneous lymphocyte antigen is a specialized form of PSGL-1 expressed on skin-homing T cells. *Nature* 1997; **389**:978-81.

317 Hirahara K, Liu L, Clark RA *et al.* The majority of human peripheral blood CD4+CD25highFoxp3+ regulatory T cells bear functional skin-homing receptors. *J Immunol* 2006; **177**:4488-94.

318 Iellem A, Colantonio L, D'Ambrosio D. Skin-versus gut-skewed homing receptor expression and intrinsic CCR4 expression on human peripheral blood CD4+CD25+ suppressor T cells. *Eur J Immunol* 2003; **33**:1488-96.

319 Malhotra N, Leyva-Castillo JM, Jadhav U *et al.* RORα-expressing T regulatory cells restrain allergic skin inflammation. *Sci Immunol* 2018; **3**:eaao6923.

320 Wohlfert EA, Grainger JR, Bouladoux N *et al.* GATA3 controls Foxp3$^+$ regulatory T cell fate during inflammation in mice. *J Clin Invest* 2011; **121**:4503-15.

321 Yamazaki S, Nishioka A, Kasuya S *et al.* Homeostasis of thymus-derived Foxp3+ regulatory T cells is controlled by ultraviolet B exposure in the skin. *J Immunol* 2014; **193**:5488-97.

322 Delacher M, Imbusch CD, Weichenhan D *et al.* Genome-wide DNA-methylation landscape defines specialization of regulatory T cells in tissues. *Nat Immunol* 2017; **18**:1160-72.

323 Harrison OJ, Linehan JL, Shih HY *et al.* Commensal-specific T cell plasticity promotes rapid tissue adaptation to injury. *Science* 2019; **363**:eaat6280.

324 Scharschmidt TC, Vasquez KS, Truong HA *et al.* A Wave of Regulatory T Cells into Neonatal Skin Mediates Tolerance to Commensal Microbes. *Immunity* 2015; **43**:1011-21.

325 Gratz IK, Truong HA, Yang SH *et al.* Cutting Edge: memory regulatory t cells require IL-7 and not IL-2 for their maintenance in peripheral tissues. *J Immunol* 2013; **190**:4483-87.

326 Scharschmidt TC, Vasquez KS, Pauli ML *et al.* Commensal Microbes and Hair Follicle Morphogenesis Coordinately Drive Treg Migration into Neonatal Skin. *Cell Host Microbe* 2017; **21**:467-77.e5.

327 Leech JM, Dhariwala MO, Lowe MM *et al.* Toxin-Triggered Interleukin-1 Receptor Signaling Enables Early-Life Discrimination of Pathogenic versus Commensal Skin Bacteria. *Cell Host Microbe* 2019; **26**:795-809.e5.

328 Sakaguchi S, Mikami N, Wing JB *et al.* Regulatory T Cells and Human Disease. *Annu Rev Immunol* 2020; **38**:541-66.

329 Bluestone JA, Buckner JH, Fitch M *et al.* Type 1 diabetes immunotherapy using polyclonal regulatory T cells. *Sci Transl Med* 2015; **7**:315ra189.

330 Brunstein CG, Miller JS, McKenna DH *et al.* Umbilical cord blood-derived T regulatory cells to prevent GVHD: kinetics, toxicity profile, and clinical effect. *Blood* 2016; **127**:1044-51.

331 Hippen KL, Merkel SC, Schirm DK *et al.* Massive ex vivo expansion of human natural regulatory T cells (T(regs)) with minimal loss of in vivo functional activity. *Sci Transl Med* 2011; **3**:83ra41.

332 Esensten JH, Muller YD, Bluestone JA, Tang Q. Regulatory T-cell therapy for autoimmune and autoinflammatory diseases: The next frontier. *J Allergy Clin Immunol* 2018; **142**:1710-18.

333 Harden PN, Game DS, Sawitzki B *et al.* Feasibility, long-term safety, and immune monitoring of regulatory T cell therapy in living donor kidney transplant recipients. *Am J Transplant* 2021; **21**:1603-11.

334 Sawitzki B, Harden PN, Reinke P *et al.* Regulatory cell therapy in kidney transplantation (The ONE Study): a harmonised design and analysis of seven non-randomised, single-arm, phase 1/2A trials. *Lancet* 2020; **395**:1627-39.

335 Fraser H, Safinia N, Grageda N *et al.* A Rapamycin-Based GMP-Compatible Process for the Isolation and Expansion of Regulatory T Cells for Clinical Trials. *Mol Ther Methods Clin Dev* 2018; **8**:198-209.

336 MacDonald KN, Piret JM, Levings MK. Methods to manufacture regulatory T cells for cell therapy. *Clin Exp Immunol* 2019; **197**:52-63.

337 Duggleby RC, Shaw TN, Jarvis LB *et al.* CD27 expression discriminates between regulatory and non-regulatory cells after expansion of human peripheral blood CD4+ CD25+ cells. *Immunology* 2007; **121**:129-39.

338 Coenen JJ, Koenen HJ, van Rijssen E *et al.* Rapamycin, and not cyclosporin A, preserves the highly suppressive CD27+ subset of human CD4+CD25+ regulatory T cells. *Blood* 2006; **107**:1018-23.

339 Ruprecht CR, Gattorno M, Ferlito F *et al.* Coexpression of CD25 and CD27 identifies FoxP3+ regulatory T cells in inflamed synovia. *J Exp Med* 2005; **201**:1793-803.

340 Nadig SN, Wieckiewicz J, Wu DC *et al.* In vivo prevention of transplant arteriosclerosis by ex vivo-expanded human regulatory T cells. *Nat Med* 2010; **16**:809-13.

341 Arroyo Hornero R, Georgiadis C, Hua P *et al.* CD70 expression determines the therapeutic efficacy of expanded human regulatory T cells. *Commun Biol* 2020; **3**:375.

342 Zhang Q, Lu W, Liang CL *et al.* Chimeric Antigen Receptor (CAR) Treg: A Promising Approach to Inducing Immunological Tolerance. *Front Immunol* 2018; **9**:2359.

343 Boardman DA, Philippeos C, Fruhwirth GO *et al.* Expression of a Chimeric Antigen Receptor Specific for Donor HLA Class I Enhances the Potency of Human Regulatory T Cells in Preventing Human Skin Transplant Rejection. *Am J Transplant* 2017; **17**:931-43.

344 MacDonald KG, Hoeppli RE, Huang Q *et al.* Alloantigen-specific regulatory T cells generated with a chimeric antigen receptor. *J Clin Invest* 2016; **126**:1413-24.

345 Noyan F, Zimmermann K, Hardtke-Wolenski M *et al.* Prevention of Allograft Rejection by Use of Regulatory T Cells With an MHC-Specific Chimeric Antigen Receptor. *Am J Transplant* 2017; **17**:917-30.

346 Matsuoka K, Koreth J, Kim HT *et al.* Low-dose interleukin-2 therapy restores regulatory T cell homeostasis in patients with chronic graft-versus-host disease. *Sci Transl Med* 2013; **5**:179ra43.

347 Hartemann A, Bensimon G, Payan CA *et al.* Low-dose interleukin 2 in patients with type 1 diabetes: a phase 1/2 randomised, double-blind, placebo-controlled trial. *Lancet Diabetes Endocrinol* 2013; **1**:295-305.

348 Yu A, Snowhite I, Vendrame F *et al.* Selective IL-2 responsiveness of regulatory T cells through multiple intrinsic mechanisms supports the use of low-dose IL-2 therapy in type 1 diabetes. *Diabetes* 2015; **64**:2172-83.

349 Castela E, Le Duff F, Butori C *et al.* Effects of low-dose recombinant interleukin 2 to promote T-regulatory cells in alopecia areata. *JAMA Dermatol* 2014; **150**:748-51.

350 von Spee-Mayer C, Siegert E, Abdirama D *et al.* Low-dose interleukin-2 selectively corrects regulatory T cell defects in patients with systemic lupus erythematosus. *Ann Rheum Dis* 2016; **75**:1407-15.

351 He J, Zhang X, Wei Y *et al.* Low-dose interleukin-2 treatment selectively modulates CD4(+) T cell subsets in patients with systemic lupus erythematosus. *Nat Med* 2016; **22**:991-93.

352 Van Gool F, Molofsky AB, Morar MM *et al.* Interleukin-5-producing group 2 innate lymphoid cells control eosinophilia induced by interleukin-2 therapy. *Blood* 2014; **124**:3572-76.

353 Hirakawa M, Matos TR, Liu H *et al.* Low-dose IL-2 selectively activates subsets of CD4(+) Tregs and NK cells. *JCI Insight* 2016; **1**:e89278.

354 Tang Q, Adams JY, Penaranda C *et al.* Central role of defective interleukin-2 production in the triggering of islet autoimmune destruction. *Immunity* 2008; **28**:687-97.

355 Weishaupt A, Paulsen D, Werner S *et al.* The T cell-selective IL-2 mutant AIC284 mediates protection in a rat model of Multiple Sclerosis. *J Neuroimmunol* 2015; **282**:63-72.

356 Rosenzwajg M, Lorenzon R, Cacoub P *et al.* Immunological and clinical effects of low-dose interleukin-2 across 11 autoimmune diseases in a single, open clinical trial. *Ann Rheum Dis* 2019; **78**:209-17.

357 Haxhinasto S, Mathis D, Benoist C. The AKT-mTOR axis regulates de novo differentiation of CD4+Foxp3+ cells. *J Exp Med* 2008; **205**:565-74.

358 Sauer S, Bruno L, Hertweck A *et al.* T cell receptor signaling controls Foxp3 expression via PI3K, Akt, and mTOR. *Proc Natl Acad Sci U S A* 2008; **105**:7797-802.

359 Tanaka A, Sakaguchi S. Regulatory T cells in cancer immunotherapy. *Cell Res* 2017; **27**:109-18.

360 Arce Vargas F, Furness AJS, Solomon I *et al.* Fc-Optimized Anti-CD25 Depletes Tumor-Infiltrating Regulatory T Cells and Synergizes with PD-1 Blockade to Eradicate Established Tumors. *Immunity* 2017; **46**:577-86.

361 Ha D, Tanaka A, Kibayashi T *et al.* Differential control of human Treg and effector T cells in tumor immunity by Fc-engineered anti-CTLA-4 antibody. *Proc Natl Acad Sci U S A* 2019; **116**:609-18.

362 Selby MJ, Engelhardt JJ, Quigley M *et al.* Anti-CTLA-4 antibodies of IgG2a isotype enhance antitumor activity through reduction of intratumoral regulatory T cells. *Cancer Immunol Res* 2013; **1**:32-42.

363 Simpson TR, Li F, Montalvo-Ortiz W *et al.* Fc-dependent depletion of tumor-infiltrating regulatory T cells co-defines the efficacy of anti-CTLA-4 therapy against melanoma. *J Exp Med* 2013; **210**:1695-710.

364 Rosat JP, Grant EP, Beckman EM *et al.* CD1-restricted microbial lipid antigen-specific recognition found in the CD8+ alpha beta T cell pool. *Journal of immunology (Baltimore, Md. : 1950)* 1999; **162**:366-71.

365 Vincent MS, Leslie DS, Gumperz JE *et al.* CD1-dependent dendritic cell instruction. *Nat Immunol* 2002; **3**:1163-8.

366 Hunger RE, Sieling PA, Ochoa MT *et al.* Langerhans cells utilize CD1a and langerin to efficiently present nonpeptide antigens to T cells. *J Clin Invest* 2004; **113**:701-8.

367 Colonna M. Skin function for human CD1a-reactive T cells. *Nat Immunol* 2010; **11**:1079-80.

368 Fujita H. The role of IL-22 and Th22 cells in human skin diseases. *J Dermatol Sci* 2013; **72**:3-8.

369 Roura-Mir C, Catalfamo M, Cheng TY *et al.* CD1a and CD1c activate intrathyroidal T cells during Graves' disease and Hashimoto's thyroiditis. *J Immunol* 2005; **174**:3773-80.

370 Pacholczyk R, Ignatowicz H, Kraj P, Ignatowicz L. Origin and T cell receptor diversity of Foxp3+CD4+CD25+ T cells. *Immunity* 2006; **25**:249-59.

371 Kasow KA, Chen X, Knowles J *et al.* Human CD4+CD25+ regulatory T cells share equally complex and comparable repertoires with CD4+CD25- counterparts. *J Immunol* 2004; **172**:6123-8.

372 Fazilleau N, Bachelez H, Gougeon ML, Viguier M. Cutting edge: size and diversity of CD4+CD25high Foxp3+ regulatory T cell repertoire in humans: evidence for similarities and partial overlapping with CD4+CD25- T cells. *J Immunol* 2007; **179**:3412-6.

373 Hsieh CS, Zheng Y, Liang Y *et al.* An intersection between the self-reactive regulatory and nonregulatory T cell receptor repertoires. *Nat Immunol* 2006; **7**:401-10.

374 Wong J, Obst R, Correia-Neves M *et al.* Adaptation of TCR repertoires to self-peptides in regulatory and nonregulatory CD4+ T cells. *J Immunol* 2007; **178**:7032-41.

375 Itoh M, Takahashi T, Sakaguchi N *et al.* Thymus and autoimmunity: production of CD25+CD4+ naturally anergic and suppressive T cells as a key function of the thymus in maintaining immunologic self-tolerance. *J Immunol* 1999; **162**:5317-26.

376 Hori S, Haury M, Coutinho A, Demengeot J. Specificity requirements for selection and effector functions of CD25+4+ regulatory T cells in anti-myelin basic protein T cell receptor transgenic mice. *Proc Natl Acad Sci U S A* 2002; **99**:8213-8.

377 Weissler KA, Caton AJ. The role of T-cell receptor recognition of peptide:MHC complexes in the formation and activity of Foxp3^{+} regulatory T cells. *Immunol Rev* 2014; **259**:11-22.

378 Föhse L, Suffner J, Suhre K *et al.* High TCR diversity ensures optimal function and homeostasis of Foxp3+ regulatory T cells. *Eur J Immunol* 2011; **41**:3101-13.

379 Lathrop SK, Santacruz NA, Pham D *et al.* Antigen-specific peripheral shaping of the natural regulatory T cell population. *J Exp Med* 2008; **205**:3105-17.

380 Wyss L, Stadinski BD, King CG *et al.* Affinity for self antigen selects Treg cells with distinct functional properties. *Nat Immunol* 2016; **17**:1093-101.

381 Sprouse ML, Shevchenko I, Scavuzzo MA *et al.* Cutting Edge: Low-Affinity TCRs Support Regulatory T Cell Function in Autoimmunity. *J Immunol* 2018; **200**:909-14.

382 Wei X, Zhang J, Gu Q *et al.* Reciprocal Expression of IL-35 and IL-10 Defines Two Distinct Effector Treg Subsets that Are Required for Maintenance of Immune Tolerance. *Cell Rep* 2017; **21**:1853-69.

383 Zemmour D, Zilionis R, Kiner E *et al.* Single-cell gene expression reveals a landscape of regulatory T cell phenotypes shaped by the TCR. *Nat Immunol* 2018; **19**:291-301.

384 Leonard JD, Gilmore DC, Dileepan T *et al.* Identification of Natural Regulatory T Cell Epitopes Reveals Convergence on a Dominant Autoantigen. *Immunity* 2017; **47**:107-17.e8.

385 Kimura T, Kobiyama K, Winkels H *et al.* Regulatory CD4(+) T Cells Recognize Major Histocompatibility Complex Class II Molecule-Restricted Peptide Epitopes of Apolipoprotein B. *Circulation* 2018; **138**:1130-43.

386 Bonertz A, Weitz J, Pietsch DH *et al.* Antigen-specific Tregs control T cell responses against a limited repertoire of tumor antigens in patients with colorectal carcinoma. *J Clin Invest* 2009; **119**:3311-21.

387 Vahl JC, Drees C, Heger K *et al.* Continuous T cell receptor signals maintain a functional regulatory T cell pool. *Immunity* 2014; **41**:722-36.

388 Levine AG, Arvey A, Jin W, Rudensky AY. Continuous requirement for the TCR in regulatory T cell function. *Nat Immunol* 2014; **15**:1070-8.

389 Walling BL, Kim M. LFA-1 in T Cell Migration and Differentiation. *Front Immunol* 2018; **9**:952.

390 So T, Lee SW, Croft M. Immune regulation and control of regulatory T cells by OX40 and 4-1BB. *Cytokine Growth Factor Rev* 2008; **19**:253-62.

391 Kumar P, Bhattacharya P, Prabhakar BS. A comprehensive review on the role of co-signaling receptors and Treg homeostasis in autoimmunity and tumor immunity. *J Autoimmun* 2018; **95**:77-99.

392 Maerten P, Shen C, Bullens DM *et al.* Effects of interleukin 4 on CD25+CD4+ regulatory T cell function. *J Autoimmun* 2005; **25**:112-20.

393 Yang W-C, Hwang Y-S, Chen Y-Y *et al.* Interleukin-4 Supports the Suppressive Immune Responses Elicited by Regulatory T Cells. *Front Immunol* 2017; **8**.

394 Mitchell RE, Hassan M, Burton BR *et al.* IL-4 enhances IL-10 production in Th1 cells: implications for Th1 and Th2 regulation. *Sci Rep* 2017; **7**:11315.

395 Pot C, Jin H, Awasthi A *et al.* Cutting edge: IL-27 induces the transcription factor c-Maf, cytokine IL-21, and the costimulatory receptor ICOS that coordinately act together to promote differentiation of IL-10-producing Tr1 cells. *J Immunol* 2009; **183**:797-801.

396 Spolski R, Kim HP, Zhu W *et al.* IL-21 mediates suppressive effects via its induction of IL-10. *J Immunol* 2009; **182**:2859-67.

397 Sabat R, Wolk K, Loyal L *et al.* T cell pathology in skin inflammation. *Semin Immunopathol* 2019; **41**:359-77.

398 Kelly R, Marsden RA, Bevan D. Exacerbation of psoriasis with GM-CSF therapy. *Br J Dermatol* 1993; **128**:468-9.

399 Scholz T, Weigert A, Brüne B *et al.* GM-CSF in murine psoriasiform dermatitis: Redundant and pathogenic roles uncovered by antibody-induced neutralization and genetic deficiency. *PLoS One* 2017; **12**:e0182646.

400 Forster S, Ilderton E, Summerly R, Yardley HJ. Epidermal phospholipase A2 activity is raised in the uninvolved skin of psoriasis. *Br J Dermatol* 1983; **109 Suppl 25**:30-5.

401 Forster S, Ilderton E, Summerly R, Yardley HJ. The level of phospholipase A2 activity is raised in the uninvolved epidermis of psoriasis. *Br J Dermatol* 1983; **108**:103-5.

402 Verhagen A, Bergers M, van Erp PEJ *et al.* Confirmation of raised phospholipase A2 activity in the uninvolved skin of psoriasis. *Br J Dermatol* 1984; **110**:731-32.

403 Forster S, Ilderton E, Norris JFB *et al.* Characterization and activity of phospholipase A2 in normal human epidermis and in lesion-free epidermis of patients with psoriasis or eczema. *Br J Dermatol* 1985; **112**:135-47.

404 Ryborg AK, Grøn B, Kragballe K. Increased lysophosphatidylcholine content in lesional psoriatic skin. *Br J Dermatol* 1995; **133**:398-402.

405 Stumhofer JS, Silver JS, Laurence A *et al.* Interleukins 27 and 6 induce STAT3-mediated T cell production of interleukin 10. *Nat Immunol* 2007; **8**:1363-71.

406 Hall AO, Beiting DP, Tato C *et al.* The cytokines interleukin 27 and interferon-γ promote distinct Treg cell populations required to limit infection-induced pathology. *Immunity* 2012; **37**:511-23.

407 Meka RR, Venkatesha SH, Dudics S *et al.* IL-27-induced modulation of autoimmunity and its therapeutic potential. *Autoimmun Rev* 2015; **14**:1131-41.

408 Meyaard L, Hovenkamp E, Otto SA, Miedema F. IL-12-induced IL-10 production by human T cells as a negative feedback for IL-12-induced immune responses. *J Immunol* 1996; **156**:2776-82.

409 Gerosa F, Paganin C, Peritt D *et al.* Interleukin-12 primes human CD4 and CD8 T cell clones for high production of both interferon-gamma and interleukin-10. *J Exp Med* 1996; **183**:2559-69.

410 Verma ND, Hall BM, Plain KM *et al.* Interleukin-12 (IL-12p70) Promotes Induction of Highly Potent Th1-Like CD4(+)CD25(+) T Regulatory Cells That Inhibit Allograft Rejection in Unmodified Recipients. *Front Immunol* 2014; **5**:190.

411 Ma X, Yan W, Zheng H *et al.* Regulation of IL-10 and IL-12 production and function in macrophages and dendritic cells. *F1000Res* 2015; **4**:1465.

412 Toomer KH, Malek TR. Cytokine Signaling in the Development and Homeostasis of Regulatory T cells. *Cold Spring Harb Perspect Biol* 2018; **10**:a028597.

413 Schmaler M, Broggi MA, Lagarde N *et al.* IL-7R signaling in regulatory T cells maintains peripheral and allograft tolerance in mice. *Proc Natl Acad Sci U S A* 2015; **112**:13330-5.

414 Xia J, Liu W, Hu B *et al.* IL-15 promotes regulatory T cell function and protects against diabetes development in NK-depleted NOD mice. *Clin Immunol* 2010; **134**:130-9.

415 Khazaie K, von Boehmer H. The impact of CD4+CD25+ Treg on tumor specific CD8+ T cell cytotoxicity and cancer. *Semin Cancer Biol* 2006; **16**:124-36.

416 Kalekar LA, Rosenblum MD. Regulatory T cells in inflammatory skin disease: from mice to humans. *Int Immunol* 2019; **31**:457-63.

417 Nussbaum L, Chen YL, Ogg GS. Role of regulatory T cells in psoriasis pathogenesis and treatment. *Br J Dermatol* 2021; **184**:14-24.

418 Kitani A, Fuss I, Nakamura K *et al.* Transforming growth factor (TGF)-beta1-producing regulatory T cells induce Smad-mediated interleukin 10 secretion that facilitates coordinated immunoregulatory activity and amelioration of TGF-beta1-mediated fibrosis. *J Exp Med* 2003; **198**:1179-88.

419 Peterson RA. Regulatory T-cells: diverse phenotypes integral to immune homeostasis and suppression. *Toxicol Pathol* 2012; **40**:186-204.

420 Rocamora-Reverte L, Melzer FL, Würzner R, Weinberger B. The Complex Role of Regulatory T Cells in Immunity and Aging. *Front Immunol* 2021; **11**:616949.

421 Deng Y, Chang C, Lu Q. The Inflammatory Response in Psoriasis: a Comprehensive Review. *Clin Rev Allergy Immunol* 2016; **50**:377-89.

422 Battaglia M, Stabilini A, Roncarolo MG. Rapamycin selectively expands CD4+CD25+FoxP3+ regulatory T cells. *Blood* 2005; **105**:4743-8.

423 Scotta C, Esposito M, Fazekasova H *et al.* Differential effects of rapamycin and retinoic acid on expansion, stability and suppressive qualities of human CD4(+)CD25(+)FOXP3(+) T regulatory cell subpopulations. *Haematologica* 2013; **98**:1291-9.

424 Liu M, Li X, Chen XY *et al.* Topical application of a linoleic acid-ceramide containing moisturizer exhibit therapeutic and preventive benefits for psoriasis vulgaris: a randomized controlled trial. *Dermatol Ther* 2015; **28**:373-82.

425 Zhang N, Bevan MJ. CD8(+) T cells: foot soldiers of the immune system. *Immunity* 2011; **35**:161-8.

426 Ochoa-Repáraz J, Rynda A, Ascón MA *et al.* IL-13 production by regulatory T cells protects against experimental autoimmune encephalomyelitis independently of autoantigen. *J Immunol* 2008; **181**:954-68.

427 Proto JD, Doran AC, Gusarova G *et al.* Regulatory T Cells Promote Macrophage Efferocytosis during Inflammation Resolution. *Immunity* 2018; **49**:666-77.e6.

428 Jung MK, Kwak JE, Shin EC. IL-17A-Producing Foxp3(+) Regulatory T Cells and Human Diseases. *Immune Netw* 2017; **17**:276-86.

429 Yawalkar N, Karlen S, Hunger R *et al.* Expression of interleukin-12 is increased in psoriatic skin. *J Invest Dermatol* 1998; **111**:1053-7.

430 Feng T, Cao AT, Weaver CT *et al.* Interleukin-12 converts Foxp3+ regulatory T cells to interferon-γ-producing Foxp3+ T cells that inhibit colitis. *Gastroenterology* 2011; **140**:2031-43.

431 Zhao J, Zhao J, Perlman S. Differential effects of IL-12 on Tregs and non-Treg T cells: roles of IFN-γ, IL-2 and IL-2R. *PLoS One* 2012; **7**:e46241.

432 Kawai K, Uchiyama M, Hester J *et al.* Regulatory T cells for tolerance. *Hum Immunol* 2018; **79**:294-303.

433 Mohseni YR, Tung SL, Dudreuilh C *et al.* The Future of Regulatory T Cell Therapy: Promises and Challenges of Implementing CAR Technology. *Front Immunol* 2020; **11**:1608.

434 Bottomley MJ, Brook MO, Shankar S *et al.* Towards regulatory cellular therapies in solid organ transplantation. *Trends Immunol* 2021.

435 Lebwohl M. Psoriasis. *Lancet* 2003; **361**:1197-204.

436 Tagami H. Triggering factors. *Clin Dermatol* 1997; **15**:677-85.

437 Singh S, Pradhan D, Puri P *et al.* Genomic alterations driving psoriasis pathogenesis. *Gene* 2019; **683**:61-71.

438 Prinz JC. Autoimmune aspects of psoriasis: Heritability and autoantigens. *Autoimmun Rev* 2017; **16**:970-79.

439 Trembath RC, Clough RL, Rosbotham JL *et al.* Identification of a major susceptibility locus on chromosome 6p and evidence for further disease loci revealed by a two stage genome-wide search in psoriasis. *Hum Mol Genet* 1997; **6**:813-20.

440 Nair RP, Henseler T, Jenisch S *et al.* Evidence for two psoriasis susceptibility loci (HLA and 17q) and two novel candidate regions (16q and 20p) by genome-wide scan. *Hum Mol Genet* 1997; **6**:1349-56.

441 Balendran N, Clough RL, Arguello JR *et al.* Characterization of the major susceptibility region for psoriasis at chromosome 6p21.3. *J Invest Dermatol* 1999; **113**:322-8.

442 Veal CD, Capon F, Allen MH *et al.* Family-based analysis using a dense single-nucleotide polymorphism-based map defines genetic variation at PSORS1, the major psoriasis-susceptibility locus. *Am J Hum Genet* 2002; **71**:554-64.

443 Nair RP, Stuart PE, Nistor I *et al.* Sequence and haplotype analysis supports HLA-C as the psoriasis susceptibility 1 gene. *Am J Hum Genet* 2006; **78**:827-51.

444 Nair RP, Duffin KC, Helms C *et al.* Genome-wide scan reveals association of psoriasis with IL-23 and NF-kappaB pathways. *Nat Genet* 2009; **41**:199-204.

445 Strange A, Capon F, Spencer CC *et al.* A genome-wide association study identifies new psoriasis susceptibility loci and an interaction between HLA-C and ERAP1. *Nat Genet* 2010; **42**:985-90.

446 Arakawa A, Siewert K, Stöhr J *et al.* Melanocyte antigen triggers autoimmunity in human psoriasis. *J Exp Med* 2015; **212**:2203-12.

447 Mabuchi T, Hirayama N. Binding Affinity and Interaction of LL-37 with HLA-C*06:02 in Psoriasis. *J Invest Dermatol* 2016; **136**:1901-03.

448 Lande R, Botti E, Jandus C *et al.* The antimicrobial peptide LL37 is a T-cell autoantigen in psoriasis. *Nat Commun* 2014; **5**:5621.

449 Knight J, Spain SL, Capon F *et al.* Conditional analysis identifies three novel major histocompatibility complex loci associated with psoriasis. *Hum Mol Genet* 2012; **21**:5185-92.

450 Okada Y, Han B, Tsoi LC *et al.* Fine mapping major histocompatibility complex associations in psoriasis and its clinical subtypes. *Am J Hum Genet* 2014; **95**:162-72.

451 Zhou F, Cao H, Zuo X *et al.* Deep sequencing of the MHC region in the Chinese population contributes to studies of complex disease. *Nat Genet* 2016; **48**:740-6.

452 Zhang X, Wei S, Yang S *et al.* HLA-DQA1 and DQB1 alleles are associated with genetic susceptibility to psoriasis vulgaris in Chinese Han. *Int J Dermatol* 2004; **43**:181-7.

453 Shawkatová I, Javor J, Párnická Z *et al.* HLA-C, DRB1 and DQB1 alleles involved in genetic predisposition to psoriasis vulgaris in the Slovak population. *Folia Microbiol (Praha)* 2013; **58**:319-24.

454 Zalzala HH, Abdullah GA, Abbas MY *et al.* Relationship between human leukocyte antigen DRB1 and psoriasis in Iraqi patients. *Saudi Med J* 2018; **39**:886-90.

455 Tsoi LC, Spain SL, Knight J *et al.* Identification of 15 new psoriasis susceptibility loci highlights the role of innate immunity. *Nat Genet* 2012; **44**:1341-8.

456 Li Y, Liao W, Cargill M *et al.* Carriers of rare missense variants in IFIH1 are protected from psoriasis. *J Invest Dermatol* 2010; **130**:2768-72.

457 Capon F, Bijlmakers MJ, Wolf N *et al.* Identification of ZNF313/RNF114 as a novel psoriasis susceptibility gene. *Hum Mol Genet* 2008; **17**:1938-45.

458 Sun LD, Cheng H, Wang ZX *et al.* Association analyses identify six new psoriasis susceptibility loci in the Chinese population. *Nat Genet* 2010; **42**:1005-9.

459 Stuart PE, Nair RP, Ellinghaus E *et al.* Genome-wide association analysis identifies three psoriasis susceptibility loci. *Nat Genet* 2010; **42**:1000-4.

460 Cargill M, Schrodi SJ, Chang M *et al.* A large-scale genetic association study confirms IL12B and leads to the identification of IL23R as psoriasis-risk genes. *Am J Hum Genet* 2007; **80**:273-90.

461 Tsunemi Y, Saeki H, Nakamura K *et al.* Interleukin-12 p40 gene (IL12B) 3'-untranslated region polymorphism is associated with susceptibility to atopic dermatitis and psoriasis vulgaris. *J Dermatol Sci* 2002; **30**:161-6.

462 Ellinghaus E, Ellinghaus D, Stuart PE *et al.* Genome-wide association study identifies a psoriasis susceptibility locus at TRAF3IP2. *Nat Genet* 2010; **42**:991-5.

463 Shaiq PA, Stuart PE, Latif A *et al.* Genetic associations of psoriasis in a Pakistani population. *Br J Dermatol* 2013; **169**:406-11.

464 Greb JE, Goldminz AM, Elder JT *et al.* Psoriasis. *Nat Rev Dis Primers* 2016; **2**:16082.

465 Raychaudhuri SK, Maverakis E, Raychaudhuri SP. Diagnosis and classification of psoriasis. *Autoimmun Rev* 2014; **13**:490-95.

466 Bjerke JR, Krogh HK, Matre R. Characterization of mononuclear cell infiltrates in psoriatic lesions. *J Invest Dermatol* 1978; **71**:340-43.

467 Griffiths CE, Barker JN. Pathogenesis and clinical features of psoriasis. *Lancet* 2007; **370**:263-71.

468 Lin AM, Rubin CJ, Khandpur R *et al.* Mast cells and neutrophils release IL-17 through extracellular trap formation in psoriasis. *J Immunol* 2011; **187**:490-500.

469 Lowes MA, Bowcock AM, Krueger JG. Pathogenesis and therapy of psoriasis. *Nature* 2007; **445**:866-73.

470 Keijsers RR, Joosten I, van Erp PE *et al.* Cellular sources of IL-17 in psoriasis: a paradigm shift? *Exp Dermatol* 2014; **23**:799-803.

471 Gabay C, Towne JE. Regulation and function of interleukin-36 cytokines in homeostasis and pathological conditions. *J Leukoc Biol* 2015; **97**:645-52.

472 Bassoy EY, Towne JE, Gabay C. Regulation and function of interleukin-36 cytokines. *Immunol Rev* 2018; **281**:169-78.

473 Quaranta M, Knapp B, Garzorz N *et al.* Intraindividual genome expression analysis reveals a specific molecular signature of psoriasis and eczema. *Sci Transl Med* 2014; **6**:244ra90.

474 Mahil SK, Catapano M, Di Meglio P *et al.* An analysis of IL-36 signature genes and individuals with IL1RL2 knockout mutations validates IL-36 as a psoriasis therapeutic target. *Sci Transl Med* 2017; **9**:eaan2514.

475 Zuo X, Sun L, Yin X *et al.* Whole-exome SNP array identifies 15 new susceptibility loci for psoriasis. *Nat Commun* 2015; **6**:6793.

476 Carrier Y, Ma HL, Ramon HE *et al.* Inter-regulation of Th17 cytokines and the IL-36 cytokines in vitro and in vivo: implications in psoriasis pathogenesis. *J Invest Dermatol* 2011; **131**:2428-37.

477 Tortola L, Rosenwald E, Abel B *et al.* Psoriasiform dermatitis is driven by IL-36-mediated DC-keratinocyte crosstalk. *J Clin Invest* 2012; **122**:3965-76.

478 Onoufriadis A, Simpson MA, Pink AE *et al.* Mutations in IL36RN/IL1F5 are associated with the severe episodic inflammatory skin disease known as generalized pustular psoriasis. *Am J Hum Genet* 2011; **89**:432-7.

479 Lizzul PF, Aphale A, Malaviya R *et al.* Differential expression of phosphorylated NF-kappaB/RelA in normal and psoriatic epidermis and downregulation of NF-kappaB in response to treatment with etanercept. *J Invest Dermatol* 2005; **124**:1275-83.

480 Goldminz AM, Au SC, Kim N *et al.* NF-κB: an essential transcription factor in psoriasis. *J Dermatol Sci* 2013; **69**:89-94.

481 Quaglino P, Ortoncelli M, Comessatti A *et al.* Circulating CD4+CD25 bright FOXP3+ T cells are up-regulated by biological therapies and correlate with the clinical response in psoriasis patients. *Dermatology* 2009; **219**:250-58.

482 Ma L, Xue H, Gao T *et al.* Notch1 Signaling Regulates the Th17/Treg Immune Imbalance in Patients with Psoriasis Vulgaris. *Mediators Inflamm* 2018; **2018**:3069521.

483 Karamehic J, Zecevic L, Resic H *et al.* Immunophenotype lymphocyte of peripheral blood in patients with psoriasis. *Med Arch* 2014; **68**:236-38.

484 Pawlaczyk M, Karczewski J, Wiktorowicz K. T regulatory CD4+CD25high lymphocytes in peripheral blood of patients suffering from psoriasis. *Postepy Dermatol Alergol* 2010; **27**:25-28.

485 Furuhashi T, Saito C, Torii K *et al.* Photo(chemo)therapy reduces circulating Th17 cells and restores circulating regulatory T cells in psoriasis. *PLoS One* 2013; **8**:e54895.

486 Zhang L, Yang XQ, Cheng J *et al.* Increased Th17 cells are accompanied by FoxP3(+) Treg cell accumulation and correlated with psoriasis disease severity. *Clin Immunol* 2010; **135**:108-17.

487 Yun WJ, Lee DW, Chang SE *et al.* Role of CD4CD25FOXP3 Regulatory T Cells in Psoriasis. *Ann Dermatol* 2010; **22**:397-403.

488 Sugiyama H, Gyulai R, Toichi E *et al.* Dysfunctional blood and target tissue CD4+CD25high regulatory T cells in psoriasis: mechanism underlying unrestrained pathogenic effector T cell proliferation. *J Immunol* 2005; **174**:164-73.

489 Bovenschen HJ, van Vlijmen-Willems IM, van de Kerkhof PC, van Erp PE. Identification of lesional CD4+ CD25+ Foxp3+ regulatory T cells in Psoriasis. *Dermatology* 2006; **213**:111-17.

490 Fujimura T, Okuyama R, Ito Y, Aiba S. Profiles of Foxp3+ regulatory T cells in eczematous dermatitis, psoriasis vulgaris and mycosis fungoides. *Br J Dermatol* 2008; **158**:1256-63.

491 Keijsers RR, van der Velden HM, van Erp PE *et al.* Balance of Treg vs. T-helper cells in the transition from symptomless to lesional psoriatic skin. *Br J Dermatol* 2013; **168**:1294-302.

492 Yan KX, Fang X, Han L *et al.* Foxp3+ regulatory T cells and related cytokines differentially expressed in plaque vs. guttate psoriasis vulgaris. *Br J Dermatol* 2010; **163**:48-56.

493 Zhang L, Li Y, Yang X *et al.* Characterization of Th17 and FoxP3(+) Treg Cells in Paediatric Psoriasis Patients. *Scand J Immunol* 2016; **83**:174-80.

494 Zhang K, Li X, Yin G *et al.* Functional characterization of CD4+CD25+ regulatory T cells differentiated in vitro from bone marrow-derived haematopoietic cells of psoriasis patients with a family history of the disorder. *Br J Dermatol* 2008; **158**:298-305.

495 Wang H, Peters T, Sindrilaru A *et al.* TGF-beta-dependent suppressive function of Tregs requires wild-type levels of CD18 in a mouse model of psoriasis. *J Clin Invest* 2008; **118**:2629-39.

496 Goodman WA, Levine AD, Massari JV *et al.* IL-6 signaling in psoriasis prevents immune suppression by regulatory T cells. *J Immunol* 2009; **183**:3170-76.

497 Zhao M, Wang LT, Liang GP *et al.* Up-regulation of microRNA-210 induces immune dysfunction via targeting FOXP3 in CD4(+) T cells of psoriasis vulgaris. *Clin Immunol* 2014; **150**:22-30.

498 Yang L, Li B, Dang E *et al.* Impaired function of regulatory T cells in patients with psoriasis is mediated by phosphorylation of STAT3. *J Dermatol Sci* 2016; **81**:85-92.

499 Harris TJ, Grosso JF, Yen HR *et al.* Cutting edge: An in vivo requirement for STAT3 signaling in TH17 development and TH17-dependent autoimmunity. *J Immunol* 2007; **179**:4313-17.

500 Ohta A, Kini R, Ohta A *et al.* The development and immunosuppressive functions of CD4(+) CD25(+) FoxP3(+) regulatory T cells are under influence of the adenosine-A2A adenosine receptor pathway. *Front Immunol* 2012; **3**:190.

501 Ohta A, Sitkovsky M. Extracellular adenosine-mediated modulation of regulatory T cells. *Front Immunol* 2014; **5**:304.

502 Yan K, Xu W, Huang Y *et al.* Methotrexate restores the function of peripheral blood regulatory T cells in psoriasis vulgaris via the CD73/AMPK/mTOR pathway. *Br J Dermatol* 2018; **179**:896-905.

503 Soler DC, Sugiyama H, Young AB *et al.* Psoriasis patients exhibit impairment of the high potency CCR5(+) T regulatory cell subset. *Clin Immunol* 2013; **149**:111-18.

504 Dong C. TH17 cells in development: an updated view of their molecular identity and genetic programming. *Nat Rev Immunol* 2008; **8**:337-48.

505 Korn T, Bettelli E, Oukka M, Kuchroo VK. IL-17 and Th17 Cells. *Annu Rev Immunol* 2009; **27**:485-517.

506 Di Cesare A, Di Meglio P, Nestle FO. The IL-23/Th17 axis in the immunopathogenesis of psoriasis. *J Invest Dermatol* 2009; **129**:1339-50.

507 Lowes MA, Kikuchi T, Fuentes-Duculan J *et al.* Psoriasis vulgaris lesions contain discrete populations of Th1 and Th17 T cells. *J Invest Dermatol* 2008; **128**:1207-11.

508 Lee E, Trepicchio WL, Oestreicher JL *et al.* Increased expression of interleukin 23 p19 and p40 in lesional skin of patients with psoriasis vulgaris. *J Exp Med* 2004; **199**:125-30.

509 Yawalkar N, Tscharner GG, Hunger RE, Hassan AS. Increased expression of IL-12p70 and IL-23 by multiple dendritic cell and macrophage subsets in plaque psoriasis. *J Dermatol Sci* 2009; **54**:99-105.

510 Tsai YC, Tsai TF. Anti-interleukin and interleukin therapies for psoriasis: current evidence and clinical usefulness. *Ther Adv Musculoskelet Dis* 2017; **9**:277-94.

511 Priyadarssini M, Divya Priya D, Indhumathi S *et al.* Immunophenotyping of T cells in the peripheral circulation in psoriasis. *Br J Biomed Sci* 2016; **73**:174-79.

512 Lochner M, Wang Z, Sparwasser T. The Special Relationship in the Development and Function of T Helper 17 and Regulatory T Cells. *Prog Mol Biol Transl Sci* 2015; **136**:99-129.

513 Zhou L, Lopes JE, Chong MM *et al.* TGF-beta-induced Foxp3 inhibits T(H)17 cell differentiation by antagonizing RORgammat function. *Nature* 2008; **453**:236-40.

514 Bovenschen HJ, van de Kerkhof PC, van Erp PE *et al.* Foxp3+ regulatory T cells of psoriasis patients easily differentiate into IL-17A-producing cells and are found in lesional skin. *J Invest Dermatol* 2011; **131**:1853-60.

515 Tovar-Castillo LE, Cancino-Diaz JC, Garcia-Vazquez F *et al.* Under-expression of VHL and over-expression of HDAC-1, HIF-1alpha, LL-37, and IAP-2 in affected skin biopsies of patients with psoriasis. *Int J Dermatol* 2007; **46**:239-46.

516 Pandiyan P, Zhu J. Origin and functions of pro-inflammatory cytokine producing Foxp3+ regulatory T cells. *Cytokine* 2015; **76**:13-24.

517 Johansen C, Usher PA, Kjellerup RB *et al.* Characterization of the interleukin-17 isoforms and receptors in lesional psoriatic skin. *Br J Dermatol* 2009; **160**:319-24.

518 Liu Y, Zhang C, Li B *et al.* A novel role of IL-17A in contributing to the impaired suppressive function of Tregs in psoriasis. *J Dermatol Sci* 2021; **101**:84-92.

519 Cordiali-Fei P, Bianchi L, Bonifati C *et al.* Immunologic biomarkers for clinical and therapeutic management of psoriasis. *Mediators Inflamm* 2014; **2014**:236060.

520 Priyadarssini M, Chandrashekar L, Rajappa M. Effect of methotrexate monotherapy on T-cell subsets in the peripheral circulation in psoriasis. *Clin Exp Dermatol* 2019; **44**:491-97.

521 Mattozzi C, Paolino G, Salvi M *et al.* Peripheral blood regulatory T cell measurements correlate with serum vitamin D level in patients with psoriasis. *Eur Rev Med Pharmacol Sci* 2016; **20**:1675-79.

522 Mucida D, Park Y, Kim G *et al.* Reciprocal TH17 and regulatory T cell differentiation mediated by retinoic acid. *Science* 2007; **317**:256-60.

523 Elias KM, Laurence A, Davidson TS *et al.* Retinoic acid inhibits Th17 polarization and enhances FoxP3 expression through a Stat-3/Stat-5 independent signaling pathway. *Blood* 2008; **111**:1013-20.

524 Kubo R, Muramatsu S, Sagawa Y *et al.* Bath-PUVA therapy improves impaired resting regulatory T cells and increases activated regulatory T cells in psoriasis. *J Dermatol Sci* 2017; **86**:46-53.

525 He X, Koenen H, Smeets RL *et al.* Targeting PKC in human T cells using sotrastaurin (AEB071) preserves regulatory T cells and prevents IL-17 production. *J Invest Dermatol* 2014; **134**:975-83.

526 Shimizu T, Kamata M, Fukaya S *et al.* Anti-IL-17A and IL-23p19 antibodies but not anti-TNFalpha antibody induce expansion of regulatory T cells and restoration of their suppressive function in imiquimod-induced psoriasiform dermatitis. *J Dermatol Sci* 2019; **95**:90-98.

527 Gu ZW, Wang YX, Cao ZW. Neutralization of interleukin-17 suppresses allergic rhinitis symptoms by downregulating Th2 and Th17 responses and upregulating the Treg response. *Oncotarget* 2017; **8**:22361-69.

528 Sakaguchi S, Miyara M, Costantino CM, Hafler DA. FOXP3+ regulatory T cells in the human immune system. *Nat Rev Immunol* 2010; **10**:490-500.

529 Dong S, Maiella S, Xhaard A *et al.* Multiparameter single-cell profiling of human CD4+FOXP3+ regulatory T-cell populations in homeostatic conditions and during graft-versus-host disease. *Blood* 2013; **122**:1802-12.

530 Smigiel KS, Richards E, Srivastava S *et al.* CCR7 provides localized access to IL-2 and defines homeostatically distinct regulatory T cell subsets. *J Exp Med* 2014; **211**:121-36.

531 Rosenblum MD, Way SS, Abbas AK. Regulatory T cell memory. *Nat Rev Immunol* 2016; **16**:90-101.

532 Szanya V, Ermann J, Taylor C *et al.* The subpopulation of CD4+CD25+ splenocytes that delays adoptive transfer of diabetes expresses L-selectin and high levels of CCR7. *J Immunol* 2002; **169**:2461-5.

533 Huehn J, Siegmund K, Lehmann JC *et al.* Developmental stage, phenotype, and migration distinguish naive- and effector/memory-like CD4+ regulatory T cells. *J Exp Med* 2004; **199**:303-13.

534 Valmori D, Merlo A, Souleimanian NE *et al.* A peripheral circulating compartment of natural naive CD4 Tregs. *J Clin Invest* 2005; **115**:1953-62.

535 Patton DT, Wilson MD, Rowan WC *et al.* The PI3K p110delta regulates expression of CD38 on regulatory T cells. *PLoS One* 2011; **6**:e17359.

536 Cai J, Wang D, Zhang G, Guo X. The Role Of PD-1/PD-L1 Axis In Treg Development And Function: Implications For Cancer Immunotherapy. *Onco Targets Ther* 2019; **12**:8437-45.

537 Solstad T, Bains SJ, Landskron J *et al.* CD147 (Basigin/Emmprin) identifies FoxP3+CD45RO+CTLA4+-activated human regulatory T cells. *Blood* 2011; **118**:5141-51.

538 Sugiyama D, Nishikawa H, Maeda Y *et al.* Anti-CCR4 mAb selectively depletes effector-type FoxP3+CD4+ regulatory T cells, evoking antitumor immune responses in humans. *Proc Natl Acad Sci U S A* 2013; **110**:17945-50.

539 Bleul CC, Wu L, Hoxie JA *et al.* The HIV coreceptors CXCR4 and CCR5 are differentially expressed and regulated on human T lymphocytes. *Proc Natl Acad Sci U S A* 1997; **94**:1925-30.

540 Qin S, Rottman JB, Myers P *et al.* The chemokine receptors CXCR3 and CCR5 mark subsets of T cells associated with certain inflammatory reactions. *J Clin Invest* 1998; **101**:746-54.

541 Yamazaki T, Yang XO, Chung Y *et al.* CCR6 regulates the migration of inflammatory and regulatory T cells. *J Immunol* 2008; **181**:8391-401.

542 Chen X, Subleski JJ, Kopf H *et al.* Cutting edge: expression of TNFR2 defines a maximally suppressive subset of mouse CD4+CD25+FoxP3+ T regulatory cells: applicability to tumor-infiltrating T regulatory cells. *J Immunol* 2008; **180**:6467-71.

543 van Mierlo GJ, Scherer HU, Hameetman M *et al.* Cutting edge: TNFR-shedding by CD4+CD25+ regulatory T cells inhibits the induction of inflammatory mediators. *J Immunol* 2008; **180**:2747-51.

544 Chen X, Wu X, Zhou Q *et al.* TNFR2 is critical for the stabilization of the CD4+Foxp3+ regulatory T. cell phenotype in the inflammatory environment. *J Immunol* 2013; **190**:1076-84.

545 Borsellino G, Kleinewietfeld M, Di Mitri D *et al.* Expression of ectonucleotidase CD39 by Foxp3+ Treg cells: hydrolysis of extracellular ATP and immune suppression. *Blood* 2007; **110**:1225-32.

546 Allard B, Longhi MS, Robson SC, Stagg J. The ectonucleotidases CD39 and CD73: Novel checkpoint inhibitor targets. *Immunol Rev* 2017; **276**:121-44.

547 Wing JB, Tay C, Sakaguchi S. Control of Regulatory T Cells by Co-signal Molecules. *Adv Exp Med Biol* 2019; **1189**:179-210.

548 Ito T, Hanabuchi S, Wang YH *et al.* Two functional subsets of FOXP3+ regulatory T cells in human thymus and periphery. *Immunity* 2008; **28**:870-80.

549 Lee DJ. The relationship between TIGIT(+) regulatory T cells and autoimmune disease. *Int Immunopharmacol* 2020; **83**:106378.

550 Anderson AC, Joller N, Kuchroo VK. Lag-3, Tim-3, and TIGIT: Co-inhibitory Receptors with Specialized Functions in Immune Regulation. *Immunity* 2016; **44**:989-1004.

551 Sun L, Jin H, Li H. GARP: a surface molecule of regulatory T cells that is involved in the regulatory function and TGF-β releasing. *Oncotarget* 2016; **7**:42826-36.

552 Kilger G, Holzmann B. Molecular analysis of the physiological and pathophysiological role of alpha 4-integrins. *J Mol Med (Berl)* 1995; **73**:347-54.

553 Springer TA. Traffic signals for lymphocyte recirculation and leukocyte emigration: the multistep paradigm. *Cell* 1994; **76**:301-14.

554 Yabkowitz R, Dixit VM, Guo N *et al.* Activated T-cell adhesion to thrombospondin is mediated by the alpha 4 beta 1 (VLA-4) and alpha 5 beta 1 (VLA-5) integrins. *J Immunol* 1993; **151**:149-58.

555 White JT, Cross EW, Kedl RM. Antigen-inexperienced memory CD8(+) T cells: where they come from and why we need them. *Nat Rev Immunol* 2017; **17**:391-400.

556 Christiaansen AF, Dixit UG, Coler RN *et al.* CD11a and CD49d enhance the detection of antigen-specific T cells following human vaccination. *Vaccine* 2017; **35**:4255-61.

557 Kraczyk B, Remus R, Hardt C. CD49d Treg cells with high suppressive capacity are remarkably less efficient on activated CD45RA- than on naive CD45RA+ Teff cells. *Cell Physiol Biochem* 2014; **34**:346-55.

558 Kleinewietfeld M, Starke M, Di Mitri D *et al.* CD49d provides access to "untouched" human Foxp3+ Treg free of contaminating effector cells. *Blood* 2009; **113**:827-36.

559 Liao YH, Jee SH, Sheu BC *et al.* Increased expression of the natural killer cell inhibitory receptor CD94/NKG2A and CD158b on circulating and lesional T cells in patients with chronic plaque psoriasis. *Br J Dermatol* 2006; **155**:318-24.

560 Yin X, Low HQ, Wang L *et al.* Genome-wide meta-analysis identifies multiple novel associations and ethnic heterogeneity of psoriasis susceptibility. *Nat Commun* 2015; **6**:6916.

561 López de Castro JA. How ERAP1 and ERAP2 Shape the Peptidomes of Disease-Associated MHC-I Proteins. *Front Immunol* 2018; **9**:2463.

562 Yao Y, Richman L, Morehouse C *et al.* Type I interferon: potential therapeutic target for psoriasis? *PLoS One* 2008; **3**:e2737.

563 Cao T, Shao S, Li B *et al.* Up-regulation of Interferon-inducible protein 16 contributes to psoriasis by modulating chemokine production in keratinocytes. *Sci Rep* 2016; **6**:25381.

564 Gudjonsson JE, Ding J, Johnston A *et al.* Assessment of the psoriatic transcriptome in a large sample: additional regulated genes and comparisons with in vitro models. *J Invest Dermatol* 2010; **130**:1829-40.

565 Agenès F, Bosco N, Mascarell L *et al.* Differential expression of regulator of G-protein signalling transcripts and in vivo migration of CD4+ naïve and regulatory T cells. *Immunology* 2005; **115**:179-88.

566 Boniface K, Diveu C, Morel F *et al.* Oncostatin M secreted by skin infiltrating T lymphocytes is a potent keratinocyte activator involved in skin inflammation. *J Immunol* 2007; **178**:4615-22.

567 Pohin M, Guesdon W, Mekouo AA *et al.* Oncostatin M overexpression induces skin inflammation but is not required in the mouse model of imiquimod-induced psoriasis-like inflammation. *Eur J Immunol* 2016; **46**:1737-51.

568 Li Q, Verma IM. NF-kappaB regulation in the immune system. *Nat Rev Immunol* 2002; **2**:725-34.

569 Grinberg-Bleyer Y, Caron R, Seeley JJ *et al.* The Alternative NF-κB Pathway in Regulatory T Cell Homeostasis and Suppressive Function. *J Immunol* 2018; **200**:2362-71.

570 Dhar A, Chawla M, Chattopadhyay S *et al.* Role of NF-kappaB2-p100 in regulatory T cell homeostasis and activation. *Sci Rep* 2019; **9**:13867.

571 Gorabi AM, Hajighasemi S, Kiaie N *et al.* The pivotal role of CD69 in autoimmunity. *J Autoimmun* 2020; **111**:102453.

572 Walker LS. Treg and CTLA-4: two intertwining pathways to immune tolerance. *J Autoimmun* 2013; **45**:49-57.

573 Ronchetti S, Ricci E, Petrillo MG *et al.* Glucocorticoid-induced tumour necrosis factor receptor-related protein: a key marker of functional regulatory T cells. *J Immunol Res* 2015; **2015**:171520.

574 Thornton AM, Shevach EM. Helios: still behind the clouds. *Immunology* 2019; **158**:161-70.

575 Remedios KA, Zirak B, Sandoval PM *et al.* The TNFRSF members CD27 and OX40 coordinately limit T(H)17 differentiation in regulatory T cells. *Sci Immunol* 2018; **3**.

576 Li C, Jiang S, Liu SQ *et al.* MeCP2 enforces Foxp3 expression to promote regulatory T cells' resilience to inflammation. *Proc Natl Acad Sci U S A* 2014; **111**:E2807-16.

577 Zhang P, Su Y, Chen H *et al.* Abnormal DNA methylation in skin lesions and PBMCs of patients with psoriasis vulgaris. *J Dermatol Sci* 2010; **60**:40-2.

578 Schmidleithner L, Thabet Y, Schönfeld E *et al.* Enzymatic Activity of HPGD in Treg Cells Suppresses Tconv Cells to Maintain Adipose Tissue Homeostasis and Prevent Metabolic Dysfunction. *Immunity* 2019; **50**:1232-48.e14.

579 Garín MI, Chu CC, Golshayan D *et al.* Galectin-1: a key effector of regulation mediated by CD4+CD25+ T cells. *Blood* 2007; **109**:2058-65.

580 Sundblad V, Morosi LG, Geffner JR, Rabinovich GA. Galectin-1: A Jack-of-All-Trades in the Resolution of Acute and Chronic Inflammation. *J Immunol* 2017; **199**:3721-30.

581 Yang YH, Song W, Deane JA *et al.* Deficiency of annexin A1 in CD4+ T cells exacerbates T cell-dependent inflammation. *J Immunol* 2013; **190**:997-1007.

582 Bai F, Zhang P, Fu Y *et al.* Targeting ANXA1 abrogates Treg-mediated immune suppression in triple-negative breast cancer. *J Immunother Cancer* 2020; **8**.

583 Beyer M, Thabet Y, Müller RU *et al.* Repression of the genome organizer SATB1 in regulatory T cells is required for suppressive function and inhibition of effector differentiation. *Nat Immunol* 2011; **12**:898-907.

584 Abadier M, Ley K. P-selectin glycoprotein ligand-1 in T cells. *Curr Opin Hematol* 2017; **24**:265-73.

585 Hirata T, Merrill-Skoloff G, Aab M *et al.* P-Selectin glycoprotein ligand 1 (PSGL-1) is a physiological ligand for E-selectin in mediating T helper 1 lymphocyte migration. *J Exp Med* 2000; **192**:1669-76.

586 Angiari S, Rossi B, Piccio L *et al.* Regulatory T cells suppress the late phase of the immune response in lymph nodes through P-selectin glycoprotein ligand-1. *J Immunol* 2013; **191**:5489-500.

587 Zibert JR, Skov L, Thyssen JP *et al.* Significance of the S100A4 protein in psoriasis. *J Invest Dermatol* 2010; **130**:150-60.

588 Grum-Schwensen B, Klingelhöfer J, Beck M *et al.* S100A4-neutralizing antibody suppresses spontaneous tumor progression, pre-metastatic niche formation and alters T-cell polarization balance. *BMC Cancer* 2015; **15**:44.

589 Ambartsumian N, Klingelhöfer J, Grigorian M. The Multifaceted S100A4 Protein in Cancer and Inflammation. *Methods Mol Biol* 2019; **1929**:339-65.

590 Therianou A, Vasiadi M, Delivanis DA *et al.* Mitochondrial dysfunction in affected skin and increased mitochondrial DNA in serum from patients with psoriasis. *Exp Dermatol* 2019; **28**:72-75.

591 Chaudhuri L, Srivastava RK, Kos F, Shrikant PA. Uncoupling protein 2 regulates metabolic reprogramming and fate of antigen-stimulated CD8+ T cells. *Cancer Immunol Immunother* 2016; **65**:869-74.

592 Martin MD, Badovinac VP. Defining Memory CD8 T Cell. *Front Immunol* 2018; **9**:2692.

593 Simonetta F, Chiali A, Cordier C *et al.* Increased CD127 expression on activated FOXP3+CD4+ regulatory T cells. *Eur J Immunol* 2010; **40**:2528-38.

594 Burr ML, Sparbier CE, Chan YC *et al.* CMTM6 maintains the expression of PD-L1 and regulates anti-tumour immunity. *Nature* 2017; **549**:101-05.

595 Lanzavecchia A, Sallusto F. Dynamics of T lymphocyte responses: intermediates, effectors, and memory cells. *Science* 2000; **290**:92-7.

596 Sallusto F, Geginat J, Lanzavecchia A. Central memory and effector memory T cell subsets: function, generation, and maintenance. *Annu Rev Immunol* 2004; **22**:745-63.

597 Zhou X, Bailey-Bucktrout SL, Jeker LT *et al.* Instability of the transcription factor Foxp3 leads to the generation of pathogenic memory T cells in vivo. *Nat Immunol* 2009; **10**:1000-7.

598 Zhang Z, Zhang W, Guo J *et al.* Activation and Functional Specialization of Regulatory T Cells Lead to the Generation of Foxp3 Instability. *J Immunol* 2017; **198**:2612-25.

599 Hu W, Wang ZM, Feng Y *et al.* Regulatory T cells function in established systemic inflammation and reverse fatal autoimmunity. *Nat Immunol* 2021; **22**:1163-74.

600 Eisenbarth SC. Dendritic cell subsets in T cell programming: location dictates function. *Nat Rev Immunol* 2019; **19**:89-103.

601 Tanne A, Bhardwaj N. Chapter 9 - Dendritic Cells: General Overview and Role in Autoimmunity. In: *Kelley and Firestein's Textbook of Rheumatology (Tenth Edition)* (Firestein GS, Budd RC, Gabriel SE *et al.*, eds): Elsevier. 2017; 126-44.e6.

602 Villani AC, Satija R, Reynolds G *et al.* Single-cell RNA-seq reveals new types of human blood dendritic cells, monocytes, and progenitors. *Science* 2017; **356**:eaah4573.

603 Swiecki M, Colonna M. The multifaceted biology of plasmacytoid dendritic cells. *Nat Rev Immunol* 2015; **15**:471-85.

604 Deckers J, Hammad H, Hoste E. Langerhans Cells: Sensing the Environment in Health and Disease. *Front Immunol* 2018; **9**:93.

605 Sallusto F, Lanzavecchia A. Efficient presentation of soluble antigen by cultured human dendritic cells is maintained by granulocyte/macrophage colony-stimulating factor plus interleukin 4 and downregulated by tumor necrosis factor alpha. *J Exp Med* 1994; **179**:1109-18.

606 Zhou LJ, Tedder TF. Human blood dendritic cells selectively express CD83, a member of the immunoglobulin superfamily. *The Journal of Immunology* 1995; **154**:3821.

607 Geijtenbeek TBH, Torensma R, van Vliet SJ *et al.* Identification of DC-SIGN, a Novel Dendritic Cell-Specific ICAM-3 Receptor that Supports Primary Immune Responses. *Cell* 2000; **100**:575-85.

608 Macatonia SE, Knight SC, Edwards AJ *et al.* Localization of antigen on lymph node dendritic cells after exposure to the contact sensitizer fluorescein isothiocyanate. Functional and morphological studies. *J Exp Med* 1987; **166**:1654-67.

609 van Wilsem EJ, Brevé J, Kleijmeer M, Kraal G. Antigen-bearing Langerhans cells in skin draining lymph nodes: phenotype and kinetics of migration. *J Invest Dermatol* 1994; **103**:217-20.

610 Stoitzner P, Tripp CH, Douillard P *et al.* Migratory Langerhans cells in mouse lymph nodes in steady state and inflammation. *J Invest Dermatol* 2005; **125**:116-25.

611 Merad M, Manz MG, Karsunky H *et al.* Langerhans cells renew in the skin throughout life under steady-state conditions. *Nat Immunol* 2002; **3**:1135-41.

612 Kanitakis J, Morelon E, Petruzzo P *et al.* Self-renewal capacity of human epidermal Langerhans cells: observations made on a composite tissue allograft. *Exp Dermatol* 2011; **20**:145-6.

613 Katz SI, Tamaki K, Sachs DH. Epidermal Langerhans cells are derived from cells originating in bone marrow. *Nature* 1979; **282**:324-6.

614 Frelinger JG, Hood L, Hill S, Frelinger JA. Mouse epidermal Ia molecules have a bone marrow origin. *Nature* 1979; **282**:321-3.

615 Merad M, Hoffmann P, Ranheim E *et al.* Depletion of host Langerhans cells before transplantation of donor alloreactive T cells prevents skin graft-versus-host disease. *Nat Med* 2004; **10**:510-7.

616 Merad M, Ginhoux F, Collin M. Origin, homeostasis and function of Langerhans cells and other langerin-expressing dendritic cells. *Nat Rev Immunol* 2008; **8**:935-47.

617 Nestle FO, Zheng XG, Thompson CB *et al.* Characterization of dermal dendritic cells obtained from normal human skin reveals phenotypic and functionally distinctive subsets. *Journal of immunology (Baltimore, Md. : 1950)* 1993; **151**:6535-45.

618 Günther C, Starke J, Zimmermann N, Schäkel K. Human 6-sulfo LacNAc (slan) dendritic cells are a major population of dermal dendritic cells in steady state and inflammation. *Clin Exp Dermatol* 2012; **37**:169-76.

619 Morelli AE, Rubin JP, Erdos G *et al.* CD4+ T Cell Responses Elicited by Different Subsets of Human Skin Migratory Dendritic Cells. *The Journal of Immunology* 2005; **175**:7905-15.

620 Larregina AT, Falo LD. Changing Paradigms in Cutaneous Immunology: Adapting with Dendritic Cells. *J Invest Dermatol* 2005; **124**:1-12.

621 Santegoets SJAM, Bontkes HJ, Stam AGM *et al.* Inducing Antitumor T Cell Immunity: Comparative Functional Analysis of Interstitial Versus Langerhans Dendritic Cells in a Human Cell Line Model. *The Journal of Immunology* 2008; **180**:4540-49.

622 Mathers AR, Janelsins BM, Rubin JP *et al.* Differential Capability of Human Cutaneous Dendritic Cell Subsets to Initiate Th17 Responses. *The Journal of Immunology* 2009; **182**:921-33.

623 Matthews K, Chung NP, Klasse PJ *et al.* Potent induction of antibody-secreting B cells by human dermal-derived CD14+ dendritic cells triggered by dual TLR ligation. *J Immunol* 2012; **189**:5729-44.

624 Chu CC, Ali N, Karagiannis P *et al.* Resident CD141 (BDCA3)+ dendritic cells in human skin produce IL-10 and induce regulatory T cells that suppress skin inflammation. *J Exp Med* 2012; **209**:935-45.

625 Nestle FO, Conrad C, Tun-Kyi A *et al.* Plasmacytoid predendritic cells initiate psoriasis through interferon-α production. *J Exp Med* 2005; **202**:135-43.

626 Lowes MA, Chamian F, Abello MV *et al.* Increase in TNF-alpha and inducible nitric oxide synthase-expressing dendritic cells in psoriasis and reduction with efalizumab (anti-CD11a). *Proc Natl Acad Sci U S A* 2005; **102**:19057-62.

627 Boffa LC, Vidali G, Mann RS, Allfrey VG. Suppression of histone deacetylation in vivo and in vitro by sodium butyrate. *J Biol Chem* 1978; **253**:3364-66.

628 Reeves R, Candido EPM. Turnover of histone acetyl groups in cultured cells is inhibited by sodium butyrate. *FEBS Lett* 1978; **91**:117-20.

629 Sealy L, Chalkley R. The effect of sodium butyrate on histone modification. *Cell* 1978; **14**:115-21.

630 Ahmadian M, Suh JM, Hah N *et al.* PPARγ signaling and metabolism: the good, the bad and the future. *Nat Med* 2013; **19**:557-66.

631 Husted AS, Trauelsen M, Rudenko O *et al.* GPCR-Mediated Signaling of Metabolites. *Cell Metab* 2017; **25**:777-96.

632 Christensen GJ, Brüggemann H. Bacterial skin commensals and their role as host guardians. *Benef Microbes* 2014; **5**:201-15.

633 Nastasi C, Candela M, Bonefeld CM *et al.* The effect of short-chain fatty acids on human monocyte-derived dendritic cells. *Sci Rep* 2015; **5**:16148.

634 Schwarz A, Bruhs A, Schwarz T. The Short-Chain Fatty Acid Sodium Butyrate Functions as a Regulator of the Skin Immune System. *J Invest Dermatol* 2017; **137**:855-64.

635 Schwarz A, Philippsen R, Schwarz T. Induction of Regulatory T Cells and Correction of Cytokine Disbalance by Short-Chain Fatty Acids: Implications for Psoriasis Therapy. *J Invest Dermatol* 2021; **141**:95-104.e2.

636 Keshari S, Balasubramaniam A, Myagmardoloonjin B *et al.* Butyric Acid from Probiotic Staphylococcus epidermidis in the Skin Microbiome Down-Regulates the Ultraviolet-Induced Pro-Inflammatory IL-6 Cytokine via Short-Chain Fatty Acid Receptor. *Int J Mol Sci* 2019; **20**:4477.

637 Sanford JA, O'Neill AM, Zouboulis CC, Gallo RL. Short-Chain Fatty Acids from *Cutibacterium acnes* Activate Both a Canonical and Epigenetic Inflammatory Response in Human Sebocytes. *The Journal of Immunology* 2019; **202**:1767-76.

638 Sanford JA, Zhang LJ, Williams MR *et al.* Inhibition of HDAC8 and HDAC9 by microbial short-chain fatty acids breaks immune tolerance of the epidermis to TLR ligands. *Sci Immunol* 2016; **1**:eaah4609.

639 Norlén L, Nicander I, Lundsjö A *et al.* A new HPLC-based method for the quantitative analysis of inner stratum corneum lipids with special reference to the free fatty acid fraction. *Archives of Dermatological Research* 1998; **290**:508-16.

640 Papavassilis C, Mach KK, Mayser PA. Medium-chain triglycerides inhibit growth of Malassezia: Implications for prevention of systemic infection. *Crit Care Med* 1999; **27**:1781-86.

641 Fischer CL, Drake DR, Dawson DV *et al.* Antibacterial Activity of Sphingoid Bases and Fatty Acids against Gram-Positive and Gram-Negative Bacteria. *Antimicrobial Agents and Chemotherapy* 2012; **56**:1157-61.

642 Gupta AK, Batra R, Bluhm R *et al.* Skin diseases associated with Malassezia species. *J Am Acad Dermatol* 2004; **51**:785-98.

643 Iwamoto K, Moriwaki M, Miyake R, Hide M. Staphylococcus aureus in atopic dermatitis: Strain-specific cell wall proteins and skin immunity. *Allergology International* 2019; **68**:309-15.

644 Kim HW, Seok YS, Rhee MS. Synergistic staphylocidal interaction of benzoic acid derivatives (benzoic acid, 4-hydroxybenzoic acid and β-resorcylic acid) and capric acid: mechanism and verification study using artificial skin. *J Antimicrob Chemother* 2019; **75**:571-75.

645 Xiang MSW, Tan JK, Macia L. Chapter 11 - Fatty Acids, Gut Bacteria, and Immune Cell Function. In: *The Molecular Nutrition of Fats* (Patel VB, ed): Academic Press. 2019; 151-64.

646 Mimori S, Okuma Y, Kaneko M *et al.* Protective effects of 4-phenylbutyrate derivatives on the neuronal cell death and endoplasmic reticulum stress. *Biol Pharm Bull* 2012; **35**:84-90.

647 Rajnavölgyi É, Laczik R, Kun V *et al.* Effects of RAMEA-complexed polyunsaturated fatty acids on the response of human dendritic cells to inflammatory signals. *Beilstein J Org Chem* 2014; **10**:3152-60.

648 Lindberg M, Färm G, Scheynius A. Differential effects of sodium lauryl sulphate and non-anoic acid on the expression of CD1a and ICAM-1 in human epidermis. *Acta Derm Venereol* 1991; **71**:384-8.

649 Gill PA, van Zelm MC, Muir JG, Gibson PR. Review article: short chain fatty acids as potential therapeutic agents in human gastrointestinal and inflammatory disorders. *Aliment Pharmacol Ther* 2018; **48**:15-34.

650 Balić A, Vlašić D, Žužul K *et al.* Omega-3 Versus Omega-6 Polyunsaturated Fatty Acids in the Prevention and Treatment of Inflammatory Skin Diseases. *Int J Mol Sci* 2020; **21**.

651 Vaughn AR, Clark AK, Sivamani RK, Shi VY. Natural Oils for Skin-Barrier Repair: Ancient Compounds Now Backed by Modern Science. *Am J Clin Dermatol* 2018; **19**:103-17.

652 de Saint-Vis B, Vincent J, Vandenabeele S *et al.* A Novel Lysosome-Associated Membrane Glycoprotein, DC-LAMP, Induced upon DC Maturation, Is Transiently Expressed in MHC Class II Compartment. *Immunity* 1998; **9**:325-36.

653 Egawa M, Mukai K, Yoshikawa S *et al.* Inflammatory Monocytes Recruited to Allergic Skin Acquire an Anti-inflammatory M2 Phenotype via Basophil-Derived Interleukin-4. *Immunity* 2013; **38**:570-80.

654 Eguíluz-Gracia I, Bosco A, Dollner R *et al.* Rapid recruitment of CD14(+) monocytes in experimentally induced allergic rhinitis in human subjects. *J Allergy Clin Immunol* 2016; **137**:1872-81.e12.

655 Tamoutounour S, Guilliams M, Montanana Sanchis F *et al.* Origins and functional specialization of macrophages and of conventional and monocyte-derived dendritic cells in mouse skin. *Immunity* 2013; **39**:925-38.

656 Hubo M, Trinschek B, Kryczanowsky F *et al.* Costimulatory Molecules on Immunogenic Versus Tolerogenic Human Dendritic Cells. *Front Immunol* 2013; **4**:82.

657 Li Z, Ju X, Silveira PA *et al.* CD83: Activation Marker for Antigen Presenting Cells and Its Therapeutic Potential. *Front Immunol* 2019; **10**:1312.

658 Zhou LJ, Tedder TF. CD14+ blood monocytes can differentiate into functionally mature CD83+ dendritic cells. *Proceedings of the National Academy of Sciences* 1996; **93**:2588-92.

659 Sassa T, Kihara A. Metabolism of very long-chain Fatty acids: genes and pathophysiology. *Biomol Ther (Seoul)* 2014; **22**:83-92.

660 Ohno Y, Suto S, Yamanaka M *et al.* ELOVL1 production of C24 acyl-CoAs is linked to C24 sphingolipid synthesis. *Proc Natl Acad Sci U S A* 2010; **107**:18439-44.

661 Oteo M, Arribas P, Setién F *et al.* Structural characterization of two CD1A allelic variants. *Hum Immunol* 2001; **62**:1137-41.

662 Gan L-H, Pan Y-Q, Xu D-P *et al.* Polymorphism of human CD1a, CD1d, and CD1e in exon 2 in Chinese Han and She ethnic populations. *Tissue Antigens* 2010; **75**:691-95.

663 Wawrzyniak M, Ochsner U, Wirz O *et al.* A novel, dual cytokine-secretion assay for the purification of human Th22 cells that do not co-produce IL-17A. *Allergy* 2016; **71**:47-57.

664 Napolitani G, Kurupati P, Teng KWW *et al.* Clonal analysis of Salmonella-specific effector T cells reveals serovar-specific and cross-reactive T cell responses. *Nat Immunol* 2018; **19**:742-54.

665 Kapteyn J, He R, McDowell ET, Gang DR. Incorporation of non-natural nucleotides into template-switching oligonucleotides reduces background and improves cDNA synthesis from very small RNA samples. *BMC Genomics* 2010; **11**:413.

666 Satija R, Farrell JA, Gennert D *et al.* Spatial reconstruction of single-cell gene expression data. *Nat Biotechnol* 2015; **33**:495-502.

667 Hao Y, Hao S, Andersen-Nissen E *et al.* Integrated analysis of multimodal single-cell data. *Cell* 2021; **184**:3573-87.e29.

668 Finak G, McDavid A, Yajima M *et al.* MAST: a flexible statistical framework for assessing transcriptional changes and characterizing heterogeneity in single-cell RNA sequencing data. *Genome Biol* 2015; **16**:278.